

**Characteristics of Tropospheric Carbon Monoxide Profiles
Retrieved from MOPITT Measurements**

Thesis submitted for the degree of
Doctor of Philosophy
at the University of Leicester

by

Nigel Andrew David Richards MPhys
Department of Physics and Astronomy
University of Leicester

August 2004

UMI Number: U188594

All rights reserved

INFORMATION TO ALL USERS

The quality of this reproduction is dependent upon the quality of the copy submitted.

In the unlikely event that the author did not send a complete manuscript and there are missing pages, these will be noted. Also, if material had to be removed, a note will indicate the deletion.



UMI U188594

Published by ProQuest LLC 2013. Copyright in the Dissertation held by the Author.
Microform Edition © ProQuest LLC.

All rights reserved. This work is protected against
unauthorized copying under Title 17, United States Code.



ProQuest LLC
789 East Eisenhower Parkway
P.O. Box 1346
Ann Arbor, MI 48106-1346

Characteristics of Tropospheric Carbon Monoxide Profiles Retrieved from MOPITT Measurements

By Nigel A. D. Richards, August 2004

Abstract

In this thesis, measurements of tropospheric carbon monoxide (CO) obtained by the Measurements of Pollution in the Troposphere (MOPITT) instrument are investigated. The MOPITT instrument and measurement techniques are discussed, and recent results from the MOPITT validation campaign are presented. MOPITT phase 1 retrieved CO profile measurements are compared to *in situ* data obtained during the ACTO campaign. These comparisons suggest that MOPITT CO profiles may possess a positive bias throughout the troposphere. The results also demonstrate the need to take into account the effects of vertical resolution and the influence of the *a priori* on MOPITT retrieved profiles through the use of the retrieval averaging kernels. Comparisons of MOPITT and TOMCAT model CO profiles are also presented. The results suggest that MOPITT profiles are biased high compared to the model, and that these biases vary greatly from location to location. Simulations conducted using MOPITT operational averaging kernels to investigate the ability of the MOPITT instrument to measure layer enhancements of CO are then discussed. It is shown that MOPITT is sensitive to layer enhancements, although it is not always possible to determine the altitude of such enhancements. The seasonal cycle in MOPITT CO profile data is derived and compared to that of six CMDL surface measuring sites. A method for detecting long range transport events with anomalous CO using a regional analysis, which achieves limited success, is presented. Finally, an investigation of the combined use of the differing sensitivity of MOPITT between day and night in order to gain extra vertical information from MOPITT data is discussed. This is the first such study of its kind and the results are encouraging. Analysis shows that by examining the difference between day and night MOPITT retrieved 'surface' data it is possible, in a number of regions and seasons, to obtain further information on the vertical structure of CO. The results are validated using the TOMCAT model to represent the 'real' atmosphere. Examinations of day-night differences in phase 1 MOPITT data suggest that it is possible to use these differences to identify CO source regions such as biomass burning and industrialised regions. It is also possible to use day-night differences to identify high altitude CO, which may be used to investigate long range transport.

Acknowledgements

As is always the way with such things, I have a lot of people to thank for helping me to get this far. First, thank you to my housemates past and present, Glen, Simon, Dave, Gary, Andrew, Udo and Ute, for putting up with my mess and my music, and for many nights out drinking and eating curry in the many fine Leicester establishments, with special thanks to Glen, Dave and Andrew for many enjoyable nights in the Fan Club!

I would especially like to thank my supervisors John Remedios and Paul Monks for giving me the opportunity to conduct this PhD and for all their help and many useful discussions throughout the past four years.

Thanks to the members of the EOS group, past and present, for all their help and for making my time at Leicester both fun and memorable. I would also like to thank the members of the Molecular Properties group, for many interesting and stimulating Friday afternoon discussions, both in the lecture theatre and with beers in the SCR.

Above all I want to thank my parents whose encouragement and support have made all this possible.

Thanks also to NERC for funding this work. Finally there is Alex who gave me 50p to mention his name in these acknowledgements.

1.	INTRODUCTION	1
1.1	The Troposphere.....	1
1.2	Tropospheric Chemistry	2
1.3	Carbon Monoxide in the Troposphere.....	4
1.3.1	The Importance of CO	4
1.3.2	Carbon Monoxide Sources and Sinks.....	6
1.3.3	The Distribution of CO	8
1.3.4	Transport of CO	11
1.4	Observing Carbon Monoxide	13
1.4.1	Ground Based Measurements of CO	13
1.4.2	Aircraft Measurements of CO.....	16
1.4.3	Measurements of CO from Space.....	18
1.5	Summary.....	21
2.	THE MOPITT INSTRUMENT	22
2.1	Introduction.....	22
2.2	Nadir Infrared Sounding.....	22
2.3	The MOPITT Technique.....	24
2.3.1	Gas Correlation Radiometry	25
2.4	The MOPITT Instrument	31
2.4.1	MOPITT Channels.....	32
2.4.2	Radiometric calibration of the MOPITT thermal channels	33
2.4.3	Operational MOPITT CO retrievals	33
2.4.4	Cloud Detection for MOPITT.....	42
2.5	MOPITT Data	44
2.5.1	Errors on retrieved MOPITT CO Profiles	45
2.5.2	Validation of MOPITT CO Profiles	46
2.6	MOPITT Instrument Status	47
2.7	Summary.....	47
3.	CHARACTERISTICS OF MOPITT CO PROFILES	49
3.1	Comparing Satellite Data with <i>in situ</i> and Model Data	49
3.2	Comparisons of MOPITT CO with <i>in situ</i> Aircraft Data	50

3.2.1	The ACTO Campaign.....	50
3.2.2	MOPITT – ACTO Profile Comparison Methodology.....	52
3.2.3	MOPITT – ACTO Profile Comparison Results	53
3.2.4	Conclusions.....	60
3.3	MOPITT – Model Comparisons.....	61
3.3.1	The TOMCAT model	61
3.3.2	MOPITT – TOMCAT Comparison Methodology.....	63
3.3.3	Global Comparisons	65
3.3.4	Profile Comparisons	76
3.4	Simulating MOPITT Measurements of CO Layer Enhancements.....	90
3.4.1	Methodology	90
3.4.2	Results.....	91
3.5	Summary.....	111
4.	THE INTERCONTINENTAL TRANSPORT OF CO AS MEASURED BY THE MOPITT INSTRUMENT.....	116
4.1	The Seasonal Cycle In MOPITT CO	116
4.1.1	Monthly Mean Comparisons to CMDL surface sites	117
4.2	Regional Analysis.....	122
4.2.1	Selected Regions.....	122
4.2.2	Methodology	123
4.2.3	Results.....	124
4.3	Summary.....	156
5.	GAINING EXTRA INFORMATION FROM MOPITT PROFILE MEASUREMENTS.....	158
5.1	Day-Night Difference Simulation Studies.....	158
5.1.1	Methodology	158
5.1.2	Results.....	158
5.2	TOMCAT model studies	166
5.2.1	Methodology	167
5.2.2	Results.....	167
5.3	Day-Night Differences in MOPITT data	172
5.3.1	African Biomass Burning	172

5.3.2	South American Biomass Burning	174
5.3.3	United States Wildfires.....	176
5.3.4	Mexico City	178
5.3.5	East Asia	179
5.3.6	Industrialised Regions.....	182
5.3.7	Long Range Transport	183
5.4	Summary.....	192
6.	SUMMARY, CONCLUSIONS AND FUTURE WORK.....	194
6.1	Carbon Monoxide in the troposphere.....	194
6.2	Characteristics of MOPITT CO profiles	194
6.3	Comparisons of MOPITT CO Profiles with TOMCAT.....	197
6.4	Observing the Intercontinental Transport of CO with MOPITT.....	198
6.5	Conclusions.....	199
6.6	Future Work.....	200
6.6.1	Characteristics of MOPITT CO profile Measurements.....	200
6.6.2	Observing Intercontinental Transport with MOPITT	200
6.6.3	Gaining Extra Information from MOPITT profile Measurements	201
6.6.4	Improvements to the MOPITT Instrument	202
APPENDIX 1. DAY-NIGHT DIFFERENCES IN MOPITT		
	‘SURFACE’ CO.....	203
REFERENCES		
		207

1. Introduction

1.1 The Troposphere

The atmosphere is split into regions characterised by vertical temperature gradients as shown in Figure 1.1 below.

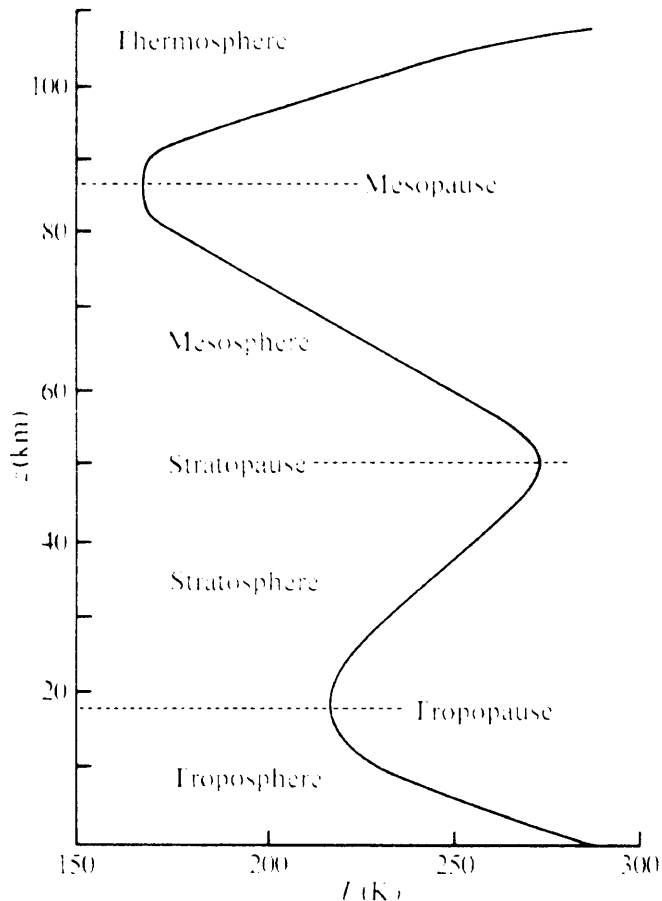


Figure 1.1: The thermal structure of the Earth's atmosphere. The curve shown represents the mean structure at 40° North during June. Taken from Wayne, 1991.

As altitude increases from the surface so temperature decreases at a rate of between 4 and 7 K km^{-1} [Wayne 1991]; this region is known as the troposphere. The troposphere extends from the surface to the tropopause which is at an altitude of approximately 18 km at the equator decreasing at higher latitudes owing to reduced convection. The region just above the tropopause is known as the stratosphere in which a temperature inversion takes place due to heating caused by the absorption of solar UV radiation by ozone.

The troposphere contains 85-90% of the Earth's atmospheric mass and the bulk of the trace gas burden. The troposphere is a dynamically unstable layer in which rapid vertical and

horizontal transport takes place. Processes occur on the timescale of days thus the troposphere is well mixed. The part of the troposphere that interacts with the surface is known as the boundary layer. The boundary layer is a region of highly turbulent mixing and is generally confined to the first 0.5-2km of the troposphere by day, and is lower at night. Most of the trace species found in the atmosphere are emitted into the troposphere from the surface and are subject to a complex series of chemical and physical transformations.

The stratosphere on the other hand is defined by small vertical mixing. Vertical transport can take place on the timescale of years rather than days and exchanges with the troposphere are slow due to the temperature inversion at the tropopause.

1.2 Tropospheric Chemistry

In general, tropospheric chemistry is analogous to a low temperature combustion system. Processes in this system however are not thermal but radical mediated and are initiated and propagated by photochemistry [Monks, 2002]. The chemistry is intrinsically linked to the chemistry of ozone.

Ozone concentrations peak in a layer in the stratosphere which is about 20 km thick and is centred on an altitude of 25-30 km [Wayne, 1991], it is often referred to as the ozone layer. It is the presence of ozone in the atmosphere that is responsible for the temperature inversion that defines the stratosphere. Ozone has unusually strong absorption between 230 and 290 nm. Molecular oxygen is capable of absorbing at wavelengths less than 230 nm but ozone is the only atmospheric species capable of attenuating solar radiation between 230 and 290 nm. Since radiation with a wavelength shorter than 290 nm damages living cells the stratospheric ozone layer is essential for the existence of life on Earth [Wayne, 1991]. Stratospheric ozone plays a large part in determining the amount of light available to cause photochemical reactions in the troposphere (the actinic flux).

Of the total amount of atmospheric ozone, only about 10% resides in the troposphere, but despite these low concentrations tropospheric ozone is still of vital importance in the atmosphere. Tropospheric ozone acts as initiator, reactant and product in much of the oxidation chemistry of the troposphere and is an important source of the hydroxyl radical

(OH). Ozone in the troposphere has two sources. The first, once thought to be the dominant source, is transport of ozone from the stratosphere to the troposphere [Junge, 1962]. The second, now believed to be the major source, is *in-situ* production by photochemical oxidation of CO and hydrocarbons catalysed by HO_x (HO + HO₂) and NO_x (NO + NO₂) [Crutzen, 1973 and Chameides and Walker, 1973]. These sources are balanced by photochemical destruction of ozone and by dry deposition at the surface.

The photodissociation of O₃ by UV radiation in sunlight to produce O(¹D), an excited oxygen atom, followed by rapid reaction of O(¹D) with water vapour forms a major source of the hydroxyl radical (OH):



In polluted regions OH may also be formed through photodissociation of nitrous acid (HONO) and hydrogen peroxide (H₂O₂). The reaction of HO₂ with NO also forms an important source of OH. This reaction is a major chain propagation step in the overall reaction mechanism for ozone formation in photochemical air pollution (see later). After formation OH rapidly inter-converts with HO₂ primarily by reactions with CO forming a steady state in sunlight. The HO_x cycle is shown in Figure 1.2, where R represents any organic hydrocarbon chain.

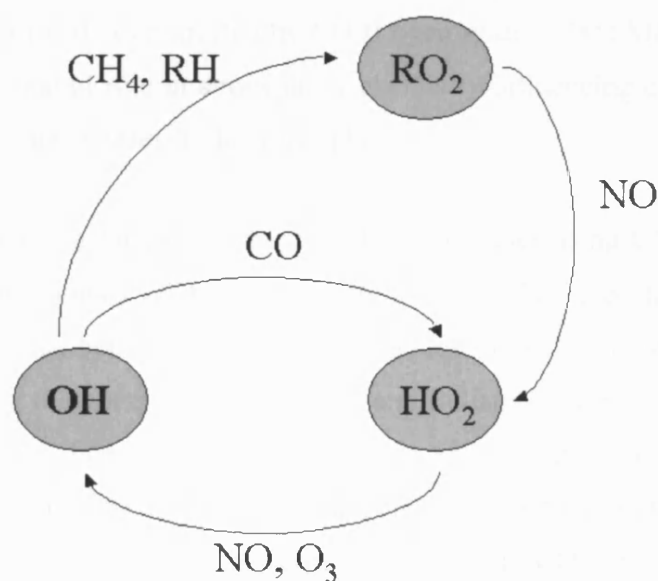


Figure 1.2: The HO_x cycle in the troposphere.

Owing to its high reactivity and relatively high tropospheric concentration, the hydroxyl radical is probably the most important of the radicals in the troposphere. The OH radical dominates daytime tropospheric chemistry and controls the oxidising capacity of the atmosphere. Reaction with the hydroxyl radical is the primary removal mechanism of many trace gases in the troposphere. In particular, hydroxyl radical chemistry provides an efficient chemical mechanism for the removal of both natural and anthropogenic pollutant trace gases. For this reason OH is known as the “detergent” of the atmosphere [Crutzen, 1994]. Free radical chain reactions oxidise greenhouse gases such as methane, hydrochlorofluorocarbons (HCFCs) and hydrofluorocarbons (HFCs) as well as CO and non-methyl hydrocarbons such as ethane and propane to CO₂ and H₂O. The rate of reaction of OH is therefore dominant in determining the tropospheric chemical lifetime of many species including the long lived greenhouse gases.

1.3 Carbon Monoxide in the Troposphere

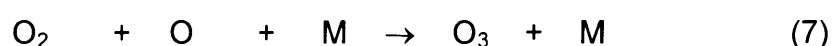
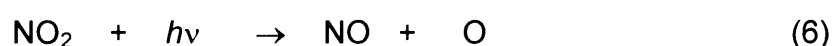
1.3.1 The Importance of CO

Carbon monoxide is an important atmospheric gas for a number of reasons. It is toxic to humans [U.S. Environmental Protection Agency (EPA), 1995] and is the main reaction partner of the hydroxyl radical. In the troposphere the reaction between CO and OH (reaction 3) represents 85% of the CO sink [Ehhalt, 1999]. Approximately 70% of tropospheric OH reacts with CO in the unpolluted troposphere [Wayne, 1991] and in many areas the removal of OH is controlled by CO [Logan *et al.*, 1981; Mészáros *et al.*, 2004]. Since OH plays a central role in atmospheric chemistry influencing climate, CO is one of the most significant trace gases in the troposphere.

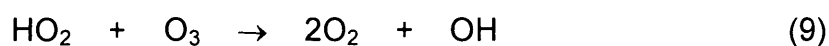
The reaction mechanism for CO destruction shows that increasing CO levels may lead to lower OH concentrations available for reaction with other greenhouse gases such as methane. The feedback between CO and OH provides CO with an indirect, but important, role in determining the chemical composition and radiative properties of the atmosphere [Novelli *et al.*, 1998]. For this reason it is known as an indirect greenhouse gas. In fact Daniel and Solomon [1998] estimate that the cumulative indirect radiative forcing due to anthropogenic CO emissions may be larger than that of N₂O. The combination of box

models with 3-D global CTM studies suggest that emitting 100 Tg(CO) is equivalent to emitting 5 Tg(CH₄) [IPCC, 2001, and references therein].

As discussed previously, ozone plays an integral part in atmospheric chemistry and CO can provide mechanisms for the production and destruction of ozone. In areas with sufficient NO_x (polluted areas, NO_x > 1ppb), HO₂ produced from oxidation of CO (reactions 3-4) can initiate photochemical reactions which result in the *net* formation of ozone (reactions 5-7). The photolysis of NO₂ and the subsequent reaction of the photoproducts with O₂ is the only known *in-situ* method of producing ozone in the troposphere. In urban and biomass burning areas where large concentrations of CO and other ozone precursors such as NO_x are produced, ozone can be formed in and downwind of the source region [Fishman and Seiler, 1983; Cros *et al.*, 1988].



Alternatively, in non-polluted regions where the NO_x levels are low (<30 pptv), the reaction of HO₂ directly with ozone leading to ozone destruction can dominate (reaction 9).



1.3.2 Carbon Monoxide Sources and Sinks

The major sources of CO are oxidation of methane (CH₄) *via* formaldehyde (HCHO) (reactions 11-14), 30-60% of tropospheric CO levels are estimated to come from oxidation of non-methane hydrocarbons (NMHC) [Poisson *et al.*, 2000], biomass burning and the incomplete combustion of fossil fuels. Other minor sources include emission by vegetation and micro-organisms and photochemical oxidation of dissolved organic matter in the oceans.

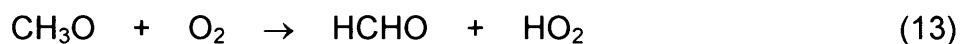
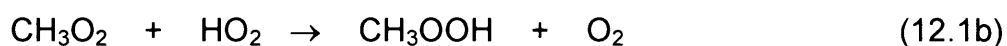
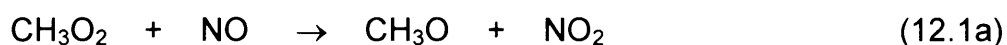
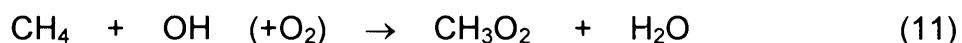


Table 1.1 shows estimates of the global budget for CO derived by several research groups. The table indicates that biomass burning accounts for about a third of the total source and that about 50% of atmospheric CO arises from direct emission due to human activity. The dominant CO sink is the reaction between CO and OH (reaction 3) which accounts for approximately 80% of CO removal with uptake by soils and transport to the stratosphere making up the rest. The table also demonstrates the large degrees of uncertainty present in estimates of both the sources and sinks of CO.

Reference:	Hauglustaine <i>et al.</i> (1998)	Bergamasschi <i>et al.</i> (2000)	WMO (1999)	IPCC SAR (1996)	IPCC TAR ^a (2001)
Sources					
Oxidation of CH ₄		795		400 - 1000	800
Oxidation of Isoprene		268		200 - 600 ^b	270
Oxidation of Terpene		136			~0
Oxidation of industrial NMHC		203			110
Oxidation of biomass NMHC		-			30
Oxidation of Acetone		-			20
Sub-total <i>in situ</i> oxidation	881	1402			1230
Vegetation		-	100	60 - 160	150
Oceans		49	50	20 - 200	50
Biomass burning ^c		768	500	300 - 700	700
Fossil & domestic fuel		641	500	300 - 550	650
Sub-total direct emissions	1219	1458	1150		1550
Total sources	2100	2860		1800 - 2700	2780
Sinks					
Surface deposition	190			250 - 640	
OH reaction	1920			1500 - 2700	
Total Sinks	2110			1750 - 3340	

Table 1.1: The global budget of CO in the Troposphere (Tg year⁻¹ of CO), taken from the Intergovernmental Panel on Climate Change (IPCC) Third Assessment Report (TAR) [2001].

1.3.3 The Distribution of CO

After CH₄, CO is the longest-lived organic species with a lifetime of up to 2 months and is one of the most abundant in the background atmosphere. It is susceptible to atmospheric transport but the lifetime is also short enough that CO will not be completely mixed. Consequently changes in CO sources and sinks generally have regional as well as global effects. The result is complex distributions of CO that depend on the size and distributions of the sources and sinks, seasonal variations in the associated chemistry, and long and short-range transport, in particular intercontinental transport.

As can be seen from Figure 1.3 the current global surface distribution of CO is asymmetric, with average surface northern hemispheric mixing ratios which are a factor of 3 higher than those of the southern hemisphere. Highest values occur at northern mid-latitudes reflecting the large anthropogenic source there. It is expected that the equatorial regions will also contribute significantly to CO production. However, the relatively constant surface CO mixing ratios in tropical regions may reflect stronger loss processes because of higher OH levels. In general, most of the biosphere related sources and anthropogenic sources occur in the northern hemisphere.

Figure 1.4 shows a composite plot of data from 30 aircraft campaigns taken over a 16 year period from 1983-1999 [Emmons *et al.*, 2000]. Although the data span a large time period, they demonstrate clearly the hemispherical differences in CO levels, it can be seen that the typical southern hemisphere CO mixing ratios are 60-70 parts per billion by volume (ppbv) and in the northern hemisphere this rises to 120-180 ppbv. Much higher concentrations can be found in localised urban and industrial areas where pollution is high and in areas of biomass burning, such as South Africa where very high CO concentration of around 460 ppbv which can be seen in the plot.

CO deseasonalized concentration (ppb)

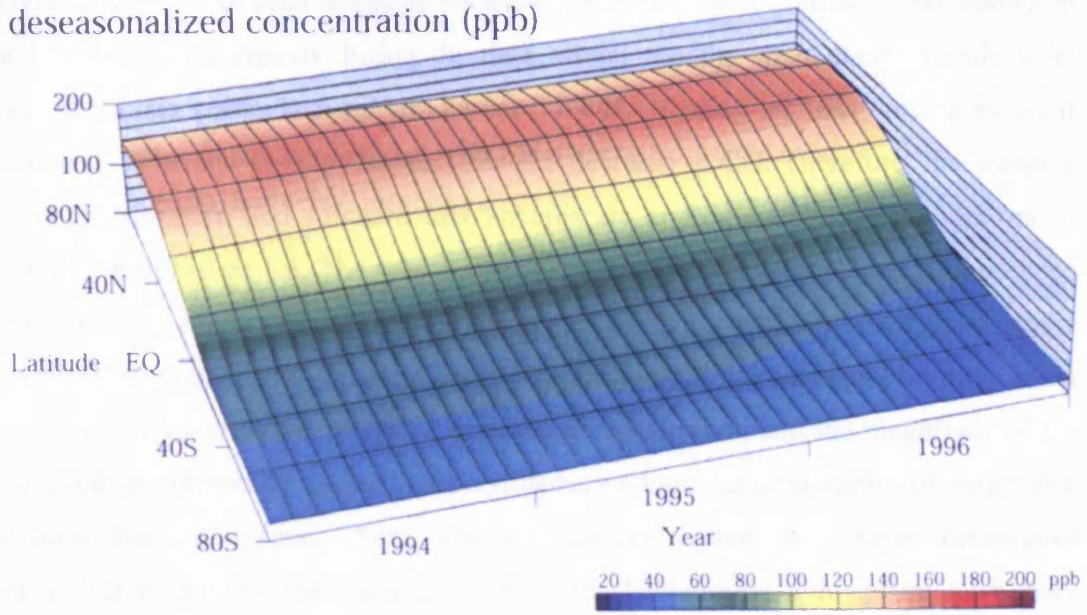


Figure 1.3: Zonally averaged deseasonalised tropospheric CO concentrations. Taken from the WMO WDCGG Data Summary, March 2002

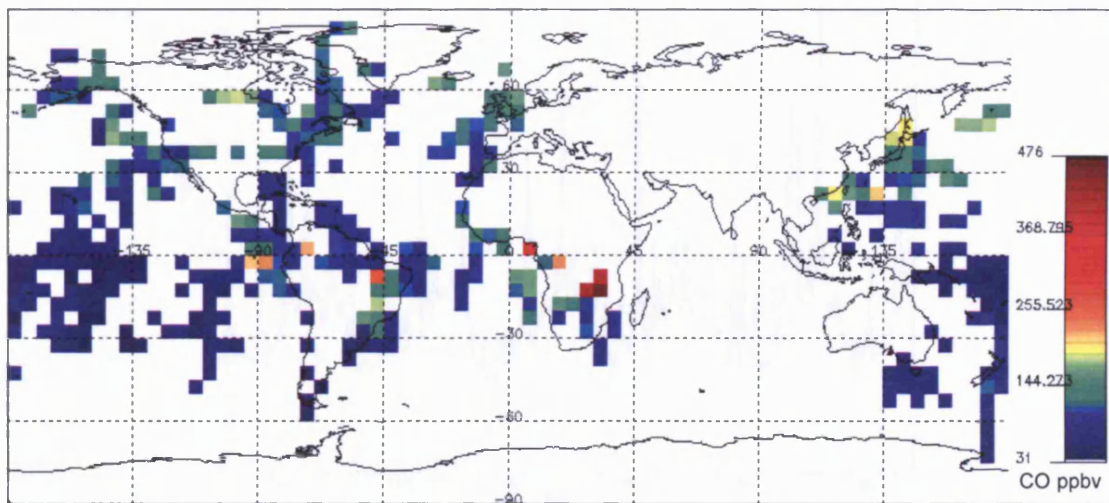


Figure 1.4 Composite aircraft CO data at 3.5 km altitude produced using data from 30 aircraft campaigns conducted over the period 1983-1999, data taken from Emmons *et al.* [2000].

Concentrations of CO in both hemispheres show a seasonal cycle similar to that shown in Figure 1.5. The CO increases during the dark winter months when there is little solar radiation to initiate photochemical production of OH. During summer, increased solar radiation leads to an increase in OH, and hence a decrease in CO. Therefore, the seasonal cycles for the northern and southern hemispheres are approximately six months out of phase as shown in Figure 1.6. The seasonal cycle in the southern hemisphere is dominated by emissions from biomass burning, and the high CO levels in the northern hemisphere winter reflect emissions from industrialisation in northern midlatitudes and burning in the northern tropics [Novelli *et al.*, 1998]. The average mixing ratio and the magnitude of the seasonal cycle are greater in the northern hemisphere where the total inputs are larger due to the large human presence there. The CO concentrations show large interannual variability, but it appears that mixing ratios in the background atmosphere have been decreasing since 1990 [Novelli *et al.*, 1998].

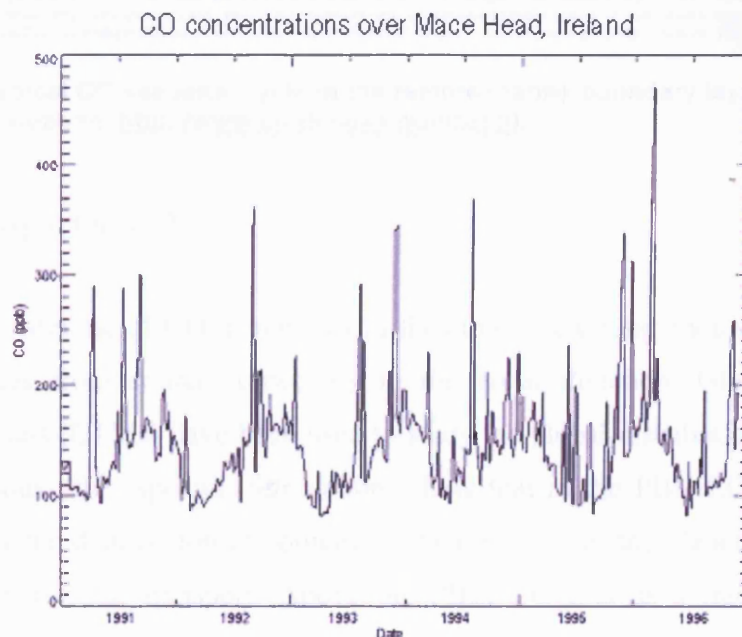
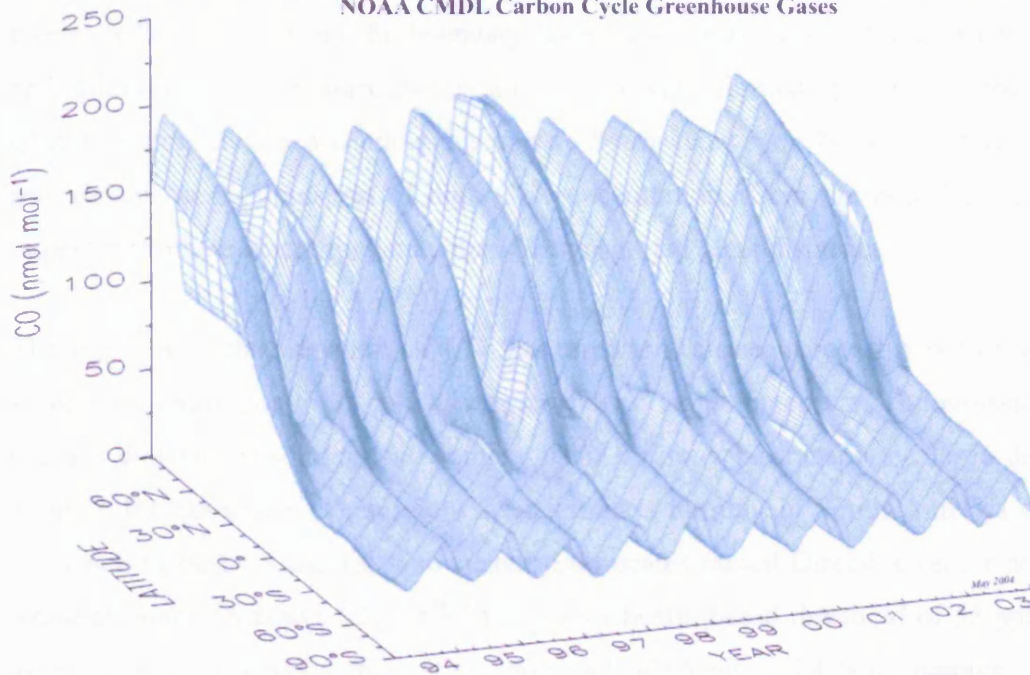


Figure 1.5: Surface CO concentrations at Mace Head for the period 1991-1996. Data supplied by NOAA CMDL (<http://www.cmdl.noaa.gov/ccgg>).

Global Distribution of Atmospheric Carbon Monoxide

NOAA CMDL Carbon Cycle Greenhouse Gases



Three dimensional representation of the latitudinal distribution of atmospheric carbon monoxide in the marine boundary layer. Data from the NOAA CMDL cooperative air sampling network were used. The surface represents data smoothed in time and latitude. Principal investigator: Paul Novelli, NOAA/CMDL Carbon Cycle Greenhouse Gases, Boulder, Colorado, (303) 497-6974 (paul.c.novelli@noaa.gov, <http://www.cmdl.noaa.gov/ccgg>).

Figure 1.6: Typical CO seasonal cycle in the remote marine boundary layer. Taken from the NOAA CMDL website (<http://www.cmdl.noaa.gov/ccgg>).

1.3.4 Transport of CO

Owing to the lifetime of CO, it remains in the atmosphere long enough to be transported large distances from source, especially in the zonal direction. Global chemistry and transport models (CTMs) have been used to study the global distributions and transport of CO and various other species. Simulations show that in the PBL CO mixing ratios are influenced by the distribution of sources, vertical mixing in the planetary boundary layer (PBL), and horizontal transport. Above the PBL, CO acts as a tracer of atmospheric motions, rising to higher altitudes and then spreading horizontally due to winds. Comparisons with observed meteorology shows that the motions of fronts and lows are mirrored as increasing mixing ratios in upper levels and the presence of high pressure in a region confines CO to lower levels [Faluvegi *et al.*, 1999]. Simulations also show that regions of high CO in upper levels move horizontally with the motion of frontal systems. Faluvegi *et al.* [1999] found upward transport in advance of fronts and subsidence behind, a finding also noted by Wang *et al.* [1996]. An important mechanism for the long range transport of pollution across the Atlantic and Pacific oceans at mid latitudes is the warm

conveyor belt (WCB) in which air rises ahead of a surface cold front [Stohl, 2001]. Warm conveyor belts reach from the boundary layer all the way up into the upper troposphere, and dilution with the surrounding air is relatively limited, preserving the chemical characteristics of the ascending air mass. Warm conveyor belts therefore provide a mechanism for the transport of high CO concentrations from the boundary layer to the upper troposphere where they may then be transported great distances.

The intercontinental transport of CO has important consequences for both regional and global air quality due to its role as a tropospheric ozone precursor. The emissions of one country will not only affect the country itself but may be transported large distances to another, for example CO emissions from biomass burning in South America and Africa can reach as far as Australia. The current European Council Directive on air pollution by ozone (Council Directive 92/72/EEC) defines a health-based threshold of 55 ppbv (8 hour average) and a vegetation protection threshold of 65 ppbv (24 hour average) [European Council of Ministers, 1992]. The transport of North American pollution can enhance surface ozone in the British Isles by up to 10 ppbv and in continental Europe by up to 8 ppbv (daily mean) [Li *et al.*, 2002]. In fact Li *et al.* [2002] find that 20% of the violations of the European Council ozone standard in the summer of 1997 over Europe would not have occurred in the absence of anthropogenic emissions from North America. Whether pollution has a regional effect or a further reaching one depends on the location of the source and also on the meteorological conditions. In general, pollution originating in North America will have an effect on both Europe and North America itself, European pollution has only a local effect on the upper troposphere over Europe, whereas Asian pollution seems to affect the whole globe [Bey, 2002]. Intercontinental transport therefore affects regional/global chemistry and the emissions policies of one country affect many others.

1.4 Observing Carbon Monoxide

In order to measure the complex spatial and temporal variations in CO distribution a number of different techniques are required. There are three main techniques used to observe CO: remote sensing from space, ground based remote measurements, and *in-situ* sampling (usually using aircraft). Each has its own strengths and weaknesses and is useful for looking at a particular aspect of the CO picture. It is likely that an integrated observing system which includes a combination of some or all of these methods is required to give a more comprehensive understanding.

1.4.1 Ground Based Measurements of CO

Ground based observations are useful for looking at trends and temporal variations of CO at a particular location. They provide very accurate long term measurements which are needed for climate change research as well as providing information on short term processes such as diurnal variations. Ground based measurement systems usually consist of a network of many fixed sites, but may also include measurements take by ships. Depending on the type of research to be carried out these sites may be located in urban areas, for the monitoring of pollution, or in remote rural sites which give an indication of what is happening in the background atmosphere away from source regions.

There are two main methods for observing CO from the ground. The first is flask sampling, where a sample of the air at the ground is taken and analysed for CO content. Methods include gas chromatography and hot mercuric oxide reduction detection (GC-HgO) and gas filter correlation (GFC) radiometry. These methods achieve low detection limits (2 ppbv) and high precision (1-2%) [Novelli *et al.*, 1998]. One such network is the NOAA Climate Modelling and Diagnostics Laboratory (CMDL) Carbon Cycle Greenhouse Gases (CCGG) cooperative air sampling network. Table 1.2 lists the measurement sites in the network and annual mean CO concentration for each.

Data from ground sampling networks of this type may be used to describe the distributions and trends of CO in the boundary layer. Figure 1.7 shows a time series of CO from two CMDL sites. Both the seasonal cycle and annual downward trend are evident.

Code	Station	Latitude	First Sample*	Annual Mean†
ALT	Alert, N.W.T., Canada	82°N	April 1992	132.8 (3.5)
ASC	Ascension Island	8°S	Feb. 1989	74.1 (3.9)
BAL	Baltic Sea	55°N	Aug. 1992	184.5 (17)
BME	Bermuda (east coast)	32°N	June 1991	128.4 (6.4)
BMW	Bermuda (west coast)	32°N	July 1991	128.0 (5.0)
BRW	Barrow, Alaska	71°N	July 1988	134.2 (3.2)
CBA	Cold Bay, Alaska	55°N	April 1992	133.8 (4.3)
CGO	Cape Grim, Tasmania	41°S	June 1991	50.7 (0.8)
CHR	Christmas Island	2°N	Dec. 1989	72.9 (2.1)
CMO	Cape Meares, Oregon	45°N	Jan. 1992	137.0 (3.6)
GMI	Guam, Mariana Islands	13°N	Oct. 1989	86.0 (3.0)
GOZ	Dwejra Point, Gozo, Malta	36°N	Oct. 1993	
ICE	Hermaey, Iceland	63°N	Oct. 1992	131.5 (2.6)
ITN	WITN, Grifton, N. Carolina	35°N	July 1992	174.1 (14)
IZO	Izaña Observatory, Tenerife	28°N	Nov. 1991	106.7 (3.7)
KEY	Key Biscayne, Florida	25°N	Aug. 1991	100.3 (4.3)
KUM	Cape Kumukahi, Hawaii	20°N	June 1989	101.8 (4.5)
MBC	Mould Bay, Canada	76°N	Feb. 1992	131.1 (3.4)
MHT	Mace Head, Ireland	54°N	June 1991	126.1 (3.4)
MID	Midway Island	28°N	Jan. 1992	113.4 (5.2)
MLO	Mauna Loa, Hawaii	20°N	July 1989	88.5 (4.8)
NWR	Niwot Ridge, Colorado	40°N	Dec. 1988	117.7 (5.4)
QPC	Qinghai Province, China	36°N	July 1991	116.2 (7.6)
RPB	Ragged Point, Barbados	13°N	March 1993	92.5 (2.8)
SEY	Mahé Island, Seychelles	4°S	Sept. 1990	80.5 (2.5)
SMO	American Samoa	14°S	Sept. 1988	55.3 (1.9)
TAP	Tae-ahn Peninsula, S. Korea	36°N	Nov. 1990	233.7 (28)
UTA	Wendover, Utah	40°N	May 1993	
UUM	Ulaan Uul, Mongolia	44°N	Jan. 1992	151.5 (6.7)

*The month and year air samples were first collected in a glass flask fitted with Teflon O-ring stopcocks and analyzed for CO.

†Preliminary 1993 mean mixing ratios and the standard error are taken from a smooth curve fit to the measured CO in flask samples as described in *Novelli et al.*, 1991.

Table 1.2: CMDL Flask Network Sites for CO Analysis and Preliminary Annual Mean CO Levels (ppb), taken from the CMDL Summary Report #22 (1992-1993).

The second is infrared solar spectroscopy [Rinsland *et al.*, 2001] which has been used to measure CO for many years. These measurements provide either integrated vertical column amounts of CO which cover the troposphere and lower stratosphere or information on two atmospheric thickness [Pougatchev *et al.*, 1999]. Spectroscopic measurements could therefore be useful for identifying plumes of CO which may pass over a site, giving information on the transport of CO from polluted to remote regions. The Network for the Detection of Stratospheric Change (NDSC) [URL: <http://www.ndsc.ncep.noaa.gov>] is an example of an observing network which uses spectroscopic techniques to measure CO in the upper troposphere and lower stratosphere (UTLS). Figure 1.8 shows the locations of the NDSC measuring sites and gives an indication of the large number of sites required to provide some kind of representative global picture of atmospheric composition.

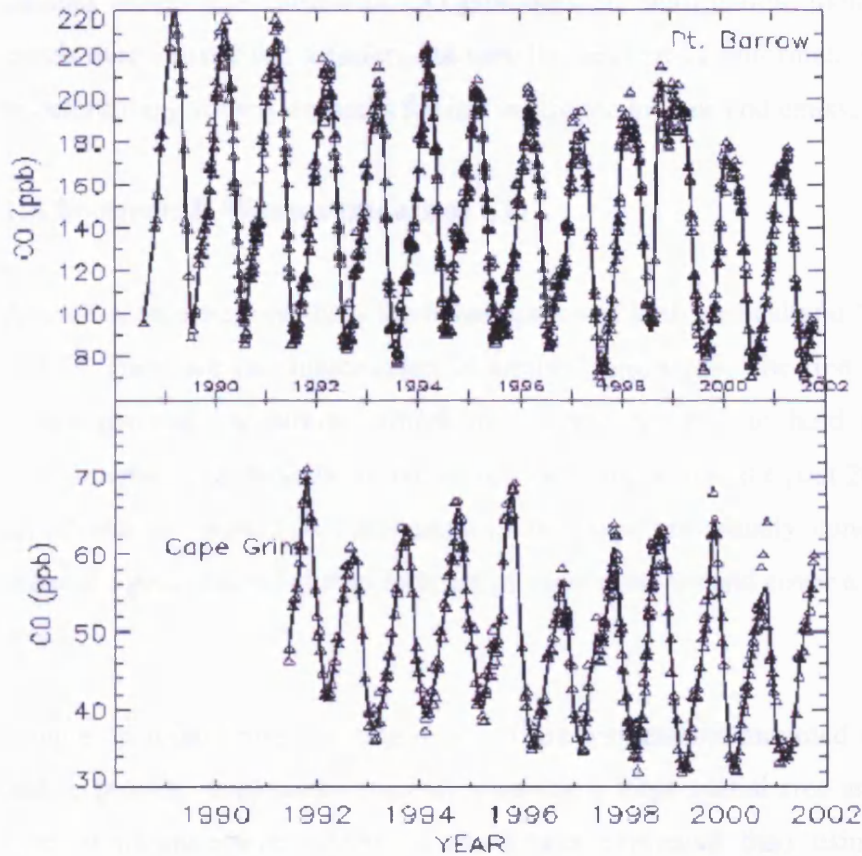


Figure 1.7: Time series of tropospheric CO mixing ratios from Pt. Barrow, Alaska, and Cape Grim, Tasmania. Triangles are the mean of a pair of flasks; the solid curves are smooth fits to the data. Taken from CMDL Summary Report #26 (2000-2001).

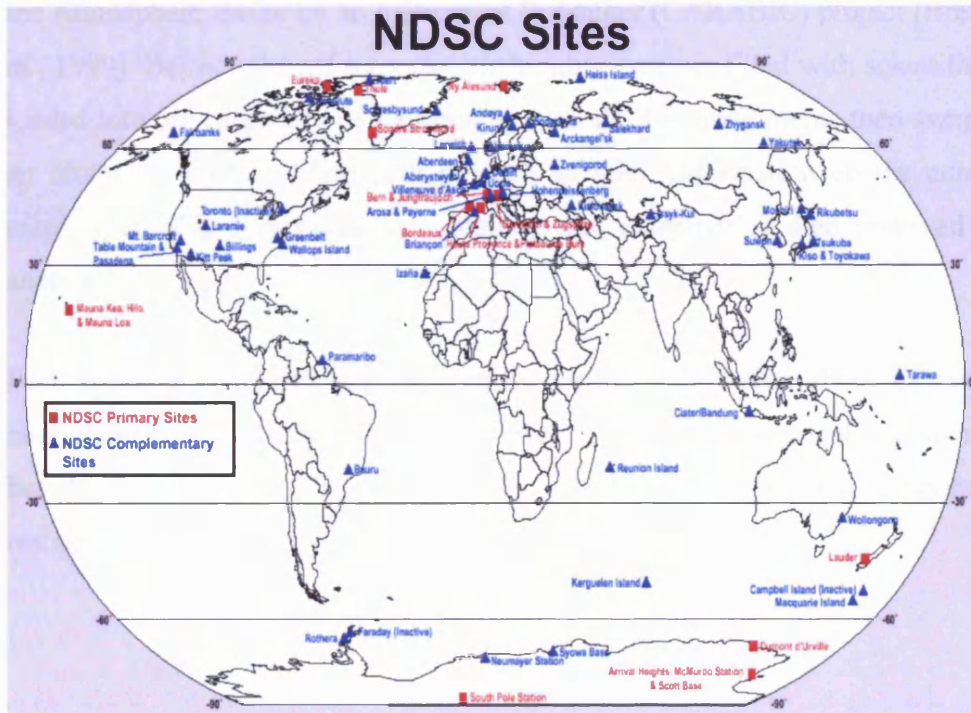


Figure 1.8: Locations of NDSC global measuring sites, taken from the NDSC web site (www.ndsc.ncep.noaa.gov).

Ground based observations of CO give accurate information about long and short term trends over a particular location, but very limited vertical information. They are also useful in determining source strengths for use in climate models and emission databases.

1.4.2 Aircraft Measurements of CO

Aircraft measurements allow the investigation of both vertical and horizontal distributions of CO. There are two major types of aircraft campaigns. The first are dedicated research campaigns that use aircraft which have been modified to hold a variety of scientific instruments. There have been many such campaigns over the past 20 years some of which are shown in Table 1.3. Campaigns of this type are usually conducted with a specific scientific goal in mind and as such are of short duration and cover a relatively small spatial area.

Long-term monitoring campaigns which use instruments mounted on commercial aircraft and so provide many measurements spanning a large spatial area are also conducted. This type of measurement system is much less expensive than using dedicated scientific research aircraft but only gives information about CO along commercial flight paths. An example of such a measurement system is the Civil Aircraft for Regular Investigation of the Atmosphere Based on an Instrument Container (CARABIC) project [Brenninkmeijer *et al.*, 1999]. Before take off a special air freight container filled with scientific equipment is loaded into the cargo bay of a passenger aircraft. The instruments then sample the outside air along the aircraft flight path through an inlet. Information on the concentrations of many species and particles are obtained, the container is then removed and the data analysed.

Both types of campaign provide vertical profile information about CO with accuracies ranging from 1 to 10 % [Emmons *et al.*, 2000] and are a useful supplement to ground based measurements. They do however give limited spatial and temporal coverage, a restriction which is better overcome using satellite systems.

Campaign	Dates
CITE-1-Hawaii	Oct-Nov 1983
CITE-1-Ames	Apr-May 1984
STRATOZ-3	June 1984
STRATOZ-3S	March 1985
ABLE-2A	July-Aug 1985
CITE-2	Aug-Sept 1986
ABLE-2B	Apr-May 1987
TROPOZ-1	Dec 1987
ABLE-3A	Jul-Aug 1988
CITE-3	Aug-Sept 1989
ABLE-3B	Jul-Aug 1990
TROPOZ-2	Jan-Feb 1991
PEM-West-A	Sept-Oct 1991
AASE-2	Jan-Mar 1992
MLOPEX-2	Apr-May 1992
TRACE-A	Sept-Oct 1992
OCTA-1	Mar-May 1993
OCTA-2	Aug-Sept 1993
OCTA-3	Jan 1994
OCTA-4	Mar-Apr 1994
PEM-West-B	Feb-Mar 1994
ACE-1	Oct-Dec 1995
TOTE	Dec 1995
VOTE	Jan-Feb 1996
SUCCESS	Apr-May 1996
PEM-Tropics-A	Aug-Oct 1996
TACIA	Sept 1996 and Aug 1997
ACSOE	1996-1998
PEM-Tropics-B	Mar-Apr 1999
INDOEX	1998-1999
MAXOX	Apr 1999
ACTO	May 2000
EXPORT	Aug 2000
SAFARI 2000	Aug-Sept 2000

Table 1.3: Some of the recent atmospheric research aircraft campaigns. Adapted from Emmons *et al.* 2000.

1.4.3 Measurements of CO from Space

We have seen that the global distribution of CO is complex and in order to understand it consistent, global observations are needed. Aircraft and ground observations are useful for looking at CO on small spatial scales, but to obtain a complete global picture satellite observations are needed to compliment these measurements. Using remote sensing techniques from space, it is possible to obtain full global coverage in just a few days. Satellite measurements attain a wide variety of spatial and temporal resolutions and use spectroscopy to infer CO concentrations from upwelling radiation from the atmosphere.

The Measurement of Air Pollution from Space (MAPS) instrument was a short duration remote sensing experiment. It was flown onboard a series of space shuttle missions in 1981, 1984 and 1994. The MAPS instrument [Reichle *et al.*, 1986] used gas correlation infrared radiometry (described in Chapter 2) to measure the global distribution of CO in the lower atmosphere (3 to 10 km above the surface) with a horizontal resolution of 17 km square and a precision of 15-20 %. The MAPS experiments provided the first coherent global observations of the distribution of CO in the troposphere [Reichle *et al.*, 1986, 1990 and 1999]. Figure 1.9 shows an example of MAPS data taken in October 1994. The interhemispheric gradient at this time of year is decreased owing to lower winter CO concentrations in the Northern hemisphere and increased emissions in the southern hemisphere because of biomass burning. Very high concentrations of CO can be seen in the southern hemisphere over South America and Africa. This is because of biomass burning which is at its peak intensity at this time of year. Also visible is a large plume over the Indonesian Islands which is presumably CO that has been transported from the biomass burning regions.

October 1994 Global Carbon Monoxide Values

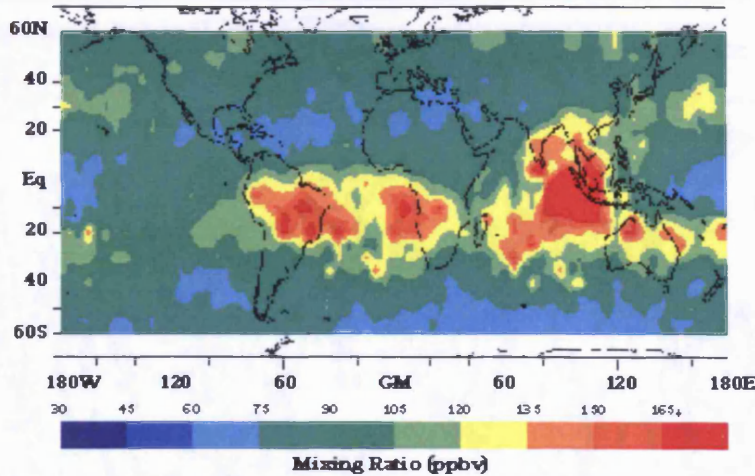


Figure 3

Figure 1.9: Map showing CO concentrations in the mid/upper troposphere (3-10 km) as measured by the MAPS instrument in October 1994. Taken from <http://oea.larc.nasa.gov/PAIS/MAPS.html>.

Most satellite missions are designed to operate for longer periods of time, typically 5-10 years. The Interferometric Monitor for Greenhouse Gases (IMG) [Kobayashi *et al.*, 1999] sensor was flown on the Japanese Advanced Earth Observing Satellite (ADEOS) satellite launched in 1996 into a sun-synchronous 830 km low Earth orbit. The instrument was a nadir-viewing Michelson-type Fourier Transform Spectrometer (FTS) that recorded detailed infrared spectra from which profile information on various greenhouse gases including CO were inferred. Figure 1.10 shows an example of IMG retrieved CO total column, taken from Clerbaux *et al.* [2001]. The horizontal resolution of IMG was 8 km x 8km and due to the large data rate of the instrument the operational mode of IMG was set to 4 days operation/10 days halt alternation [Clerbaux *et al.*, 2003]. The plot demonstrates the kind of coverage achieved by the IMG instrument over the course of a 4 day set of measurements. The accuracy of the retrieved CO column ranges from 5% to 40% and exhibits large spatial variability [Clerbaux *et al.*, 2001]. Unfortunately the ADEOS mission only lasted 10 months when the satellite suddenly lost power on June 30, 1997 due to structural damage to its solar paddle.

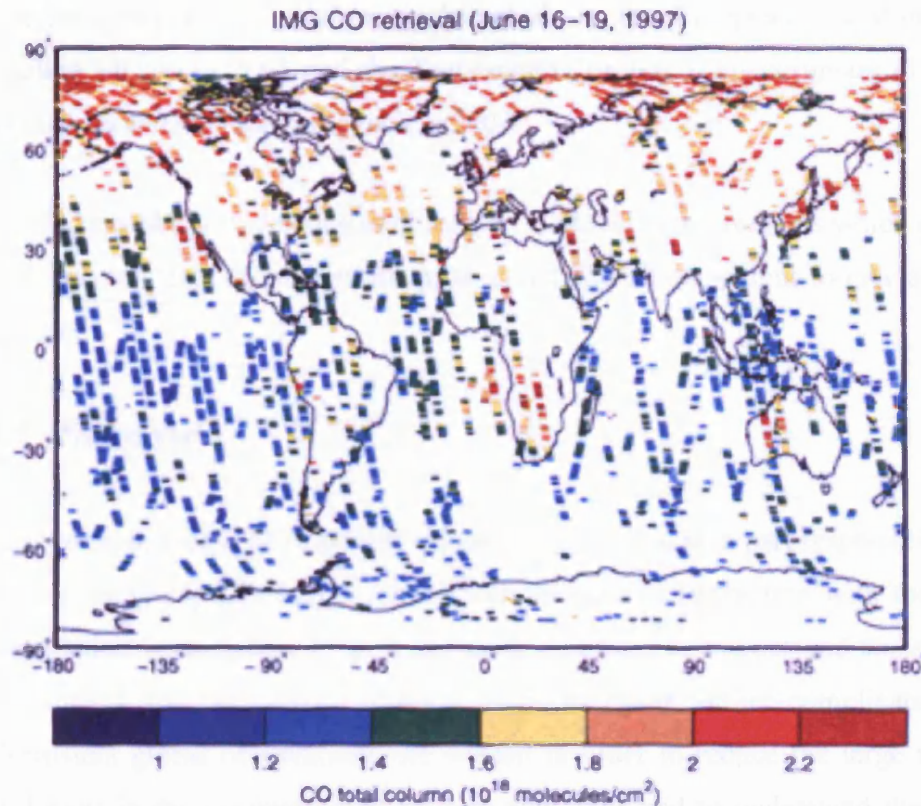


Figure 1.10: Global distribution of CO total column (molecules/cm²) for June 16-19, 1997, as retrieved from cloud-filtered Infrared Monitor for Greenhouse Gases (IMG) spectra, taken from Clerbaux *et al.* [2001]

The Measurements Of Pollution In The Troposphere (MOPITT) is an example of a currently flying instrument designed to measure CO. The MOPITT, described in detail in the next chapter, uses gas correlation radiometry to measure CO profiles. The instrument was designed to obtain long term measurements of the distribution of CO offering nearly continuous measurements throughout its expected 5 year lifetime, thus, providing improved temporal coverage than was possible with MAPS. The MOPITT instrument is able to achieve global coverage approximately every 3 days, which represents an improvement in spatial coverage over the IMG and MAPS instruments. Another advantage of the MOPITT instrument over previous missions such as MAPS is its ability to provide measurements of vertical profile of CO in the troposphere with improved vertical resolution.

There are many more instruments which will measure the composition of the atmosphere planned for the future. Such instruments include, the Scanning Imaging Absorption SpectroMeter for Atmospheric ChartographY (SCIAMACHY) on the European Environmental Satellite (ENVISAT), launched in March 2002, the Infrared Atmospheric Sounding

Interferometer (IASI) due to be launched on the European operational meteorology satellite MetOp in 2005 and the Tropospheric Emission Spectrometer (TES) on NASA's EOS-Aura satellite due for launch in 2004.

Satellites could provide consistent long term global measurements which can be combined with accurate data taken from the ground and aircraft campaigns to give a complete global picture.

1.5 Summary

Carbon monoxide is an important atmospheric gas and is in part responsible for controlling the oxidising capacity of the atmosphere through its interaction with the OH radical. Its distribution is complex owing to seasonal variations in sources and sinks. The lifetime of CO means that both long and short range transport further complicate its distribution. Consistent global observations are needed in order to reduce the large uncertainties that still exist in the magnitudes of sources and sinks and to understand the distribution and transport of CO.

Satellite measurements are needed in conjunction with other data obtained from ground and airborne sensors to give a complete picture of CO in the atmosphere. Satellites provide the opportunity to obtain global coverage on a daily basis over long periods of time. Satellites are capable of measuring vertical profiles of CO with accuracies of up to 10%. These datasets are needed to understand both the long and short term behaviour of CO and to provide information on the source distribution and transport of this important atmospheric species.

The MOPITT instrument provides the first opportunity to routinely obtain regular global observations of the horizontal and vertical distribution of CO in the troposphere. In order for the MOPITT data to be useful for climate research it must first be understood and characterised.

2. The MOPITT Instrument

2.1 Introduction

The Measurements of Pollution In The Troposphere, (MOPITT) experiment was launched on December 18th 1999, onboard the NASA EOS-Terra satellite. It is a downward looking (nadir view) infrared radiometer which targets measurements of carbon monoxide (CO) and methane. Terra is in a 705 km, sun-synchronous orbit with a 10:30am equator crossing time, which together with the MOPITT swath width, of about 600km, means total global coverage can be achieved in approximately 3 days. The primary objective of MOPITT is to enhance knowledge of the lower atmosphere system and particularly interactions with the surface/ocean/biomass systems. The particular focus is the distribution, transport, sources and sinks of CO and CH₄ in the troposphere. In this thesis, CO measurements only are discussed. A more complete description of the MOPITT instrument can be found in the MOPITT mission description document [Drummond, 1996].

2.2 Nadir Infrared Sounding

The monochromatic infrared radiance $L(\nu)$ arriving at a satellite instrument situated above the atmosphere looking down in a nadir view (i.e. placed at infinity) is given by the equation of radiative transfer:

$$L(\nu, \infty) = \varepsilon B(\nu, 0) \tau(\nu, 0, \infty) + \int_0^{\infty} B(\nu, z) \frac{d\tau}{dz}(\nu, z, \infty) dz + R \quad (2.1)$$

The first term on the right hand side of the equation represents the radiance from the Earth's surface. The second term represents the emerging radiance due to the atmospheric layer dz which absorbs radiation from the layer below and re-emits it at the layer temperature. The third term, R , represents atmospheric radiation which has been reflected by the surface. At these wavelengths, this term is usually small and can be neglected, as the emissivity of the Earth's surface, ε , is generally close to unity. The term B_ν is black body radiance i.e. the Planck function, z is altitude and τ is the atmospheric transmittance.

It can be seen from equation 2.1 that the surface emissivity and temperature of a measurement scene will determine the contribution of the surface to the total measured radiance at the top of the atmosphere. Therefore, scenes with low surface temperatures, such as snow or ice, will provide lower signals than those with high surface temperatures, such as deserts. It is also clear that the radiance contribution from the atmosphere not only depends on the absorption properties of the gas constituents but also their black body emission which itself is dependent on the temperature of the emitting atmospheric layer. This means that in order to retrieve any vertical information on trace gas concentrations the temperatures of the vertical layers to be retrieved must be different enough to provide distinct features in the radiation field. The atmospheric temperature profile is therefore important in determining the achievable vertical resolution of a nadir viewing instrument, and as such, the vertical resolution will be low over locations where the atmospheric temperature profile is quite flat such as high latitudes during the winter.

The measurement, \mathbf{y} , obtained by a radiometer such a MOPITT is related to the radiance, L_v , by an instrument function which describes the instrument and the detector used, \mathbf{F}_1 :

$$\mathbf{y} = \mathbf{F}_1 \int_{\nu_0}^{\nu_1} L_v \quad (2.2)$$

For any remote measurement, \mathbf{y} is some vector valued function \mathbf{F} of the unknown state vector \mathbf{x} (the quantity you wish to retrieve):

$$\mathbf{y} = \mathbf{F}(\mathbf{x}) + \boldsymbol{\varepsilon} \quad (2.3)$$

where \mathbf{F} is the forward function which describes the complete physics of the measurement, including the radiative transfer theory required to relate the state to the measured signal. The error term, $\boldsymbol{\varepsilon}$, includes errors from sources such as detector noise, which are not related to the forward function parameters. In the linear case, this can be represented as:

$$\mathbf{y} = \mathbf{K}\mathbf{x} + \boldsymbol{\varepsilon} \quad (2.4)$$

where \mathbf{K} is known as the weighting function matrix, and is equal to $\partial y / \partial x$ and is the sensitivity of the measurement to a change in the state vector \mathbf{x} and is a function of both frequency and altitude.

2.3 The MOPITT Technique

The MOPITT instrument makes measurements of radiation emerging from the atmosphere in two spectral bands for the retrieval of CO columns and profiles. The first band targets thermal infrared emission at 4.7 μm and the second focuses on reflected solar radiation at 2.3 μm ; The focus here will be on the thermal infrared since in the current MOPITT operational retrieval algorithm only the 4.7 μm channels are used. The 4.7 μm band lies in a region of the spectrum which contains signals from gases other than CO, in particular N_2O and water vapour, and the lines of interest are mixed with those of these interfering species, see Figure 2.1. In principle it is possible to measure total emission or transmission in a spectral band, and then correct for the contributions of the interfering species to arrive at a measurement of the species of interest. However, in this case the contributions of the other species are comparable or larger than those of the gas of interest, and their amounts are often not known with sufficient accuracy. The uncertainties of the corrections may significantly degrade, or even mask, the detection of changes in the gas of interest.

The MOPITT technique overcomes this problem by increasing its spectral sensitivity to CO and separating the CO emission lines from the general radiation field through the use of gas correlation radiometry.

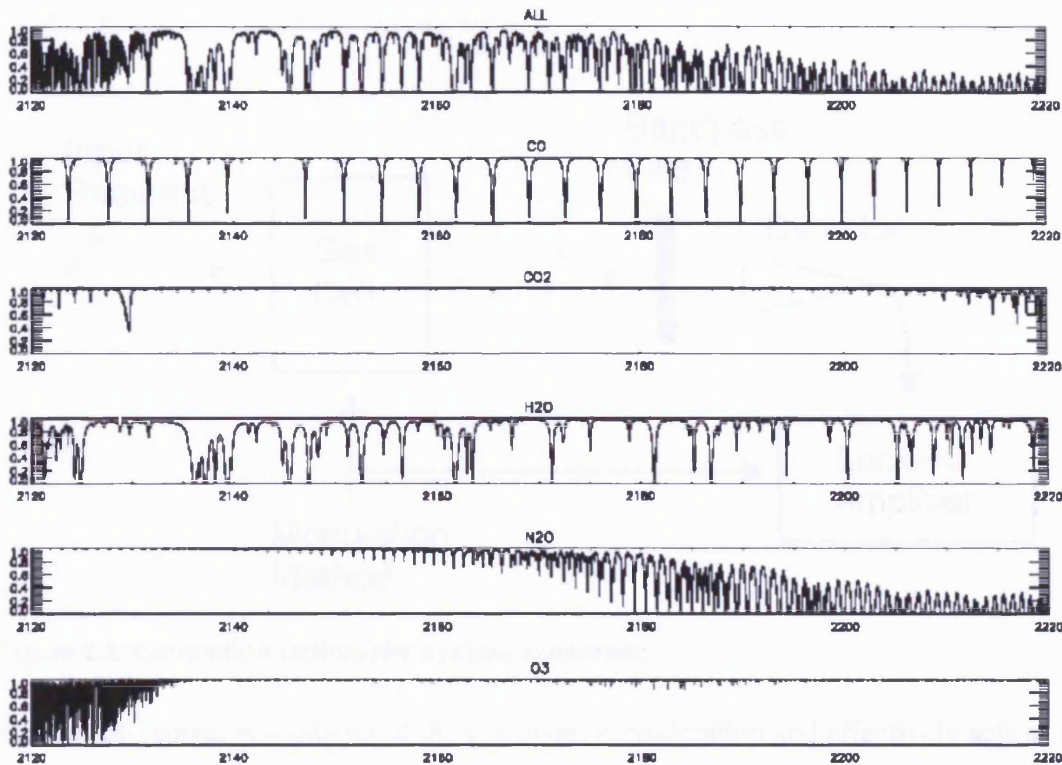


Figure 2.1: Surface to top of the atmosphere transmissions of species in the MOPITT 4.7 μm channel, calculated using the line by line radiative transfer code, the Oxford RFM (<http://www.atm.ox.ac.uk/RFM>). Transmissions are shown for CO, CO₂, H₂O, N₂O and O₃.

2.3.1 Gas Correlation Radiometry

Gas correlation spectroscopy has been used to remotely sense atmospheric parameters for more than 30 years. The first instrument to use the technique in space was the selective chopper radiometer (SCR) instrument on the Nimbus 4 satellite, launched in 1970 [Abel *et al.*, 1970]. The principle is that of spectral selection of radiation emission or absorption by a gas using a sample of the same gas as the filter. In the absence of Doppler shifts, the spectral lines of a gas must align perfectly with themselves and the spectral alignment of the system will be perfect without the need for sensitive dispersive elements. A schematic of a correlation radiometry system is shown in Figure 2.2.

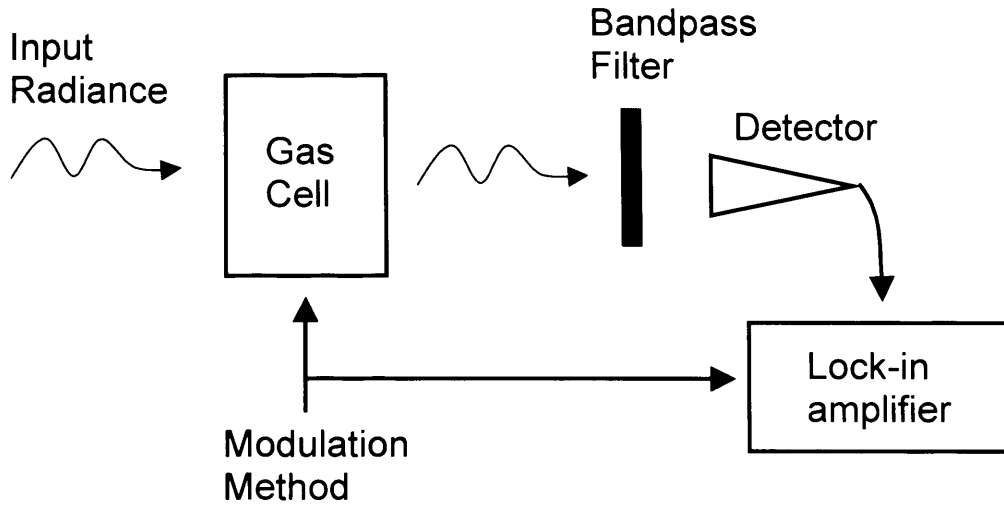


Figure 2.2: Correlation radiometry system schematic.

The gas cell contains a sample of the gas under consideration and effectively acts as a filter attenuating only those lines belonging to the target gas, the resulting signal is as shown in Figure 2.3 for two different amounts of gas in the cell. By cycling the amount of gas in the cell between the two states, the detector looks alternately through two different filters, with only the target gas lines changing. The transmission through the correlation cell can be characterised by the definition of two effective transmission profiles [Tolton and Drummond, 1997]. The effective average transmission (EAT) (equation 2.5) corresponds to the average transmission (τ) through two states of the cell (s_1 and s_2). When using the EAT, the system effectively acts as a filter radiometer and provides little sensitivity to the gas in the cell. Providing that the cell pressure is high enough, the transmission will be zero at the target gas lines due to absorption by the gas in the cell, as shown in Figure 2.4. The effective difference transmission (EDT) (equation 2.6) corresponds to the difference in transmission between the two gas states. The EDT of the system approaches zero between the spectral lines of the gas in the cell, eliminating interfering signals from other gases and is a maximum at the target lines as shown in Figure 2.4.

$$EAT(\nu) = \left[\frac{(\tau_{s_1}(\nu) + \tau_{s_2}(\nu))}{2} \right] \quad (2.5)$$

$$EDT(\nu) = \tau_{s_1}(\nu) - \tau_{s_2}(\nu) \quad (2.6)$$

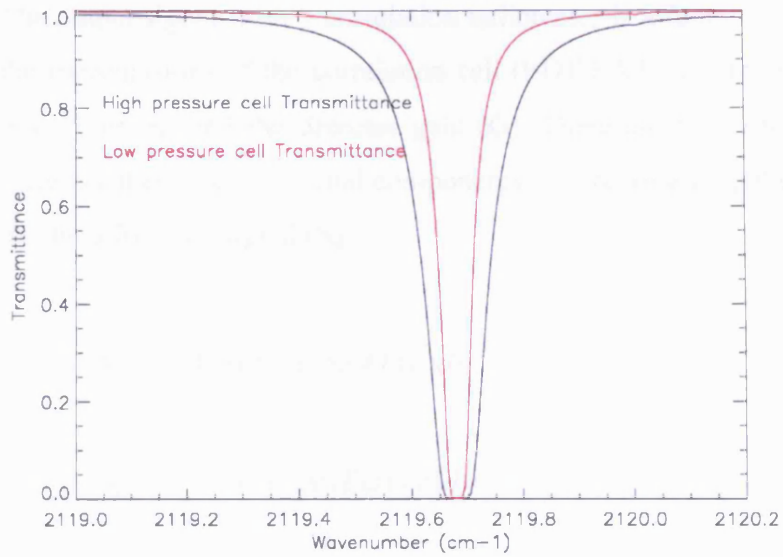


Figure 2.3: High and low pressure cell transmittances for a CO pressure modulator cell (PMC). The transmittances were calculated using the Oxford RFM for a 1cm long cell, with low and high pressures of 50 and 100 mb respectively, at a temperature of 300K.

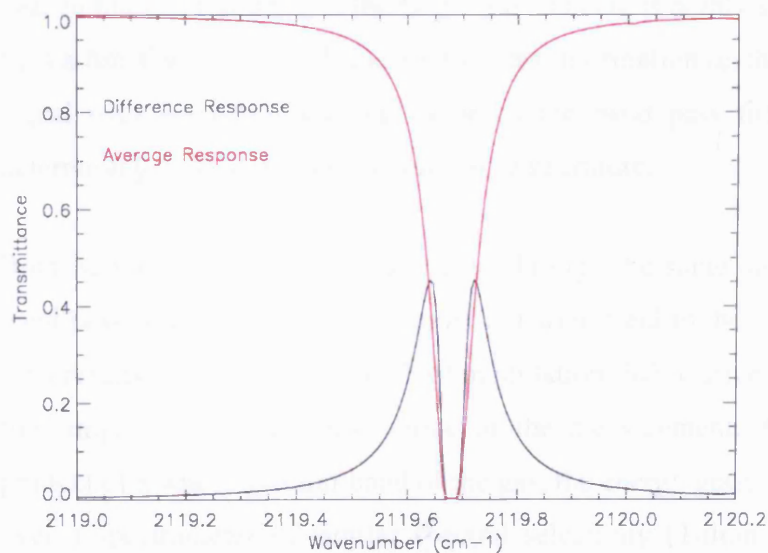


Figure 2.4: Average and difference responses for a pressure modulated cell (PMC). The responses were calculated using the Oxford RFM for a 1cm long cell, with low and high pressures of 50 and 100 mb respectively, at a temperature of 300K.

The positions of the EDT maxima on the gas absorption lines depend on the pressure of the gas in the cell. Therefore by using cells with different amounts of gas it is possible to look at different parts of the line wings and thus, because of atmospheric pressure broadening, different altitudes.

The output signal from a correlation radiometer is a function of the incident radiation (L), the transmissions of the correlation cell (EDT/EAT), the transmission of the narrow band pass filter (τ_f) and the detector gain (G). There are two effective cell transmissions and therefore there are two signal components, one representing the average signal (S_a) and one for the difference signal (S_d).

$$S_a = G \int_{\nu_1}^{\nu_2} L(\nu) \tau_f(\nu) EAT(\nu) d\nu \quad (2.7)$$

$$S_d = G \int_{\nu_1}^{\nu_2} L(\nu) \tau_f(\nu) EDT(\nu) d\nu \quad (2.8)$$

Both signals provide information about the spectral properties of the incident radiation. Since S_d is a function of the EDT, it provides information only at the wave numbers at or near to the spectral lines of the target gas, making it highly sensitive to that gas. However, S_a is a function of the EAT and so provides information on the stronger contributions to the signal over the entire spectral range of the band pass filter. It is therefore useful for determining surface properties, such as temperature.

Both S_a and S_d must intrinsically pass through the same spectral filter. This is a narrow band pass filter to limit the measured radiation field to the spectral band of the target gas. This results in an increased depth of modulation (S_d) relative to the background signal (S_a), thus improving the dynamic range of the measurement. Also, since the signals are a product of a whole spectral band of the gas, the energy grasp of the radiometer is improved over a spectrometer of similar spectral selectivity [Tolton and Drummond, 1997]. The MOPITT instrument uses two different methods for the modulation of the gas cell opacity, pressure and length modulation.

2.3.1.1 The Pressure Modulated Cell (PMC)

The pressure modulated cell [Taylor *et al.*, 1972] was developed in the early 1970s. The configuration of a pressure modulated radiometer (PMR) is shown in Figure 2.5. The opacity of the cell in a PMR is varied by modulating the pressure of the cell between a high and a low state using a piston as shown, the resulting EDT can be seen in Figure 2.6. This transmission curve was constructed by using the Oxford RFM to calculate the radiation

transmitted through a 1 cm gas cell containing pure CO at pressures of 50 and 100 mb, and a temperature of 300K, and subtracting the resulting signals. Due to the compression and expansion of the gas in the cell its temperature also varies in a cyclic fashion and in order for the technique to be of any use in remote sensing the pressure and temperature cycle must be fully understood and characterised.

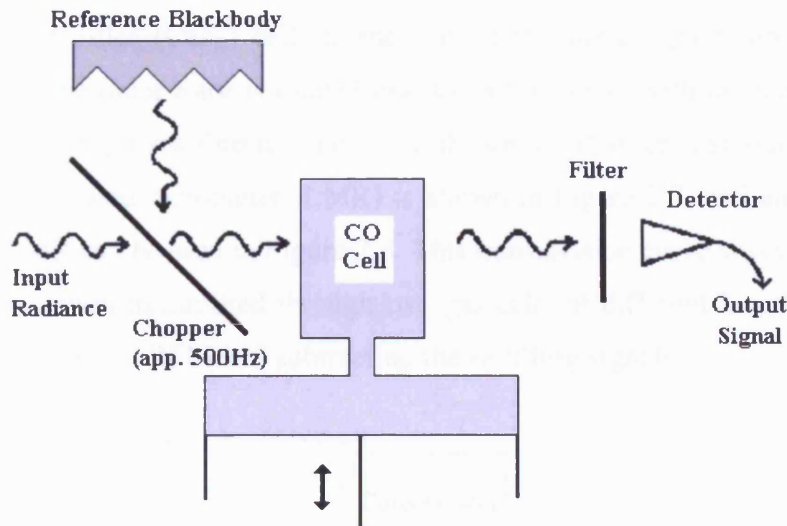


Figure 2.5: Schematic for a pressure modulated radiometer (PMR). Taken from the MOPITT mission description document [Drummond, 1996].

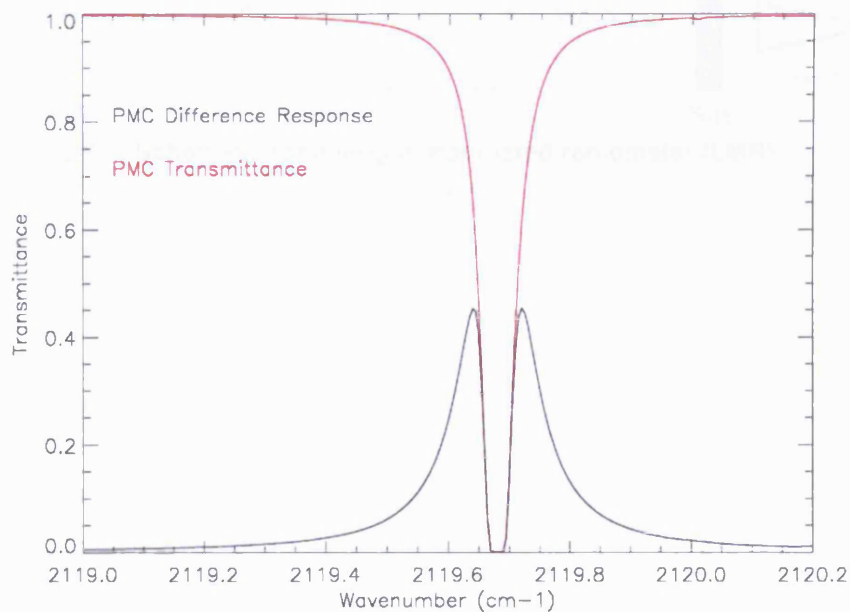


Figure 2.6: Example effective difference transmission curve (EDT) for a pressure modulated cell (PMC). The transmittances were calculated using the Oxford RFM for a 1cm long cell, with low and high pressures of 50 and 100 mb respectively, at a temperature of 300K.

2.3.1.2 The Length Modulated Cell (LMC)

Length modulated cells were first developed in the late 1980s [Drummond 1989]. In an LMC the gas density in the cell is modulated by changing the optical path length through the gas within the cell. Path length modulation is performed by the rotation of an optically inert filler (CaF_2) cell in and out of the optical path through the correlation cell. A compensator rotor is rotated exactly out of phase with the main rotor so that the radiation always passes through the same thickness of filler material. A schematic of the length modulated radiometer (LMR) is shown in Figure 2.7, and an example of the EDT for an LMR can be seen in Figure 2.8. This transmission curve was constructed by calculating the radiation transmitted through two gas cells of different lengths containing pure CO using the Oxford RFM and subtracting the resulting signals.

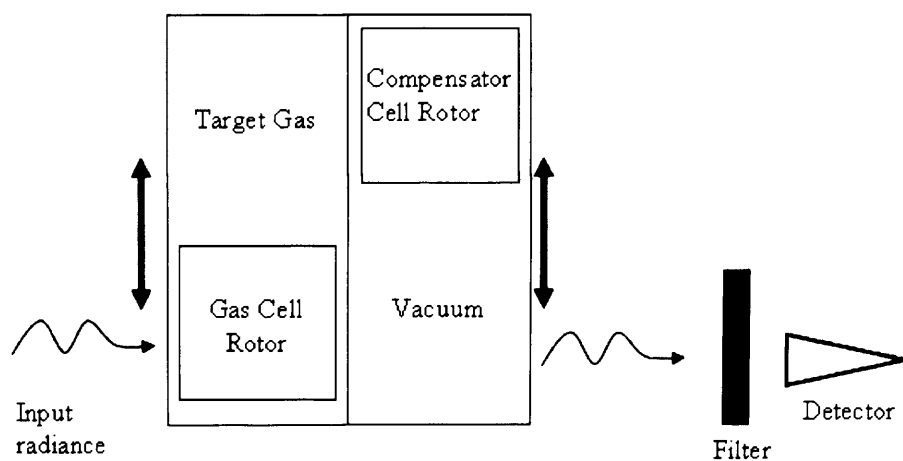


Figure 2.7: Schematic for a length modulated radiometer (LMR).

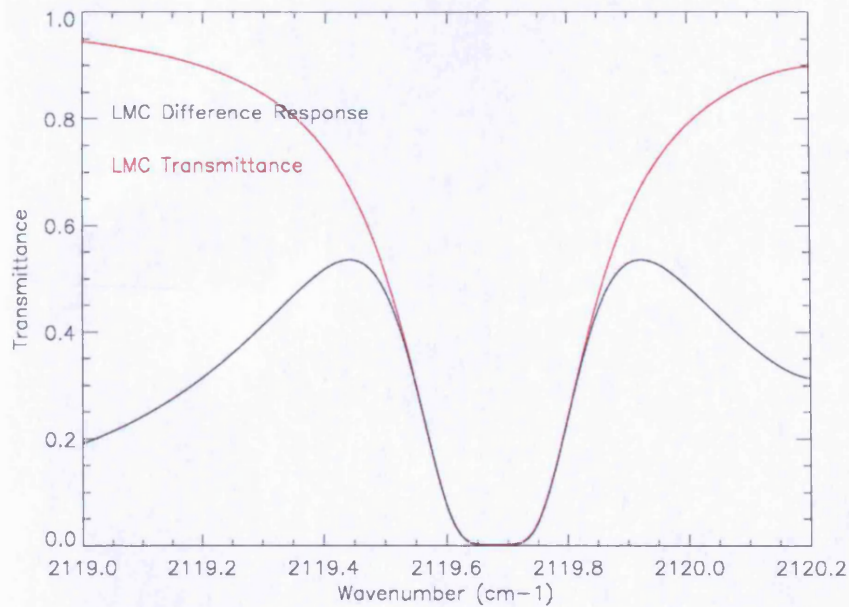


Figure 2.8: Example effective difference transmission curve (EDT) for a length modulated cell (LMC). The responses were calculated using the Oxford RFM for a cell pressure of 200 mb and cell lengths of 2 and 10 mm, at a temperature of 300K.

2.3.1.3 PMR vs. LMR

As the cell pressure increases, the PMR requires more power to operate, so PMRs are generally only used at lower pressures (25-100 mb for MOPITT) which means they are useful for measuring the upper troposphere only. The LMR may operate at much higher pressures (200-800 mb for MOPITT) and are therefore more suited to measuring the mid to lower troposphere. A combination of both techniques would therefore give good vertical coverage, and the MOPITT instrument takes advantage of this.

2.4 The MOPITT Instrument

The MOPITT instrument is designed as a nadir viewing instrument providing a horizontal resolution of 22 km by 22 km. The MOPITT instrument makes measurements by scanning across the satellite flight track to +/- 26.1 degrees in 13 seconds, pausing for approximately 0.45 seconds to record data. Each of these measurements is called a 'stare' and consists of four 22km by 22km pixels. This cross-track scanning increases the spatial coverage in each satellite orbit. Figure 2.9 shows an example of the MOPITT scan pattern. As a result the MOPITT instrument has a swath width of approximately 600 km and achieves global coverage in approximately 3 days.

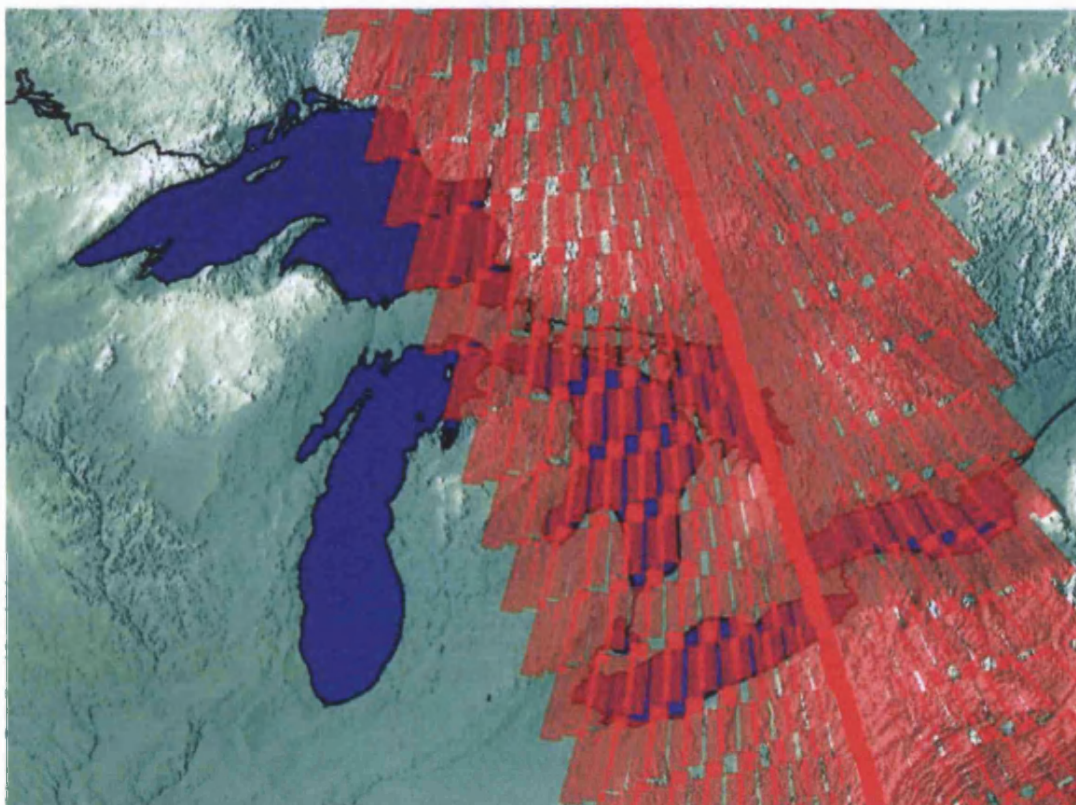


Figure 2.9: The MOPITT scan pattern. Taken from Drummond, 1992.

2.4.1 MOPITT Channels

As described earlier, the MOPITT instrument makes CO measurements in two spectral regions, thermal infrared emission at $4.7\ \mu\text{m}$ and reflected solar radiation at $2.3\ \mu\text{m}$. Here we will concentrate on the thermal infrared channels only since the solar channels are not currently used in any CO retrievals, as the calibration of these channels is yet to be fully understood. The $4.7\ \mu\text{m}$ region covers the R branch of the CO(0-1) fundamental band in the spectral region $2110\text{-}2230\ \text{cm}^{-1}$. In this region, the solar spectrum is relatively weak and the ground reflectivity is low, $\sim 2\%$ over the ocean [Edwards *et al.*, 1999]. The top of the atmosphere radiance in this region is therefore dominated by thermal emission from the surface and the atmosphere. Table 2.1 shows how the MOPITT instrument makes use of two PMCs and four LMCs to form eight spectral channels, six are designed to be used for CO retrievals and two for CH₄. By using a series of PMRs and LMRs at different cell pressures the MOPITT instrument is able to obtain information on the vertical distribution of CO by sampling different parts of the line wings.

Channel Number	Primary Purpose	Modulator Type and Number	Cell Pressure (mb)	Cell Temperature (K)	Cell Length (mm)	Centre Wavenumber (cm ⁻¹)
1	CO	LMC1	200	300	2-10	2166 (52)
2	CO	LMC1	200	300	2-10	4285 (40)
3	CO	PMC1	50-100	300	10	2166 (52)
4	CH ₄	LMC2	800	300	2-10	4430 (140)
5	CO	LMC3	800	300	2-10	2166 (52)
6	CO	LMC3	800	300	2-10	4285 (40)
7	CO	PMC2	25-50	300	10	2166 (52)
8	CH ₄	LMC4	800	300	2-10	4430 (140)

Table 2.1: The MOPITT instrument channel characteristics, numbers in parentheses denote standard deviation, adapted from the NCAR MOPITT web site (<http://www.eos.ucar.edu/mopitt>).

2.4.2 Radiometric calibration of the MOPITT thermal channels

The MOPITT instrument employs two separate radiometric calibration systems to minimise any offset and gain errors due to instrument thermal variations, condensation and damage to the optics, or detector degradation [McKernan, 2001]. The first system is a fast optical chopper (500-600 Hz), which calibrates for thermal drifts in the section of the instrument behind it and allows for the reduction of 1/f noise. The second system consists of a space-viewing port and a warm blackbody target. Every two minutes (10 swaths) the instrument scan mirror rotates to look at deep space for 5 stares, establishing the instrument offset. After every fifth space-view i.e. every 10 minutes, the scan mirror rotates to view an internal blackbody target for 20 stares. The blackbody targets are maintained at 295 K and provide a channel gain correction.

2.4.3 Operational MOPITT CO retrievals

2.4.3.1 MOPITT forward modelling

Forward modelling for the MOPITT instrument is described in detail by Edwards *et al.* [1999] and only a short description will be given here. Gas correlation spectroscopy requires high spectral resolution radiative transfer calculations to model the measurement

process [Edwards *et al.*, 1999]. Calculations of this type must be performed by using line-by-line radiation code, which is too slow for operational retrieval use but is used to generate high spectral resolution databases on which fast operational models are based. The MOPITT line-by-line calculations, described by Pan *et al.* [1995], were performed using the general purpose line-by-line transmittance and radiance model GENLN2 [Edwards, 1992].

The fast forward model developed for the MOPITT instrument is called MOPFAS [Edwards *et al.* 1999]. The aim of this model is to solve the radiative transfer equation after having first performed the spectral integrations off-line. It reproduces MOPITT channel signals taking into account their dependence on temperature, mixing ratios of target and contaminating gases, and satellite and solar zenith angles. A regression scheme is applied to establish a correspondence between channel-integrated transmittances and atmospheric profiles so that when given a profile MOPFAS is able to quickly infer a corresponding transmittance. The regression coefficients are pre-computed using a least squares fit over a representative atmospheric ensemble. The accuracy of MOPFAS is within ~0.5% of a full line-by-line calculation, and the code runs 10^5 times faster.

The MOPFAS model is used to produce simulated MOPITT signals and calculate weighting functions needed for the retrieval process, which is described in the next section.

2.4.3.2 The MOPITT Operational Retrieval Algorithm

2.4.3.2.1 Retrieval Algorithm Formulation

The operational MOPITT retrieval uses a non-linear optimal estimation algorithm [Rodgers, 2000; Pan *et al.*, 1998] and the MOPFAS fast forward model (see last section) to invert the measured average and difference signals to determine tropospheric concentrations of CO. The CO retrieval algorithm used for MOPITT exploits the maximum *a posteriori* (MAP) solution which is a specific type of optimal estimation technique [Rodgers, 2000]. For the thermal band signals the average and difference signals for each channel are included directly in the measurement vector. The thermal band signals are not only dependent on the CO profile being measured but also the atmospheric temperature and water vapour profiles, and the surface temperature and longwave

emissivity. Therefore, accurate values for all these parameters must be obtained in order to produce accurate retrievals [Deeter *et al.*, 2003]. Atmospheric temperature and water vapour profiles are obtained by spatially and temporally interpolating NCEP reanalysis profiles to the time and location of each MOPITT pixel. Values for the surface temperature and emissivity are retrieved simultaneously with the CO profile from information contained in the thermal band signals.

The measurement and state vectors for a given pixel can be written generally as

$$y = (y_i) = \begin{Bmatrix} S_1^A \\ \vdots \\ S_4^A \\ S_1^D \\ \vdots \\ S_4^D \end{Bmatrix} \quad x = (x_i) = \begin{Bmatrix} \epsilon_{sfc} \\ T_{sfc} \\ q_1 \\ q_2 \\ \vdots \\ q_i \end{Bmatrix} \quad (2.9)$$

where y is the measurement vector, S^A and S^D represent the average and difference signals respectively for each thermal channel, x represents the state vector which contains the surface emissivity ϵ_{sfc} , the surface temperature T_{sfc} and q_i which represents the CO mixing ratio at the i th pressure level of the pressure grid. The MOPITT operational retrieval pressure level grid has seven levels which include the surface, 850, 700, 500, 350, 250 and 150 mb. A Newtonian iterative form of the maximum a posteriori solution is found which combines the state vector, determined solely from the measurements, and the *a priori* state vector, inversely weighted by their respective covariances. If the error terms are neglected, the MOPITT retrieved CO profile \hat{x} can be expressed as a linear combination of the true profile x_t and an *a priori* profile, x_a , through the matrix relation [Rodgers, 2000]

$$\hat{x} \approx Ax_t + (I - A)x_a \quad (2.10)$$

where I is the identity matrix and A is the averaging kernel matrix. The averaging kernels indicate the sensitivity of the retrieval to the atmospheric state ($\partial \hat{x} / \partial x$) and provide the relative weighting between the true and *a priori* profile. The ideal situation would be one

where \mathbf{A} equals \mathbf{I} then from equation 2.10 we see that $\hat{\mathbf{x}} \approx \mathbf{x}_t$ and the retrieved profile reflects the true profile, generally though this is not the case and changes in the true profile result in finite changes to all elements of the retrieved profile. Thus, the averaging kernel gives some indication of the vertical resolution and sensitivity of the retrieval and the influence of the *a priori*. Averaging kernels are calculated from the *a priori* covariance matrix (\mathbf{C}_a) and the retrieval error covariance matrix ($\mathbf{C}_{\hat{\mathbf{x}}}$), determined for each retrieval:

$$\mathbf{A} = \mathbf{I} - \mathbf{C}_{\hat{\mathbf{x}}} \mathbf{C}_a^{-1} \quad (2.11)$$

The retrieval covariance matrix is calculated using the *a priori* covariance matrix, the weighting function (\mathbf{K}), and the radiance error matrix (\mathbf{C}_e):

$$\mathbf{C}_{\hat{\mathbf{x}}} = (\mathbf{C}_a^{-1} + \mathbf{K}^T \mathbf{C}_e^{-1} \mathbf{K})^{-1} \quad (2.12)$$

The square roots of the diagonal elements of the retrieval error covariance matrix provide the retrieval errors for each profile retrieval.

Expanding equations 2.11 and 2.12, the averaging kernel may be expressed as:

$$\mathbf{A} = \mathbf{I} - (\mathbf{C}_a^{-1} + \mathbf{K}^T \mathbf{C}_e^{-1} \mathbf{K})^{-1} \mathbf{C}_a^{-1} \quad (2.13)$$

Thus, the averaging kernel is directly related to the weighting function which describes the sensitivity of the measurement to the vertical distribution of the species of interest in the atmosphere.

2.4.3.2.2 Operational Retrievals

The signals used to perform operational MOPITT CO profile retrievals include channels 7A, 1D, 3D and 7D. Channel 5D was excluded because of an apparent radiance bias which degraded the retrieval considerably. Channels 1A, 3A and 5A were excluded because of the redundancy of information with the 7A signal, as all these channels are primarily sensitive to surface temperature and emissivity. The solar channels are also excluded from the retrievals due to low signal-to-noise ratios. Figure 2.10 shows typical weighting functions for the three difference signals used in the retrievals. These weighting functions

were calculated [Deeter *et al.*, 2003] using the MOPITT *a priori* profile (described in the next section) and show that the MOPITT instrument is most sensitive to the mid-troposphere (~500 mb). Operational weighting functions exhibit significant variability due to changes in the true CO profile and surface temperature. The geographical and seasonal variability of the weighting functions will therefore lead to significant variability in the vertical sensitivity of the retrievals [Deeter *et al.*, 2003].

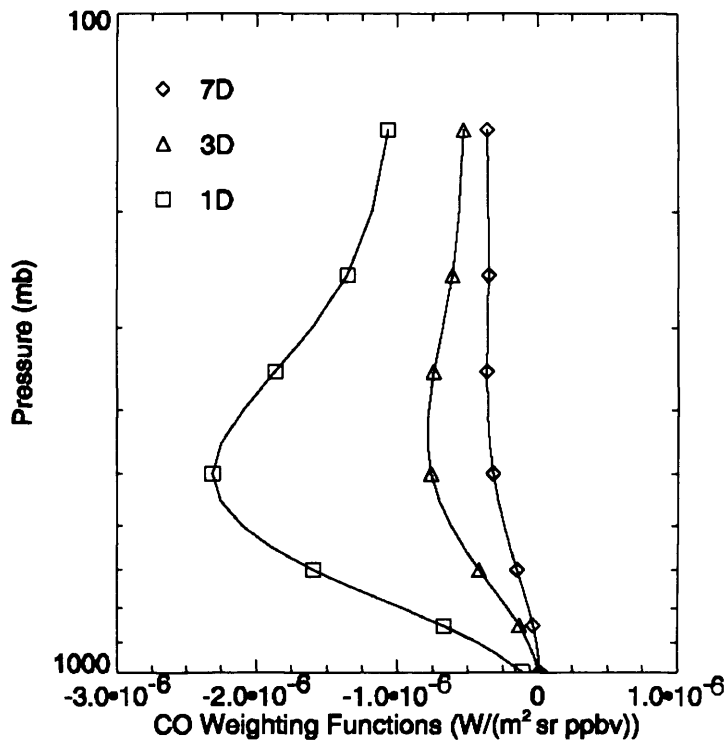


Figure 2.10: Typical weighting functions for the MOPITT thermal band D signals used in operational retrievals taken from Deeter *et al.*, 2003.

2.4.3.2.3 MOPITT *a priori*

The MOPITT radiances themselves are not sufficient to uniquely determine the atmospheric vertical distributions of CO. Therefore, the inversions must be constrained with *a priori* information about the concentrations and variability of CO in the atmosphere. Operational MOPITT retrievals use a fixed global *a priori* profile for all CO retrievals. This profile and its uncertainties can be seen in Figure 2.11. A fixed *a priori* has been chosen rather than one which varies in space and/or time for three reasons. First, the use of a spatially varying *a priori* would produce corresponding spatial features in the retrieved

profiles which would not be associated with the MOPITT measured radiances. Second, as the *a priori* becomes more specific, the *a priori* variances and covariances would decrease and in the retrieval scheme used this would reduce the relative weight given to the measured radiances. The final reason is a practical one, the use of a fixed *a priori* covariance matrix simplifies the averaging kernel calculations.

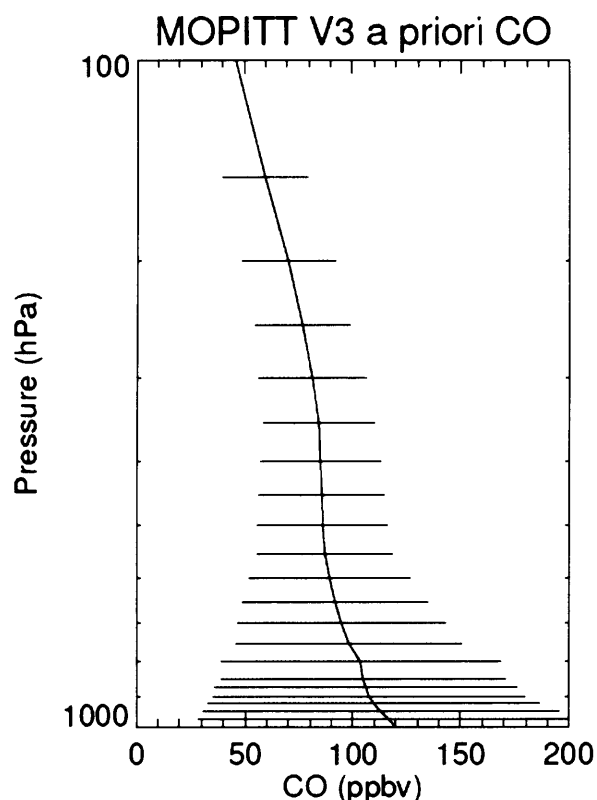


Figure 2.11: The MOPITT *a priori* profile and uncertainties (the square root of the diagonal elements of the covariance matrix) used in MOPITT retrievals, taken from Deeter *et al.*, 2003.

The MOPITT *a priori* is generated from 525 *in situ* profiles measured by aircraft during eight field campaigns (TROPOZ-II, STRATOZ-III, TRACE-A, PEMWEST-A, PEMWEST-B, PEMTROP-A, ABLE-3A and ABLE-3B) and from two fixed sites (Carr, Colorado and Cape Grim, Australia). Typically these profiles extend from the surface to approximately 400 mb. The profiles are then extended to cover the higher MOPITT levels with monthly climatological data from the chemistry transport model MOZART [Hauglustaine *et al.*, 1998].

The *a priori* value of the surface temperature is interpolated from NCEP reanalysis at each pixel. The longwave surface emissivity is obtained from a surface emissivity database [Wilber *et al.*, 1999] coupled to a geographical database of surface types [Belward and Loveland, 1996].

2.4.3.2.4 Operational MOPITT Averaging Kernels

Figure 2.11 shows example averaging kernels for MOPITT retrievals conducted at night over the central Pacific. Ideal averaging kernels would have a peak of one at the required altitude and are zero at all others, and good averaging kernels have elements that sum to one. It can be seen that operational MOPITT kernels are far from ideal. The averaging kernel for each retrieval level does not necessarily peak at the desired altitude, for example the surface, 850 and 700 mb averaging kernels show sensitivity to all seven levels and peak at 500 mb in this case. The 500 mb kernel does indeed peak at 500 mb and the 350, 250 and 150 mb kernels show greatest sensitivity in the upper troposphere as desired. The problem is that all seven averaging kernels are rather broad and overlap with each other and this indicates that the seven retrieval levels are not generally independent, leading to lower vertical resolution, typically MOPITT is able only to distinguish between upper and lower tropospheric CO levels. This is partially due to the fact that the number of retrieval levels is greater than the number of CO sensitive signals used in the retrieval [Deeter *et al.*, 2003]. The correlation between the lower retrieval levels can be traced to the low sensitivity of all three thermal channel difference signals to CO in the boundary layer as indicated by the weighting functions shown in Figure 2.10. This implies that CO at higher levels heavily influences the retrieved values at these lower levels.

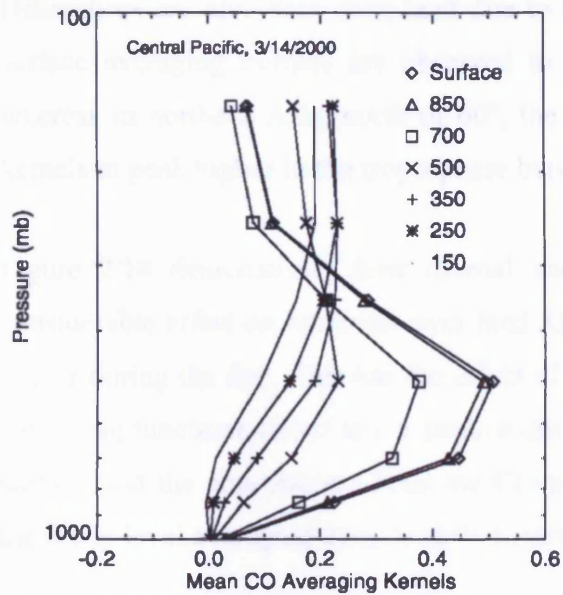


Figure 2.12: Mean MOPITT retrieval averaging kernels obtained by averaging all night time kernels over the central pacific ocean on March 14, 2000. Taken from Deeter *et al.*, 2003.

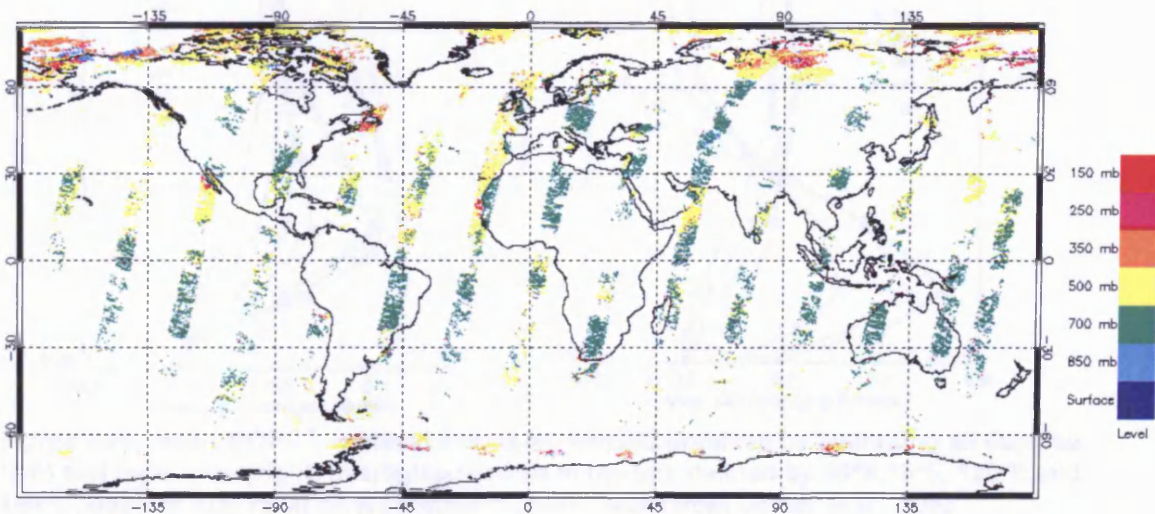


Figure 2.13: Map showing the altitude at which the MOPITT surface averaging kernel peaks. The data shown is for MOPITT daytime retrievals on the 14th May 2000.

Figure 2.13 shows a map indicating the altitude at which the MOPITT daytime surface averaging kernel peaks for the 14th May 2000. The figure shows that MOPITT averaging kernels exhibit significant variability this is mostly due to variability of the atmospheric temperature profile, surface temperature and emissivity, and the actual CO profile being measured. Differences between land and ocean scenes are evident with averaging kernels peaking at higher altitudes over the oceans, for example surface averaging kernels for retrievals conducted over northwestern Africa peak at 700 mb whereas those just off the coast, over the North Atlantic, peak at 500 mb, and in some cases as high as 250 mb.

Differences are also seen over land due to different surface properties. For example the surface averaging kernels are observed to peak at 700 mb for much of central Asia, whereas in northern Asia, north of 60°, the presence of snow and ice causes the surface kernels to peak higher in the troposphere between 500 and 250 mb.

Figure 2.14 demonstrates how diurnal variations of surface temperature can have a considerable effect on retrievals over land. Generally the land surface temperature is much higher during the day. This has the effect of shifting the thermal channel difference signal weighting functions closer to the surface due to the increased thermal contrast between the surface and the atmosphere. Thus the CO near the surface becomes more detectable and the lower level averaging kernels shift downwards.

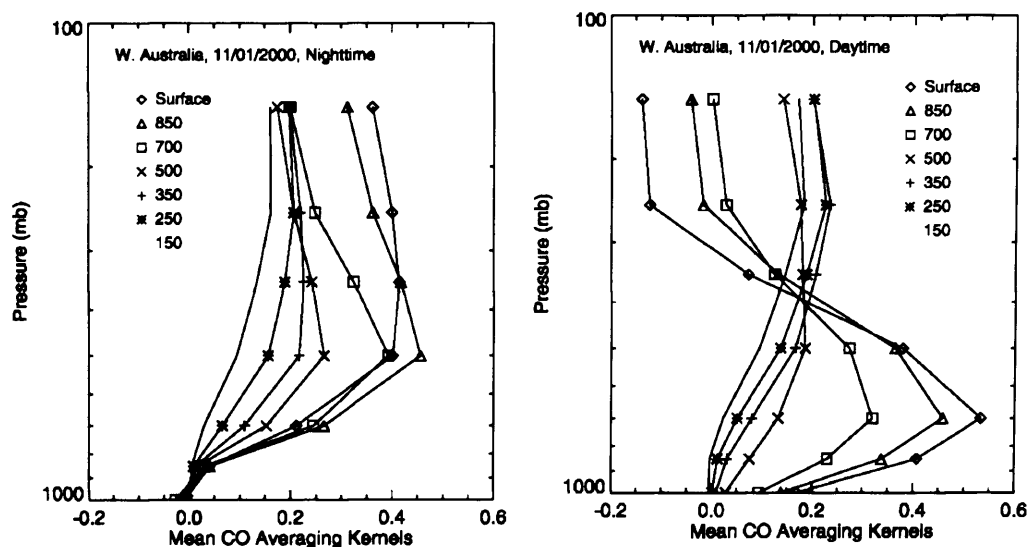


Figure 2.14: Mean MOPITT retrieval averaging kernels obtained by averaging all daytime (left) and night time (right) averaging kernels in the box defined by 30°S, 15°S, 120°E and 140°E (western Australia) on November 1, 2000. Taken from Deeter *et al.*, 2003

The diurnal variability of the averaging kernels should be a maximum over dry, sparsely vegetated regions such as deserts where diurnal variability of surface temperature is greatest, and a minimum over oceans [Deeter *et al.*, 2003].

Seasonal and geographic variability in the atmospheric temperature profile will also lead to averaging kernel variability and this effect is greatest at mid-latitudes and at the poles. Figure 2.15 shows an example of averaging kernels obtained for retrievals over the Canadian Plains in November 2000. The weaker temperature profile gradient and the low surface temperature have caused the averaging kernels to become less distinct. Thus, at

higher latitudes the vertical resolution of MOPITT CO retrievals will generally be lower over the winter hemisphere than the summer hemisphere, particularly over land [Deeter *et al.*, 2003].

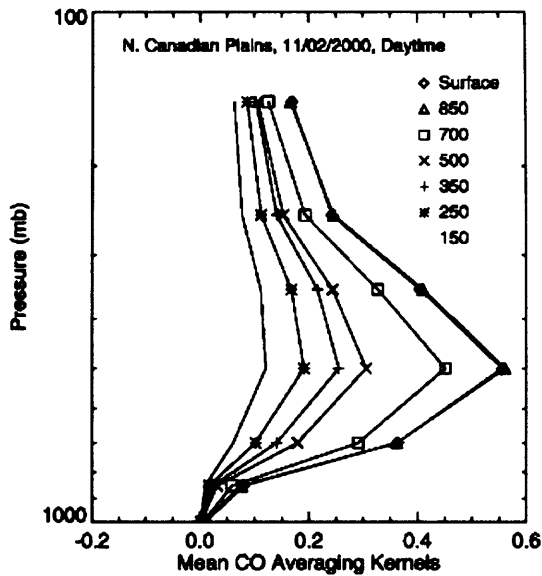


Figure 2.15: Mean MOPITT daytime averaging kernels for the North-western Canadian plains on November 2nd 2000. Taken from Deeter *et al.*, 2003.

Whenever MOPITT data are used, the averaging kernels must be taken into account, especially if the data are to be compared to model or *in situ* data. The averaging kernel variations described above mean that it is not possible to use fixed averaging kernels when using MOPITT data and that the averaging kernel specific to each retrieved profile should be used.

2.4.4 Cloud Detection for MOPITT

Many cloud detection methods make use of spectral information to determine if a scene is cloudy or not, because of the limited number of spectral channels available to MOPITT it is not possible to use such techniques. Instead, MOPITT cloud detection uses a thermal threshold method called MOPCLD which is described in detail by Warner *et al.*, [2001]. Generally clouds are characterised as being colder than the planet surface. Temperature differences between clear and cloudy scenes will show up in the thermal channel average signals and these may be used to infer the presence of clouds. Observed radiances from one of the thermal channels (1A) are compared with forward model calculated clear sky radiances and the ratio of the two ($R_{\text{observed}}/R_{\text{calculated}}$) found. The threshold used to define

the presence of clouds is $R_{\text{observed}}/R_{\text{calculated}} \leq 0.955$; this threshold is only used for latitudes within 65° North and South to avoid complications owing to temperature inversions and snow and ice coverage [Warner *et al.*, 2001]. The MOPITT solar channels should also provide information on clouds due to the increased solar reflectance they produce, however at this time they are not used in the detection process as a detailed study of the calibration of these channels is still underway.

In order to improve MOPITT cloud detection and to extend the MOPITT coverage beyond 65° North and South the MODIS (MODerate-resolution Imaging Spectroradiometer) cloud mask is also used to locate cloudy MOPITT pixels. Both the MOPITT and MODIS instruments are aboard the same satellite platform, the MODIS swaths are more than twice the width of those of MOPITT and therefore provide complete overlap with MOPITT measurements. The MODIS cloud mask has a spatial resolution of 1x1 km and therefore each MOPITT pixel is collocated with approximately 484 MODIS pixels.

Both MOPCLD and the MODIS cloud mask are combined in the MOPITT cloud detection algorithm. A MOPITT pixel is considered clear when both MODIS and MOPCLD indicate it is clear and when there is only low cloud in the MOPITT field of view, since low cloud doesn't affect the CO retrieval, owing to the low sensitivity of MOPITT to the boundary layer. A MOPITT pixel determined to be clear by use of the MODIS cloud mask means that there is less than 5% cloud in that pixel. If MODIS determines a pixel to be cloudy and MOPCLD indicates clear, unless the cloud is low cloud, then the MODIS cloud flagging overrides the MOPCLD result and the pixel is determined to be cloudy and no retrieval is performed. Table 2.2 shows the possible combinations of the two detection schemes which lead to a clear pixel determination, also included is the corresponding cloud flag which can be found in the MOPITT level 2 data file. The use of the MODIS cloud mask means that the MOPITT coverage is extended past 65° North and South, but only the MODIS cloud mask is used at latitudes higher than 65°. In regions where the MODIS cloud mask is not available then only MOPCLD is used.

In the current retrieval scheme, only cloud-free pixels are included, and retrievals are not performed on cloudy pixels.

Flag	MOPCLD	MODIS	Cloudy/Clear
1	Clear	Not available	Clear
2	Clear	Clear	Clear
3	Cloudy	Clear	Clear
4	Clear	Cloudy (low cloud)	Clear
5	Polar Regions (not Used)	Clear	Clear

Table 2.2: MOPCLD and MODIS cloud decisions leading to a MOPITT pixel being classified as clear.

2.5 MOPITT Data

As previously stated, MOPITT CO profile data is provided on 7 levels starting at the surface and extending up to 150 mb with a horizontal resolution of 22 by 22 km. The vertical resolution of MOPITT data is highly variable and is intrinsically linked to the retrieval averaging kernels, but in general, MOPITT is able to provide only two pieces of independent information on the vertical structure of CO. MOPITT coverage extends to ± 80 degrees latitude but data at latitudes greater than 65 degrees should be treated with care as only the MODIS cloud mask is used for cloud detection and problems with ice and snow cover may affect the MOPITT retrieval process. In the current operational retrieval scheme, retrievals are performed only on pixels which are determined to be either cloud free or have low cloud as detected by MODIS, no attempt at cloud clearing is made.

MOPITT data are provided in EOS-HDF format and is freely available for download from the NASA Langley DAAC via the world wide web (http://eosweb.larc.nasa.gov/PRODOCS/mopitt/table_mopitt.html). The data file contains MOPITT CO profile and total column values and errors as well as all the information required to construct the averaging kernel for each profile.

2.5.1 Errors on retrieved MOPITT CO Profiles

The uncertainties on MOPITT retrieved profiles depend on smoothing error, model parameter error, forward model error, and error due to instrument noise [Rodgers, 1990]. These uncertainties are represented by the square root of the diagonal elements of the retrieval covariance matrix, and are provided within the MOPITT data file for each retrieved profile. Table 2.3 shows global means and standard deviations of reported MOPITT errors for all retrieved profiles obtained on the 1st May 2000, obtained from the MOPITT level 2 data product. The errors are largest in the lower troposphere, where the MOPITT measurements are least sensitive, and decrease with increasing altitude. The errors also exhibit large temporal and spatial variability, this is because of changes in the instrument sensitivity as discussed in Section 2.4.3.2.4. These errors suggest that MOPITT CO profile data are more representative of the real atmosphere in the upper troposphere (above 500 mb) than in the lower troposphere. MOPITT CO profile data below 500 mb should be treated with care and wherever possible data from other independent sources should be used in order to assess the validity of MOPITT retrieved concentrations, particularly at or near the surface.

Despite the seemingly large errors on lower level retrievals, the errors for all levels are still lower than the corresponding *a priori* uncertainties (see Section 2.4.3.2.3). This means that the MOPITT retrieved CO profiles are able to provide new and improved information about CO in the troposphere, over that which is currently available.

Pressure (mb)	Global Mean Error (%)
'Surface'	69.4 (13.3)
850	37.6 (9.4)
700	25.9 (6.7)
500	17.4 (3.5)
350	13.0 (3.6)
250	11.8 (3.1)
150	13.9 (2.0)

Table 2.3: Global mean errors for MOPITT retrieved CO profiles obtained on 1st May 2000. The numbers in parentheses denote the standard deviation.

2.5.2 Validation of MOPITT CO Profiles

The validation of remotely sensed satellite data is important for providing an assessment of the satellite retrievals which may be used to improve retrieval biases in future data versions. Validation also provides a means by which to characterise the satellite measurements and examine the usability of retrieved profiles in further activities such as pollution monitoring and climate change studies. Correlative measurements made using *in situ* techniques such as aircraft and ground stations are an important part of the validation exercise and provide the opportunity to characterise the retrieved satellite profiles with those made by sampling the real atmosphere. The MOPITT validation program consists of comparing MOPITT data to those recorded by both ground stations and aircraft in a set of carefully organised validation campaigns designed to sample profiles coincident with MOPITT overpasses. The validation also extends to data from any other campaigns and field measurements available which although not designed to coincide with MOPITT overpasses do fall within a suitable spatial and temporal scale for comparison.

The validation of MOPITT CO profiles and total columns is currently underway and the first results were reported by Emmons *et al.* [2004]. The MOPITT CO retrievals have been validated using *in situ* CO measurements from aircraft. These measurements were obtained as part of a regular sampling program coordinated by NOAA CMDL, as well as coincident research experiments. In total, 69 profiles were sampled during the Phase 1 (March 2000–May 2001) of MOPITT measurements [Emmons *et al.*, 2004]. The measurements were recorded over North and South America, Africa and the North and South Pacific Oceans. The results of this validation exercise can be found in Table 2.4. For Phase 1, on average the bias is positive throughout the troposphere with slightly larger differences in the lower troposphere than the upper levels. The large standard deviation of these mean biases, particularly in the lower troposphere (20 ppbv, 20%), indicates that the biases exhibit large variability. During both Phase 1 and Phase 2, larger biases are seen in clean environments, such as the South Pacific [Emmons *et al.*, 2004]. At the time of this thesis, this work was ongoing but clearly there are gaps in the geographic coverage of the validation measurements to date, such as the North and South Atlantic and Europe.

Level	Absolute Bias ^a	Percentage Bias
Surface	5.7 ± 20.6	8.1 ± 21.5
850 hPa	4.1 ± 18.8	8.1 ± 22.2
700 hPa	4.2 ± 14.5	6.5 ± 16.1
500 hPa	2.7 ± 9.8	3.8 ± 10.1
350 hPa	1.7 ± 11.9	2.6 ± 12.3
250 hPa	0.7 ± 11.5	1.7 ± 13.0
150 hPa	-0.8 ± 10.5	-0.2 ± 15.8
Column	0.7 ± 1.9	4.9 ± 10.8

Table 2.4: MOPITT validation results showing the absolute and percentage biases (Mean and Standard Deviation) for each MOPITT retrieval level and total column for phase 1 MOPITT data, taken from Emmons *et al.* [2004].

2.6 MOPITT Instrument Status

In May 2001 the MOPITT instrument suffered a failure of one of its coolers. This resulted in the loss of half of the instrument channels (Channels 1-4). The periods before and after the failure are referred to as phase 1 and phase 2 respectively. As described in section 2.4.3.2.2 the signals from channels 1D, 3D, 7D and 7A were used in phase 1 retrievals of CO profiles. After the failures, significant work was done to understand and correct for the bias found in channel 5D radiances and an empirical correction factor was found. Operational CO profile retrievals for phase 2 data use the signals from channels 5A, 5D and 7D and although this leads to a degradation in vertical resolution the Phase 1 and Phase 2 data are now considered by the MOPITT team to be of comparable quality.

2.7 Summary

The MOPITT instrument was launched aboard the EOS Terra satellite in December 1999 and became operational in March 2000. MOPITT is a nadir viewing infrared instrument which uses a combination of pressure and length modulated radiometers to obtain global measurements of column and profile amounts of carbon monoxide and methane. MOPITT CO profile data is provided on 7 levels extending from the surface up to 150 mb with a horizontal resolution of 22 by 22 km, which along with a swath width of approximately 600 km allows MOPITT to obtain global coverage approximately every 3 days. The MOPITT vertical resolution is intrinsically linked to the retrieval averaging kernels for

each measured profile which are themselves highly variable in both space and time and typically MOPITT is only able to obtain two pieces of independent vertical information from each measurement, providing only lower and upper tropospheric CO concentrations. The errors on MOPITT retrieved CO profiles are such that, they are able to provide new and improved information about CO in the troposphere, over that which is currently available.

The results of the MOPITT validation campaign show that on average, MOPITT exhibits a positive bias throughout the troposphere with slightly larger differences in the lower troposphere than the upper levels. The large standard deviation of these mean biases, particularly in the lower troposphere (20 ppbv, 20%), indicates that the biases exhibit significant variability. During both Phase 1 and Phase 2, larger biases are seen in clean environments, such as the South Pacific [Emmons *et al.*, 2004]. At the time of this thesis, this work was ongoing but clearly there are gaps in the geographic coverage of the validation measurements to date, such as the North and South Atlantic and Europe.

One aim of this thesis is to characterise MOPITT CO profile measurements, and assess the ability of the instrument to obtain vertical information on CO under the many different situations encountered in the atmosphere. Owing to the failure of MOPITT channels 1-4 in May 2001, and the resulting differences in the characteristics of CO profile measurements made before (phase 1) and after (phase 2) the failure, only phase 1 data (April 2000-April 2001) will be used for this study as these measurements contain a greater degree of vertical information.

3. Characteristics of MOPITT CO Profiles

Before satellite measurements such as MOPITT CO profiles can be used for atmospheric research, they must first be characterised and understood. In this chapter, profiles of CO retrieved from the MOPITT instrument measurements are compared to both *in situ* and model data in order to determine the characteristics of MOPITT profile measurements in varying regimes. The data are compared on both monthly averaged and daily timescales using both global datasets and single profile case studies. For this study, the ACTO aircraft campaign has been chosen as this campaign covers the UK and the North Atlantic, two regions which are absent from the current MOPITT validation exercise. Although the flights were not designed to coincide with MOPITT overpasses, the measurement region does overlap a MOPITT measurement swath on two of the flights. For the model comparisons the TOMCAT model is used. This model was chosen because TOMCAT is a full global chemistry transport model that is used by the UK community to investigate and understand chemical and dynamical processes in the troposphere, and in the planning and direction of research aircraft campaigns.

Simulations are also performed using operational MOPITT averaging kernels to test the ability of the MOPITT instrument to measure enhanced vertical layers of CO.

3.1 Comparing Satellite Data with *in situ* and Model Data

Atmospheric measurements made by remote sensing satellite instruments such as MOPITT are fundamentally different to those of *in situ* instruments and to the output of models. There are two main differences which need to be considered before comparisons of the different datasets can be made. The first is vertical resolution. In general the vertical resolution of an *in situ* measurement or model output can be approximated as a delta function whereas for a remote sensing instrument the retrieval is sensitive to some non-uniformly weighted layer of the atmosphere. The second, is the influence of *a priori* information in the maximum likelihood retrieval scheme which is used in the MOPITT data processing (see Section 2.4.3.2).

The retrieval averaging kernel matrix intrinsically accounts for the finite vertical resolution inherent of the satellite measurement and the effects of *a priori* information in the retrieval. The rows of \mathbf{A} define the averaging kernels for each level in the retrieved profile.

The averaging kernel matrix may therefore be used to transform the model/*in situ* profile into a form which can be directly compared with the MOPITT profile by degrading its vertical resolution and giving it the same dependence on *a-priori* information as the retrieved MOPITT profile. Each MOPITT retrieved profile has its own averaging kernel which can be highly variable as discussed in Section 2.4.3.2.4. Each comparison between a MOPITT profile and a model or *in situ* CO profile, therefore requires the appropriate averaging kernel to be applied to the model/*in situ* profile.

The MOPITT averaging kernel is applied to the model/*in situ* profile through the linear transformation [Emmons *et al.*, 2004]

$$\mathbf{x}_{\text{final}} \equiv \mathbf{x}_a + \mathbf{A}(\mathbf{x}_{\text{model}} - \mathbf{x}_a) \quad (3.1)$$

where $\mathbf{x}_{\text{model}}$ is the original model/*in situ* profile and $\mathbf{x}_{\text{final}}$ is the model/*in-situ* profile with the averaging kernel applied which can now be compared directly with the MOPITT retrieved profile. The profile $\mathbf{x}_{\text{final}}$ represents what the MOPITT instrument would have observed had $\mathbf{x}_{\text{model}}$ been the true atmospheric profile.

3.2 Comparisons of MOPITT CO with *in situ* Aircraft Data

3.2.1 The ACTO Campaign

The ACTO (Atmospheric Chemistry and Transport of Ozone) campaign was a NERC UTLS-funded project, whose main objective was to study the budget of ozone in the upper troposphere. The campaign was based around the UKMO C-130 Hercules aircraft to enable measurements of carbon monoxide, ozone, NO_y species, water vapour, formaldehyde, hydrogen peroxide, peroxy radicals and a range of hydrocarbons in the mid and upper troposphere. The campaign took place between the 7th and the 19th of May 2000 during which the aircraft made flights over the Atlantic, the west of Scotland and over the UK mainland. Owing to instrument problems, carbon monoxide data was only available for two and a half of the ACTO flights. Data for the flights on the 14th (flight A755) and

3.2.2 MOPITT – ACTO Profile Comparison Methodology

In order to compare ACTO CO with that of the MOPITT instrument an average CO profile for each ACTO flight was constructed. These were achieved by averaging the CO data into ten 100 mb wide pressure bins centred at pressures from 1000 mb up to 100 mb along the whole of the flight track. This is illustrated in Figure 3.3 and Figure 3.4 which show the CO time series for the two flights colour coded by the altitude bin into which the measurements fall. A mean profile for each flight was constructed by averaging all measurements of the same colour (altitude bin).

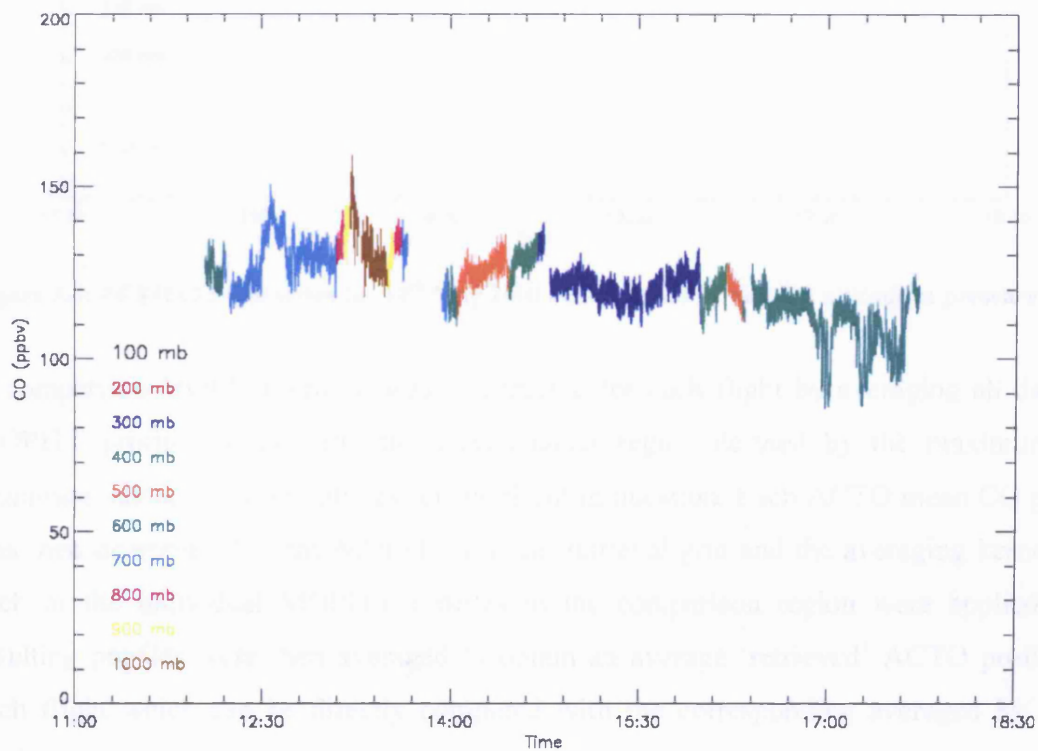


Figure 3.3: ACTO CO time series for 14th May 2000 colour coded by aircraft altitude in pressure units of mb.

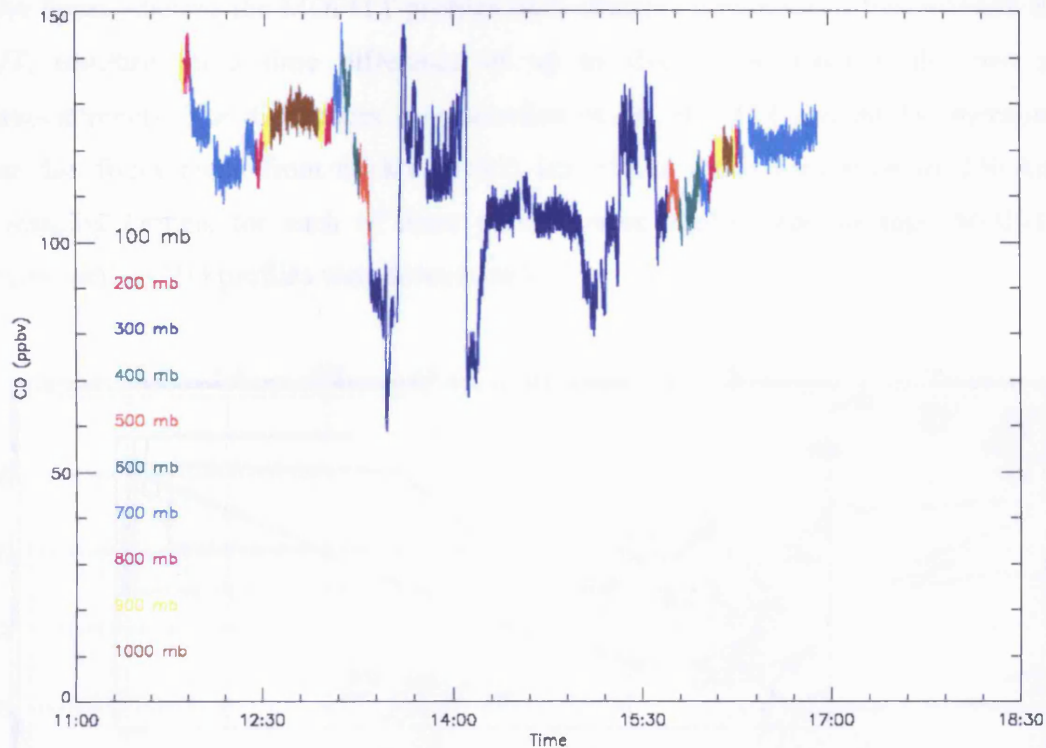


Figure 3.4: ACTO CO timeseries for 19th May 2000 colour coded by aircraft altitude in pressure units

A comparison MOPITT profile was constructed for each flight by averaging all daytime MOPITT profiles which fall into a rectangular region defined by the maximum and minimum latitudes and longitudes for the flight in question. Each ACTO mean CO profile was then interpolated to the MOPITT vertical retrieval grid and the averaging kernels for each of the individual MOPITT profiles in the comparison region were applied. The resulting profiles were then averaged to obtain an average ‘retrieved’ ACTO profile for each flight which can be directly compared with the corresponding averaged MOPITT profile.

3.2.3 MOPITT – ACTO Profile Comparison Results

3.2.3.1 Flight A755

On flight A755 the aircraft took off from Prestwick on the west coast of Scotland and flew north-west over the Atlantic. Figure 3.5 shows the aircraft flight track and its corresponding bounding box used to select MOPITT profiles for comparison. On this occasion, there were ten coincident MOPITT profiles. The aircraft measurements were made continuously from 11:40 UT until 16:35 UT, covering a time window of more than

five hours whereas the MOPITT profiles were obtained within just a few seconds at 11:48 UT, resulting in a time difference of up to five hours between the two sets of measurements. The differences in collocation of the MOPITT and ACTO measurements for this flight range from 60 km to 425 km with a mean separation of 230 km. The averaging kernels for each of these profiles were applied and average MOPITT and ‘retrieved’ ACTO profiles were constructed.

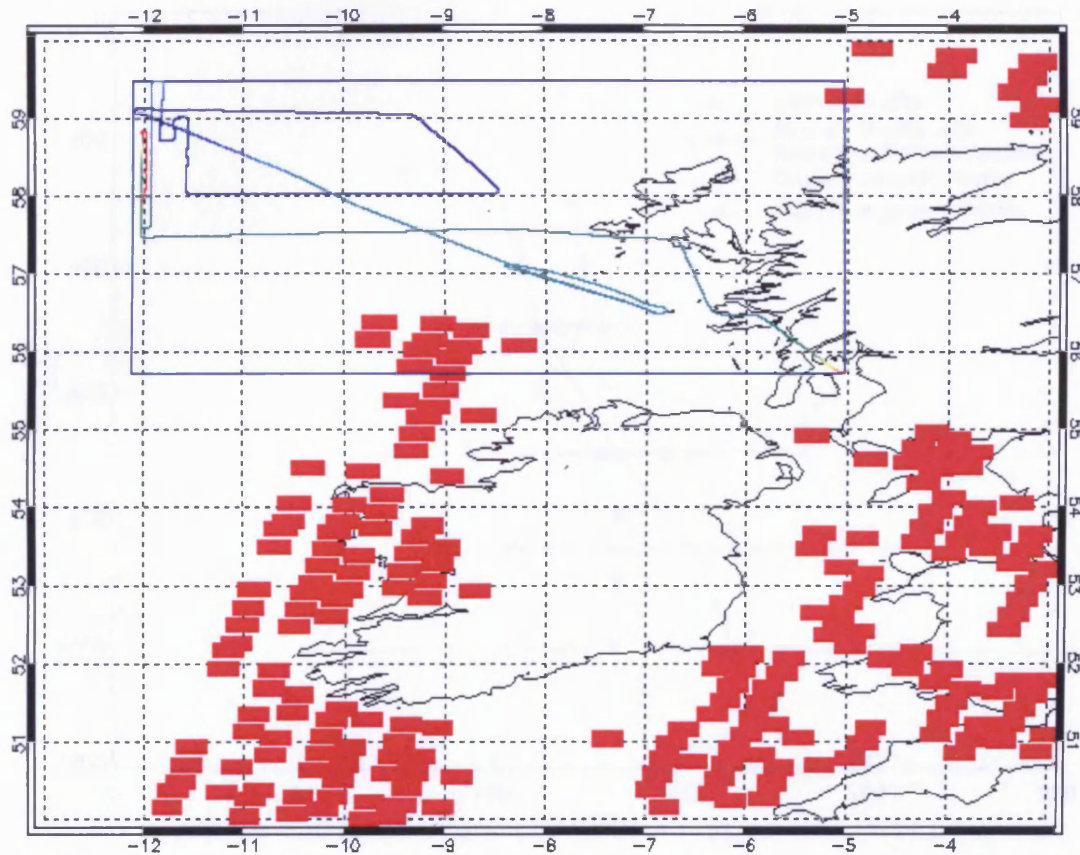


Figure 3.5: Map showing the location of MOPITT pixels (red) and the ACTO flight region (blue box) for 14th May 2000

Figure 3.6 shows the results of the profile comparison. Before application of the MOPITT averaging kernels, the aircraft data (dashed blue line) apparently indicate lower levels of CO than MOPITT (solid red line) in the lower troposphere and the opposite is true in the upper troposphere. Although the two instruments agree within errors on the magnitude of the CO concentrations, the shape of the two profiles are quite different. The MOPITT profile is rather flat and shows a steady decrease in CO concentrations with increasing altitude from 170 ppbv at the surface to approximately 60 ppbv at 150 mb. The aircraft measurements show a smaller decrease with altitude and a small pocket of cleaner air

between 700 and 500 mb is evident. After applying the MOPITT averaging kernels to the aircraft profile the comparison is excellent. The aircraft profile (solid blue line) now resembles the MOPITT profile much more closely and the two profiles are similar in both shape and magnitude. The feature observed between 500 and 700 mb in the original aircraft profile is no longer significant in the comparison because of the lower vertical resolution of the MOPITT instrument.

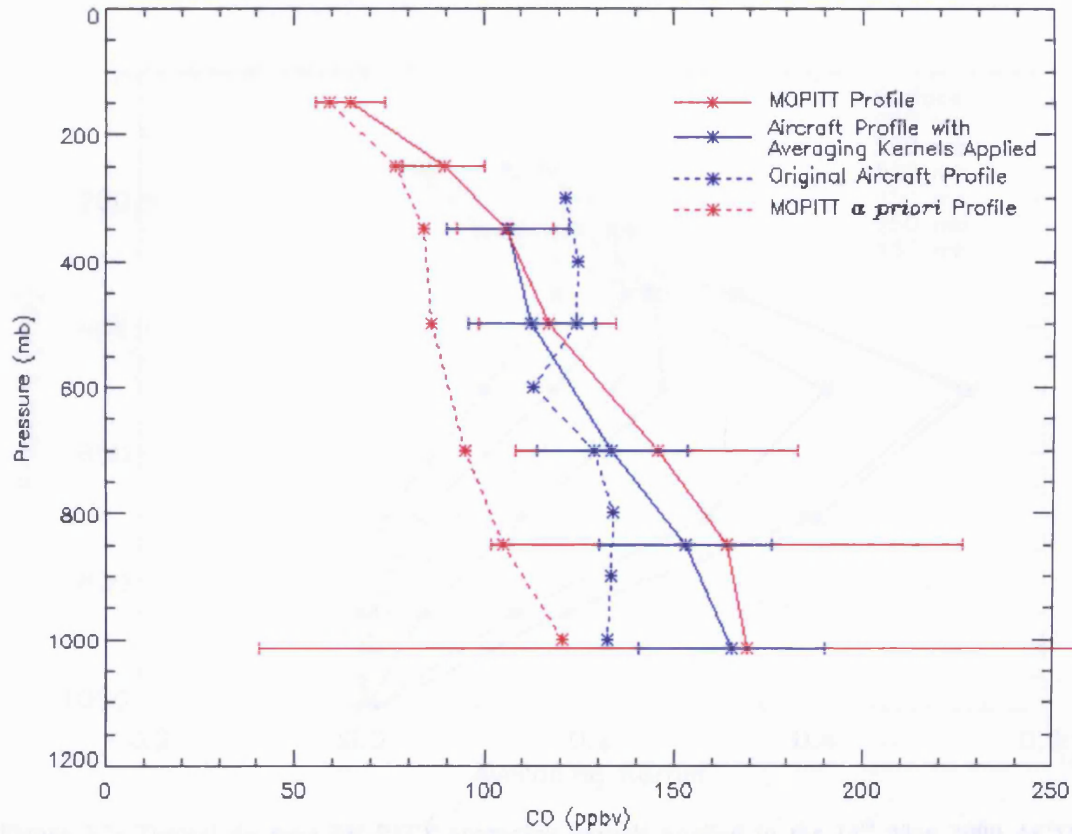


Figure 3.6: Averaged MOPITT vs. ACTO CO profiles for coincidence on the 14th May 2000, the time difference between MOPITT and ACTO measurements was up to five hours. The error bars represent the mean reported errors for each instrument, which in the case of MOPITT correspond to the mean retrieval uncertainty at each level.

Figure 3.7 shows a typical example of averaging kernels that have been applied to the aircraft data. The averaging kernels show that there are essentially only 2 pieces of independent information which contribute to the MOPITT profile, with the kernels for the lower levels (surface up to 500 mb) all peaking at 500 mb and those for the upper levels peaking at 350 mb. All of the averaging kernels are quite broad indicating that the lower profile levels are sensitive to the whole of the lower to mid troposphere (850-250 mb) with

greatest sensitivity at 500 mb, and the upper levels are sensitive to the mid to upper troposphere between 500 and 150 mb with sensitivities peaking at 350 mb. This indicates that MOPITT is only really distinguishing between lower and upper tropospheric CO levels and could explain the flat appearance of the profile. This would also explain why when the averaging kernels are applied to the aircraft data, the profile is smoothed out and the cleaner region between 500 and 700 mb evident in the original aircraft profile disappears.

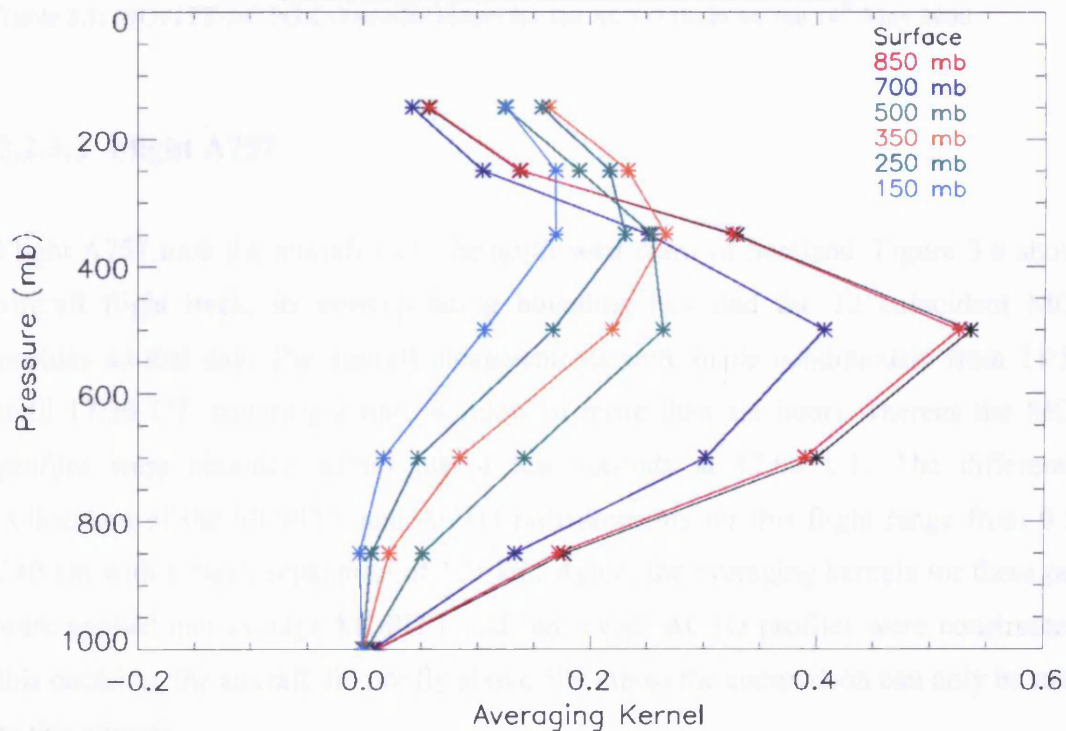


Figure 3.7: Typical daytime MOPITT averaging kernels applied to the 14th May 2000 ACTO CO profile.

Table 3.1 shows the bias between the MOPITT and ‘retrieved’ ACTO profiles as a function of altitude. The MOPITT CO levels show a small positive bias (less than 10 %) throughout much of the profile with a very small negative bias (-0.53 %) at 350 mb. Unfortunately, the aircraft did not fly above 350 mb so it is unclear if this effect is systematic.

Pressure (mb)	% Bias (MOPITT-ACTO)
1000 (Surface)	2.54
850	6.9
700	8.3
500	3.6
350	-0.53

Table 3.1: MOPITT-ACTO CO profile biases for the ACTO flight on the 14th May 2000

3.2.3.2 Flight A757

Flight A757 took the aircraft over the north-west coast of Scotland. Figure 3.8 shows the aircraft flight track, its corresponding bounding box and the 12 coincident MOPITT profiles on that day. The aircraft measurements were made continuously from 11:52 UT until 17:30 UT, covering a time window of more than six hours whereas the MOPITT profiles were obtained within just a few seconds at 12:06 UT. The differences in collocation of the MOPITT and ACTO measurements for this flight range from 0 km to 240 km with a mean separation of 125 km. Again, the averaging kernels for these profiles were applied and average MOPITT and ‘retrieved’ ACTO profiles were constructed. On this occasion, the aircraft did not fly above 500 mb so the comparison can only be made up to this altitude.

The results of this comparison are shown in Figure 3.9. Before the application of MOPITT averaging kernels the comparison is very similar to the previous case with the aircraft apparently showing lower levels than MOPITT in the lower troposphere and higher values in the upper troposphere. Again, application of the averaging kernels increases the CO gradient through the troposphere in the equivalent ‘retrieved’ aircraft profile. This can be explained by examining the averaging kernels (Figure 3.10); the kernels are rather broad as information from the lower and upper levels is mixed, enhancing the CO levels in the lower troposphere and diluting them in the upper troposphere, thus smoothing out the profile. The two profiles compare well within the MOPITT errors.

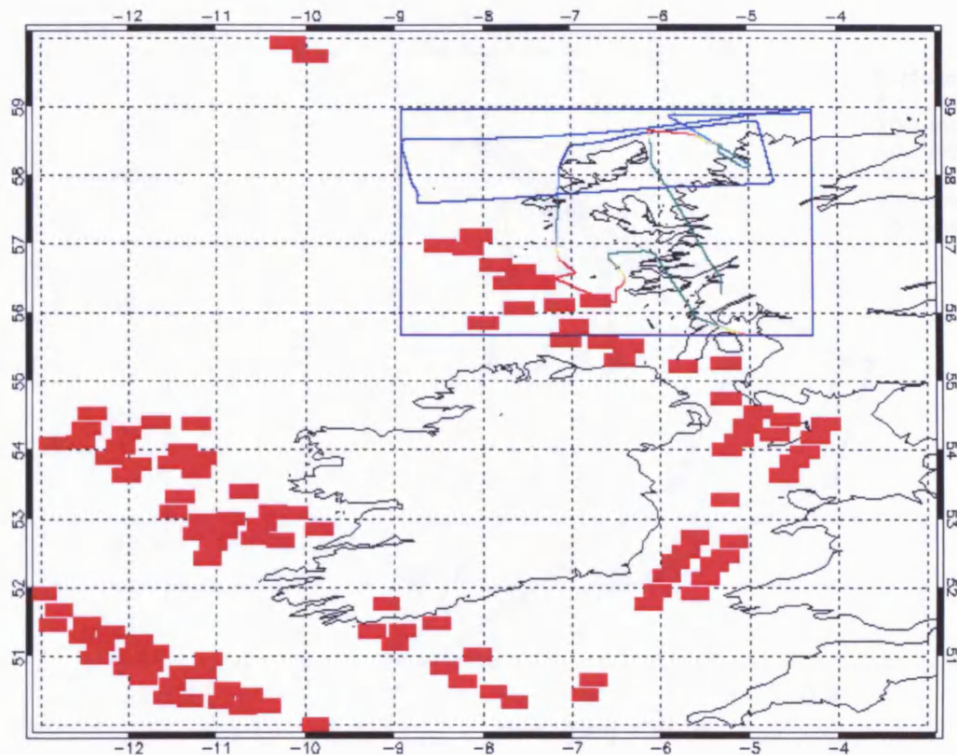


Figure 3.8: Map showing the location of MOPITT pixels (red) and the ACTO flight region (blue box) for 19th May 2000

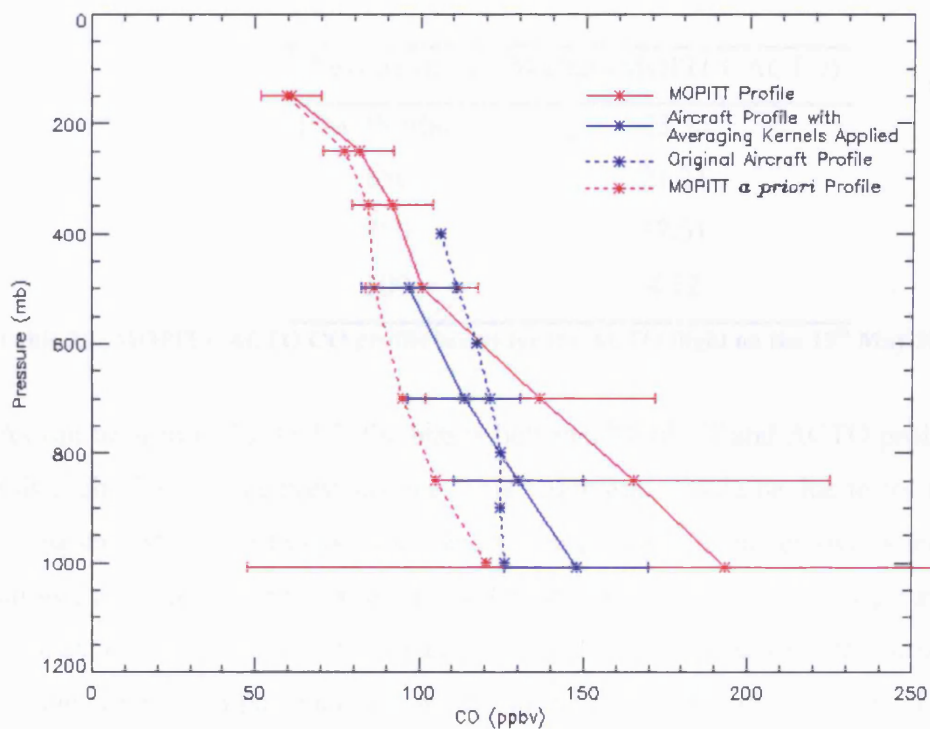


Figure 3.9: Averaged MOPITT vs ACTO CO profiles for coincidence on the 19th May 2000, the time difference between MOPITT and ACTO measurements was up to five hours. The error bars represent the mean reported errors for each instrument, which in the case of MOPITT correspond to the mean retrieval uncertainty at each level.

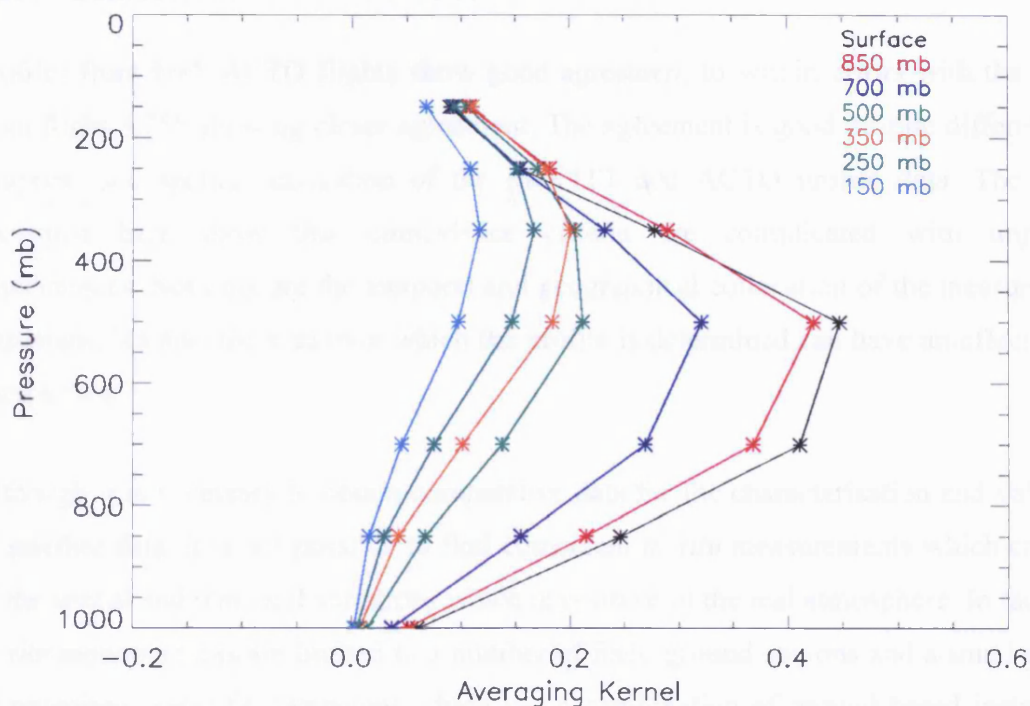


Figure 3.10: Typical daytime MOPITT averaging kernels applied to the 19th May 2000 ACTO CO profile

Pressure (mb)	% Bias (MOPITT-ACTO)
1000 (Surface)	23.55
850	21.21
700	17.01
500	4.12

Table 3.2: MOPITT-ACTO CO profile biases for the ACTO flight on the 19th May 2000

As can be seen in Table 3.2, the biases between MOPITT and ACTO profile are larger for this flight than for the previous one. This observation could be due to the aircraft covering a smaller distance on this occasion and so the profile is averaged over a much smaller area allowing small localised variations in CO concentrations to have a greater affect on the final average. Also, all of the coincident MOPITT pixels fall over the ocean whereas most of the aircraft flight track is over land which could also account for some of the differences.

3.2.4 Conclusions

Profiles from both ACTO flights show good agreement to within errors with the profile from flight A755 showing closer agreement. The agreement is good despite differences in temporal and spatial collocation of the MOPITT and ACTO profile data. The results presented here show that coincidence criteria are complicated with unplanned coincidences. Not only are the temporal and geographical collocation of the measurements important, but also the area over which the profile is determined can have an effect on the comparison.

Although it is necessary to obtain comparative data for the characterisation and validation of satellite data, it is not possible to find coincident *in situ* measurements which cover all of the spatial and temporal variations which may occur in the real atmosphere. In fact, such *in situ* measurements are limited to a number of fixed ground stations and a small number of organised scientific campaigns which use a combination of ground-based instruments and research aircraft flights. The campaigns are infrequent and usually designed to study a particular atmospheric process or region and as such do not cover the wide range of atmospheric conditions encountered by a satellite instrument. Global chemistry transport models are able to provide a more complete picture and, in the absence of appropriate *in situ* data, can be a useful tool for the validation, characterisation and interpretation of satellite data.

3.3 MOPITT – Model Comparisons

3.3.1 The TOMCAT model

The model employed in this study is the tropospheric chemistry transport model, TOMCAT which is a global off-line, Eulerian model [Law *et al.*, 1998]. It has monthly varying surface emissions, based on the IPCC Third Assessment Report [IPCC, 2001], and also aircraft and lightning emissions. Figure 3.19 shows the TOMCAT total CO emissions for May 2000. Large amounts of CO are emitted into the boundary layer over populated and industrial regions of the northern hemisphere such as the United States and Europe. The largest sources for this month appear to be over Asia and Africa where biomass burning produces large amounts of CO at this time of year. The TOMCAT model includes dry deposition, large scale advective transport, subscale convective and boundary layer exchanges, chemical and photochemical transformations including a tropospheric chemistry scheme for NO_x, HO_x, CO and CH₄ and some NMHC chemistry as well as wet scavenging. The model is forced using ECMWF analysed meteorology and has a horizontal resolution of approximately 2.8 x 2.8 degrees. It calculates the distributions and evolution of 41 of the main tropospheric chemical species on 31 levels between the surface and 10 hPa.

Several studies have been conducted to validate the TOMCAT model, most of which concentrate its ability to correctly model tropospheric ozone concentrations. Law *et al.* [1998] carried out a comparison of TOMCAT modelled ozone with data collected by passenger aircraft as part of the Measurement of Ozone by Airbus In-Service Aircraft (MOZAIC) project. The model was found to show good agreement with seasonally averaged data at cruise altitudes in the upper troposphere and with individual profiles obtained during takeoff and landing operations. TOMCAT has also been validated through participation in an intercomparison of several CTMs with two years of MOZAIC data [Law *et al.* 2000]. The performance of TOMCAT was generally good in relation to the other models, although it did tend to overestimate ozone at cruise altitudes in the tropics and mid-latitudes.

Prather *et al.* [2001] compared TOMCAT modelled ozone and CO with several other models, ozonesondes and ground-based observations at various altitudes and latitudes. The TOMCAT model was able to capture the seasonal cycle in observed CO in the tropics and

in the northern mid and high latitudes. However, both TOMCAT and the other models overestimated CO at the remote site of Cape Grim, this suggests that Southern Hemisphere emissions of CO were overestimated in the IPCC recommendations.

More recently, Brunner *et al.* [2003] performed an evaluation of the performance of five chemistry transport models, including TOMCAT, with data obtained by research aircraft. The comparisons show that TOMCAT exhibits too much CO in the lower stratosphere, whereas concentrations in the upper troposphere are too low. The low upper tropospheric CO concentrations are more pronounced at northern mid-latitudes than in the southern hemisphere. Brunner *et al.* [2003] suggest that a likely explanation for this deficiency is that TOMCAT tends to underestimate convective transport and occurring convection is biased towards the tropics.

An example of TOMCAT data can be seen in Figure 3.11 which shows a global map of CO at 681 mb. In this case the data represents a ‘snapshot’ of the state of the TOMCAT model atmosphere at 00:00 UT on 1st May 2000. The hemispheric gradient in CO is evident with Northern Hemisphere concentrations which are on average a factor 3 higher than those in the southern hemisphere. High concentrations are observed over populated source regions in the Northern Hemisphere such as the United States and Europe. Large amounts of CO are also present over biomass burning regions in Africa, South America and East Asia. There is also evidence of CO transport, with high concentrations of CO over the oceans. For example, large amounts of CO are observed stretching across the North Pacific, between 30 and 60 degrees north, from East Asian sources towards the United States. The transport of CO across the Atlantic from the U.S. towards Europe is also evident, with high concentrations observed over Greenland and Iceland.

Figure 3.12 shows an example of a typical TOMCAT CO profile over the UK on the 1st May 2000. The profile shows how over a populated region such as the UK high concentrations of CO are found in the boundary layer where most of the CO is emitted into the atmosphere. The CO concentrations decrease with increasing altitude as vertical mixing occurs between the polluted boundary layer and the cleaner free troposphere. Also evident in this profile is an enhanced layer of CO centred on 400 mb which could be due to the transport of CO rich air from distant sources.

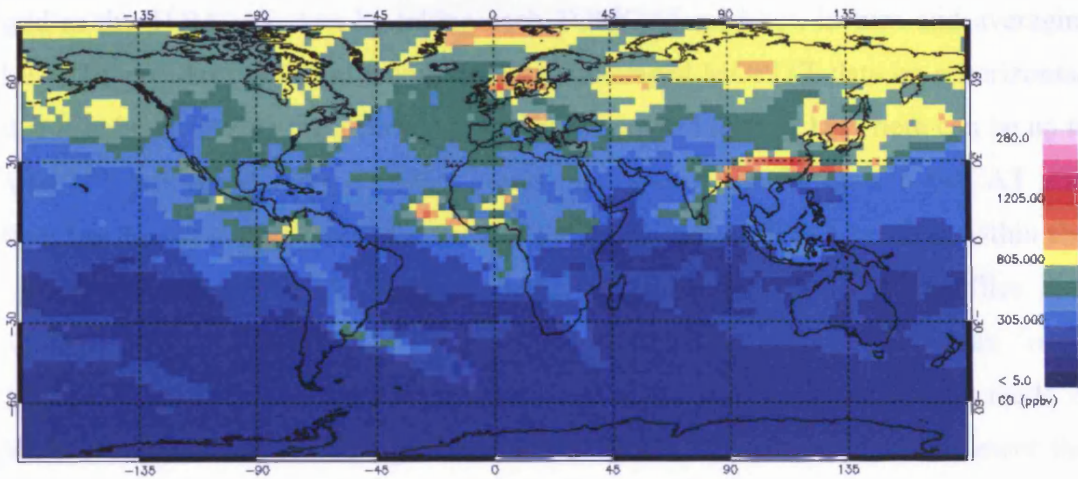


Figure 3.11: Map of TOMCAT global CO at 681 mb at 00:00 UT on 01/05/00

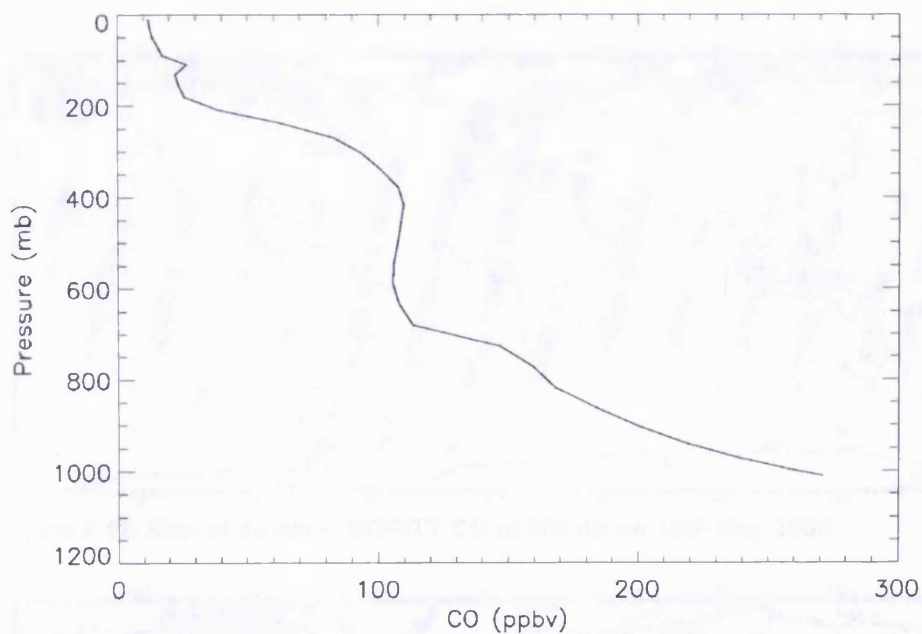


Figure 3.12: TOMCAT CO profile over the UK located at 51.6° N, 0°W at 00:00 UT on 01/05/00

3.3.2 MOPITT – TOMCAT Comparison Methodology

TOMCAT data for the month of May 2000 were made available by Cambridge University for this study. The MOPITT data for the day to be examined is first separated into daytime and night time measurements according to the solar zenith angle reported with each data point (see Figure 3.13 and Figure 3.14). The separation is necessary because of the differing sensitivities of the MOPITT instrument between day and night. Here for profile comparisons only daytime profiles are used. The MOPITT data are averaged onto the same

grid as the TOMCAT data by taking each TOMCAT grid box in turn and averaging the MOPITT profiles contained therein to obtain averaged MOPITT data on a horizontal grid that is coincident with the TOMCAT data as shown in Figure 3.15. There can be up to 200 MOPITT profiles within a TOMCAT grid box. The profile for each TOMCAT grid box then has the averaging kernel for each of the coincident MOPITT profiles within the grid box applied to it. This produces a number of ‘retrieved’ TOMCAT profiles for each original TOMCAT profile. These are then averaged to produce the mean ‘retrieved’ TOMCAT profile which represents the measurement that would have been made by the MOPITT instrument for that grid box if the TOMCAT data were to represent the real atmosphere.

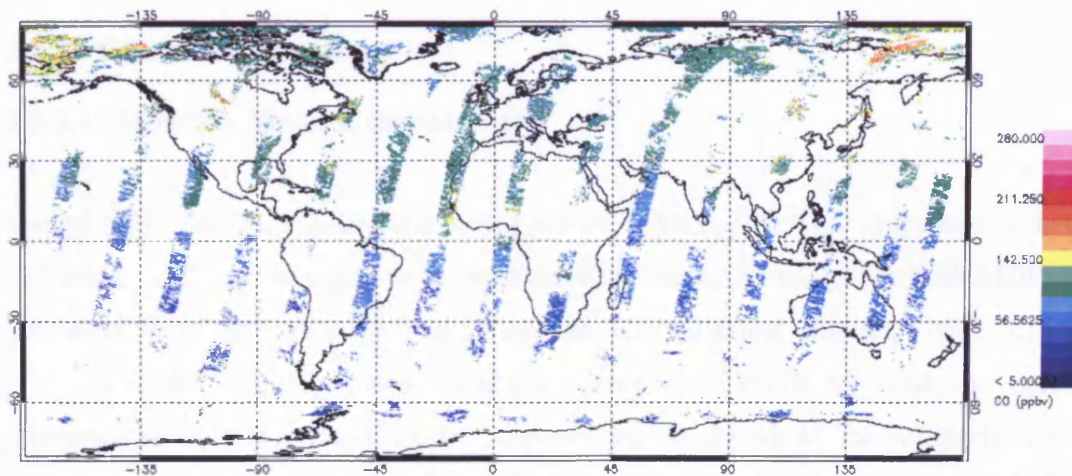


Figure 3.13: Map of daytime MOPITT CO at 500mb on 14th May 2000

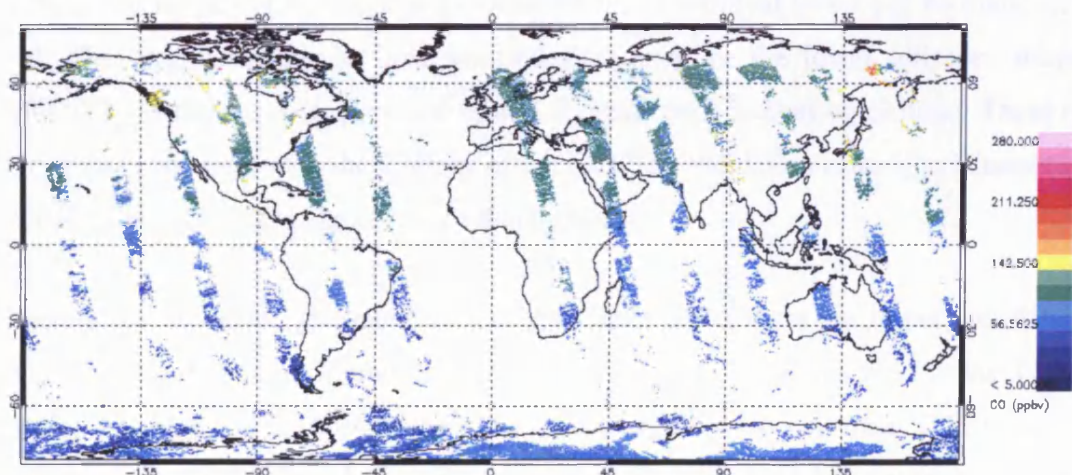


Figure 3.14: Map of night time MOPITT CO at 500mb on 14th May 2000

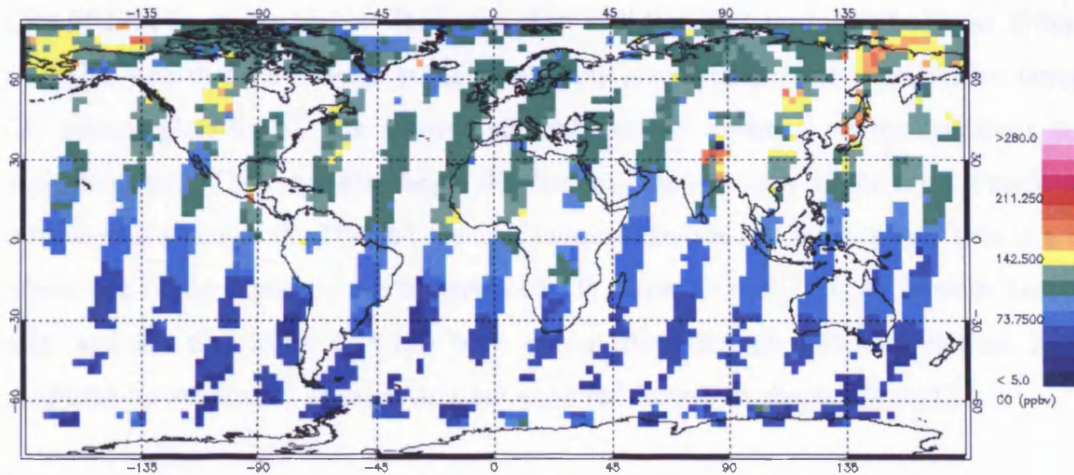


Figure 3.15: Daytime MOPITT data averaged onto TOMCAT coincidence grid at 500mb on 14th May 2000

3.3.3 Global Comparisons

3.3.3.1 Monthly Mean Comparisons

The MOPITT and TOMCAT data for the whole of May 2000 were processed as described in Section 3.3.2 and averaged to produce monthly mean CO values for both MOPITT and ‘retrieved’ TOMCAT as a function of latitude, longitude and altitude. Figure 3.16-Figure 3.18 show the monthly mean MOPITT, ‘retrieved’ TOMCAT and the percentage difference between the two at 700 mb respectively. On the whole, the comparison between the two datasets is rather good. Globally, MOPITT is slightly higher than TOMCAT by 20% at 700 mb; the differences at the other MOPITT retrieval levels can be found in Table 3.3. The largest differences and uncertainties occur in the lower altitudes where the MOPITT instrument is least sensitive, and decrease with increasing altitude. These results are in fact consistent with the findings of the MOPITT validation campaign [Emmons *et al.* 2004], published during the course of this thesis.

Despite the excellent agreement on a global mean scale, there are important differences which are worth noting. Figure 3.19 shows the total CO emissions used in the TOMCAT model for May 2000. The largest differences appear to occur near TOMCAT source regions. For example, excluding Antarctica, where snow and ice cover may affect the MOPITT retrievals, the only locations where the ‘retrieved’ TOMCAT CO levels are higher than those of MOPITT are over a very intense TOMCAT emission in the region of Calcutta and a smaller source region over northeast Columbia. Conversely, over Mexico

City MOPITT reports higher CO levels than TOMCAT of up to 50%. These differences could indicate that the sources in the model may give approximately the correct amount of CO release globally but the relative strengths of the different source locations may be underestimated. There are also larger differences than the mean in the north Pacific region off the west coast of the US and the east coast of Russia and over Japan. This is a region where one might expect to see transport of CO across to the US from Eastern Europe and may indicate that more CO has been transported through this region than has been predicted by the model. These issues are explored further in chapters 4 and 5.

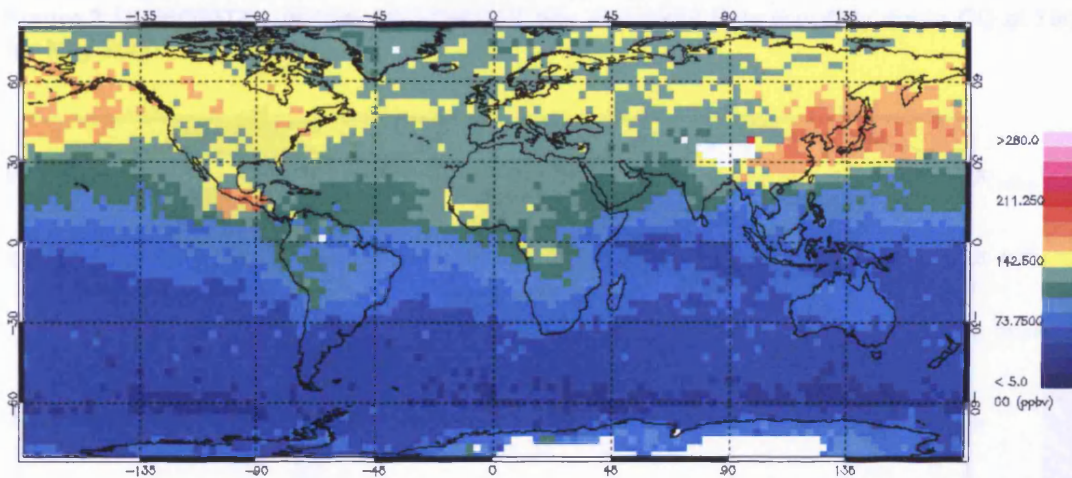


Figure 3.16: Monthly mean day and night time averaged MOPITT CO at 700 mb for May 2000

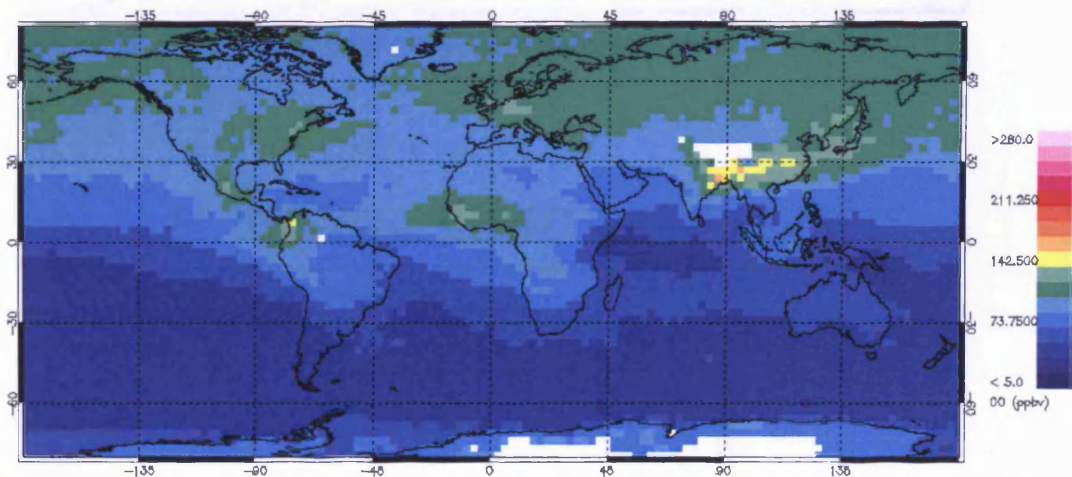


Figure 3.17: Monthly mean day and night time 'retrieved' TOMCAT CO at 700 mb for May 2000

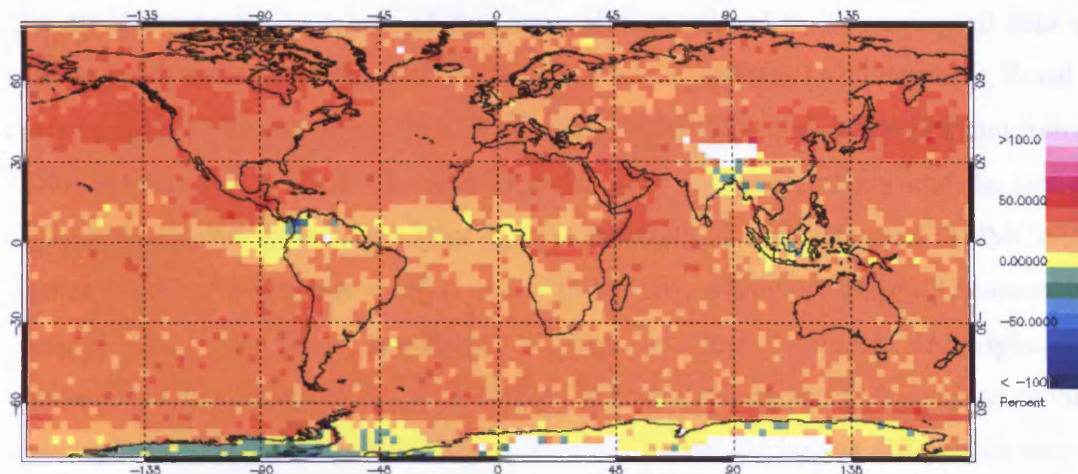


Figure 3.18: MOPITT – ‘retrieved’ TOMCAT day and night time monthly mean CO at 700 mb for May 2000

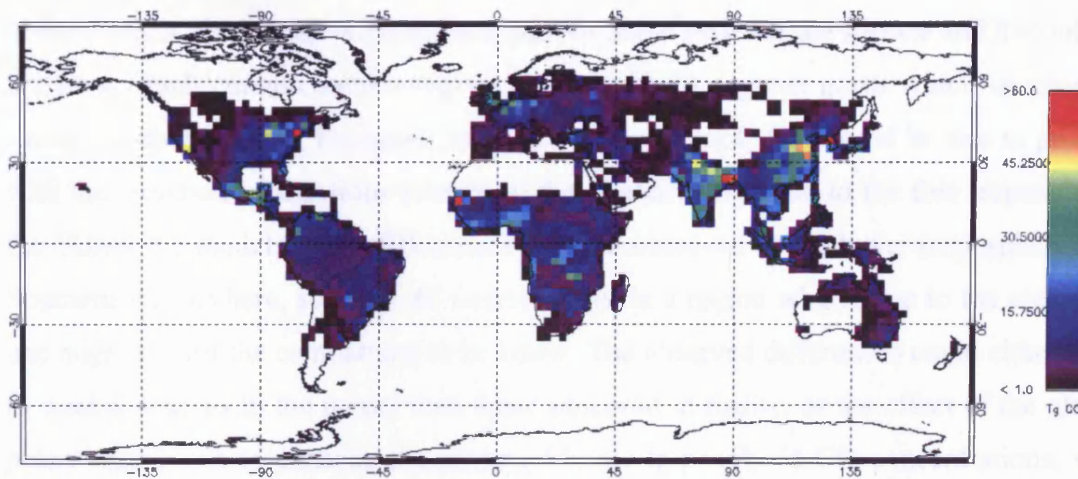


Figure 3.19: The TOMCAT total CO emissions for May 2000

Pressure (mb)	MOPITT – ‘retrieved’ TOMCAT (%)
Surface	19.54 (15.74)
850	23.51 (12.33)
700	20.18 (9.14)
500	16.20 (7.39)
350	14.63 (8.49)
250	12.71 (8.65)
150	10.83 (9.09)

Table 3.3: Global mean differences between MOPITT and ‘retrieved’ TOMCAT monthly means for May 2000. The numbers in parentheses denote the standard deviation.

The zonal means for both sets of data were also calculated by averaging all data within latitude bands defined by the width of each TOMCAT grid box (~2.8 degrees). Zonal mean cross-sections of the monthly mean CO levels for May 2000 from MOPITT and 'retrieved' TOMCAT can be found in Figure 3.20 and Figure 3.21 respectively and the percentage difference between the two in Figure 3.22. Both MOPITT and 'retrieved' TOMCAT show similar structure in both the vertical and with latitude, with the highest CO concentrations located over the most populated regions in the Northern Hemisphere. The interhemispherical gradient in CO is evident in both datasets and both seem to capture the intertropical convergence zone (ITCZ) quite well. Again, the largest differences seem to be at those latitudes which contain source regions.

In the vertical, the largest differences appear to occur between the surface and 850 mb over latitudes which contain source regions such as 30-50 degrees north which encompasses strong North American, European and East Asian sources. This could be due to problems with the transport of CO from sources in the boundary layer up to the free troposphere in the TOMCAT model. Large differences are also observed in the lower troposphere in the Southern Hemisphere, south of 40 degrees. This is a region where, due to the cleaner air, one might expect the comparison to be better. The observed differences could either be due to weaker sources in the model than those observed in reality, or the effect of the global *a priori* which acts to enhance the retrieved lower tropospheric CO concentrations, where MOPITT is less sensitive.

Figure 3.23 shows a scatter plot of the zonal mean May 2000 average for MOPITT and 'retrieved' TOMCAT, the plot is coloured by altitude and the equation for the line of best fit and the correlation coefficient for each altitude is displayed. The results show that the comparison between the two is excellent with correlation coefficients of better than 0.95 for all altitudes and MOPITT generally reporting higher CO levels than TOMCAT. The exception is a number of points at the lower altitudes near source regions over South America and India which are consistent with the findings above.

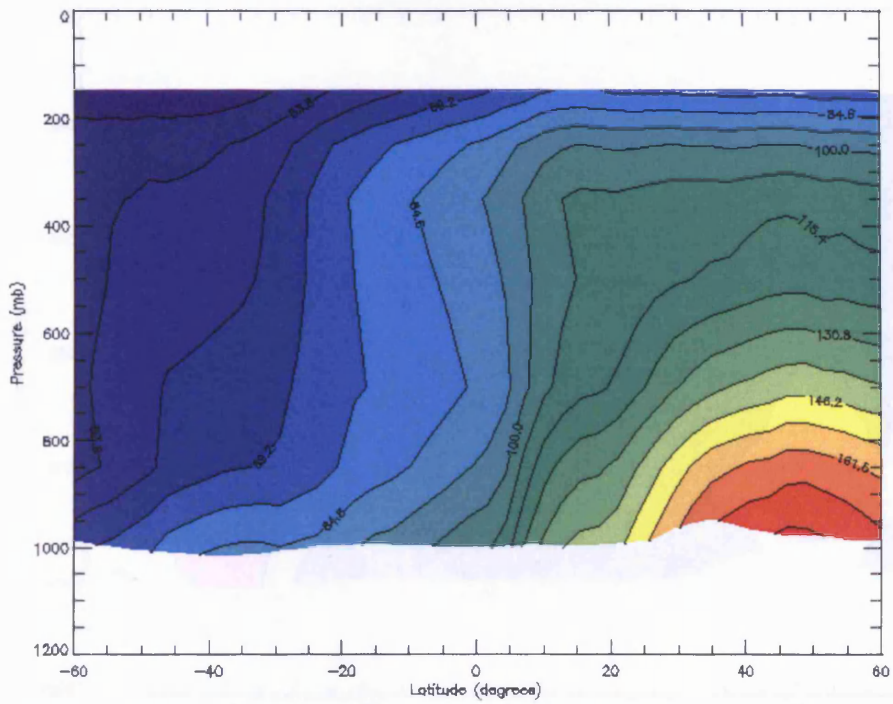


Figure 3.20: Zonal mean cross-section of MOPITT monthly mean CO data for May 2000

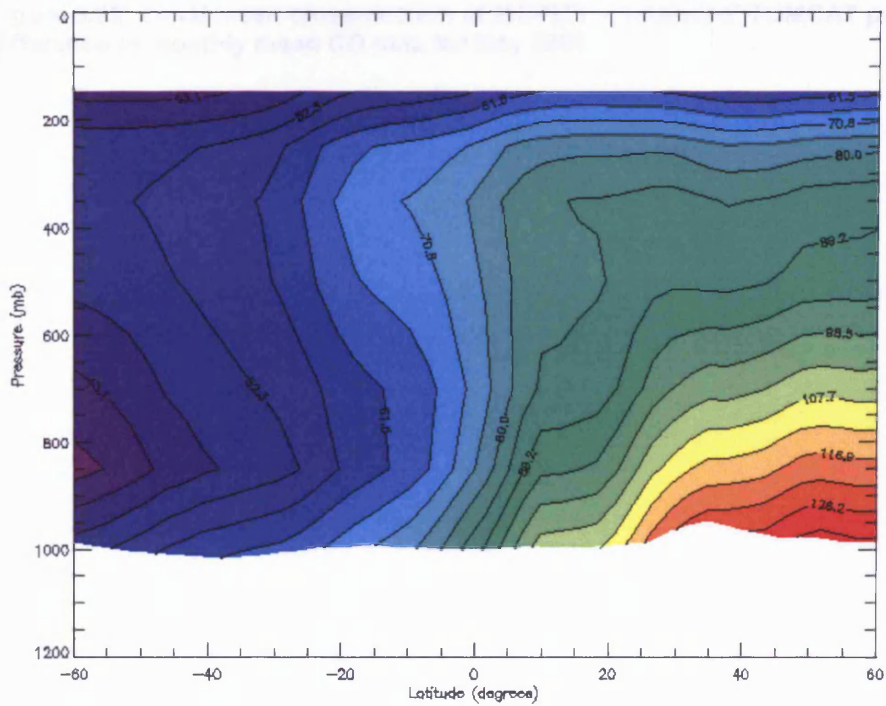


Figure 3.21: Zonal mean cross-section of 'retrieved' TOMCAT monthly mean CO data for May 2000

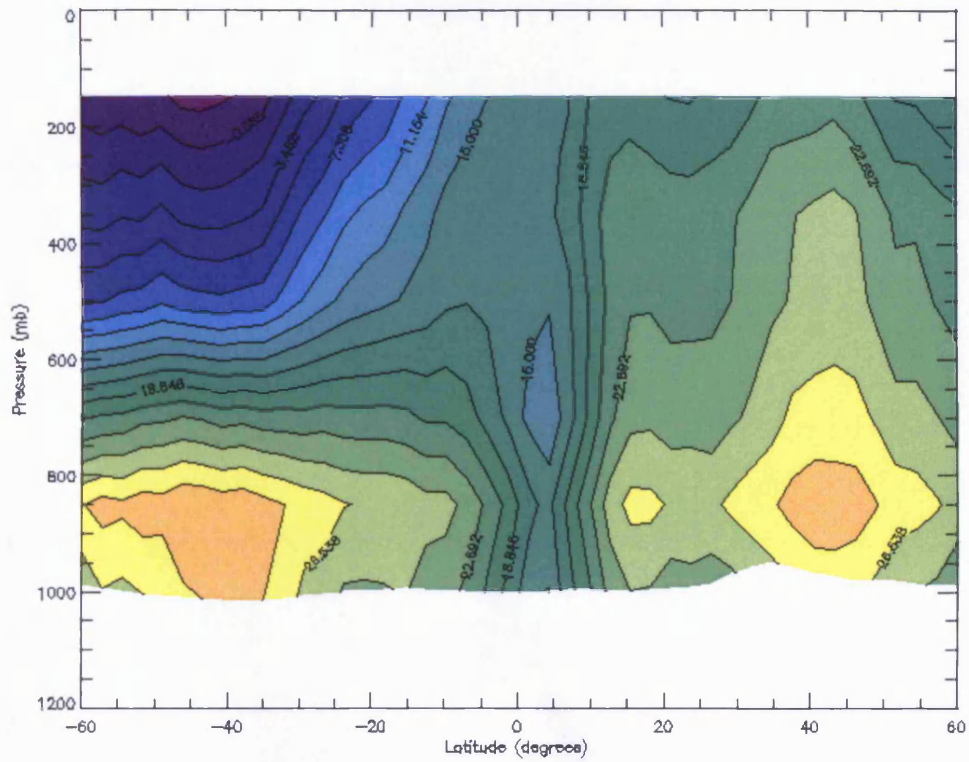


Figure 3.22: Zonal mean cross-section of MOPITT – ‘retrieved’ TOMCAT percentage difference in monthly mean CO data for May 2000

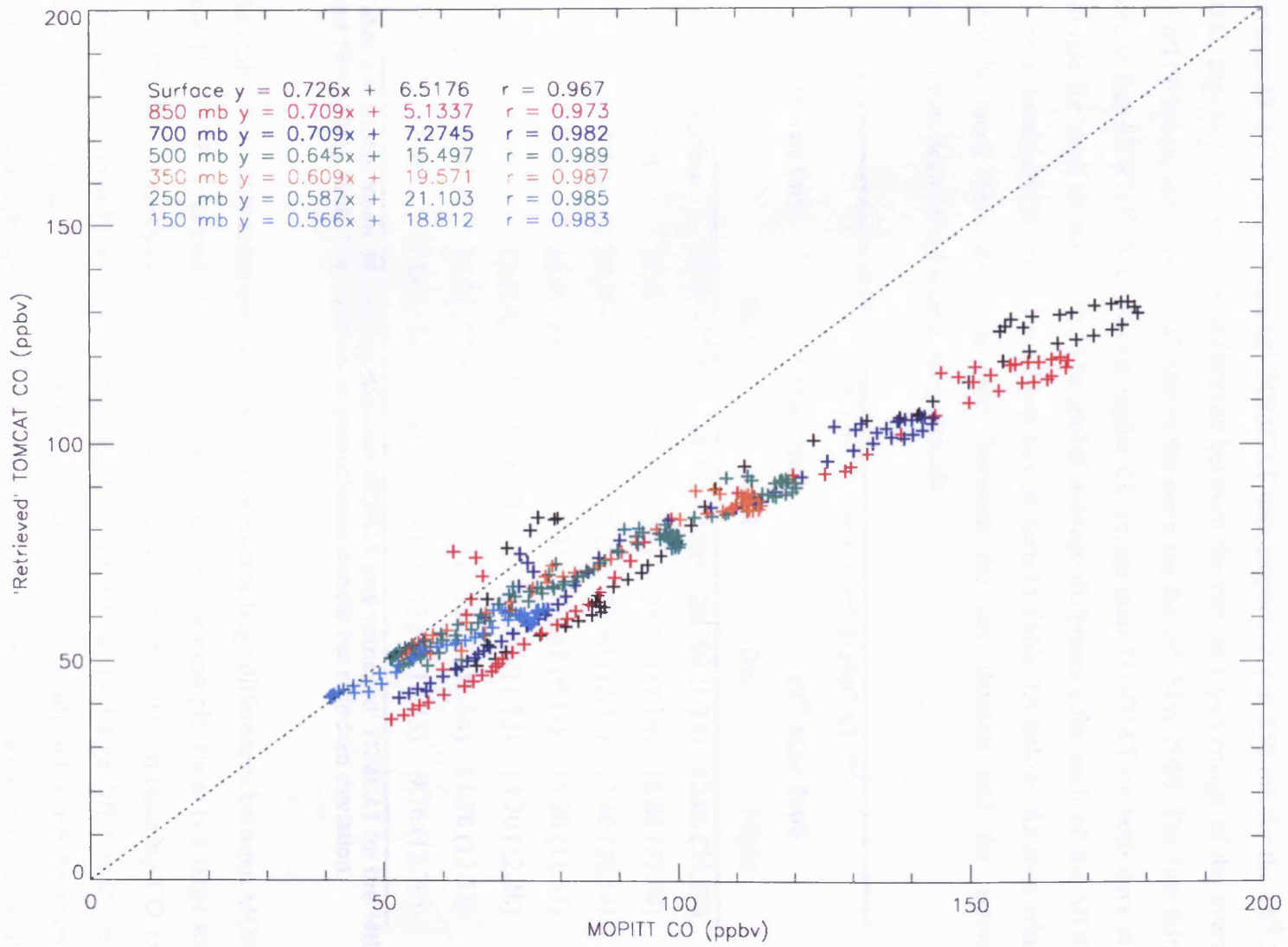


Figure 3.23: MOPITT vs 'retrieved' TOMCAT May 2000 monthly mean CO zonal mean scatter plot

3.3.3.2 MOPITT-TOMCAT Daily Comparisons

Daily data for May 2000 were also examined. Figure 3.24 and Figure 3.25 show averaged daytime MOPITT and ‘retrieved’ TOMCAT data respectively at 850 mb for the 14th May 2000. Figure 3.26 shows the difference between the two as a percentage of the averaged MOPITT values and Figure 3.27 shows the same for the 19th May 2000. The first thing to note is that MOPITT data indicate higher CO levels than TOMCAT on both days at this altitude for most of the globe. The global average differences for each of the MOPITT retrieval levels on the two days shown can be seen in Table 3.4 below. As seen with the monthly mean data, the differences between the two datasets and the associated uncertainties decrease with increasing altitude.

MOPITT – ‘retrieved’ TOMCAT (%)				
Pressure (mb)	14 th May 2000		19 th May 2000	
	Day	Night	Day	Night
Surface	18.91 (23.73)	14.88 (32.68)	20.70 (21.23)	12.06 (35.59)
850	22.55 (20.92)	20.37 (22.07)	24.22 (17.16)	18.83 (27.58)
700	20.34 (13.98)	17.18 (18.25)	21.50 (12.37)	17.40 (20.54)
500	16.97 (19.65)	15.17 (11.33)	17.67 (9.39)	15.20 (11.51)
350	15.66 (17.29)	13.97 (12.21)	15.87 (11.73)	13.70 (12.48)
250	13.98 (13.98)	12.22 (12.21)	13.87 (12.54)	11.70 (12.13)
150	12.02 (14.55)	10.51 (13.12)	11.54 (18.43)	9.76 (12.70)

Table 3.4: Global mean differences between MOPITT and ‘retrieved’ TOMCAT for the 14th and 19th of May 2000. The numbers in parentheses denote the standard deviation.

As with the monthly mean comparisons, it appears that large differences between MOPITT and TOMCAT occur over TOMCAT source regions. For example, there is a large source over Calcutta in north-east India and this coincides with MOPITT measuring CO levels which are less than 50% of the corresponding TOMCAT values. Large differences are also seen over or near to TOMCAT source regions over Africa, South and North America and East Asia. These differences could be due to the use of monthly mean emissions in the TOMCAT model which would not reproduce daily variations in source strengths and specific pollution events such as forest fires that may be captured in the MOPITT measurements. There also seem to be large positive differences over parts of the Pacific

where the comparison might be expected to be much better as these regions are away from source regions. However, these differences could be due to the transport of CO from specific pollution events such as forest fires which again may not be represented in the model emissions. Chapter 5 explores these factors more fully.

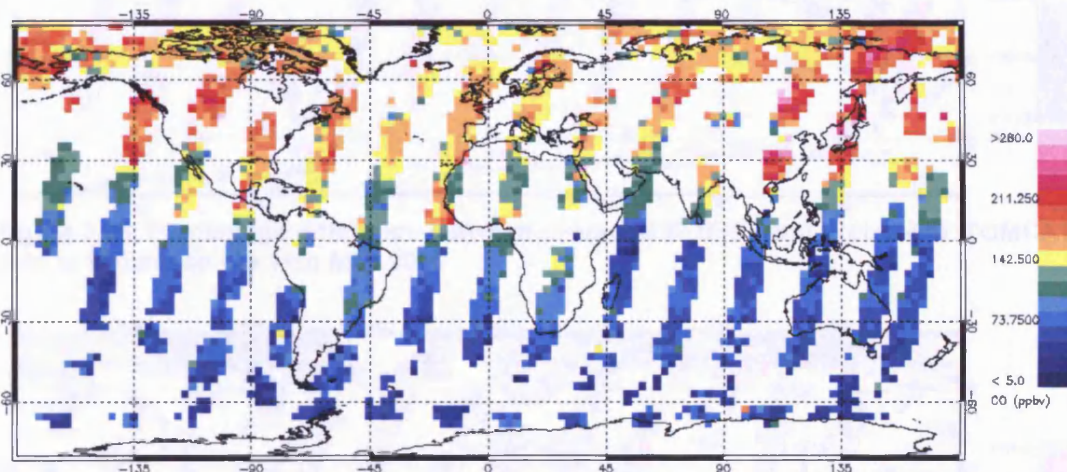


Figure 3.24: Averaged daytime MOPITT CO data at 850 mb on the 14th May 2000

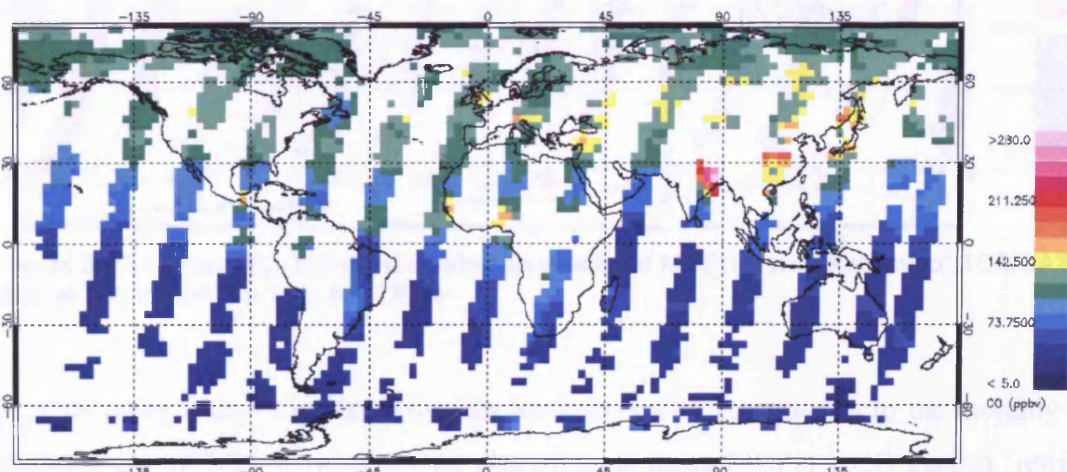


Figure 3.25: Averaged 'Retrieved' TOMCAT CO data at 850 mb on the 14th May 2000

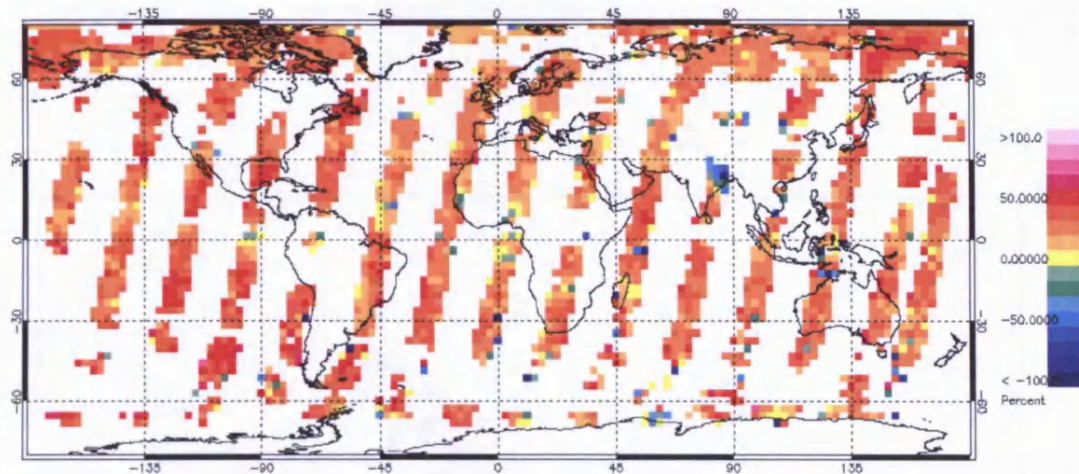


Figure 3.26: Percentage difference between averaged MOPITT and 'Retrieved' TOMCAT CO data at 850 mb on the 14th May 2000

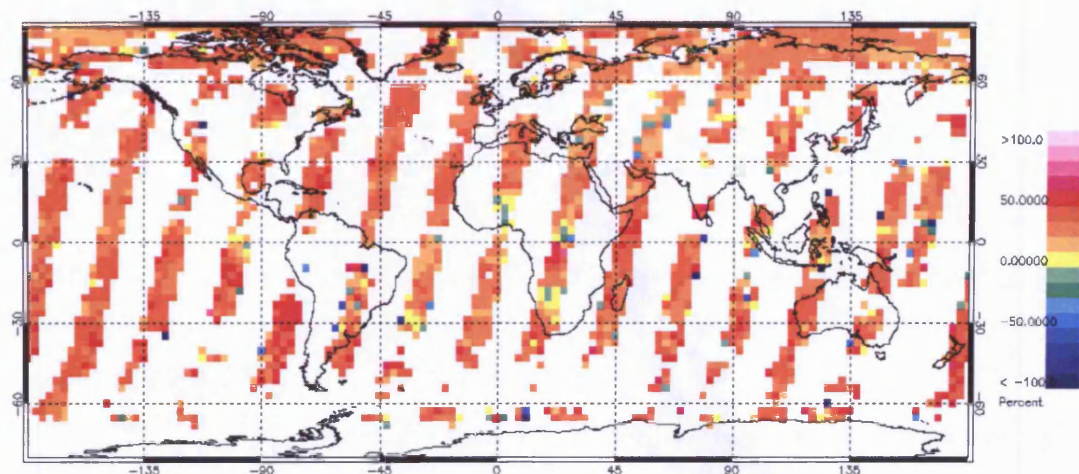


Figure 3.27: Percentage difference between averaged MOPITT and 'Retrieved' TOMCAT CO data at 850 mb on the 19th May 2000

A zonal mean analysis of the daily data leads to similar conclusions to the monthly mean analysis. Figure 3.28 shows a scatter plot of zonal mean MOPITT CO against 'retrieved' TOMCAT CO coloured by altitude for both day and night time data on 14th May 2000. The agreement between the two datasets is again excellent with correlation coefficients in excess of 0.97 for all altitudes. Table 3.5 shows the correlation coefficients for daytime and night time comparisons for both the 14th and the 19th of May. The good agreement between the two datasets seems to hold for both day and night with the correlation at lower levels dropping from day to night as expected.

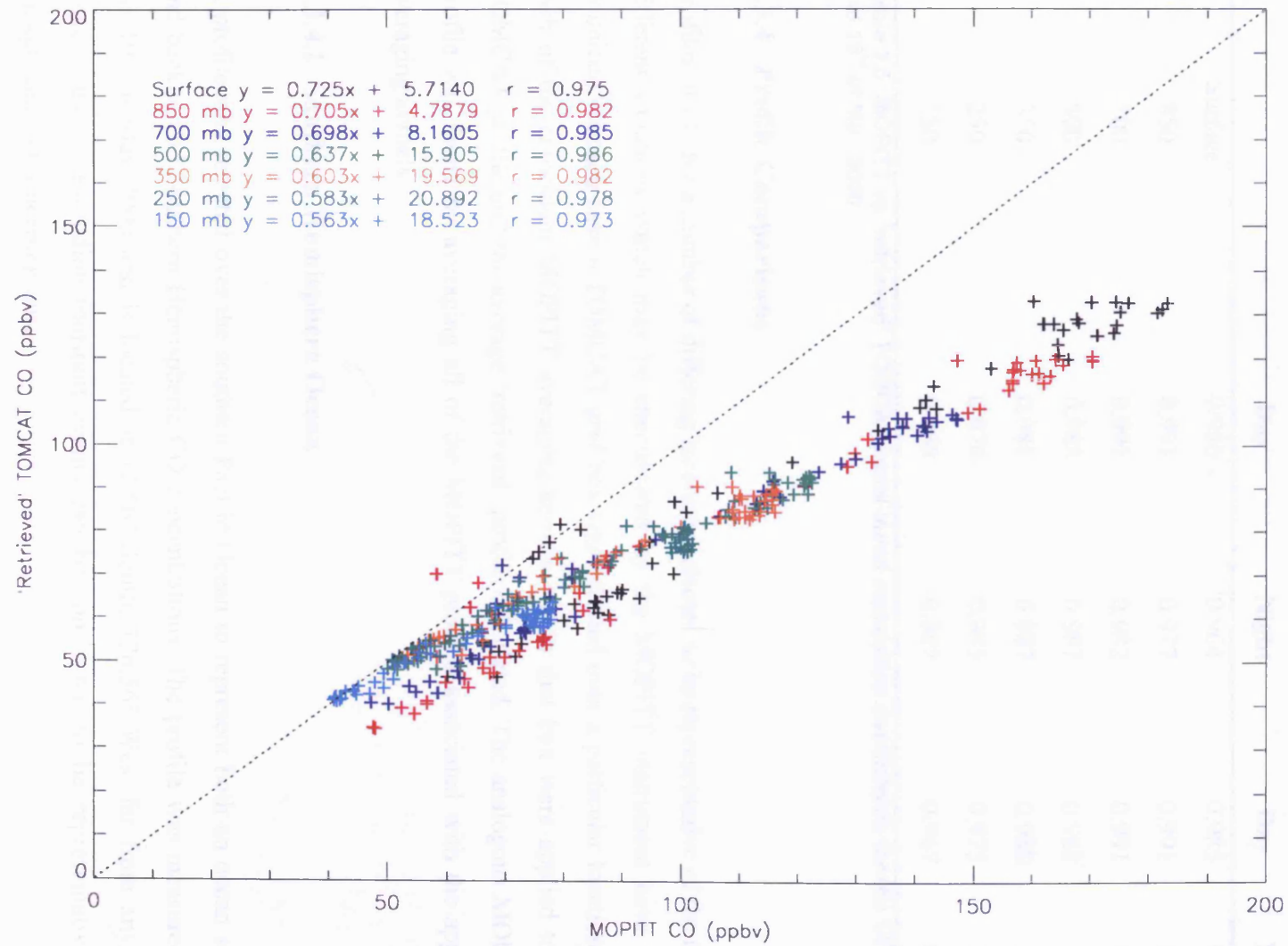


Figure 3.28: MOPITT vs 'retrieved' TOMCAT day/night zonal mean CO scatter plot for 14th May 2000

MOPITT vs 'retrieved' TOMCAT Zonal Mean Correlation
Coefficient

Pressure (mb)	14 th May 2000		19 th May 2000	
	Day	Night	Day	Night
Surface	0.986	0.964	0.985	0.938
850	0.991	0.977	0.991	0.953
700	0.991	0.982	0.991	0.966
500	0.988	0.987	0.988	0.987
350	0.981	0.987	0.980	0.987
250	0.976	0.985	0.975	0.985
150	0.969	0.982	0.967	0.984

Table 3.5: MOPITT vs 'retrieved' TOMCAT zonal mean correlation coefficients for the 14th and 19th of May 2000

3.3.4 Profile Comparisons

Profiles of CO for a number of differing locations selected to be representative of the many different situations which may be encountered by the MOPITT instrument have been examined. In each case a TOMCAT grid box was selected over a particular location and each of the coincident MOPITT averaging kernels within that box were applied to the TOMCAT profile and the average 'retrieved' profile calculated. The analogous MOPITT profile was found by averaging all of the MOPITT profiles associated with the applied averaging kernels.

3.3.4.1 Southern Hemisphere Ocean

A profile was selected over the southern Pacific Ocean to represent both an ocean scene and background Southern Hemispheric CO concentrations. The profile was measured on the 19th of May 2000 and is located at 12.56° South, 126.56° West far from any CO sources and so excluding transport events can be considered to be representative of background CO concentrations.

Figure 3.29 shows the results of the comparison, the solid red line represents the averaged MOPITT profile, the dotted red line is the MOPITT *a priori* used for the MOPITT retrieval, the solid blue line is the average 'retrieved' TOMCAT profile and the dotted blue

line represents the TOMCAT profile before the application of the averaging kernels. Applying the MOPITT averaging kernels seems to have little effect on the TOMCAT profile which suggests that for profiles of the shape seen here over ocean, i.e. in the absence of strong layering, MOPITT CO profiles may be considered to be representative of the real atmospheric CO profile. This is true despite the apparently low sensitivity to the lower troposphere evident in the MOPITT averaging kernels (Figure 3.30). This is due to the profile being quite smooth in this region, so even though MOPITT obtains most of the information for the lower levels from a layer centred at 700 mb, the CO concentrations at this altitude are similar and correlate well with those at 850 mb and the surface.

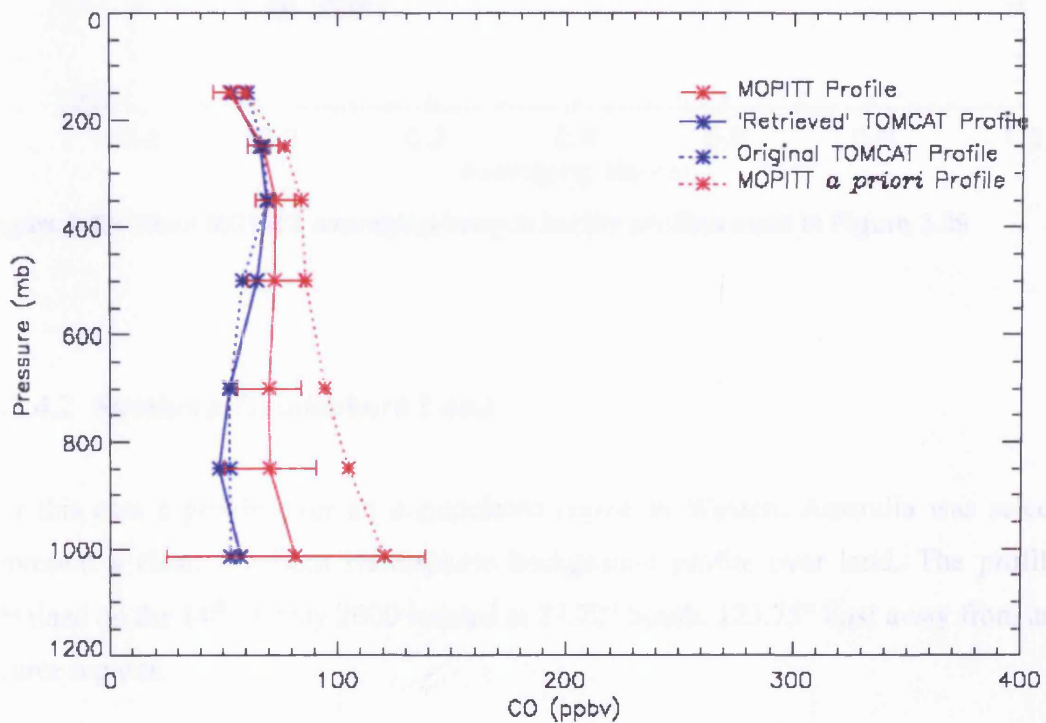


Figure 3.29: Averaged MOPITT and TOMCAT CO profiles located at 12.56° South, 126.56° West, over the southern Pacific on the 19th of May 2000. The error bars on the MOPITT profile represent the mean reported retrieval uncertainty at each MOPITT level for all coincident profiles.

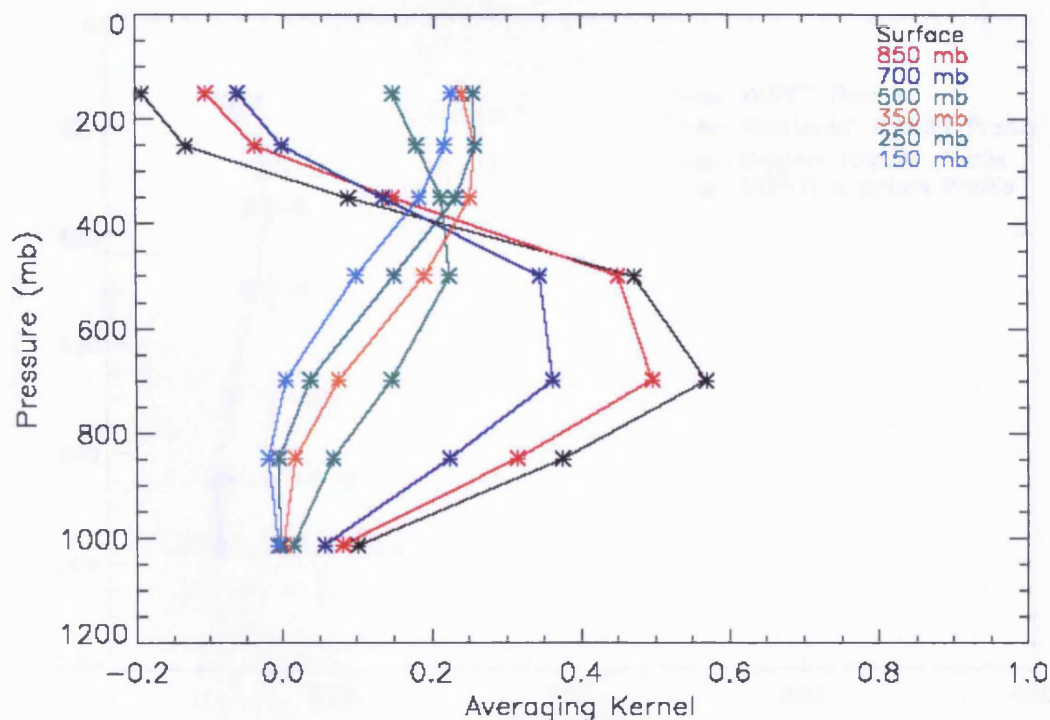


Figure 3.30: Mean MOPITT averaging kernels for the profiles used in Figure 3.29

3.3.4.2 Southern Hemisphere Land

For this case a profile over an unpopulated region in Western Australia was selected to represent a clean Southern Hemisphere background profile over land. The profile was obtained on the 14th of May 2000 located at 23.72° South, 123.75° East away from any CO source regions.

The results for this comparison can be seen in Figure 3.31. As with the ocean case, the application of MOPITT averaging kernels has done very little to alter the TOMCAT profile. This is especially true in the lower levels where the MOPITT averaging kernels suggest little sensitivity (Figure 3.32). This again is due to the shape of the TOMCAT CO profile which is quite uniform throughout the whole of the troposphere and the correlation of information between levels. This suggests that in regions where the air is considered to be vertically well mixed and represent background or aged conditions, MOPITT CO profiles may be considered to represent the true atmospheric profile.

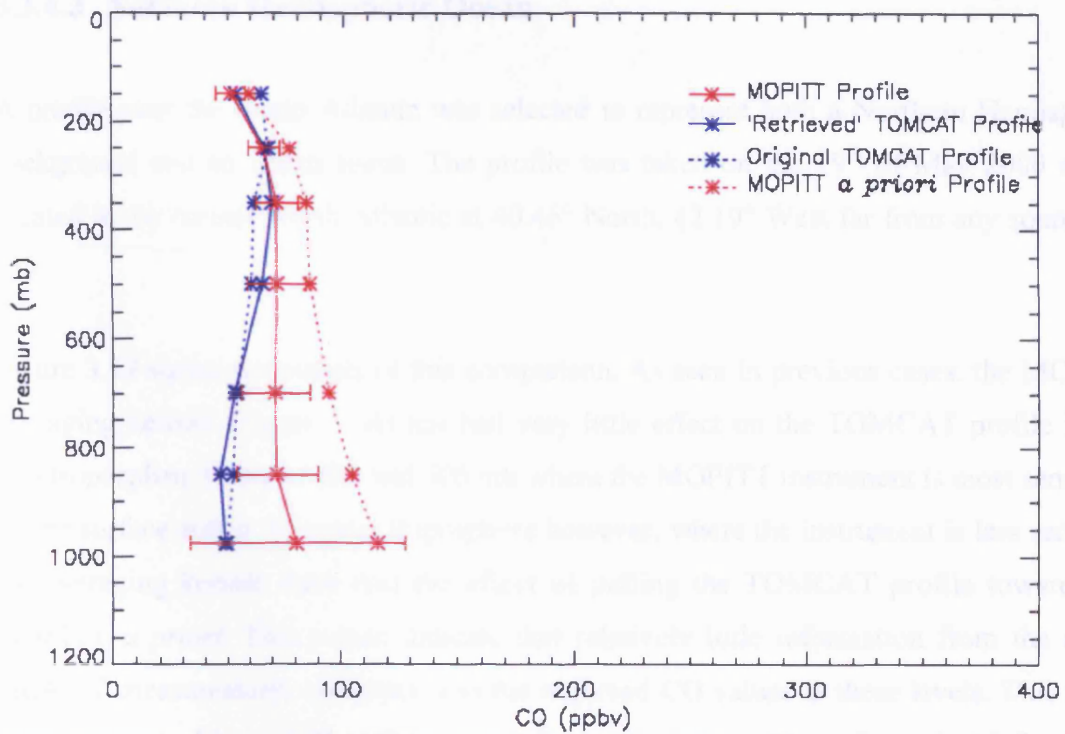


Figure 3.31: Averaged MOPITT and TOMCAT CO profiles located at 23.72° South, 123.75° East, over Western Australia on the 14th of May 2000. The error bars on the MOPITT profile represent the mean reported retrieval uncertainty at each MOPITT level for all coincident profiles.

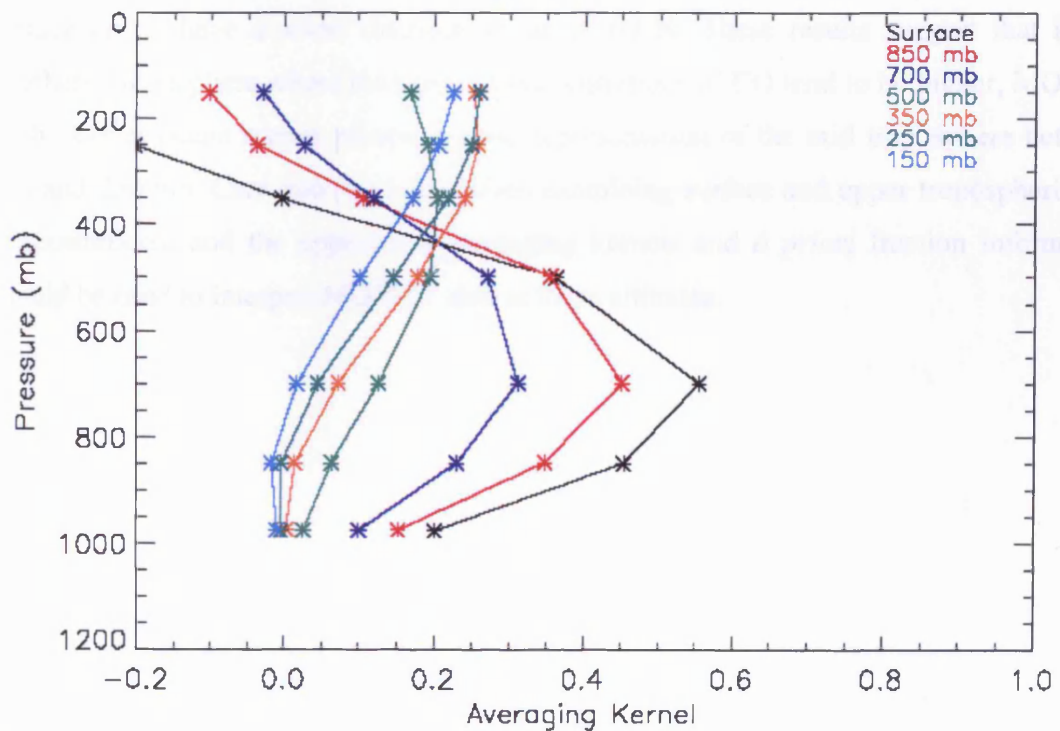


Figure 3.32: Mean MOPITT averaging kernels for the profiles used in Figure 3.31

3.3.4.3 Northern Hemispheric Ocean

A profile over the North Atlantic was selected to represent both a Northern Hemispheric background and an ocean scene. The profile was taken on the 19th of May 2000 and is located in the remote North Atlantic at 40.46° North, 42.19° West far from any sources of CO.

Figure 3.33 shows the results of this comparison. As seen in previous cases, the MOPITT averaging kernels (Figure 3.34) has had very little effect on the TOMCAT profile in the mid troposphere between 850 and 500 mb where the MOPITT instrument is most sensitive. At the surface and in the upper troposphere however, where the instrument is less sensitive the averaging kernels have had the effect of pulling the TOMCAT profile towards the MOPITT *a priori*. This would indicate that relatively little information from the actual MOPITT measurements contributed to the retrieved CO values at these levels. This effect can be seen in Figure 3.35 which shows the average percentage of *a priori* information used at each altitude level for the profiles used in the comparison. The mid tropospheric levels (850 – 250 mb) for which the averaging kernel application made little or no difference have less than 30 % *a-priori* information whereas the upper tropospheric and surface layers have *a-priori* fractions of up to 60 %. These results suggest that in the Northern Hemisphere where background concentrations of CO tend to be higher, MOPITT profiles over ocean scenes present a good representation of the mid troposphere between 850 and 250 mb. Care must be taken when examining surface and upper tropospheric CO concentrations, and the appropriate averaging kernels and *a priori* fraction information should be used to interpret MOPITT data at these altitudes.

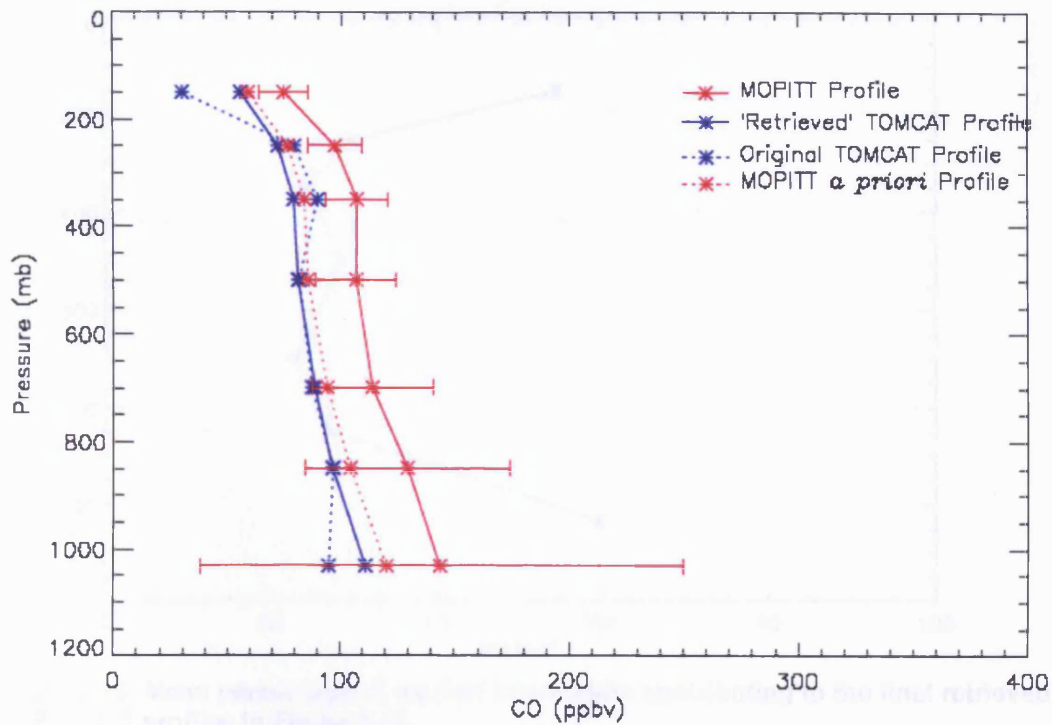


Figure 3.33: Averaged MOPITT and TOMCAT CO profiles located at 40.46° North, 42.19° West, over the North Atlantic on the 19th of May 2000. The error bars on the MOPITT profile represent the mean reported retrieval uncertainty at each MOPITT level for all coincident profiles.

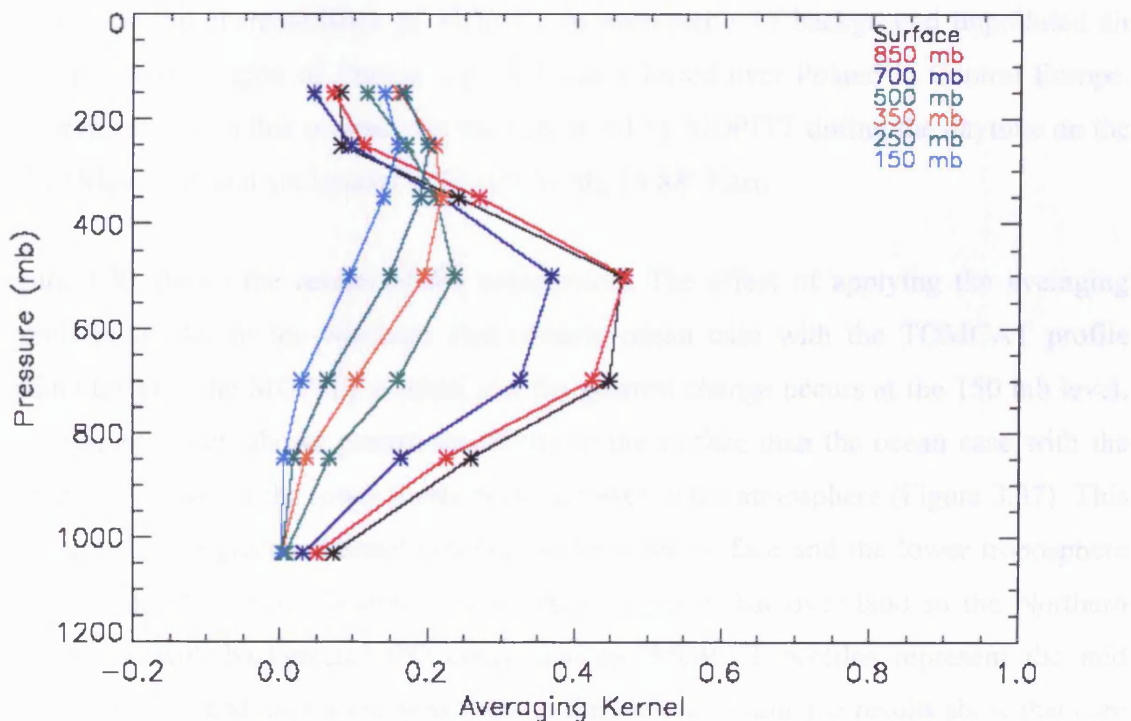


Figure 3.34: Mean MOPITT averaging kernels for the profiles used in Figure 3.33.

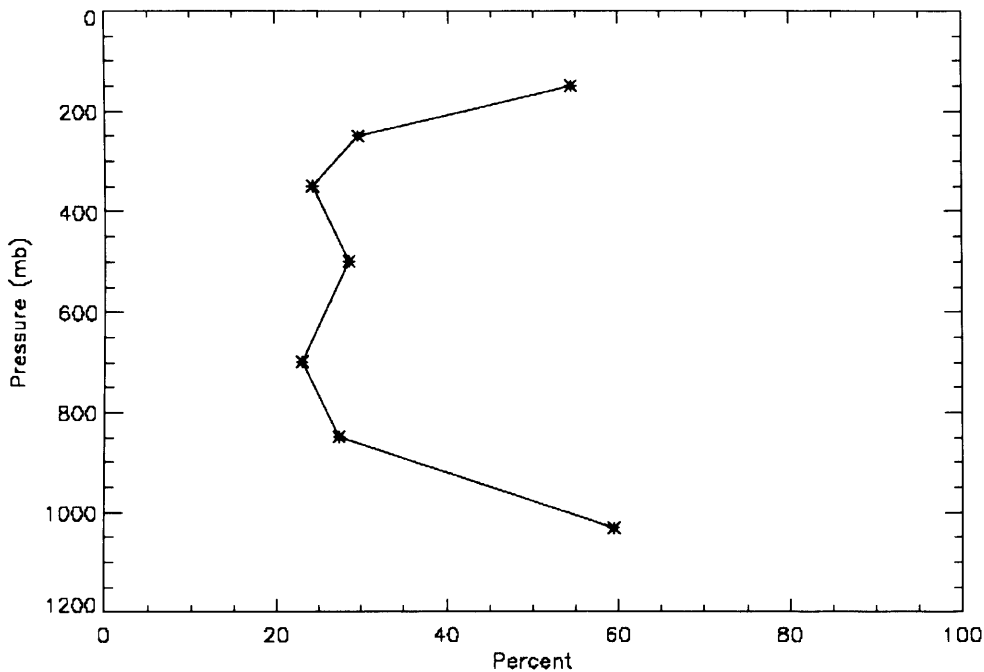


Figure 3.35: Mean percentage of *a-priori* information contributing to the final retrieved MOPITT CO profiles in Figure 3.33

3.3.4.4 European Background

To examine the characteristics of MOPITT measurements of background unpolluted air over land in the region of Europe a profile was selected over Poland in Central Europe. The profiles used in this comparison were recorded by MOPITT during the daytime on the 14th of May 2000 and are located at 51.62° North, 16.88° East.

Figure 3.36 shows the results of the comparison. The effect of applying the averaging kernels is similar to the Northern Hemispheric ocean case with the TOMCAT profile tending towards the MOPITT *a priori* and the greatest change occurs at the 150 mb level. This case however, shows greater sensitivity to the surface than the ocean case with the averaging kernels for the lower levels peaking lower in the atmosphere (Figure 3.37). This is because of the greater thermal contrast between the surface and the lower troposphere over land due to surface heating. These results suggest that over land in the Northern Hemisphere with background CO concentrations, MOPITT profiles represent the mid troposphere well and have some sensitivity to the surface. Again, the results show that care must be taken when interpreting MOPITT CO profiles under these conditions and the appropriate averaging kernels should be taken into account in any such study.

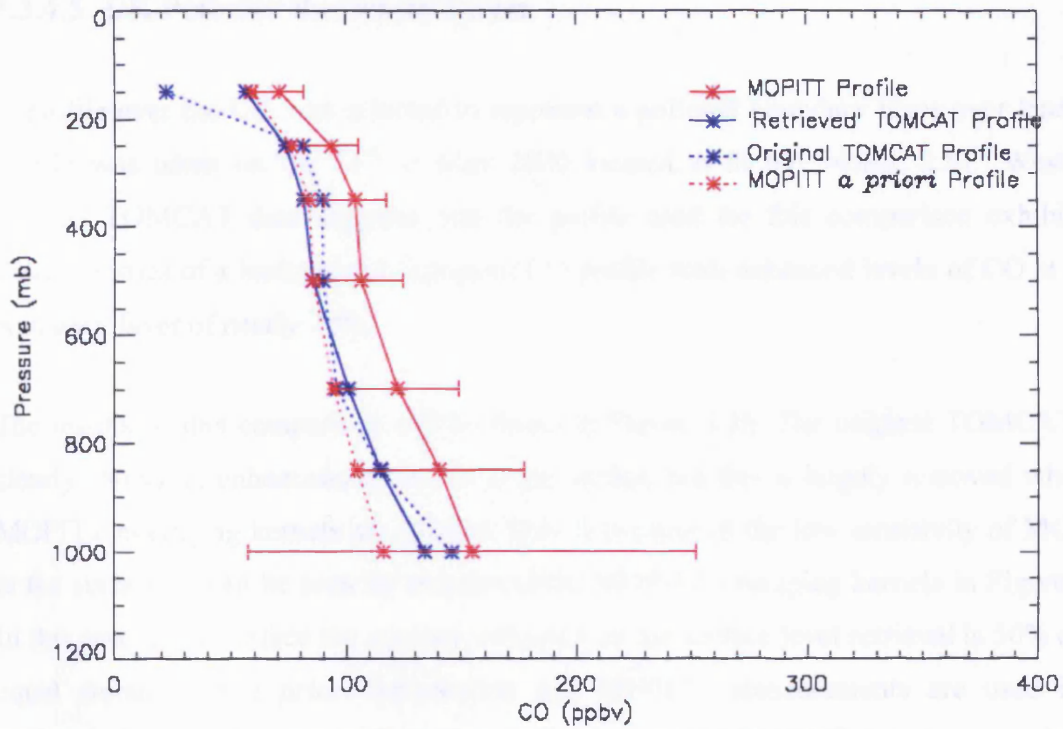


Figure 3.36: Averaged MOPITT and TOMCAT CO profiles located over Poland at 51.62° North, 16.88° East, on the 19th of May 2000. The error bars on the MOPITT profile represent the mean reported retrieval uncertainty at each MOPITT level for all coincident profiles.

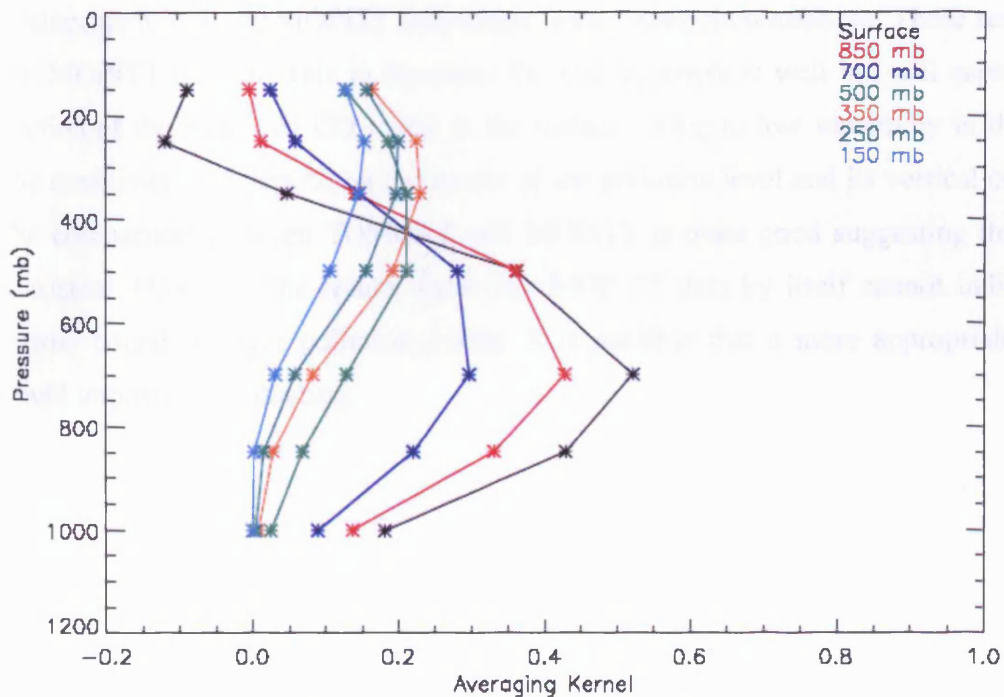


Figure 3.37: Mean MOPITT averaging kernels for the profiles used in Figure 3.36.

3.3.4.5 UK Polluted Boundary Layer

A profile over the UK was selected to represent a polluted boundary layer over land. The profile was taken on the 14th of May 2000 located at 51.63° North, 2.81° West. The original TOMCAT data suggests that the profile used for this comparison exhibits the characteristics of a background European CO profile with enhanced levels of CO at in the boundary layer of nearly 70%.

The results of this comparison can be found in Figure 3.38. The original TOMCAT data clearly shows an enhancement of CO at the surface but this is largely removed when the MOPITT averaging kernels are applied. This is because of the low sensitivity of MOPITT at the surface as can be seen by examining the MOPITT averaging kernels in Figure 3.39. In this case at the surface the *a priori* influence on the surface level retrieval is 50% and so equal amounts of *a priori* information and MOPITT measurements are used in the retrieval. The surface level enhancement shown in the TOMCAT data is approximately 70% and this is comparable with the average MOPITT error at the surface for the profiles used in this comparison, so one might not expect to be able to observe such an enhancement with the MOPITT instrument under these circumstances. These results show that MOPITT is again able to represent the mid troposphere well but will capture only a fraction of the enhanced CO levels at the surface owing to low sensitivity in this region. The sensitivity will depend on the nature of the pollution level and its vertical correlation. The comparison between TOMCAT and MOPITT is quite good suggesting the data are consistent. However, the results show that MOPITT data by itself cannot indicate these narrow boundary layer pollution events. It is possible that a more appropriate *a priori* would improve this situation.

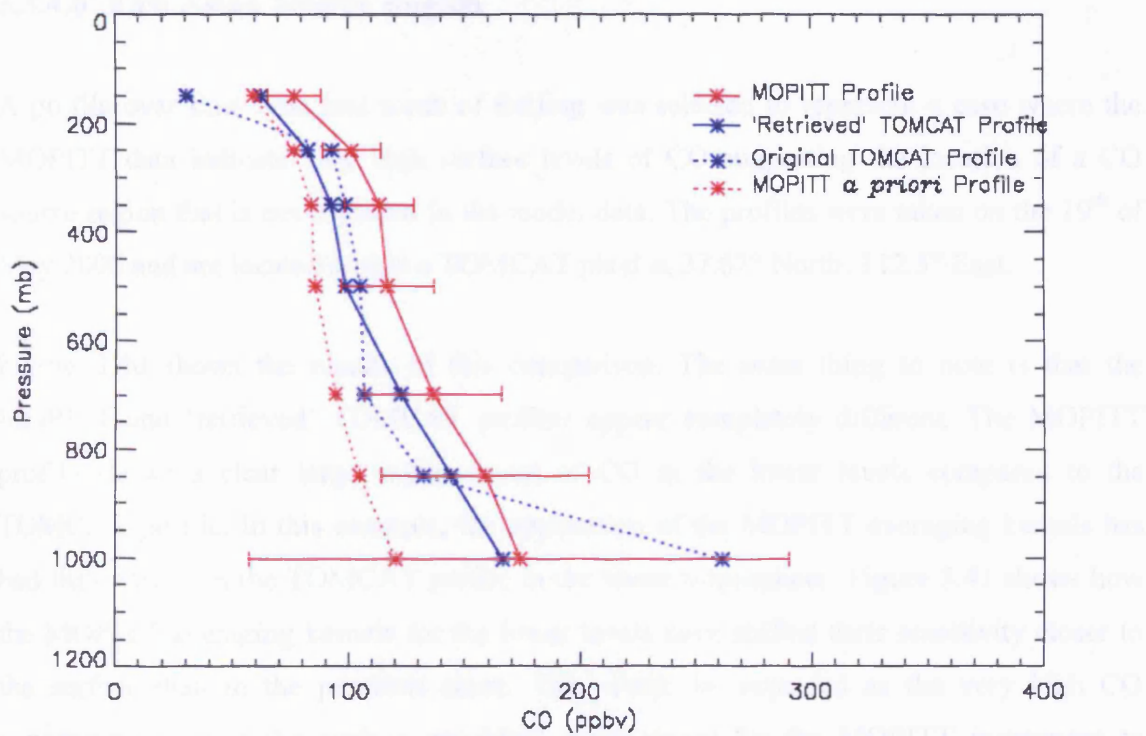


Figure 3.38: Averaged MOPITT and TOMCAT CO profiles located over the UK at 51.63° North, 2.81° West, on the 14th of May 2000. The error bars on the MOPITT profile represent the mean reported retrieval uncertainty at each MOPITT level for all coincident profiles.

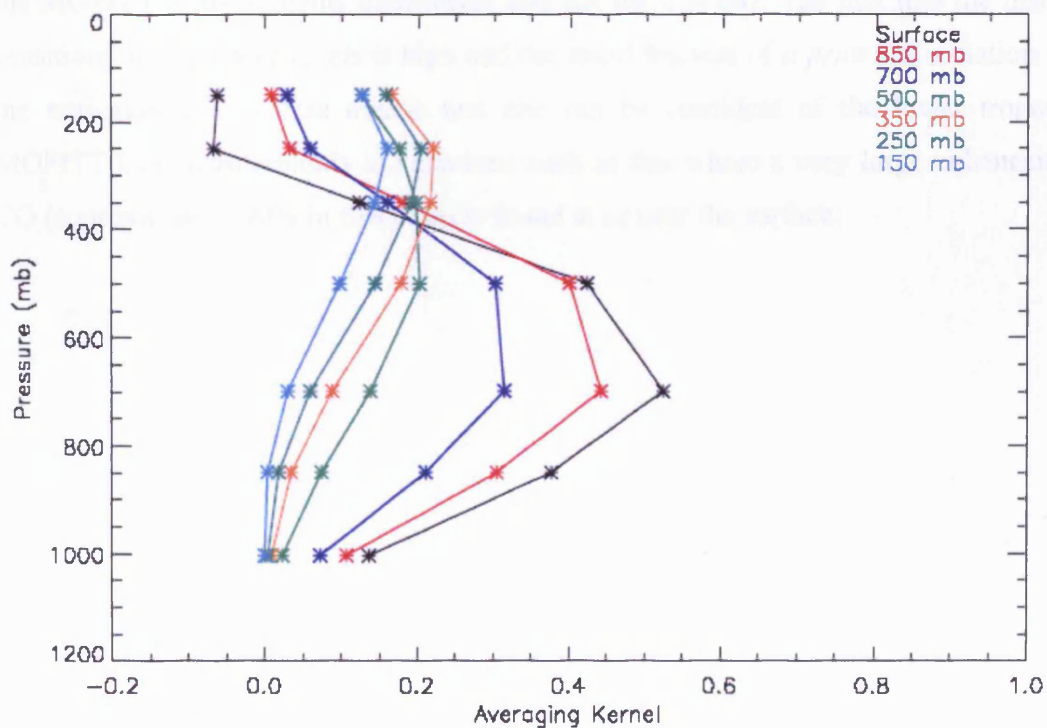


Figure 3.39: Mean MOPITT averaging kernels for the profiles used in Figure 3.38.

3.3.4.6 East Asian Source Region

A profile over East Asia just south of Beijing was selected to represent a case where the MOPITT data indicate very high surface levels of CO suggesting the location of a CO source region that is not captured in the model data. The profiles were taken on the 19th of May 2000 and are located within a TOMCAT pixel at 37.67° North, 112.5° East.

Figure 3.40 shows the results of this comparison. The main thing to note is that the MOPITT and ‘retrieved’ TOMCAT profiles appear completely different. The MOPITT profile shows a clear large enhancement of CO in the lower levels compared to the TOMCAT profile. In this example, the application of the MOPITT averaging kernels has had little effect on the TOMCAT profile in the lower troposphere. Figure 3.41 shows how the MOPITT averaging kernels for the lower levels have shifted their sensitivity closer to the surface than in the previous cases. This would be expected as the very high CO concentrations near the surface providing more signal for the MOPITT instrument to measure. It is clear from Figure 3.42, that most of the information for the lower troposphere used in the retrieval of the MOPITT profiles used in this case has come from the MOPITT measurements themselves and not the *a priori*. The fact that the instrument sensitivity to the lower levels is high and the small fraction of *a priori* information used in the retrievals in this case means that one can be confident of the lower tropospheric MOPITT CO measurements in situations such as this where a very large enhancement of CO (approximately 90% in this case) is found at or near the surface.

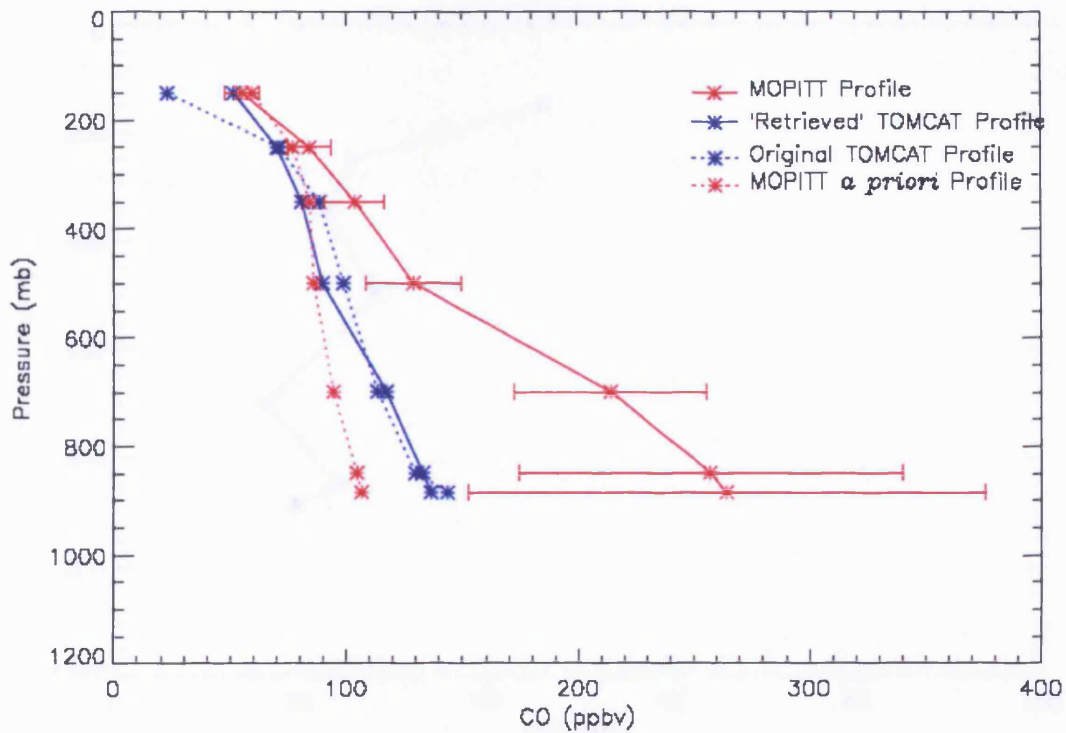


Figure 3.40: Averaged MOPITT and TOMCAT profiles located over East Asia at 37.67° North, 112.5° East, on the 19th of May 2000. The error bars on the MOPITT profile represent the mean reported retrieval uncertainty at each MOPITT level for all coincident profiles.

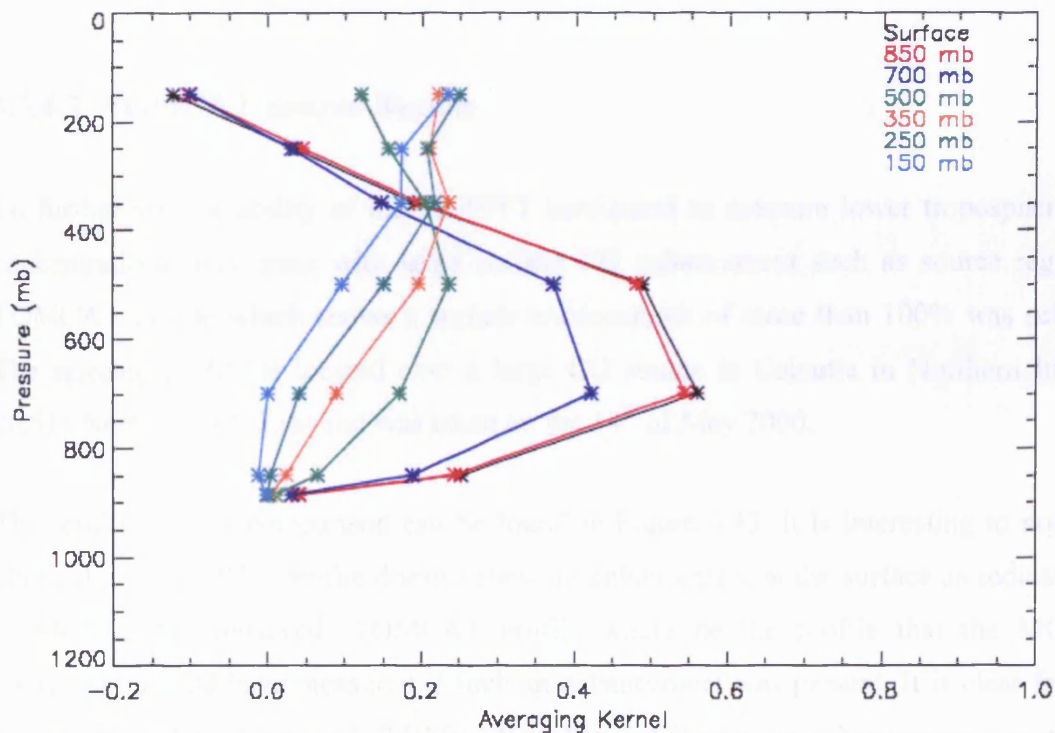


Figure 3.41: Mean MOPITT averaging kernels for the profiles used in Figure 3.40.

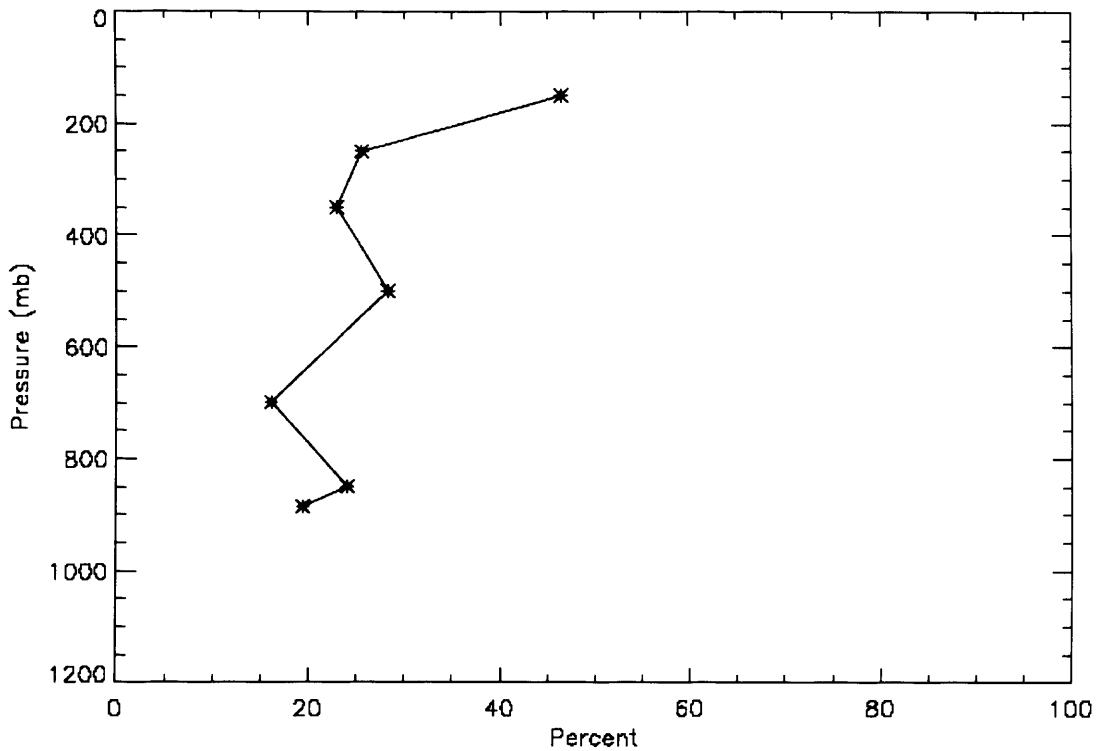


Figure 3.42: Mean percentage of *a-priori* information used in the retrieval of the MOPITT CO profiles in Figure 3.40.

3.3.4.7 TOMCAT Source Region

To further test the ability of the MOPITT instrument to measure lower tropospheric CO concentrations over areas with large surface CO enhancement such as source regions a TOMCAT profile which shows a surface enhancement of more than 100% was selected. The selected profile is located over a large CO source in Calcutta in Northern India at 26.51° North, 84.37° East and was taken on the 14th of May 2000.

The results for this comparison can be found in Figure 3.43. It is interesting to note that although the MOPITT profile doesn't show an enhancement at the surface as indicated by TOMCAT, the 'retrieved' TOMCAT profile would be the profile that the MOPITT instrument should have measured if such an enhancement was present. It is clear from an examination of the 'retrieved' TOMCAT profile that if such an enhancement was present the MOPITT measurements would have reflected this albeit to a lesser extent due to mixing of information between the layers. In reality, if such a profile was measured by MOPITT one might expect the enhancement at the surface to cause the lower level

averaging kernels to shift sensitivity towards the surface and thereby increasing the importance of the lower tropospheric layers in the profile retrieval. The fact that the enhancement is seen in the TOMCAT data and not by MOPITT could be due to problems with sources in the model as described earlier.

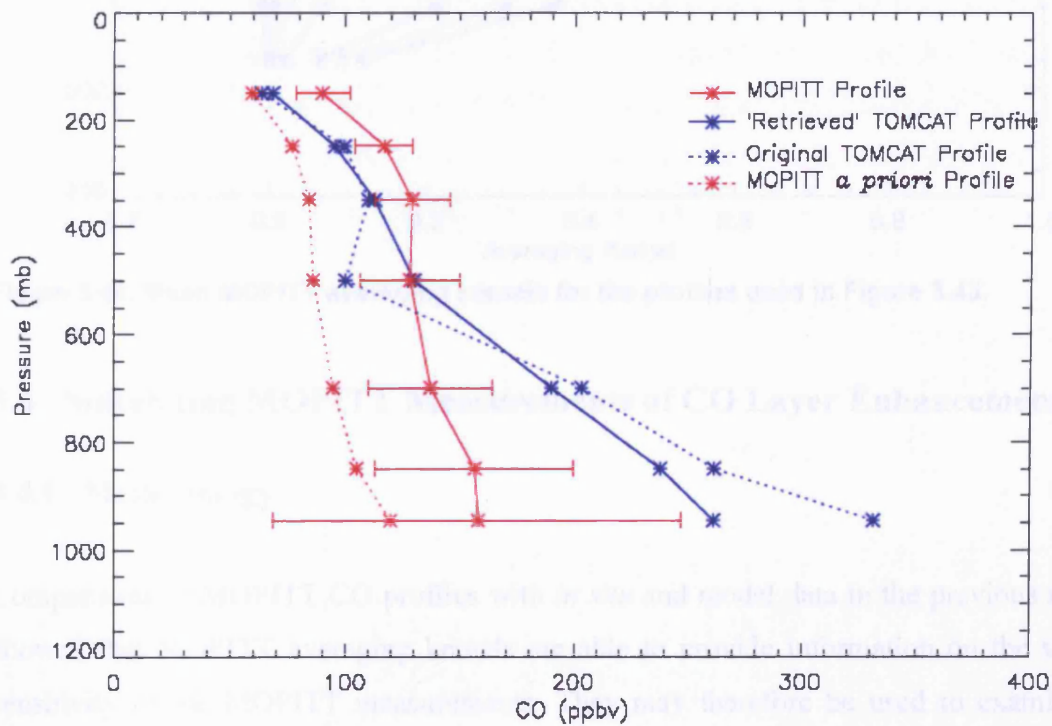


Figure 3.43: Averaged MOPITT and TOMCAT profiles located over Calcutta at 26.51° North, 84.37° East, on the 14th of May 2000. The error bars on the MOPITT profile represent the mean reported retrieval uncertainty at each MOPITT level for all coincident profiles.

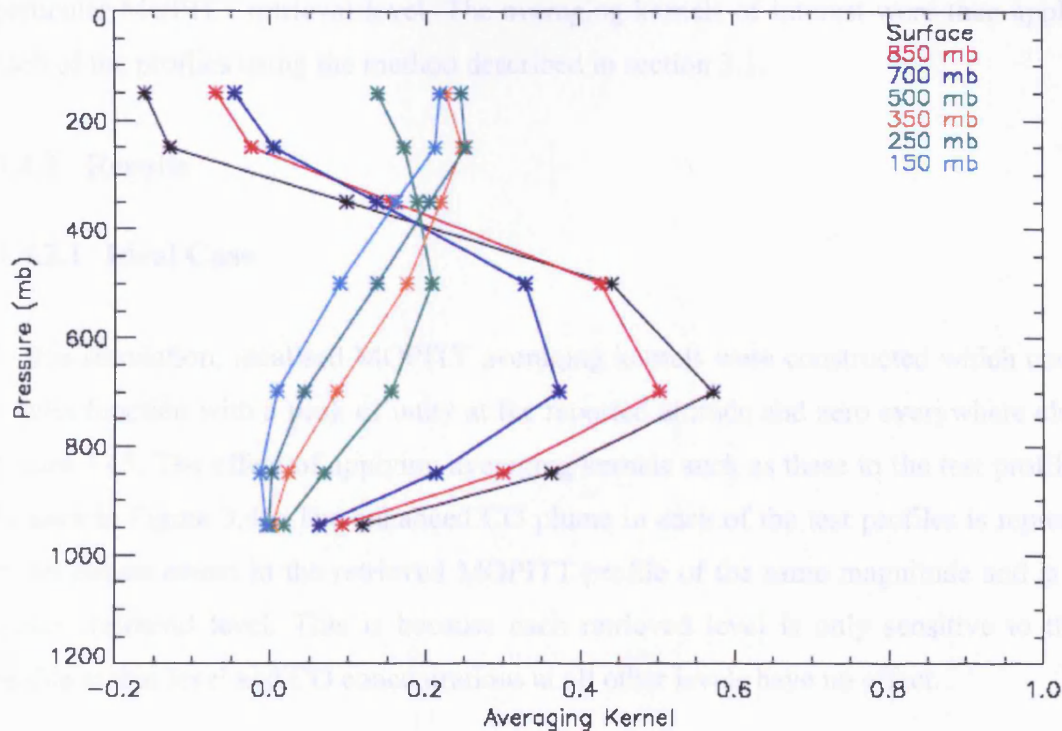


Figure 3.44: Mean MOPITT averaging kernels for the profiles used in Figure 3.43.

3.4 Simulating MOPITT Measurements of CO Layer Enhancements

3.4.1 Methodology

Comparisons of MOPITT CO profiles with *in situ* and model data in the previous section showed that MOPITT averaging kernels are able to provide information on the vertical sensitivity of the MOPITT measurements. They may therefore be used to examine the ability of the instrument to make CO profile measurements under different atmospheric and surface conditions. One is then able to determine if it is possible for the MOPITT instrument to detect plumes or layers of enhanced CO which have a limited vertical extent by applying averaging kernels to known profiles to simulate the effect of using MOPITT to measure such profiles. Simulations of this type were performed using MOPITT averaging kernels for different situations under which one might want to observe plumes of enhanced CO. A profile based on the MOPITT *a priori* profile was constructed. An enhancement of 200% was then applied to this profile in a layer stretching from the surface (1100 mb) to 900 mb. This layer was then moved successively upwards through the profile in 200 mb steps to form 7 test profiles each with a 200 mb wide CO enhancement covering a

particular MOPITT retrieval level. The averaging kernels of interest were then applied to each of the profiles using the method described in section 3.1.

3.4.2 Results

3.4.2.1 Ideal Case

In this simulation, idealised MOPITT averaging kernels were constructed which comprise a delta function with a peak of unity at the reported altitude and zero everywhere else, see Figure 3.45. The effect of applying averaging kernels such as these to the test profiles can be seen in Figure 3.46. The enhanced CO plume in each of the test profiles is represented by an enhancement in the retrieved MOPITT profile of the same magnitude and is at the correct retrieval level. This is because each retrieved level is only sensitive to the CO profile at that level and CO concentrations at all other levels have no effect.

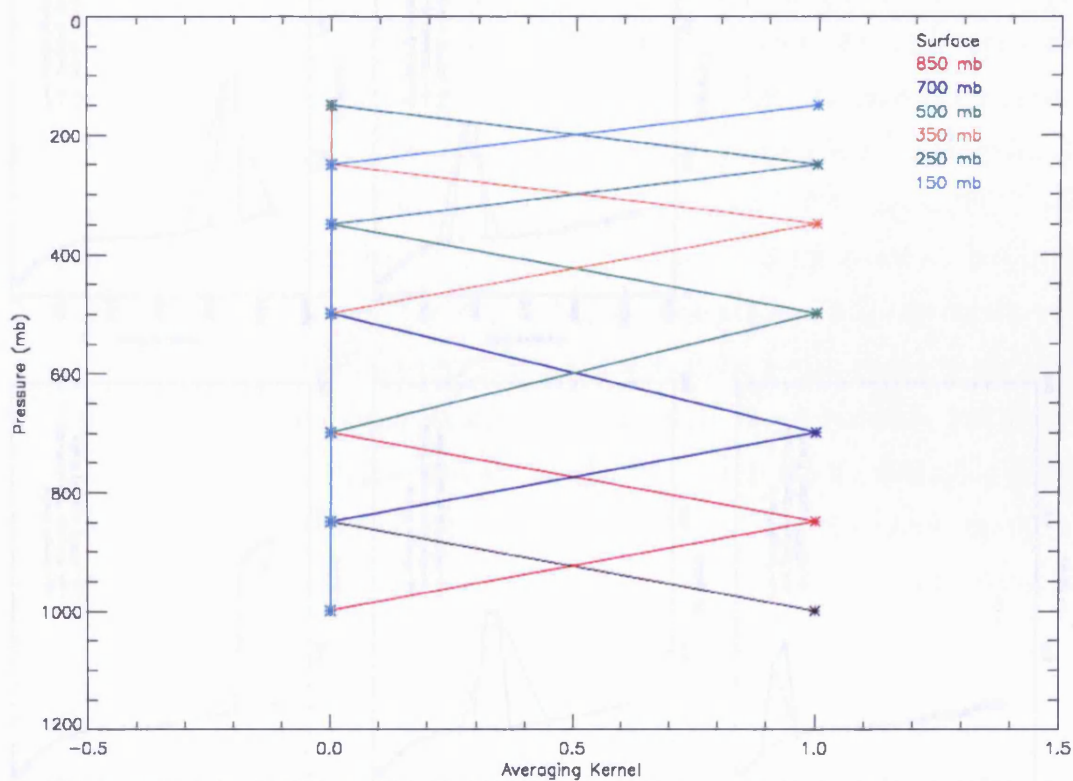


Figure 3.45: Idealised MOPITT averaging kernels. Each averaging kernel peaks at unity at the chosen level and is zero at all other levels.

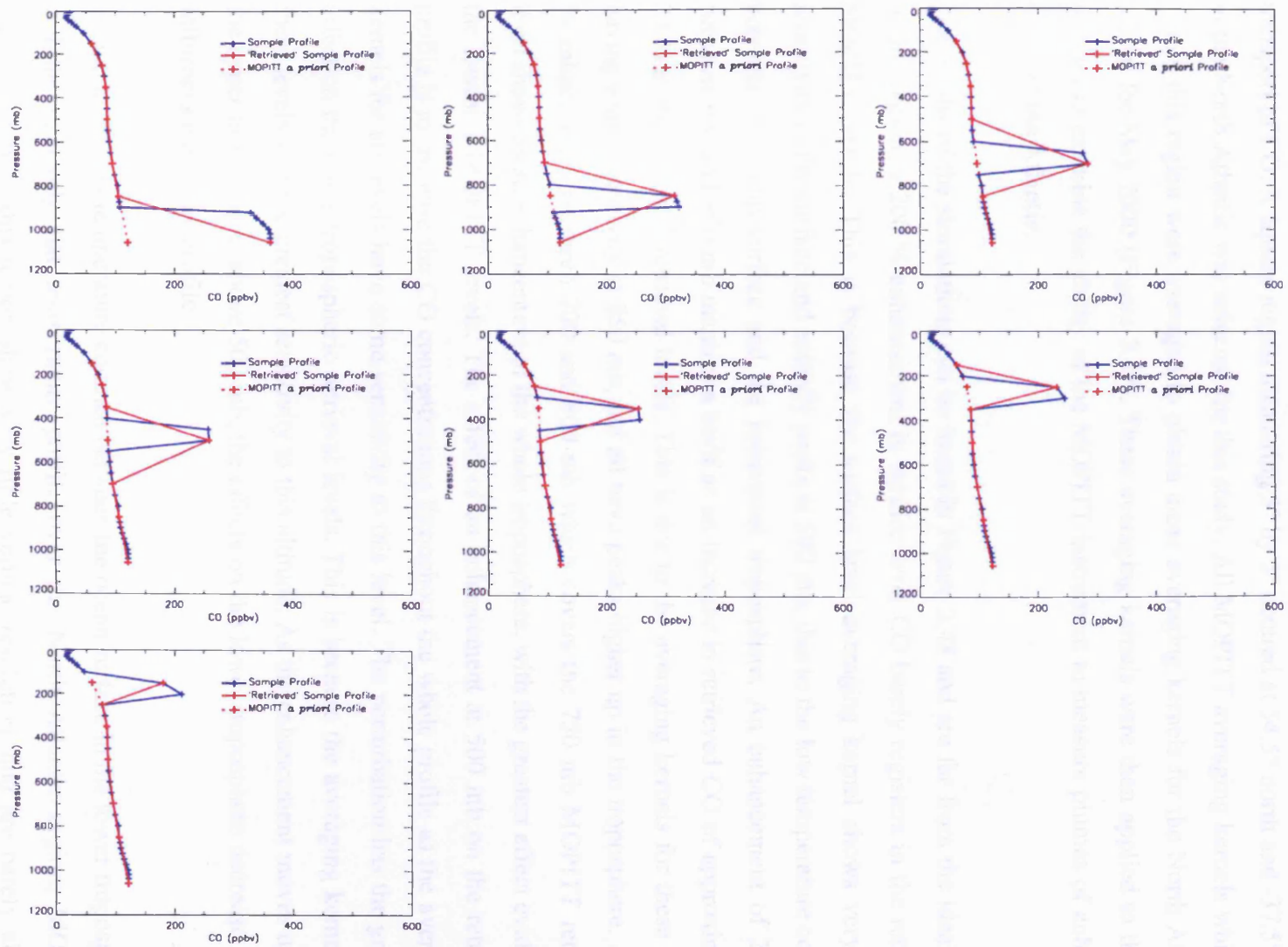


Figure 3.46: Results of simulations conducted using ideal MOPITT averaging kernels

3.4.2.2 North Atlantic May 2000

The North Atlantic region is an important region when examining the intercontinental transport of CO. A square region measuring 5° by 5° centred at 54.5° north and -37.5° west in the North Atlantic was selected for this study. All MOPITT averaging kernels which lie within this region were averaged to obtain mean averaging kernels for the North Atlantic region for May 2000 (Figure 3.47). These averaging kernels were then applied to the test profiles to examine the ability of the MOPITT instrument to measure plumes of enhanced CO over the Atlantic.

The results of the simulations can be found in Figure 3.48 and are far from the ideal case. In this region, a 200 % enhancement in surface level CO barely registers in the retrieved MOPITT profile. This is because the surface level averaging kernel shows very little sensitivity to the surface and actually peaks at 500 mb, due to the low temperature contrast between the ocean surface and the lowermost troposphere. An enhancement of 200 % between 800 and 900 mb manifests itself as an increase in retrieved CO of approximately 20 % at the lowest 3 retrieval levels. This is due to the averaging kernels for these levels having some sensitivity at 850 mb, but all have peaks higher up in the troposphere. A 200 % enhancement between 700 and 800 mb which covers the 750 mb MOPITT retrieval level shows as an enhancement of the whole troposphere, with the greatest effect evident in the lowest 3 MOPITT levels. The effect of an enhancement at 500 mb on the retrieved profile is to increase the CO concentrations throughout the whole profile as the averaging kernels for all levels have some sensitivity to this level. The perturbation has the greatest effect on the lower tropospheric retrieval levels. This is because the averaging kernels for these levels all have greatest sensitivity to this altitude. As the enhancement moves up into the upper troposphere, above 500 mb, the effects on the lower troposphere decrease and it influences the whole profile.

Owing to the low temperature contrast between the ocean surface in the lower troposphere, and the relatively flat temperature profile over the North Atlantic region, MOPITT measurements in this region show very little vertical resolution, and are barely able to distinguish between lower and upper tropospheric CO. The measurements are most sensitive to changes in CO in the mid troposphere between 700 and 350 mb with no sensitivity to the surface.

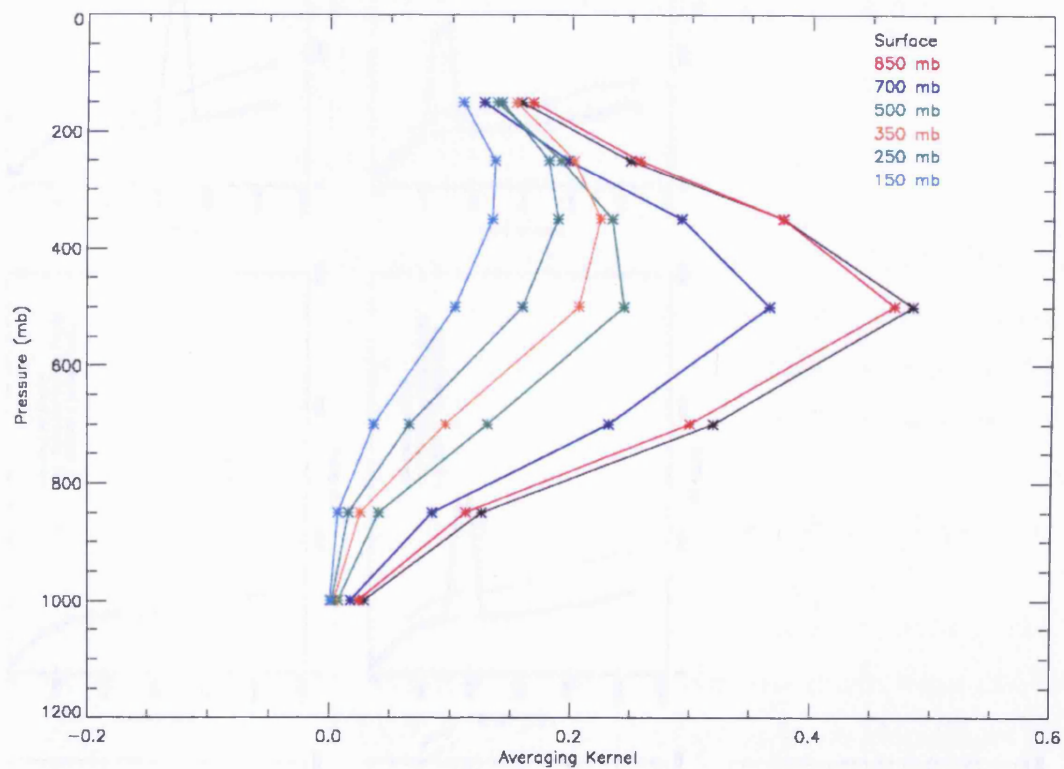


Figure 3.47: Mean MOPITT averaging kernels for the North Atlantic in May 2000

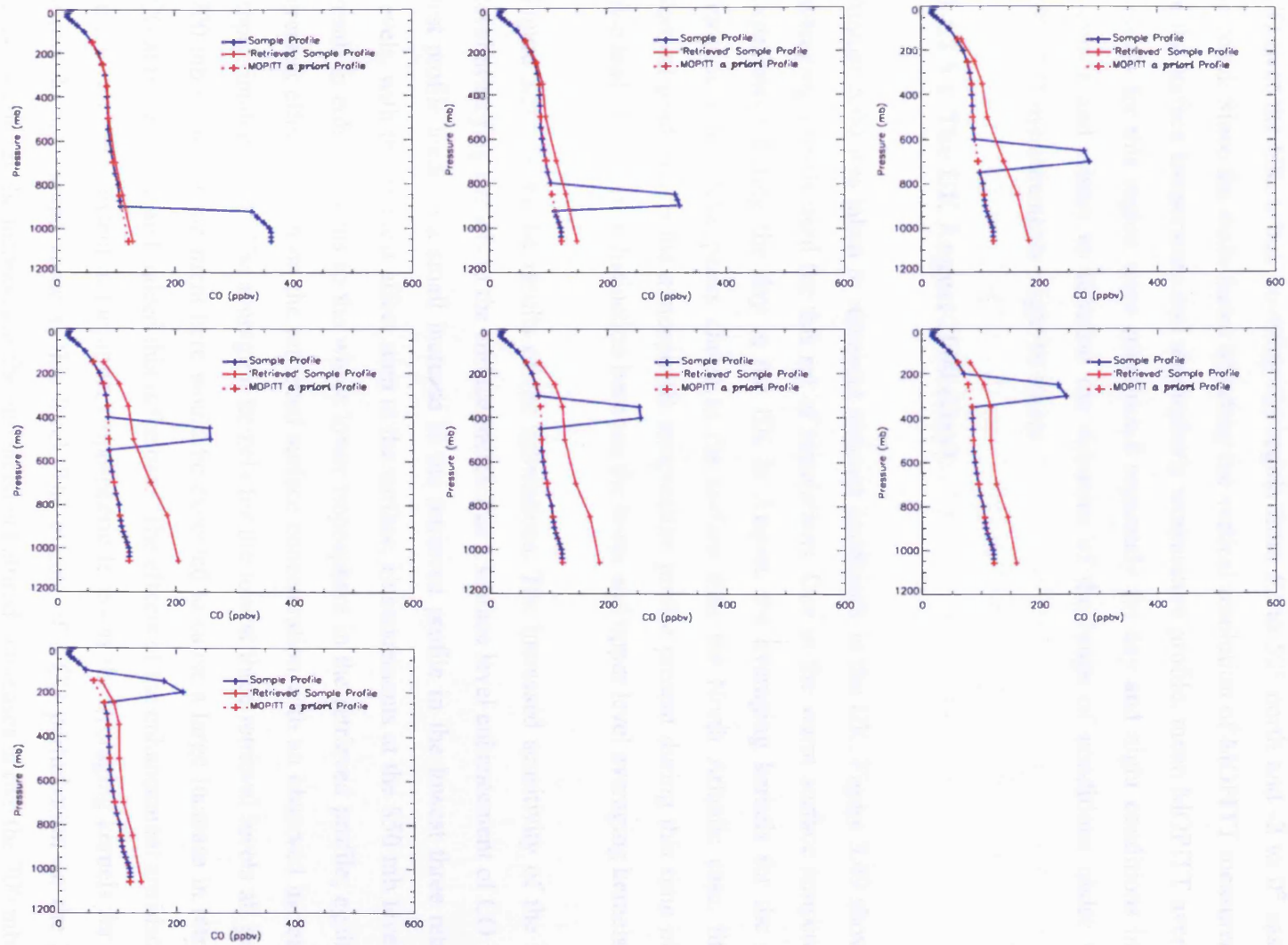


Figure 3.48: Results of simulations conducted using mean averaging kernels for the North Atlantic in May 2000

3.4.2.3 The UK

In order to examine the ability of the MOPITT instrument to measure plumes of enhanced CO over the UK, a box covering the region from 52 to 53° north and -2 to 0° east was selected. Since the main factor affecting the vertical resolution of MOPITT measurements is the surface temperature and atmospheric temperature profile, mean MOPITT averaging kernels for this region were constructed separately for day and night conditions in both summer and winter to simulate the extremes of the range of conditions under which MOPITT measurements might be taken.

3.4.2.3.1 The UK August 2000 (Day)

August 2000 was taken to represent summer conditions in the UK. Figure 3.49 shows the averaging kernels used for this set of simulations. Due to the warm surface temperatures experienced during the day in the UK in August, the averaging kernels for the lower retrieval levels have peaks closer to the surface than the North Atlantic case. Steeper vertical gradients in the atmospheric temperature profile present during this time of year also lead to more of a distinction between the lower and upper level averaging kernels.

Figure 3.50 shows the results of the simulations. The increased sensitivity of the lower level averaging kernels to the surface means that a surface level enhancement of CO in the test profile leads to a small increase in the retrieved profile in the lowest three retrieval levels, with the greatest effect seen at the surface. Enhancements at the 850 mb level also result in enhancements to the whole lower troposphere in the retrieved profile; again, the greatest effect is seen on the retrieved surface concentration with an observed increase of approximately 80%. The averaging kernels for the lowest three retrieval levels all peak at 700 mb so an enhancement here would be expected to cause a large increase in retrieved CO at these levels, and indeed this is the case. The effects of the enhancement are also seen to a much lesser extent in the upper tropospheric levels as the averaging kernels for these levels do have some value at this level. The effects of a CO perturbation on the lower tropospheric levels decreases as the enhancement altitude increases above the 700 mb level as the averaging kernels for these levels fall away. An enhancement at 500 mb has an effect on the whole of the retrieved profile, although the effects are more pronounced in the lower troposphere. The results show that increased CO concentrations in the upper

troposphere have the greatest effect on the upper tropospheric retrieved profile, with enhancements above 300 mb actually acting to reduce the retrieved CO concentrations at the surface and in the lower troposphere in the retrieved profile. This is due to the averaging kernels for the lower levels having negative values above this altitude, indicating that increasing the CO in the upper troposphere will lead to a decrease in the retrieved concentrations in the lower troposphere.

These results show that under the conditions used in this simulation, the MOPITT instrument is able to differentiate between upper and lower tropospheric enhancements in CO, with greatest sensitivity to the lower troposphere at 700 mb, and at 350 mb in the upper troposphere. The simulations also indicate some sensitivity to the surface.

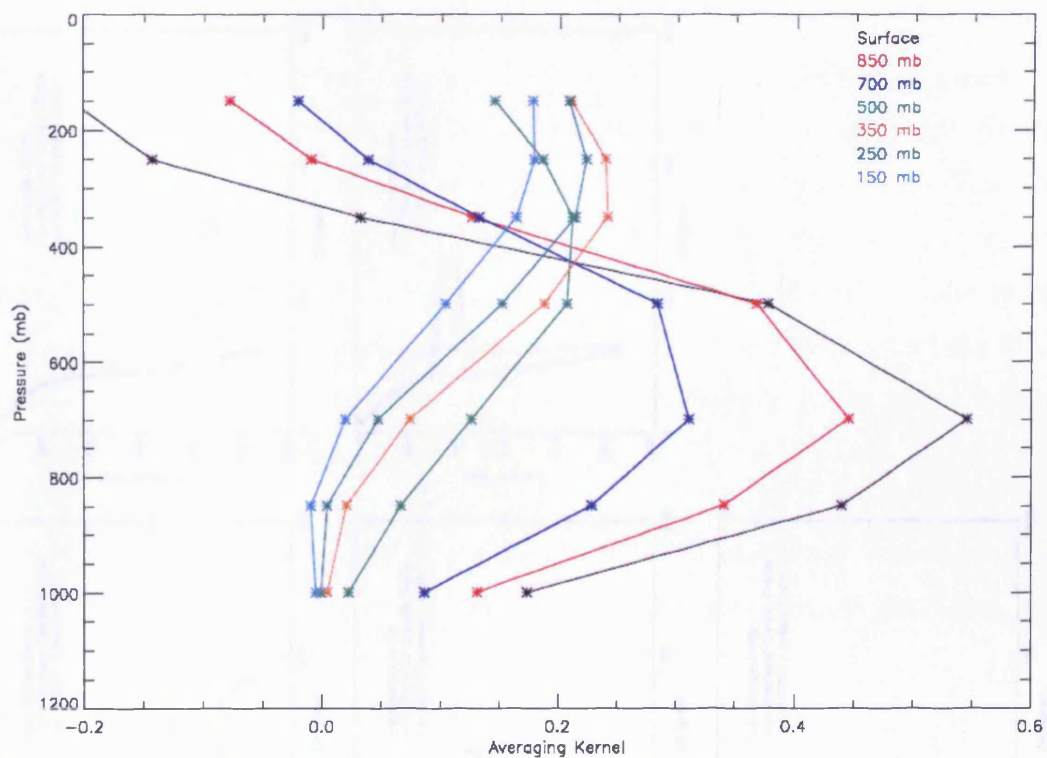


Figure 3.49: Mean daytime MOPITT averaging kernels for the UK in August 2000

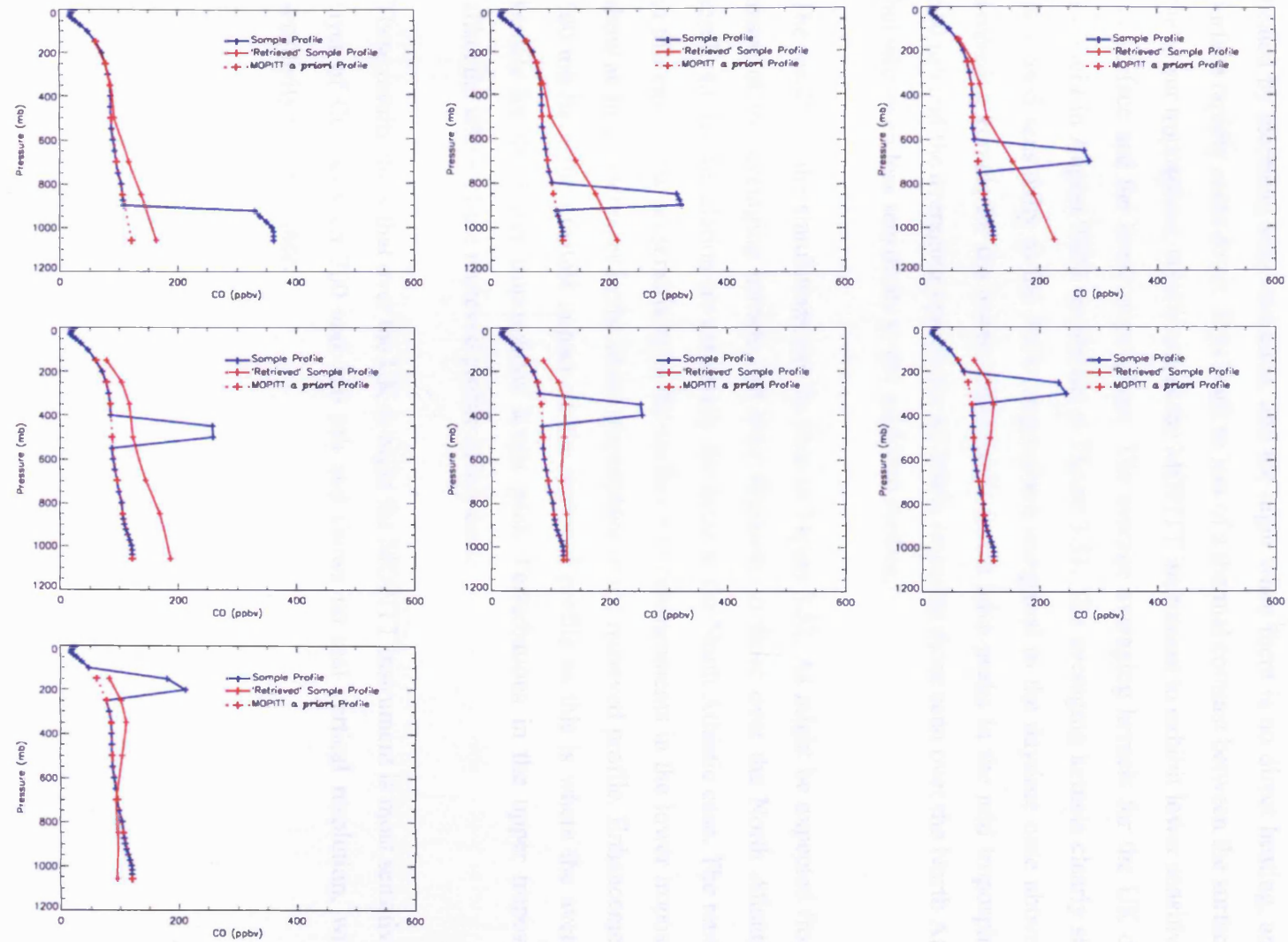


Figure 3.50: Results of simulations conducted using mean daytime averaging kernels for the UK in August 2000

3.4.2.3.2 The UK August 2000 (Night)

The surface temperature over land can vary rapidly between the day, when the surface is heated by incoming solar radiation, and the night when there is no direct heating, and the surface rapidly cools down. This leads to less of a thermal contrast between the surface and the lower troposphere, which causes the MOPITT instrument to exhibit lower sensitivity to the surface and the lower troposphere. The average averaging kernels for the UK during the night in August 2000 are shown in Figure 3.51. The averaging kernels clearly show a decreased sensitivity to the lower troposphere compared to the daytime case above. The averaging kernels for the lower tropospheric levels have peaks in the mid troposphere at 500 mb and the averaging kernels for all levels resemble those seen over the North Atlantic but with even less sensitivity to the cold land surface.

The results of the simulations can be seen in Figure 3.52. As might be expected from the shape of the averaging kernels and their similarity to those over the North Atlantic the results of this simulation are essentially the same as the North Atlantic case. The retrievals in this case show no sensitivity to the surface and enhancements in the lower troposphere show as small increases in the lower troposphere in the retrieved profile. Enhancements at 500 mb have the greatest impact on the retrieved profile as this is where the averaging kernels for the lower tropospheric levels peak. Perturbations in the upper troposphere affect the whole of the retrieved profile in this case.

These results show that over the UK at night the MOPITT instrument is most sensitive to a layer of CO between 700 and 350 mb and shows no real vertical resolution, with no sensitivity to the surface.

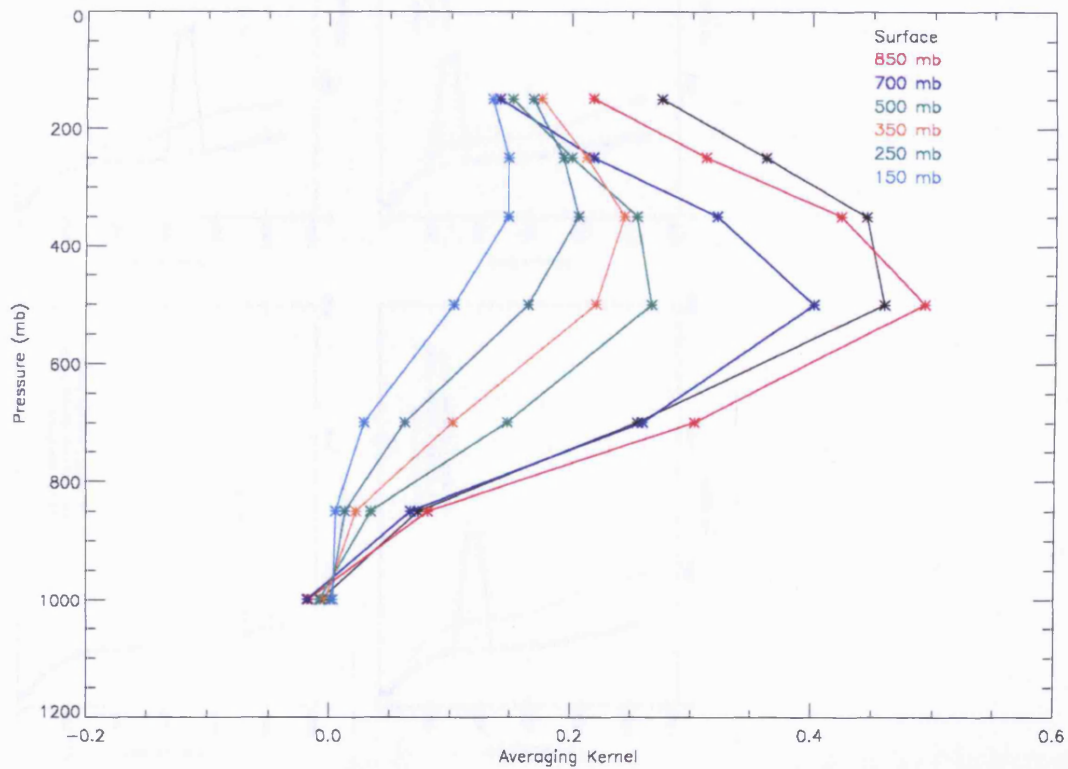


Figure 3.51: Mean night time MOPITT averaging kernels for the UK in August 2000.

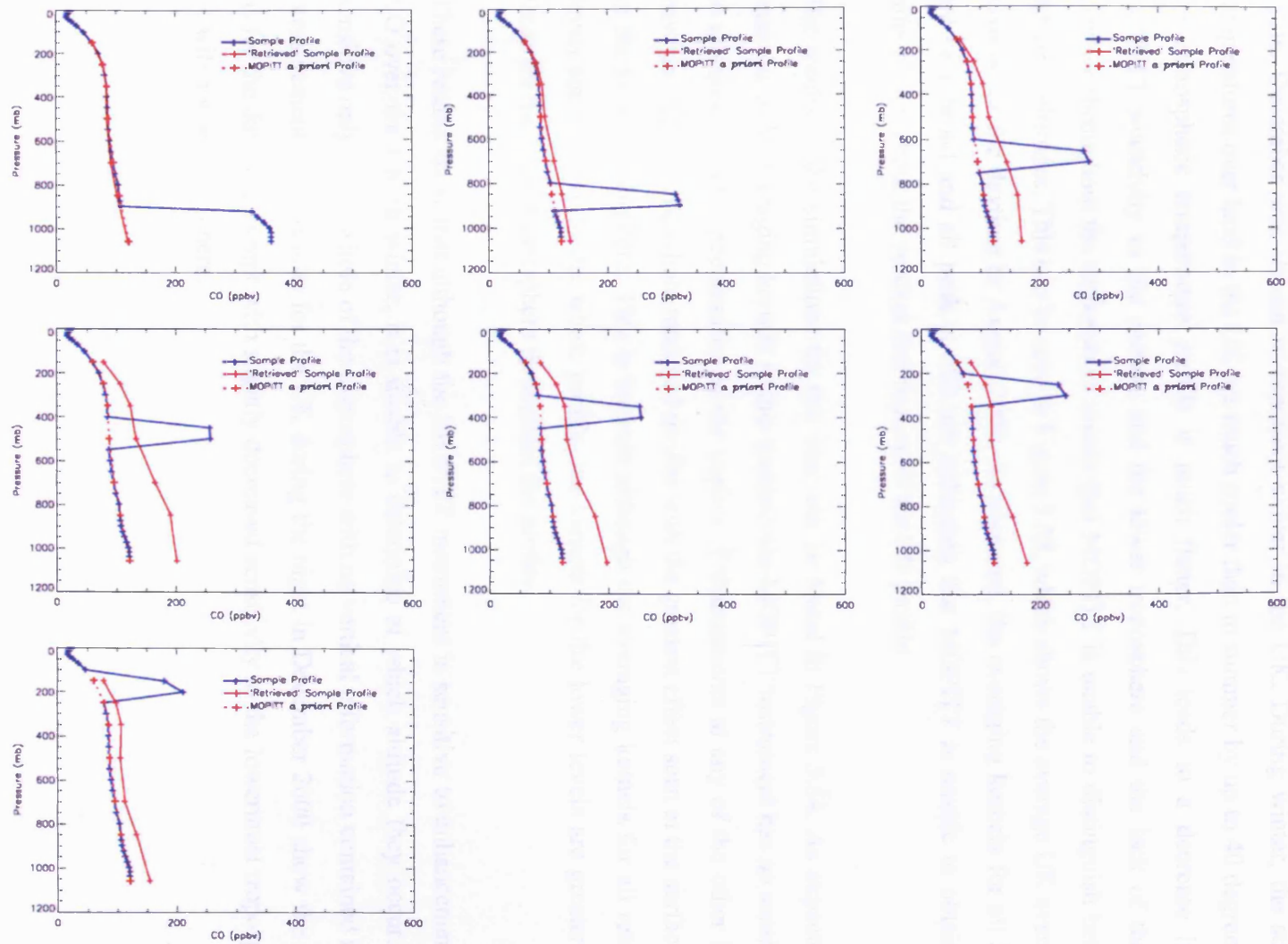


Figure 3.52: Results of simulations conducted using mean night time averaging kernels for the UK in August 2000

3.4.2.3.3 The UK December (Day) 2000

As well as the diurnal variation in surface temperature over land, there is also a seasonal cycle. December was chosen to represent winter in the UK. During winter, the surface temperatures over land in the UK are much cooler than in summer by up to 40 degrees and the atmospheric temperature profile is much flatter. This leads to a decrease in the MOPITT sensitivity to the surface and the lower troposphere and the lack of thermal contrast throughout the troposphere means that MOPITT is unable to distinguish between different altitudes. This can be seen in Figure 3.53, which shows the average UK averaging kernels for the daytime in August 2000. As expected, the averaging kernels for all levels are very broad and all peak at 500 mb indicating that MOPITT is unable to obtain any information about the vertical distribution of the CO profile.

The results of the simulations for this case can be found in Figure 3.54. As expected by examining the averaging kernels in this scenario the MOPITT instrument has no sensitivity to changes in CO concentrations at the surface. Enhancements at any of the other levels have an affect on the whole retrieved profile with the greatest effect seen at the surface and in the lower troposphere. This is because although the averaging kernels for all retrieval levels are sensitive to the whole profile, the kernels for the lower levels are greater than those for the upper troposphere throughout the profile.

These results show that although the MOPITT instrument is sensitive to enhancements in CO over the UK in winter, it is unable to determine at which altitude they occur. It is sensitive only to the whole of the troposphere with no vertical information contained in the measurements. The results for the UK during the night in December 2000 show the same as for the day case except with slightly decreased sensitivity to the lowermost troposphere so will not be shown here.

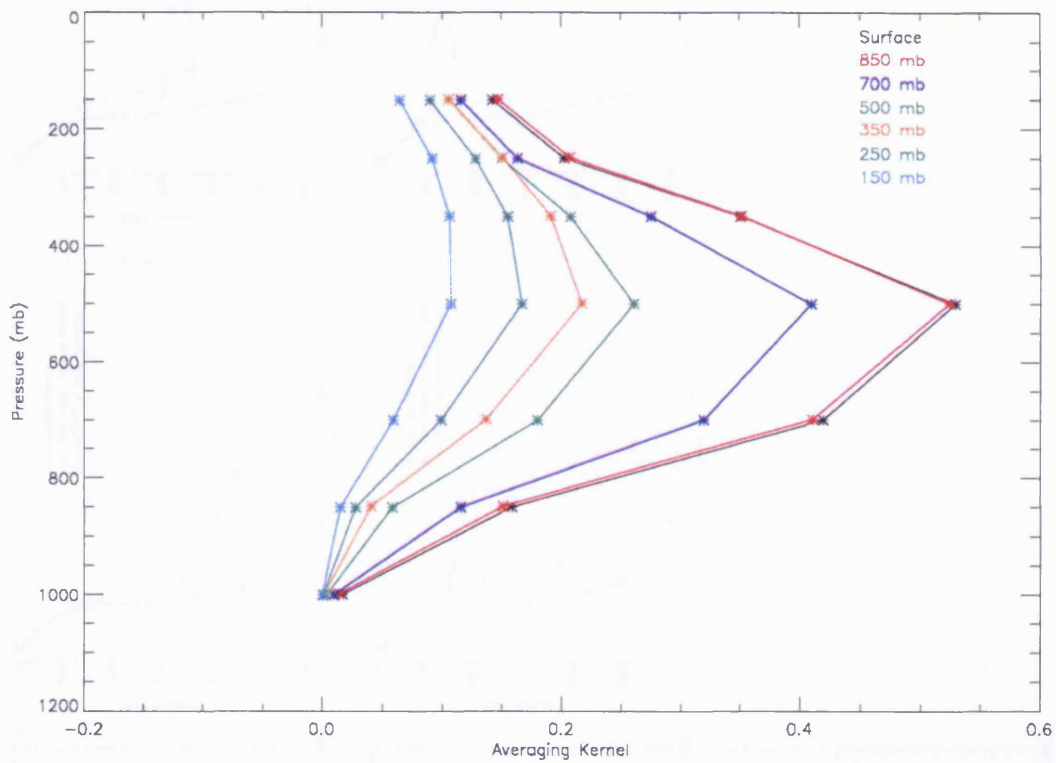


Figure 3.53: Mean daytime MOPITT averaging kernels for the UK in December 2000

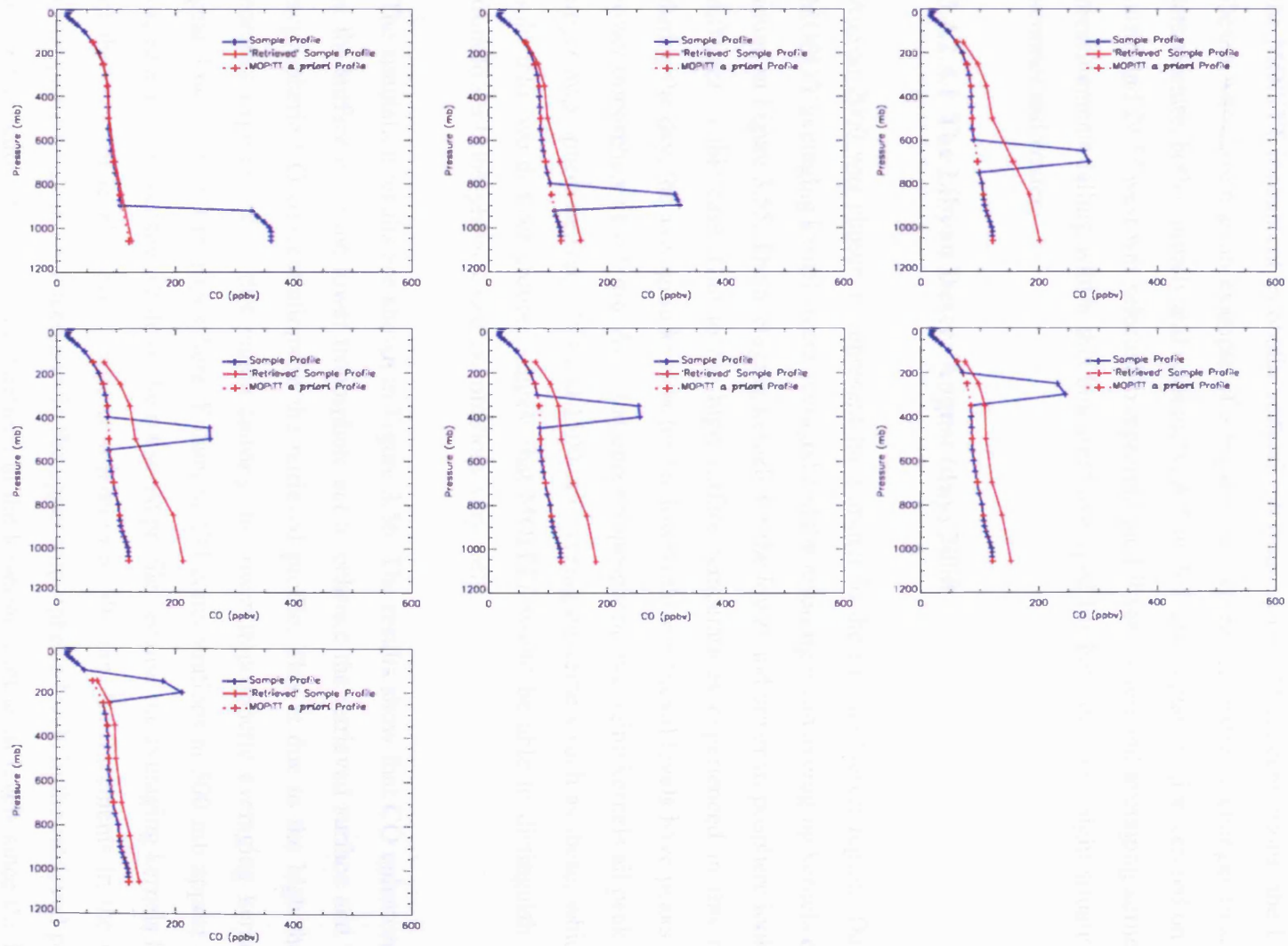


Figure 3.54: Results of simulations conducted using mean daytime averaging kernels for the UK in December 2000

3.4.2.4 The Libyan Desert

Since the surface temperature of the measurement scene has a great effect on the ability of the MOPITT instrument to obtain vertical information on CO concentrations, the Libyan Desert was chosen as an example of a region that experiences extreme changes in surface temperature, both diurnally and seasonally. A 5 by 5 degree square region centred on 23.5° north and 24.5° west was selected to represent the Libyan Desert and averaging kernels for measurements falling within this box were averaged for both day and night situations in summer and winter.

3.4.2.4.1 The Libyan Desert August (day) 2000

August 2000 was chosen to represent the summer in the Libyan Desert region. Daytime MOPITT averaging kernels were averaged and the resulting mean averaging kernels can be found in Figure 3.55. The averaging kernels for the lower and upper troposphere look very different in this case. Due to the high surface temperatures experienced in this region during the day, the averaging kernels for the lowest three retrieval levels have peaks in the lower troposphere at 700 mb. Also, the upper tropospheric averaging kernels all peak in the upper troposphere between 250 and 1500 mb. Averaging kernels such as these, which are split into two distinct groups, suggest that MOPITT would be able to distinguish upper from lower tropospheric CO concentrations very well.

The simulation results are shown in Figure 3.56. The results show that CO enhancements at the surface or in the lower troposphere act to enhance the retrieved surface and lower tropospheric CO concentrations in the retrieved profile. This is due to the high thermal contrast experienced in this region causing the lower tropospheric averaging kernels to peak low down in the troposphere. Enhanced CO concentrations at 500 mb appear as an increase in CO over the whole of the retrieved profile because the averaging kernels for all of the retrieval levels have a large contribution at 500 mb. Enhancements in the upper troposphere result in enhancements in the upper tropospheric levels in the retrieved profile and act to reduce the CO concentrations in the lowermost retrieval levels since the lower tropospheric averaging kernels have a negative peak in the upper troposphere.

These results demonstrate that under the conditions simulated here the MOPITT instrument is able to distinguish upper and lower tropospheric CO concentrations very well. This is due to the large thermal contrast between the surface and the atmosphere experienced over such a region in summer.

The results of simulations for the Libyan Desert at night in August are extremely similar to those for August at night in the UK and therefore will not be shown here. Simulations were also performed for the Libyan Desert during daytime in December 2000 but due to the quite stable nature of the surface temperature of desert regions, which show little seasonal variation during the day, the results are very similar to those for the same region during the day in August and so will not be shown.

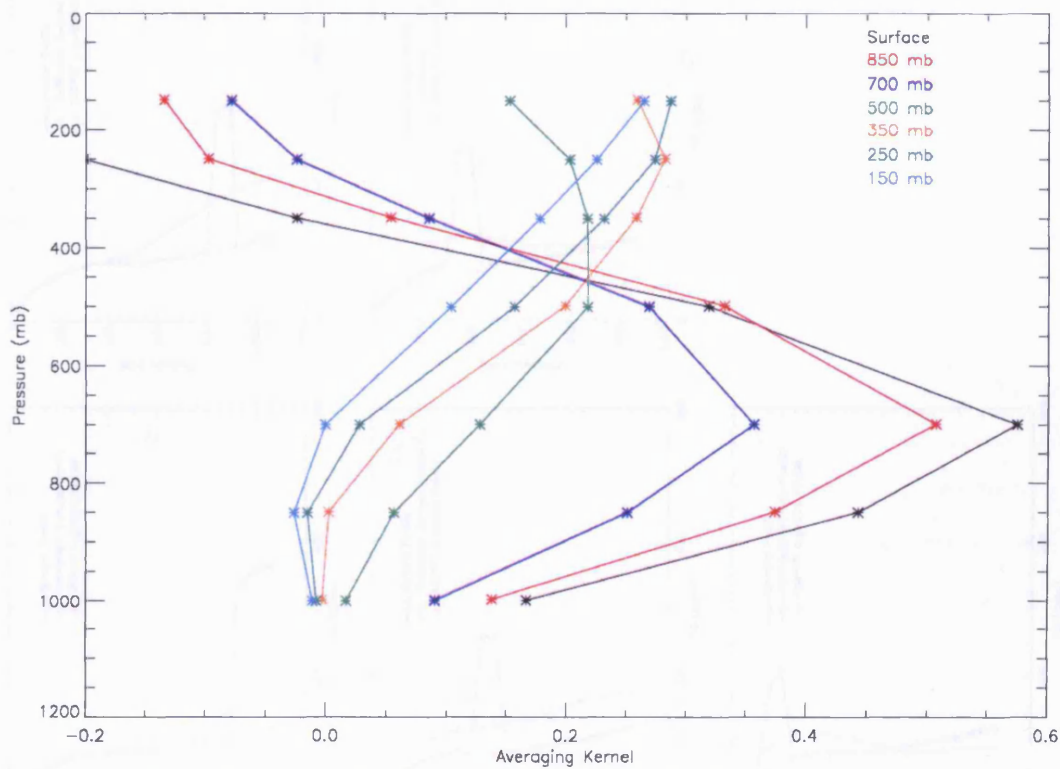


Figure 3.55: Mean daytime MOPITT averaging kernels for the Libyan Desert in August 2000.

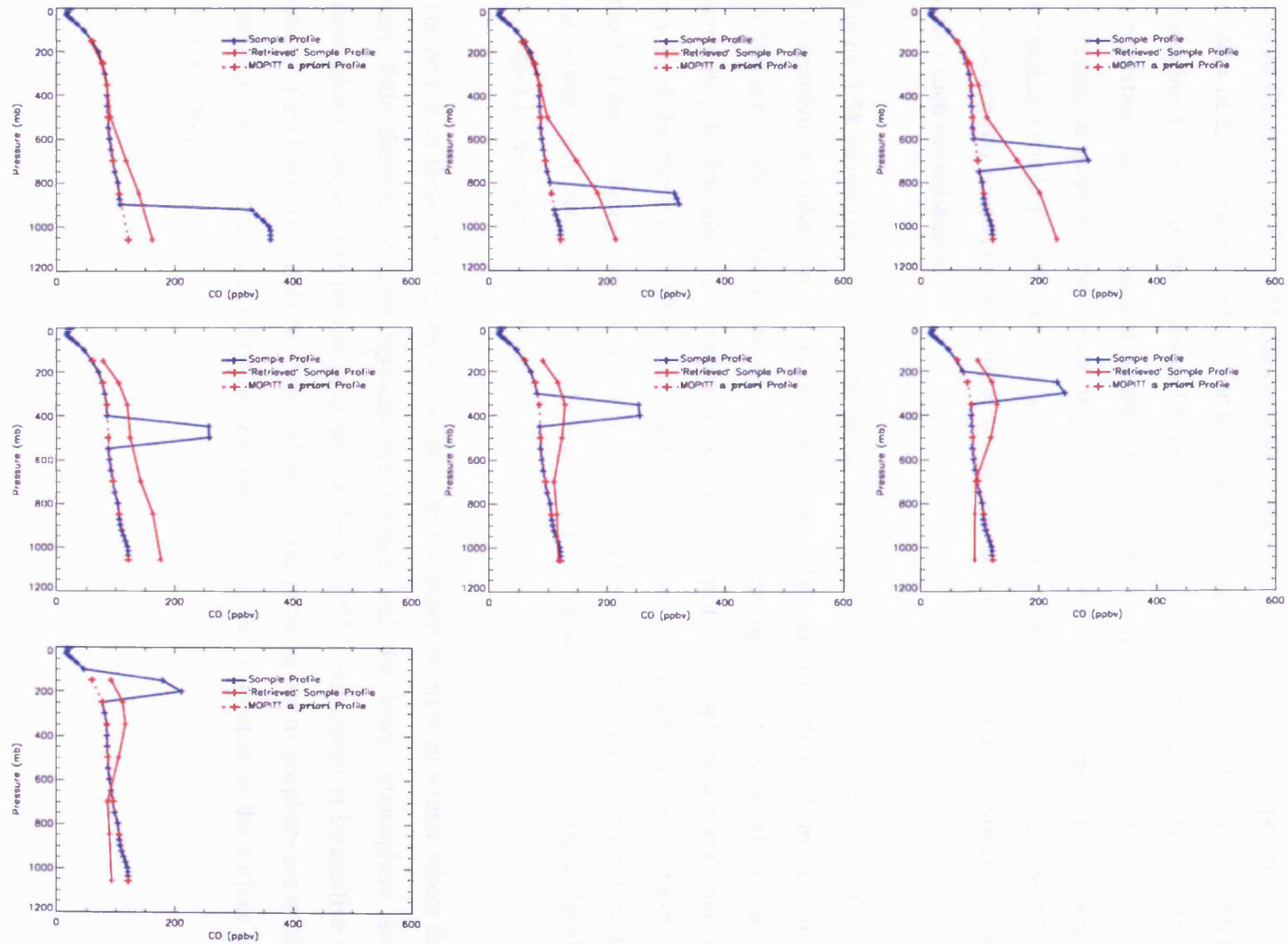


Figure 3.56: Results of simulations conducted using mean daytime averaging kernels for the Libyan Desert in August 2000

3.4.2.4.2 The Libyan Desert December (Night) 2000

Owing to the very large diurnal variations in temperature experienced in desert regions, the Libyan Desert at night in December experiences very cold surface temperatures. This is evident in the averaging kernels for the region, Figure 3.57 shows the average MOPITT averaging kernels for the Libyan Desert at night in December 2000. Due to the cold temperatures, and little thermal contrast between the lower atmosphere and the surface, the averaging kernels for the lower troposphere all peak in the upper troposphere. The averaging kernels for all retrieval levels look very similar indicating that the MOPITT instrument has no vertical resolution and is only sensitive to CO in the upper troposphere under such circumstances.

Figure 3.58 shows the results of the simulations. As expected, the retrieved profiles show no sensitivity to enhancements in the lower troposphere below 500 mb. Limited sensitivity to 500 mb is shown due to the averaging kernels for most retrieval levels having some sensitivity to this altitude. Enhancements in the upper troposphere are reflected in the whole of the retrieved profile with greatest sensitivity to perturbations at 350 mb, where most of the averaging kernels peak. Upper tropospheric enhancements are most evident in the lower three retrieved profile levels as the averaging kernels for these levels are strongest in the upper troposphere.

The results of these simulations show that over the desert at night in winter where there is very little thermal contrast between the surface and the lower atmosphere and the atmospheric temperature profile is quite flat the MOPITT instrument is insensitive to the whole of the lower troposphere. Only enhancements in the upper troposphere are evident in retrieved profiles and their affect on the retrieved profile is greatest at the surface and in the lower troposphere.

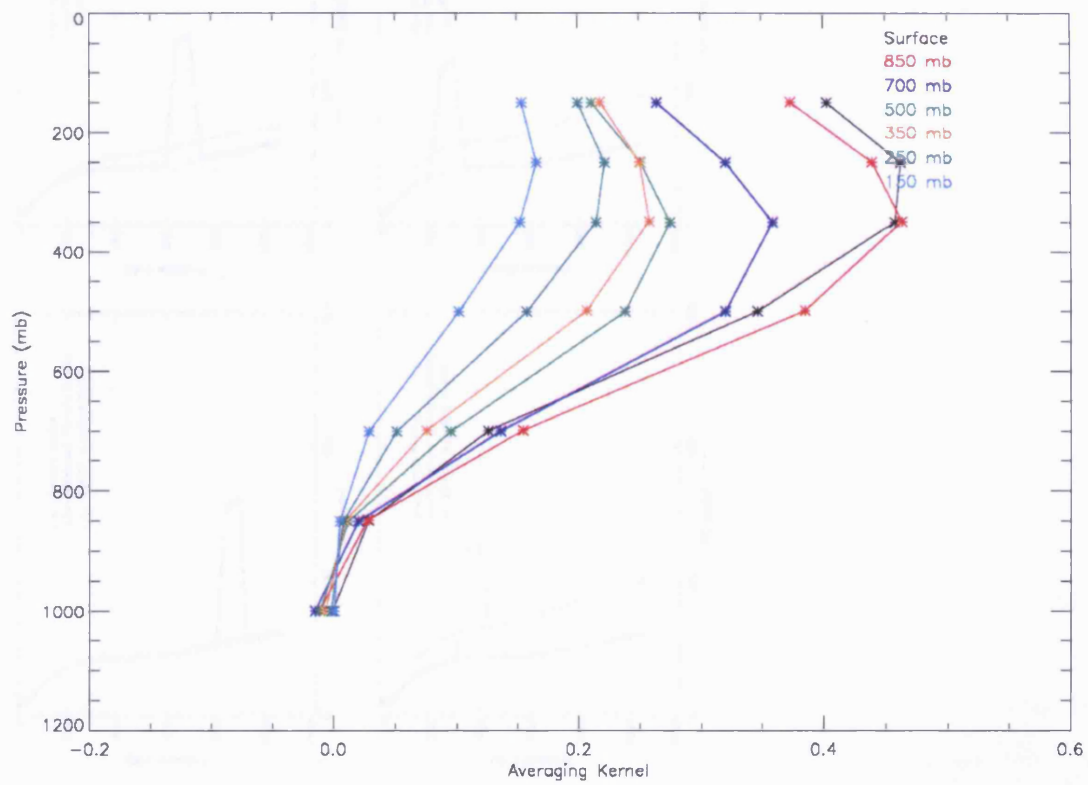


Figure 3.57: Mean MOPITT averaging kernels for the Libyan Desert at night in December 2000

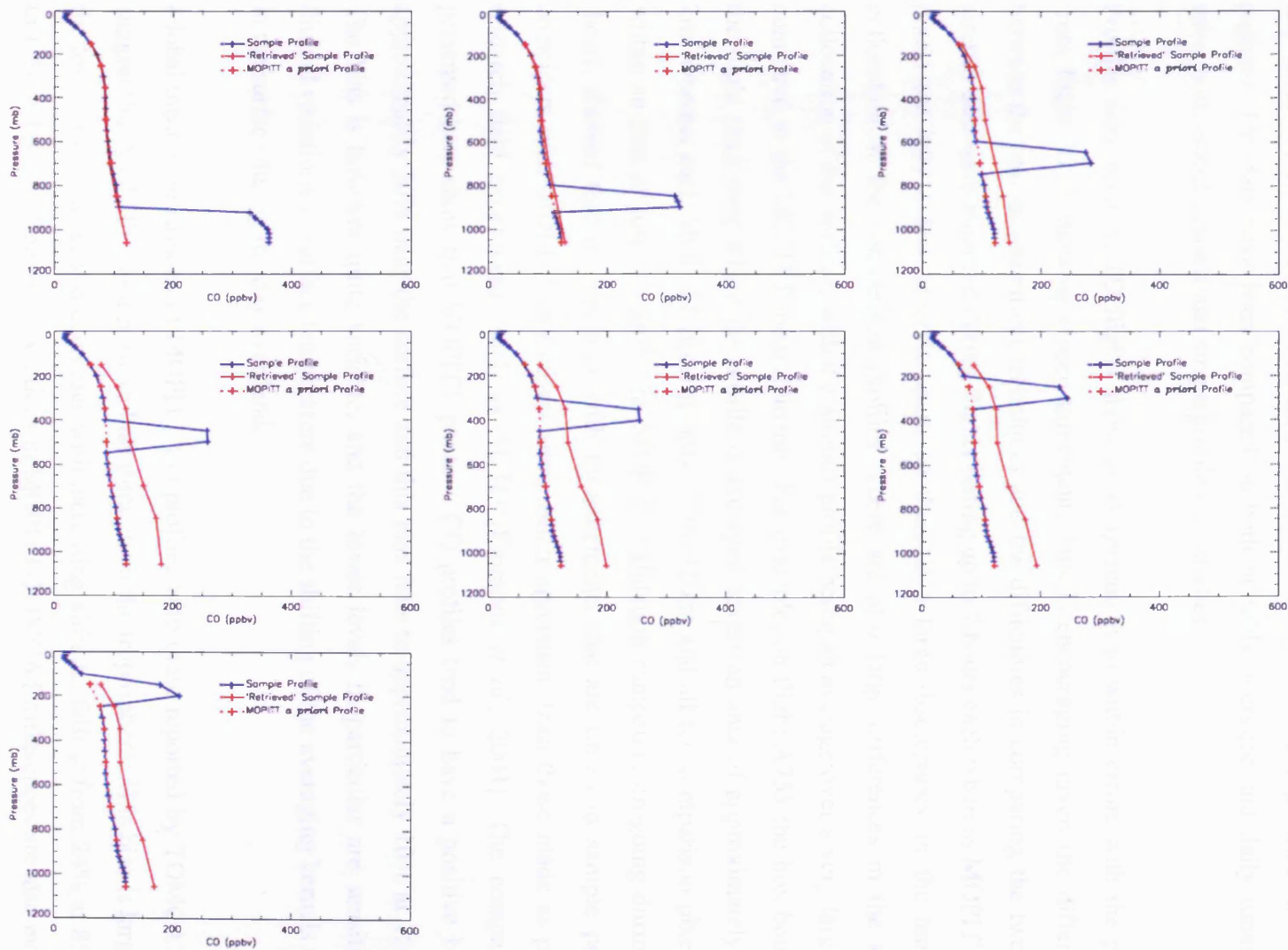


Figure 3.58: Results of simulations conducted using mean night time averaging kernels for the Libyan Desert in December 2000

3.5 Summary

Phase 1 profiles of CO from the MOPITT instrument have been compared to both *in situ* and model data in order to determine the characteristics of such profiles in varying regimes. The data have been compared on both monthly averaged and daily timescales using both global datasets and single profile case studies

Profiles from both ACTO flights show good agreement to within errors with the profile from flight A755 showing closer agreement. This is encouraging given the differences between the two measurement techniques and the difficulties in comparing the two. The aircraft data were recorded during flights lasting up to 7 hours each whereas MOPITT data pixels are only a few seconds apart, so there is a large discrepancy in the temporal collocation of the comparison profiles. There are also large differences in the spatial collocation of the profiles, with the aircraft profile being an average over a very large area compared to the MOPITT measurements. For example, on flight A755 the box bounding the flight track over which the profile is averaged covers an area of approximately 2800 km² whereas each MOPITT pixel is only 22 by 22 km and all ten comparison pixels fall within an area of just 216 km². The MOPITT validation campaign, on-going during this thesis, showed that comparisons with measurements that are timed to sample profiles coincident with MOPITT overpasses show better agreement than those made as part of research field experiments such as ACTO [Emmons *et al.*, 2004]. The comparisons presented here show that MOPITT phase 1 CO profiles tend to have a positive bias of approximately 20% near the surface and this bias falls to approximately 10% at 150 mb. The bias is however quite variable, and the lower levels in particular are sensitive to diurnal variations in surface temperature due to the shifting of the averaging kernels closer to the surface during the day over land.

Global mean comparisons of MOPITT CO profiles with those reported by TOMCAT also suggest that MOPITT has a positive bias throughout the troposphere. This bias is largest in the lower troposphere, and decreases with increasing altitude, falling from 24% at 850 mb to 11% at 150 mb. Regional variations in MOPITT-TOMCAT differences are also evident, with the largest differences observed near TOMCAT source regions. For example, excluding Antarctica, where snow and ice cover may affect the MOPITT retrievals. The only locations where the 'retrieved' TOMCAT CO levels are higher than those of

MOPITT are over a very intense TOMCAT emission in the region of Calcutta and a smaller source region over northeast Columbia. Conversely over Mexico City, MOPITT reports higher CO levels than TOMCAT of up to 50%. These differences could indicate that the sources in the model may give approximately the correct amount of CO release globally, but the relative strengths of the different source locations may be underestimated. Large differences are also observed over the North Pacific off the east coast of Russia and over Japan, stretching as far as the west coast of the U.S. These differences indicate that the model may underestimate the amount of CO transport across the North Pacific.

Zonal mean comparisons of MOPITT and TOMCAT CO profiles are excellent, with correlation coefficients of in excess of 0.97 for all altitudes. These comparisons also suggest a positive bias in MOPITT data of approximately 25% at the surface, falling to approximately 5% at 150 mb. However, these biases vary considerably with latitude. The largest differences are observed in the lower troposphere, over those latitudes which contain strong source regions such as 30-50 degrees north, which encompasses strong North American, European and East Asian sources. These differences may again be due to problems with source strengths, or with the transport of CO from sources in the boundary layer up to the free troposphere in the TOMCAT model.

Comparisons of MOPITT profiles with those reported by the TOMCAT model show that one must be careful when interpreting MOPITT profiles in differing regimes. The results suggest that in regions of low CO concentrations, where the air is considered to be well mixed in the vertical, MOPITT profiles may be used to represent the real atmosphere, although a positive bias in the lower troposphere still remains. In the Northern Hemisphere, where background CO concentrations tend to be higher, MOPITT profiles obtained over both ocean and land scenes present a good representation of the mid troposphere between 850 and 250 mb with greater sensitivity to the surface over land. The MOPITT measurements seem to have a decreased sensitivity to the polluted boundary layer compared to the mid-troposphere, but do show enhancements when the surface level enhancement is sufficiently high (approximately 90% in the cases studied) to shift the averaging kernel sensitivity towards the surface such as in source regions.

The results of comparisons of MOPITT with *in situ* aircraft and TOMCAT model data appear to be consistent with the results of the MOPITT validation campaign [Emmons, *et*

al., 2004], published during the course of this thesis. However, the interpretation of the TOMCAT results is further complicated by uncertainties in the validity of the model data. Therefore, it is difficult to determine if the observed differences are truly representative of biases in the MOPITT data, or simply due to errors in the model field.

The results presented here indicate that MOPITT profiles should be used with care in examining tropospheric CO concentrations. The need to take into account the *a priori* influence and averaging kernels used in the retrieval of such profiles is evident. Wherever possible, correlative measurements such as *in situ* or model data should be used in conjunction with MOPITT in order to gain a much fuller understanding of the behaviour of CO in the troposphere.

Simulations were performed using MOPITT averaging kernels to examine the ability of the instrument to identify CO enhancements with limited vertical extent. The results of this study show that the ability of the MOPITT instrument to obtain measurements of the vertical structure of CO depends greatly on both the surface and atmospheric conditions of the measurement scene. Surface temperature plays a key role in determining whether or not MOPITT has sensitivity to the lower troposphere, and this parameter can vary greatly with location, time of day and season of the year.

Water has a large heat capacity and so sea surface temperature varies very slowly with time. This means that there is not much difference in surface temperature between day and night over ocean scenes and therefore the vertical resolution of MOPITT measurements made over such areas does not have an appreciable diurnal variation due to surface temperature changes. There is also little seasonal variation in averaging kernel shape over a location such as the North Atlantic, where although surface temperatures undergo a seasonal change, this change isn't sufficiently large so as to have an effect on the retrievals. However, MOPITT averaging kernels do show some diurnal variation over ocean scenes. This is likely the result of a difference in the uncertainties in the retrieved surface emissivity between day and night [Emmons *et al.* 2004]. At night, the MOPITT thermal band radiances are more sensitive to surface emissivity, therefore the night time retrievals are less constrained by the *a priori* emissivity values. Since this quantity is retrieved simultaneously, the CO retrievals will have a greater reliance on the *a priori* CO.

This is not the case however over land. The land surface temperature of a scene can vary either very rapidly or quite slowly depending on the type of land and its location. The surface temperature over urban regions such as the UK can vary greatly on both diurnal and seasonal timescales. This is due to the complex surface types found in such regions, which may consist of a mixture of concrete, asphalt and vegetation. The concrete and asphalt are both heated quickly to high temperatures during the day in direct sunlight and quickly cool down in the evening. This behaviour, although somewhat lessened by the presence of the vegetation, has a large effect on the MOPITT averaging kernels for such regions. During the day in the summer, when the surface temperature is high and strong gradients in the atmospheric temperature profile exist, the MOPITT averaging kernels for the lower troposphere peak lower down closer to the surface. This allows the MOPITT instrument to distinguish between upper and lower tropospheric CO concentrations. However, at night or in the winter over the UK the surface temperature is much lower and there is no longer a strong thermal contrast between the surface and the atmosphere. The atmospheric temperature profile is also quite flat and this acts to degrade the vertical resolution of MOPITT, which is no longer able to determine any information about the vertical structure of the CO profile. This effect is much more pronounced over the Libyan Desert, which has a surface consisting predominantly of sand. Sand reacts very quickly to changes in temperature, and during the summer the very high surface temperatures experienced in desert regions enable the MOPITT instrument to obtain a good distinction between lower and upper tropospheric CO concentrations. However, at night during the winter, the very cold temperatures experienced in such regions shift the sensitivity of all the retrieval levels to the upper troposphere, and the instrument is able to obtain information about upper tropospheric CO only. In reality however, the amount of CO in the measured profile also affects the sensitivity of the instrument. Hence, the enhancement itself will have an effect on the averaging kernels and therefore the ability of the instrument to measure it.

The results show that it is possible for the MOPITT instrument to measure layer enhancements of CO under the right circumstances. Although it is possible to detect enhanced CO concentrations over most surface types, in order to gain the most information about the vertical distribution of the enhancement, measurements are best made over land during the summer where there is a large thermal contrast between the surface and the lower atmosphere.

It is therefore possible to use MOPITT data to examine the long range transport of CO providing that considerations such as time of year and surface type are taken into account and the averaging kernels for the retrievals are used to determine the validity of any vertical information.

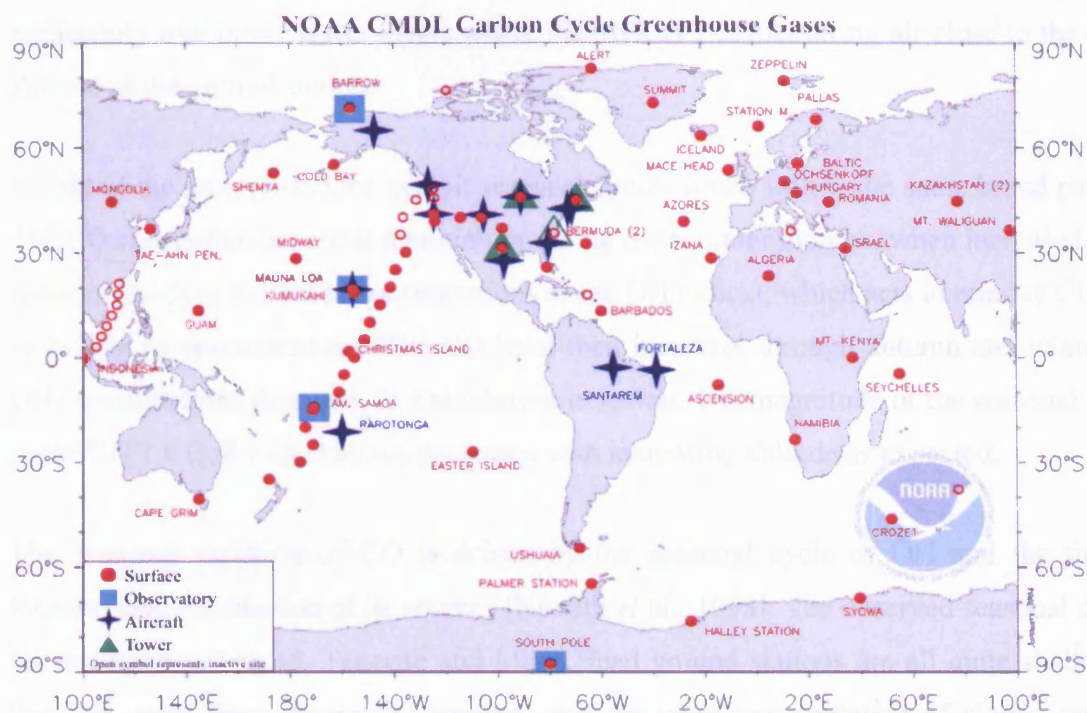
4. The Intercontinental Transport of CO as Measured by the MOPITT Instrument

As described in Section 1.3.4, the intercontinental transport of CO has important consequences for both regional and global air quality. Transport events are episodic in nature and occur on large spatial scales. It is therefore difficult to obtain information on the frequency and distribution of such events on a global scale using *in situ* aircraft and ground station data. Satellite instruments such as MOPITT are able to provide regular global coverage, and so are useful for quantifying these parameters, providing the opportunity to understand the transport of pollution on a global scale.

MOPITT CO profile data exhibits a seasonal cycle due to seasonal variations in background CO levels, owing to local sources and chemistry. Superimposed on this cycle are short term fluctuations which may be caused by transport. In order to examine the intercontinental transport of CO using MOPITT data, it is first necessary to disassociate the seasonal variability from the high frequency short-term fluctuations due to transport. This is achieved by subtracting monthly mean CO concentrations from daily data. The result is a CO anomaly field which indicates daily fluctuations from the mean.

4.1 The Seasonal Cycle In MOPITT CO

Before removing the seasonal cycle from MOPITT data, it is necessary to make sure that the form of this cycle is correctly captured in the data. This is accomplished by comparing monthly mean MOPITT data to *in situ* data collected by surface stations to see if they exhibit similar seasonal trends. The *in situ* data selected for this comparison are taken from surface monitoring sites which form part of the NOAA (National Oceanic and Atmospheric Administration) CMDL (Climate Modelling & Diagnostics Laboratory) CCGG (Carbon Cycle Greenhouse Gases) network (see Figure 4.1).



The NOAA CMDL Carbon Cycle Greenhouse Gases group operates 4 measurement programs. In situ measurements are made at the CMDL baseline observatories: Barrow, Alaska; Mauna Loa, Hawaii; Tutuila, American Samoa; and South Pole, Antarctica. The cooperative air sampling network includes samples from fixed sites and commercial ships. Measurements from tall towers and aircraft began in 1992. Presently, atmospheric carbon dioxide, methane, carbon monoxide, hydrogen, nitrous oxide, sulfur hexafluoride, and the stable isotopes of carbon dioxide and methane are measured. Group Chief: Dr. Pieter Tans, Carbon Cycle Greenhouse Gases, Boulder, Colorado, (303) 497-6678 (pieter.tans@noaa.gov, <http://www.cmdl.noaa.gov/ccgg>).

Figure 4.1: Map of the NOAA CMDL monitoring network (taken from <http://www.cmdl.noaa.gov/ccgg>).

4.1.1 Monthly Mean Comparisons to CMDL surface sites

Table 4.1 shows the six CMDL sites which were selected for comparison, to be representative of North America, the North Atlantic and Europe. A 100 km box was selected around each site, and all daytime MOPITT profiles which fell within these boxes were averaged to form monthly mean MOPITT profiles for each location, for the 14 month period from April 2000 to May 2001 (MOPITT phase 1 data). In the comparison of these data, MOPITT averaging kernels are not applied since the *in situ* data consists of single point measurements, and only the shape of the seasonal trend is required for comparison, not the absolute concentrations of CO.

The results of the comparison can be found in Figure 4.2-Figure 4.7. The shape of the MOPITT seasonal cycle compares well with all six of the selected stations. This is

particularly true in the lower layers where the MOPITT is measuring air close to the same altitude as the ground station.

All six of the ground stations exhibit seasonal cycles which follow the same broad pattern. The CO concentrations are at a minimum during the summer months, when increased solar radiation leads to increased concentrations of the OH radical, which acts to remove CO and so reduce its concentrations. The CO level then increases through autumn and winter, as OH concentrations decrease, to a maximum in spring. The magnitude of the seasonal cycle in MOPITT CO, for all stations, decreases with increasing altitude as expected.

The seasonal variation of CO is driven by the seasonal cycle of OH and the timing, location, and distribution of its sources [Novelli *et al.*, 1998]. The observed seasonal cycles for the Azores, Iceland, Tenerife and Mace Head ground stations are all quite shallow as they are away from strong CO sources, and are more representative of slowly varying background concentrations. Florida and Bermuda on the other hand exhibit a much stronger cycle. Owing to the strong CO sources present in Florida, CO concentrations rapidly increase as solar radiation begins to decrease in September. Bermuda, whilst not representing a strong source region itself, is located in a region which experiences high CO concentrations due to the regular outflow of pollution from the southern United States. This leads to a rapid increase in CO concentrations in September, when high concentrations of CO from strong sources in the United States are transported to this remote location.

The seasonal cycles for the Azores, Bermuda and Florida exhibit more small-scale structure. This variability may be caused by the long range transport of CO over these regions from distant sources, as these three stations are located along a major transport path for pollution from the United States to Europe [Stohl, 2001]. These fluctuations are not evident in the CMDL data as these represent surface concentrations and the transport is occurring at higher altitudes, to which MOPITT is sensitive.

These results suggest that MOPITT is able to correctly capture the observed seasonal cycle in CO. The observation of higher frequency variations within the seasonal cycle over a number of sites suggests that the MOPITT instrument may be able to detect enhancements in CO due to long range transport events.

Code	Site Name and Location	Latitude (degrees)	Longitude (degrees)	Altitude (m.a.s.l.)
AZR	Terceira Island, Azores, Portugal	38.77	-27.38	40
BME	St. Davids Head, Bermuda, United Kingdom	32.37	-64.65	30
ICE	Storhofdi, Vestmannaeyjar, Iceland	63.34	-20.29	127
IZO	Tenerife, Canary Islands, Spain	28.30	-16.48	2360
KEY	Key Biscayne, Florida, United States	25.67	-80.20	3
MHD	Mace Head, County Galway, Ireland	53.33	-9.90	25

Table 4.1: The six NOAA CMDL surface sites selected for comparison with MOPITT data.

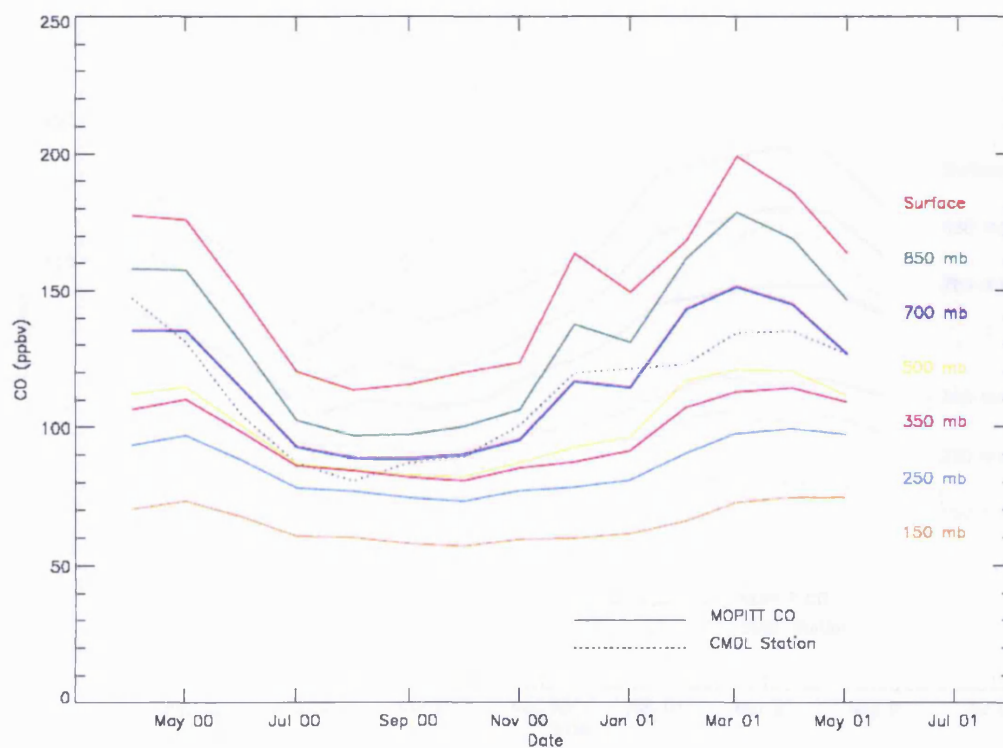


Figure 4.2: Monthly mean MOPITT profile and CMDL surface CO data for the Azores ground station, for the period April 2000-May 2001.

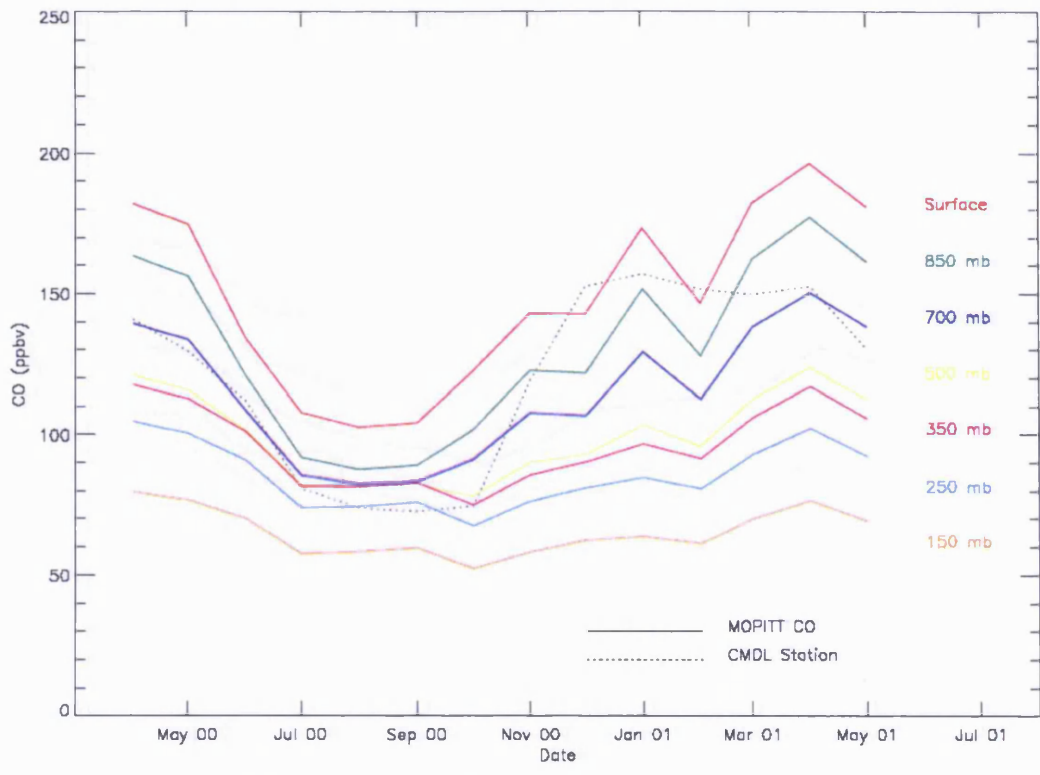


Figure 4.3: Monthly mean MOPITT profile and CMDL surface CO data for the Bermuda ground station, for the period April 2000-May 2001.

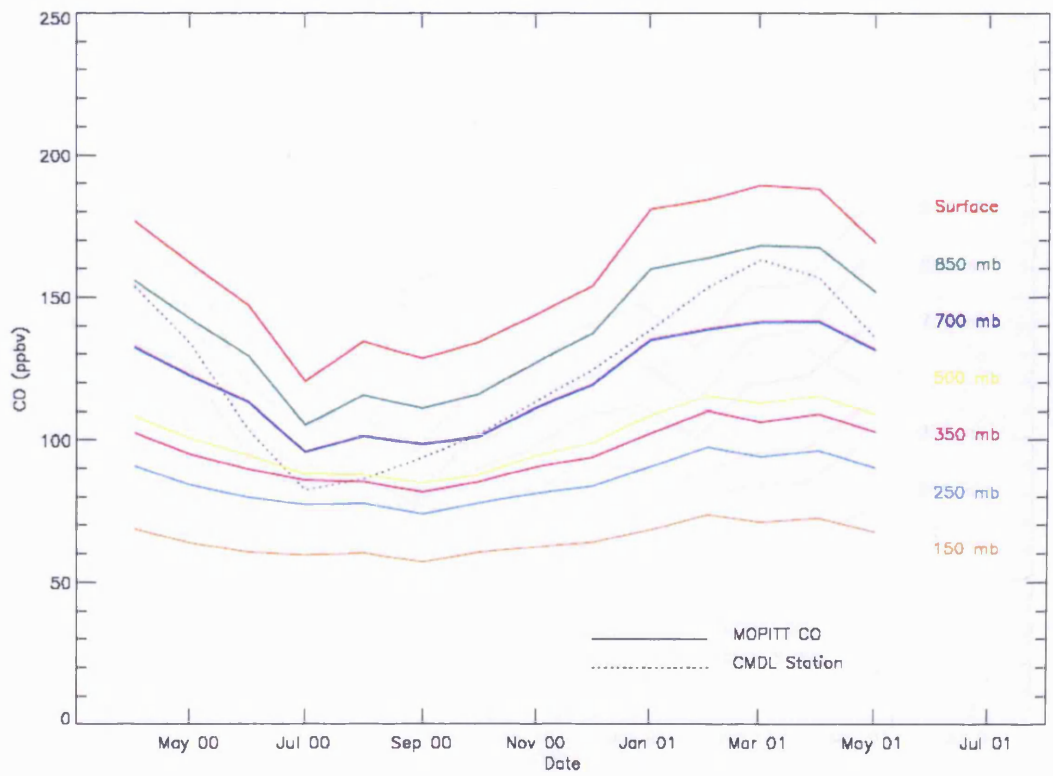


Figure 4.4: Monthly mean MOPITT profile and CMDL surface CO data for the Iceland ground station, for the period April 2000-May 2001.

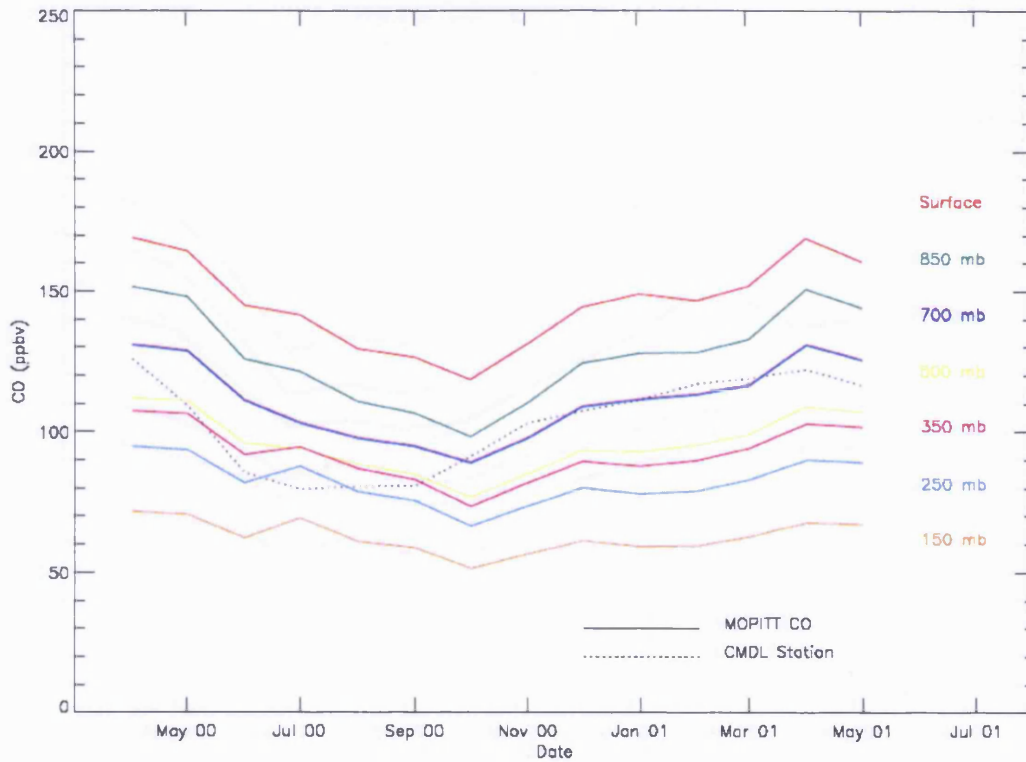


Figure 4.5: Monthly mean MOPITT profile and CMDL surface CO data for the Tenerife ground station, for the period April 2000-May 2001.

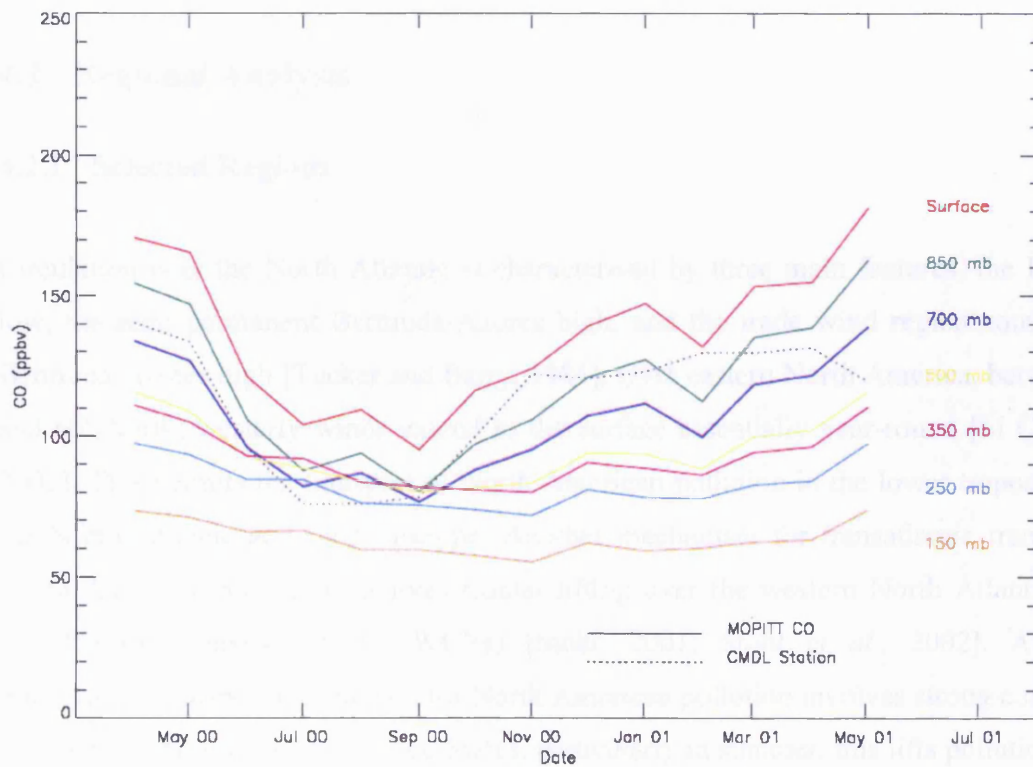


Figure 4.6: Monthly mean MOPITT profile and CMDL surface CO data for the Florida ground station, for the period April 2000-May 2001.

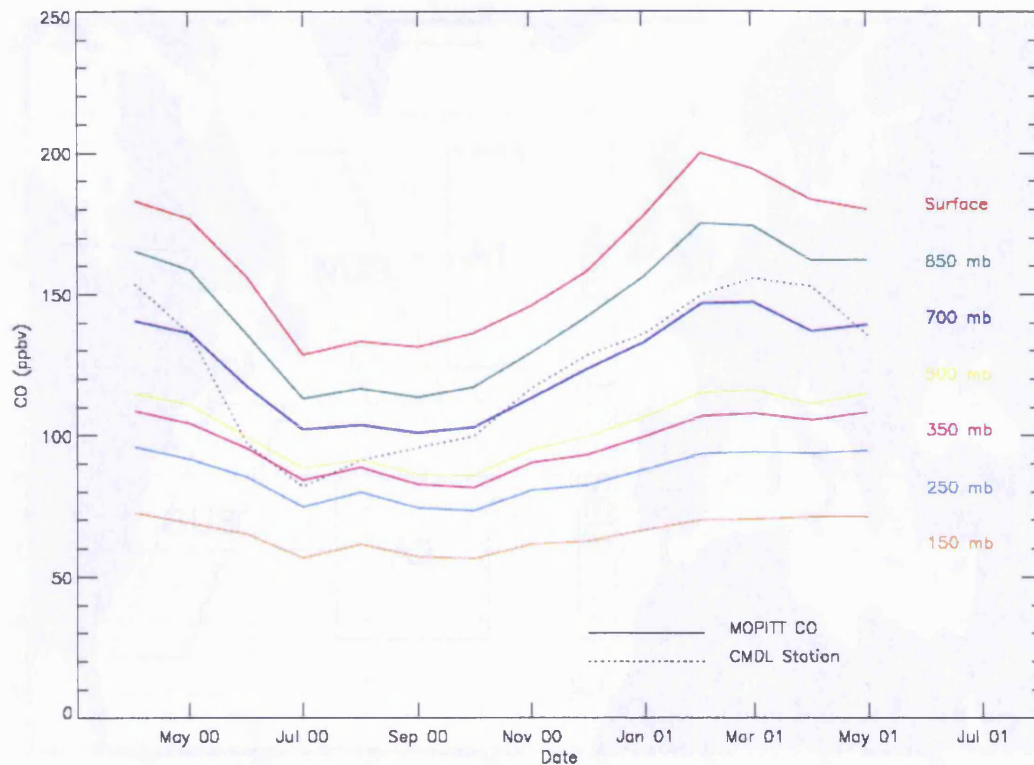


Figure 4.7: Monthly mean MOPITT profile and CMDL surface CO data for the Mace Head ground station, for the period April 2000-May 2001.

4.2 Regional Analysis

4.2.1 Selected Regions

Circulation over the North Atlantic is characterised by three main features, the Icelandic low, the semi permanent Bermuda-Azores high, and the trade wind region south of the Bermuda-Azores high [Tucker and Barry, 1984]. Over eastern North America, between 30° and 60° North, westerly winds extend to the surface essentially year-round [Li Q., *et al.*, 2002]. This permits the transport of North American pollution in the lower troposphere to the North Atlantic and on to Europe. Another mechanism for transatlantic transport of North American pollution involves frontal lifting over the western North Atlantic by so called warm conveyor belts (WCBs) [Stohl, 2001; Stohl *et al.*, 2002]. A further transatlantic transport mechanism for North American pollution involves strong convection over the central and eastern United States, particularly in summer, this lifts pollution to the middle and upper troposphere where it is then exported by westerly winds [Jacob *et al.*, 1993].

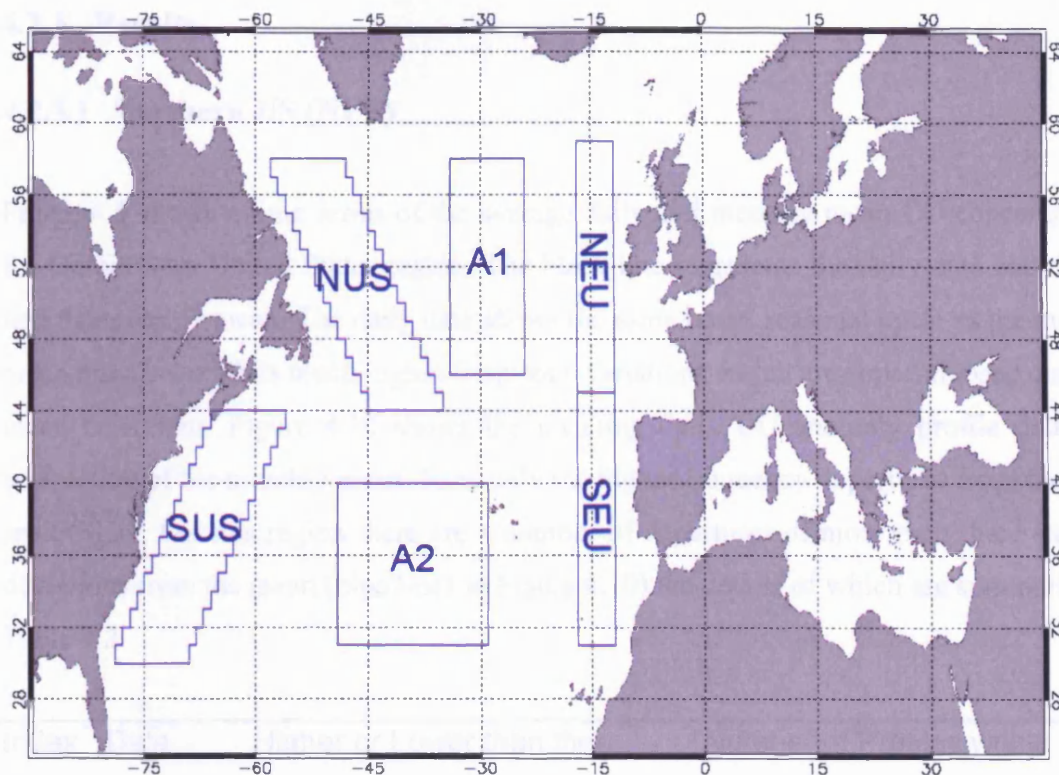


Figure 4.8: Map showing the six regions selected to try and capture the long range transport of CO across the North Atlantic.

With these transport mechanisms in mind, six regions were selected to try and capture the transport of CO over the North Atlantic region (see Figure 4.8). These regions cover the east coast of the United States (NUS and SUS), the central North Atlantic (A1 and A2) and the west coast of Europe (NEU and SEU).

4.2.2 Methodology

Monthly mean CO profiles for each of the selected regions were calculated for the 14 month period from April 2000 to May 2001. These data were then subtracted from the daily data for the same period to produce daily CO anomalies from the mean for each region. The mean and standard deviation of these departures from the monthly mean were calculated. Those days which exhibit CO concentrations which are greater than 3 standard deviations from the mean were selected as possible candidates for transport detection.

4.2.3 Results

4.2.3.1 Northern US (NUS)

Figure 4.9 shows a time series of the average daily and monthly mean CO concentrations for the northern United States region. The black line represents the daily data and the red line the monthly mean. The daily data shows the same broad seasonal cycle as the monthly mean but also exhibits much higher frequency variations which are superimposed onto this mean behaviour. Figure 4.10 shows the resulting daily CO anomaly profile data after subtraction of the monthly mean. Now only the higher frequency departures from the mean are evident. For this region there are a number of departures of more than three standard deviations from the mean (blue lines in Figure 4.10) the details of which are summarised in Table 4.2.

Index	Date	Higher or Lower than the mean	Number of Profiles within region
1	30/11/00	Higher	1
2	26/03/01	Higher	22
3	02/08/00	Higher	166
4	13/09/00	Higher	37
5	11/09/00	Higher	3
6	11/09/00	Lower	3
7	17/09/00	Lower	24
8	12/05/00	Lower	5

Table 4.2: Days on which the average MOPITT CO profile for the NUS region is greater than 3 standard deviations from the mean.

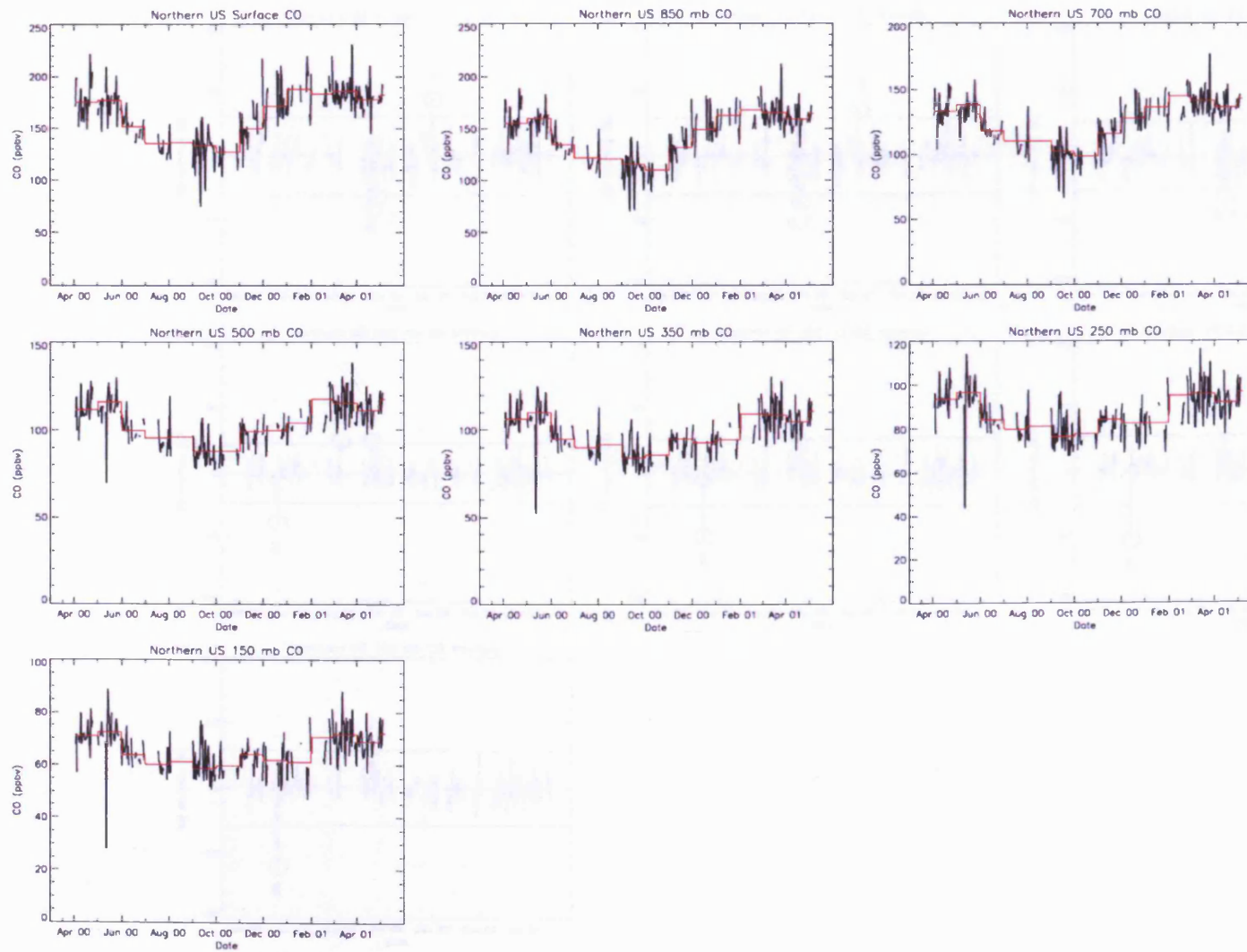


Figure 4.9: Northern United States region (NUS) average daily (black) and monthly mean (red) CO profile time series.

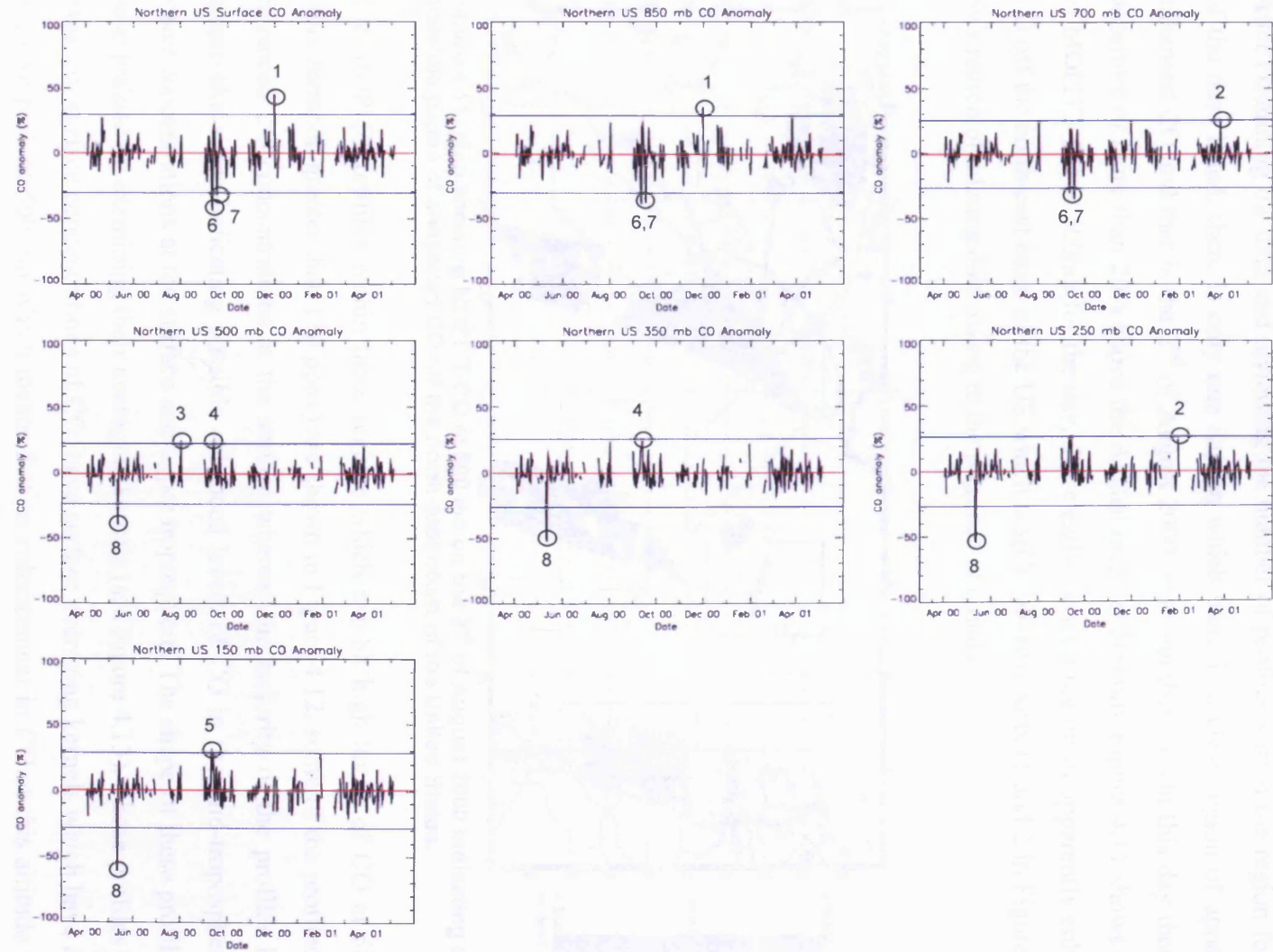


Figure 4.10: Northern United States region (NUS) average daily CO anomaly (black), the red line indicates the mean anomaly for the whole time period and the blue lines represent +/- 3 standard deviations from this mean.

After examining the data and reviewing the number of profiles within the region for each of the days listed, there is only one day on which there is a clear region of apparently enhanced CO and that is the 2nd of August 2000 (case number 3). On this day there is a departure of more than 20% above the August mean at 500 mb. Figure 4.11 shows a map of MOPITT CO at 500mb for the day, this clearly shows a region of apparently enhanced CO off the north-east coast of the US which is split into two parts (1 and 2 in Figure 4.11) by a region of missing data owing to the presence of clouds.

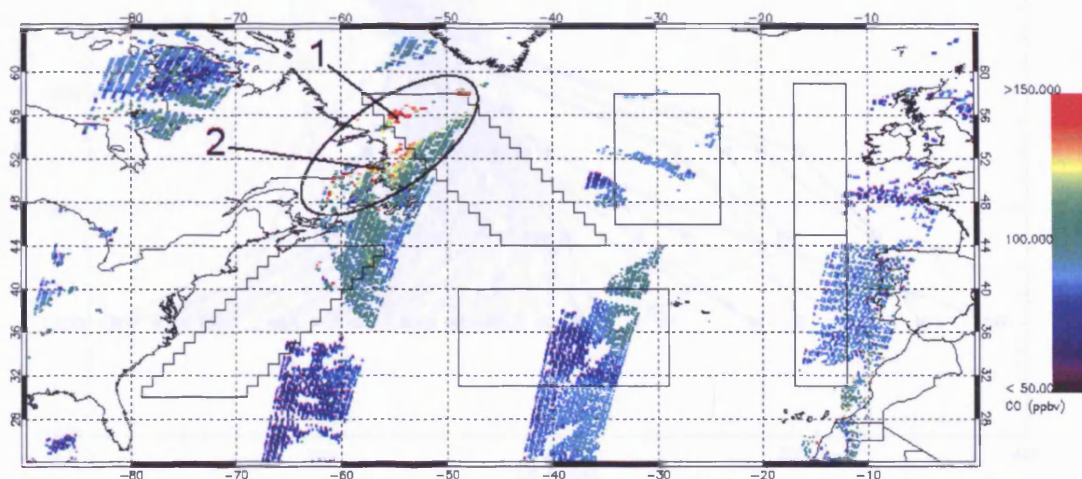


Figure 4.11: Map showing MOPITT CO at 500 mb on the 2nd of August 2000 indicating a possible plume of enhanced CO off the north-east coast of the United States.

The MOPITT profiles within these regions which exhibit high levels of CO at 500 mb (concentration greater than 130 ppbv) are shown in Figure 4.12, some of the profiles show enhanced CO concentrations at the surface whereas the majority of the profiles have a plume-like shape indicating possible enhanced levels of CO in the mid-troposphere and lower concentrations at the surface and upper troposphere. The shape of these profiles can be explained by examining their averaging kernels (see Figure 4.13). Those profiles which have low surface concentrations of CO, have surface averaging kernels which have a large negative peak at 500 mb which means that an enhancement in CO at this altitude would lead to a reduction in CO concentrations at the surface in the retrieved profile. These profiles also have surface and 850 mb averaging kernels which have a large positive peak in the upper troposphere, above 250 mb, indicating that most of the information for these levels comes from the upper troposphere where CO concentrations are generally lower, and therefore this leads to lower retrieved concentrations at the surface and 850 mb. The averaging kernels for all levels have an abnormal shape in the lower troposphere between

the surface and 850 mb, compared with those in Figure 3.34, which exhibit a more conventional shape for retrievals over the North Atlantic.

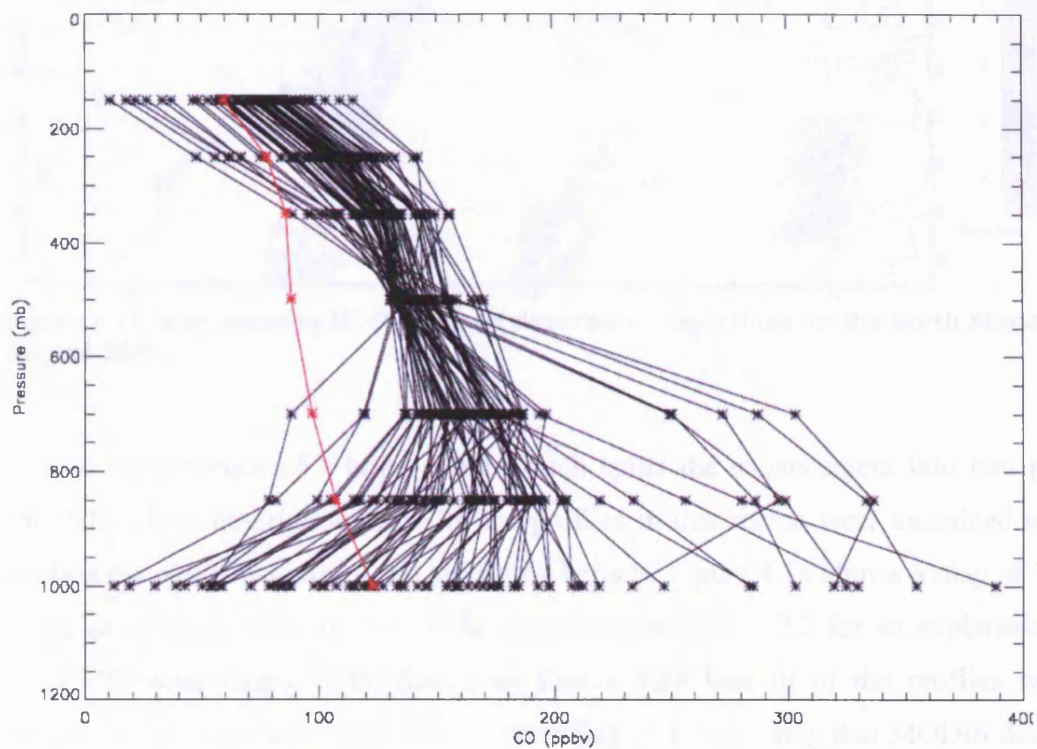


Figure 4.12: MOPITT CO profiles for those pixels in regions 1 and 2 in Figure 4.11. The red profile indicates the monthly mean profile for the NUS region for August 2000.

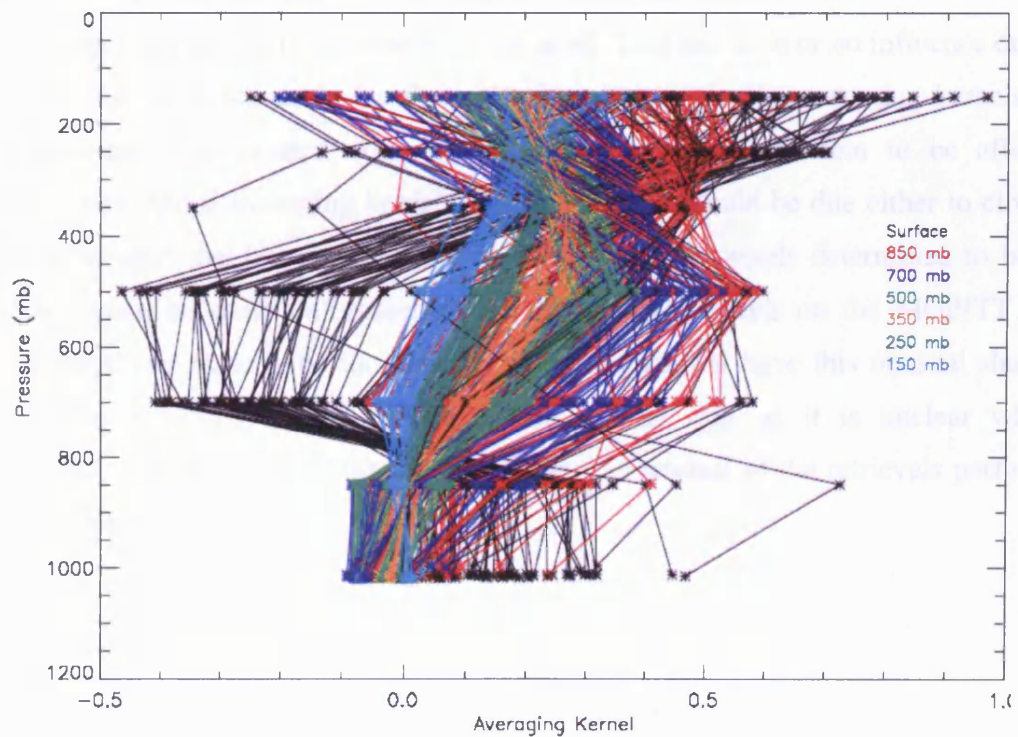


Figure 4.13: The MOPITT averaging kernels for the profiles shown in Figure 4.12.

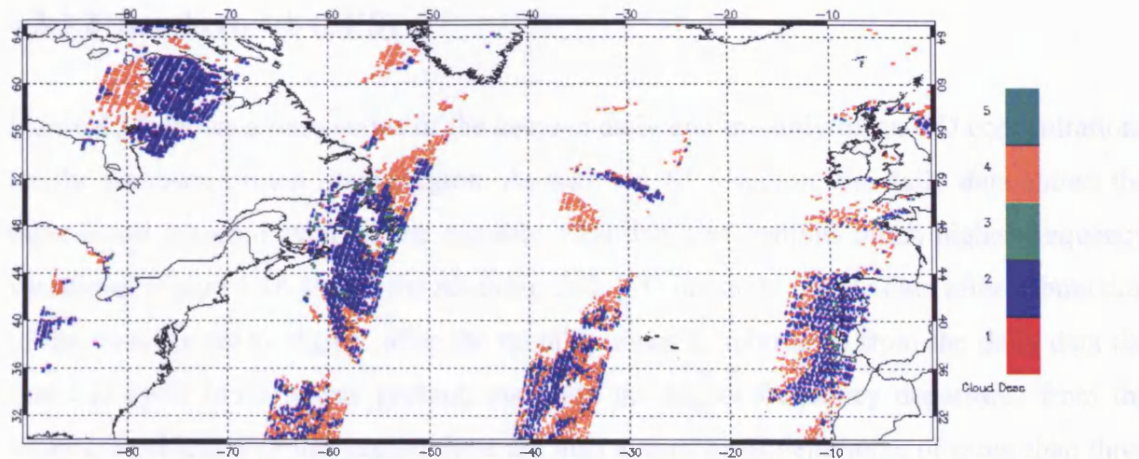


Figure 4.14: Map showing MOPITT cloud description flag values for the North Atlantic on 2nd August 2000.

Due to the presence of a large cloud, which splits the enhancement into two parts, the MOPITT cloud description flags for the profiles in this region were examined to try and explain the odd behaviour of the averaging kernels. Figure 4.14 shows a map of MOPITT cloud description flags for the 2nd August 2000 (see Table 2.2 for an explanation of the MOPITT cloud flags). It is clear from Figure 4.14 that all of the profiles within the enhanced region are associated with a cloud flag of 4, indicating that MODIS detected the presence of low level cloud and MOPITT retrievals were still conducted for these pixels as low level clouds are thought not to have a large effect on the MOPITT thermal channels. Although it is generally believed that low level cloud has little or no influence on MOPITT retrievals conducted using the thermal infrared channels, the averaging kernels for those measurements associated with low level cloudy pixels do seem to be affected. The abnormal shaped averaging kernels for these profiles could be due either to clouds which have escaped the detection scheme or partially cloudy pixels determined to be clear, or there could be some unforeseen effect of low level clouds on the MOPITT retrievals. Whatever the reason, the fact that the averaging kernels have this unusual shape, means that the retrievals should not be trusted in this case as it is unclear whether the enhancement detected at 500mb is real or just an artefact of the retrievals performed over this cloudy scene.

4.2.3.2 Southern US (SUS)

Figure 4.15 shows a time series of the average daily and monthly mean CO concentrations for the southern United States region. As with the NUS region, the daily data shows the same broad seasonal cycle as the monthly mean but also exhibits much higher frequency variations. Figure 4.16 shows the resulting daily CO anomaly profile data after subtraction of the monthly mean. Again, after the monthly mean is subtracted from the daily data the seasonal cycle is no longer present, and only the higher frequency departures from the mean are evident. For this region there are also a number of departures of more than three standard deviations from the mean as indicated in Figure 4.16 the details of which are summarised in Table 4.3.

For this region there are an insufficient number of profiles in each of the cases selected in Table 4.3 to be able to determine the presence of an enhanced CO plume. The exception to this is the 2nd of February 2000 where there were 101 profiles indicating that the average for the region was lower than the monthly mean. Unfortunately, there were not enough days of data for that particular month to obtain a reliable monthly mean.

Index	Date	Higher or Lower than the mean	Number of Profiles within region
1	22/12/00	Higher	37
2	23/07/00	Higher	45
3	30/07/30	Lower	16
4	02/02/01	Lower	101
5	04/03/01	Lower	72
6	06/03/01	Lower	1
7	19/03/01	Lower	4

Table 4.3: Days on which the average MOPITT CO profile for the SUS region is greater than 3 standard deviations from the mean.

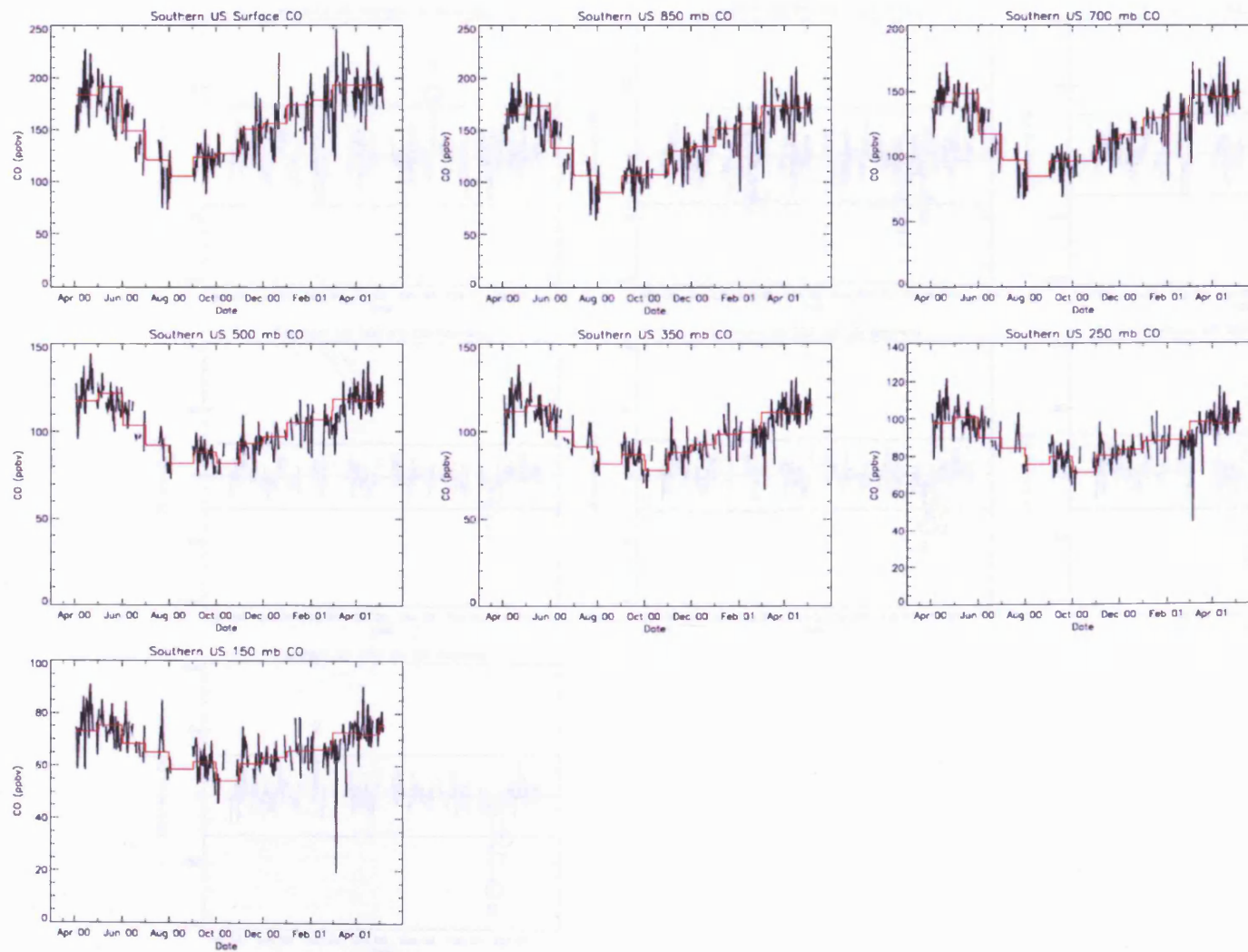


Figure 4.15: Southern United States region (SUS) average daily (black) and monthly mean (red) CO profile time series.

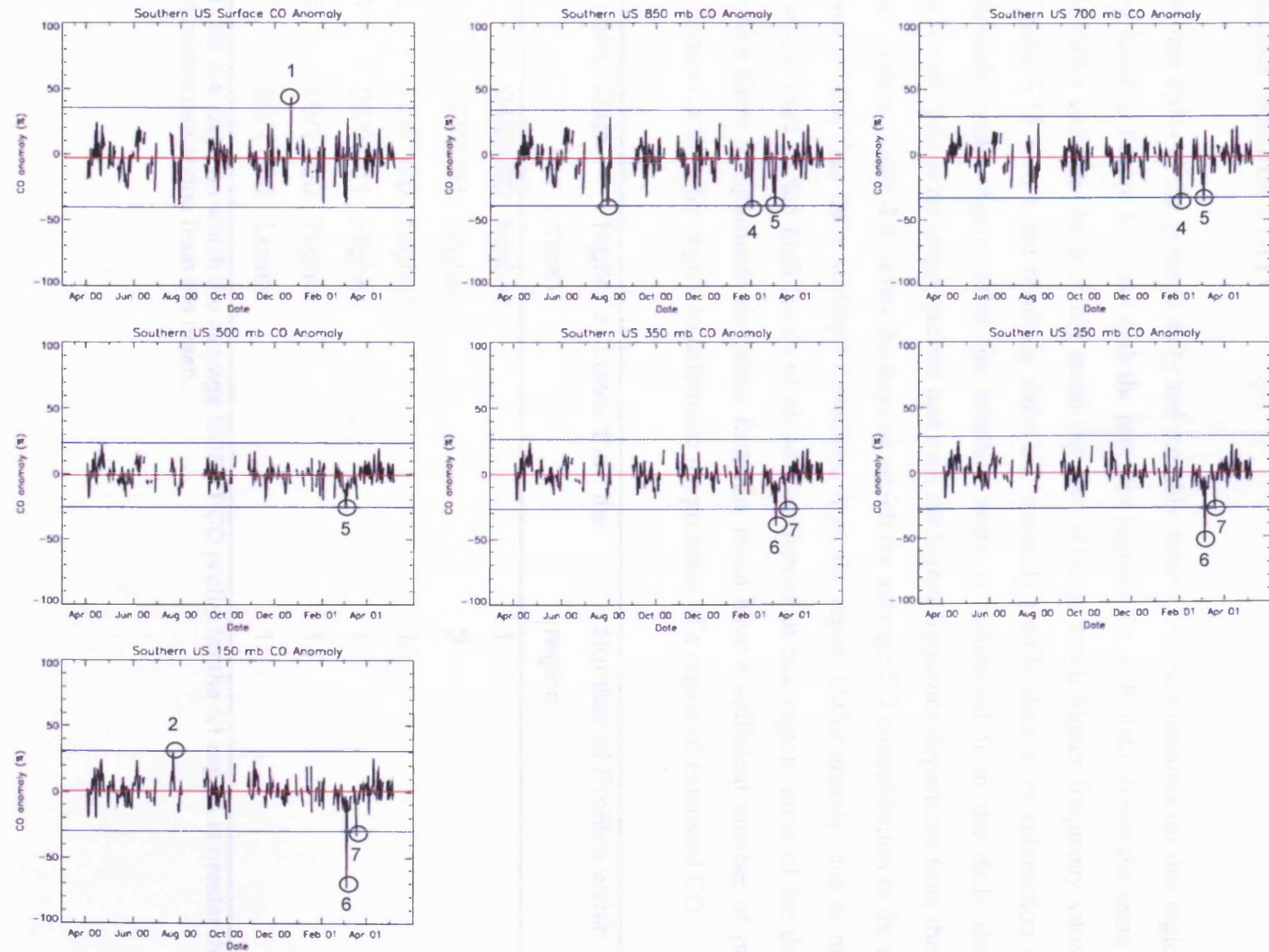


Figure 4.16: Southern United States region (SUS) average daily CO anomaly (black), the red line indicates the mean anomaly for the whole time period and the blue lines represent ± 3 standard deviations from this mean.

4.2.3.3 Atlantic 1 (A1)

A time series of the average daily and monthly mean CO concentrations for this region can be found in Figure 4.17. As with the previous regions the daily data shows the same broad seasonal cycle as the monthly mean but also exhibits much higher frequency variations. Figure 4.18 shows the resulting daily CO anomaly profile data after subtraction of the monthly mean. Again, after the monthly mean is subtracted from the daily data the seasonal cycle is no longer present and only the higher frequency departures from the mean are evident. Table 4.4 shows the days on which the average CO concentration in the region was greater than three standard deviations from the mean. Unfortunately, due to missing data, caused by the high levels of cloud experienced in this region, none of the days on which there is significant deviation from the mean have a sufficient number of profiles contained within the region to determine the presence of a region of enhanced CO.

Index	Date	Higher or Lower than the mean	Number of Profiles within region
1	04/09/00	Higher	1
2	17/02/01	Higher	2
3	18/07/00	Higher	10
4	06/04/01	Higher	1
5	09/11/00	Higher	1
6	09/11/00	Lower	1

Table 4.4: Days on which the average MOPITT CO profile for the A1 region is greater than 3 standard deviations from the mean.

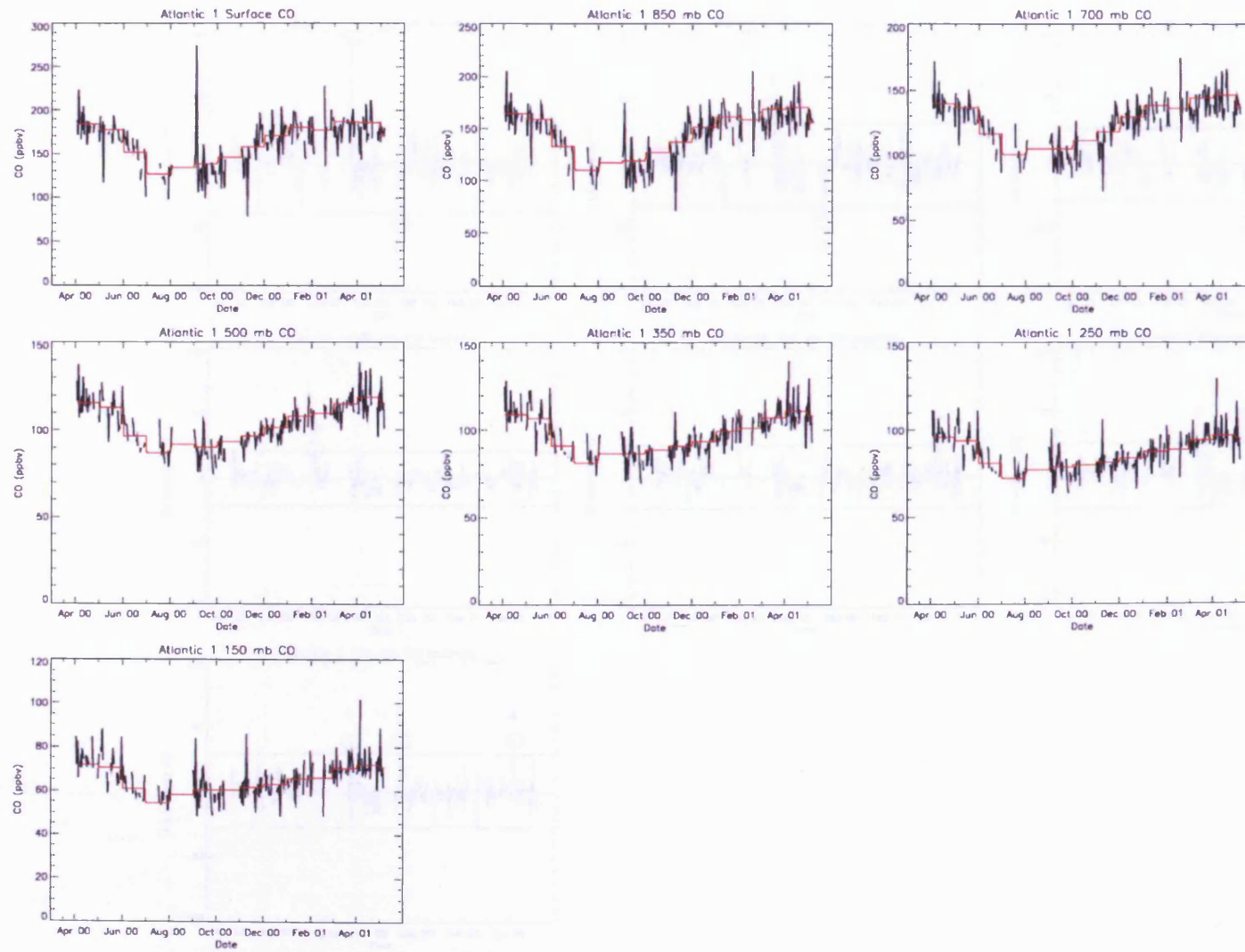


Figure 4.17: Atlantic region 1 (A1) average daily (black) and monthly mean (red) CO profile time series.

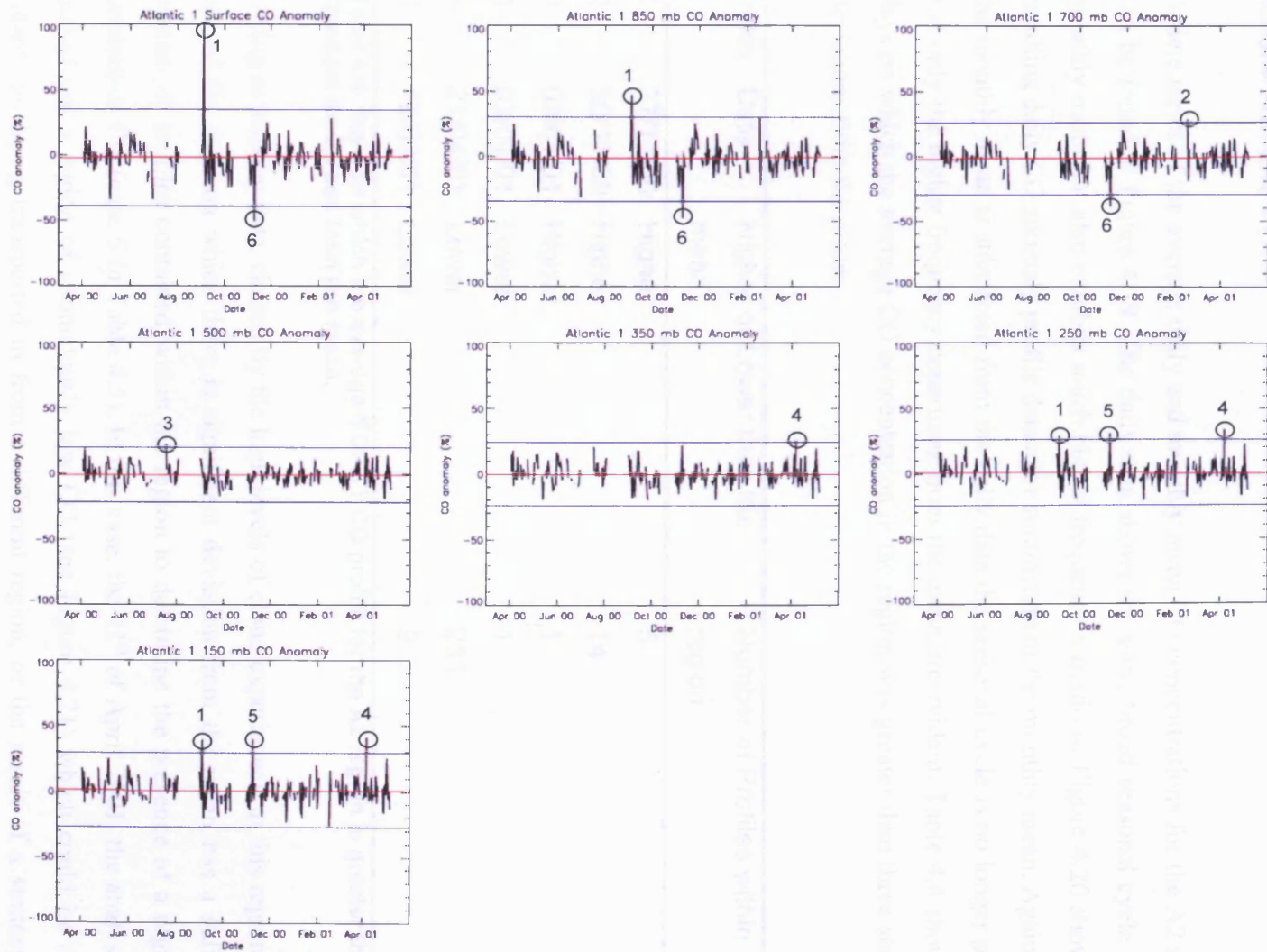


Figure 4.18: Atlantic region 1 (A1) average daily CO anomaly (black), the red line indicates the mean anomaly for the whole time period and the blue lines represent +/- 3 standard deviations from this mean.

4.2.3.4 Atlantic 2 (A2)

A time series of the average daily and monthly mean CO concentrations for the A2 region can be found in Figure 4.19. The daily data shows the same broad seasonal cycle as the monthly mean but also exhibits much higher frequency variations. Figure 4.20 shows the resulting daily CO anomaly profile data after subtraction of the monthly mean. Again, after the monthly mean is subtracted from the daily data the seasonal cycle is no longer present and only the higher frequency departures from the mean are evident. Table 4.4 shows the days on which the average CO concentration in the region was greater than three standard deviations from the mean.

Index	Date	Higher or Lower than the mean	Number of Profiles within region
1	27/11/00	Higher	5
2	30/11/00	Higher	14
3	03/01/01	Higher	1
4	03/01/01	Lower	1
5	21/04/01	Lower	231
6	19/03/01	Lower	9

Table 4.5: Days on which the average MOPITT CO profile for the A2 region is greater than 3 standard deviations from the mean.

Owing to missing data, caused by the high levels of cloud experienced in this region, only one of the days on which there is significant deviation from the mean has a sufficient number of profiles contained within the region to determine the presence of a region of anomalous CO (case 5 in Table 4.5). In this case, the 21st of April 2001, the analysis has picked out a region of anomalously low CO (see Figure 4.21) which could be due to cleaner air being transported in from a different region, or the result of a stratospheric intrusion bringing “CO poor” stratospheric air down into the troposphere.

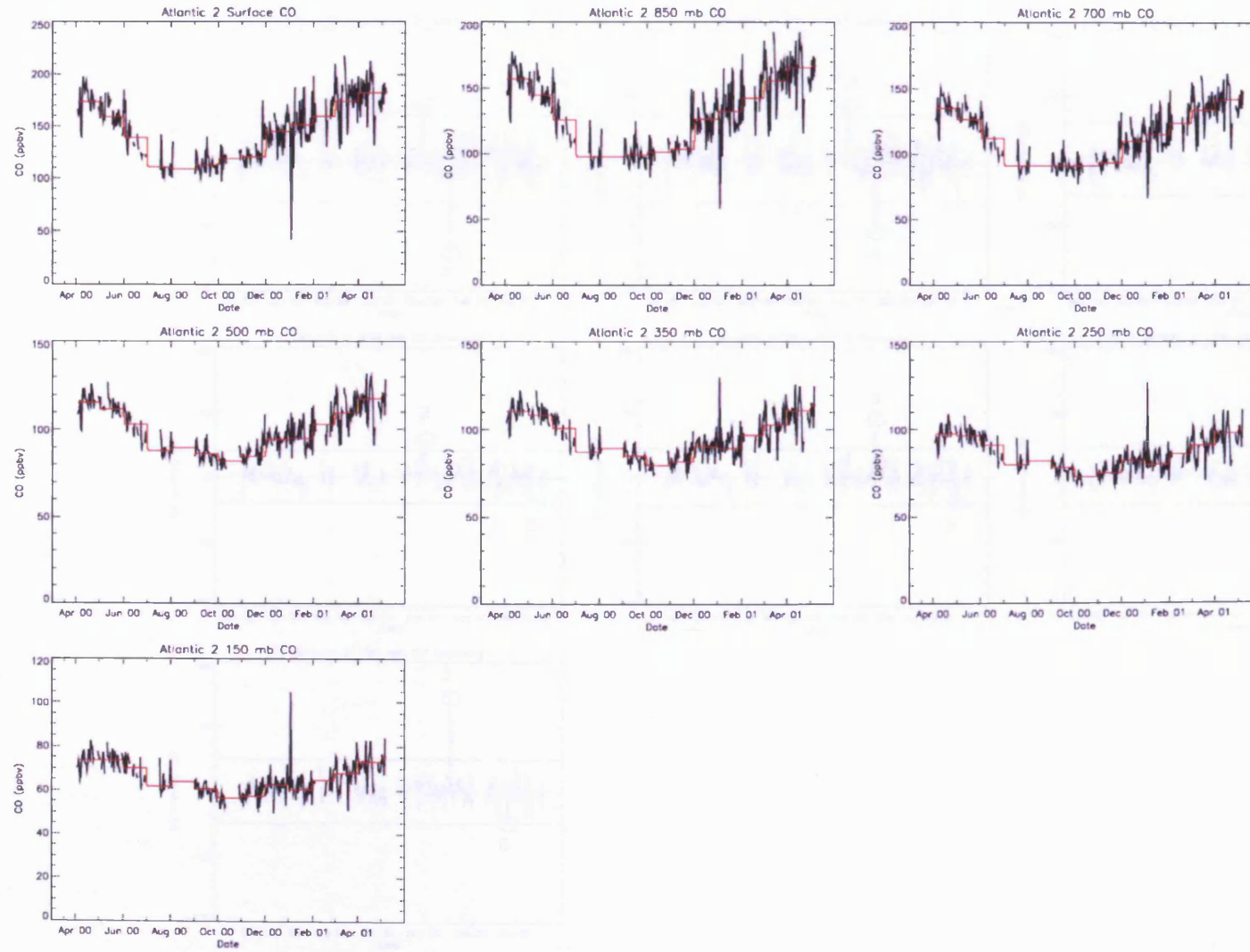


Figure 4.19: Atlantic region 2 (A2) average daily (black) and monthly mean (red) CO profile time series.

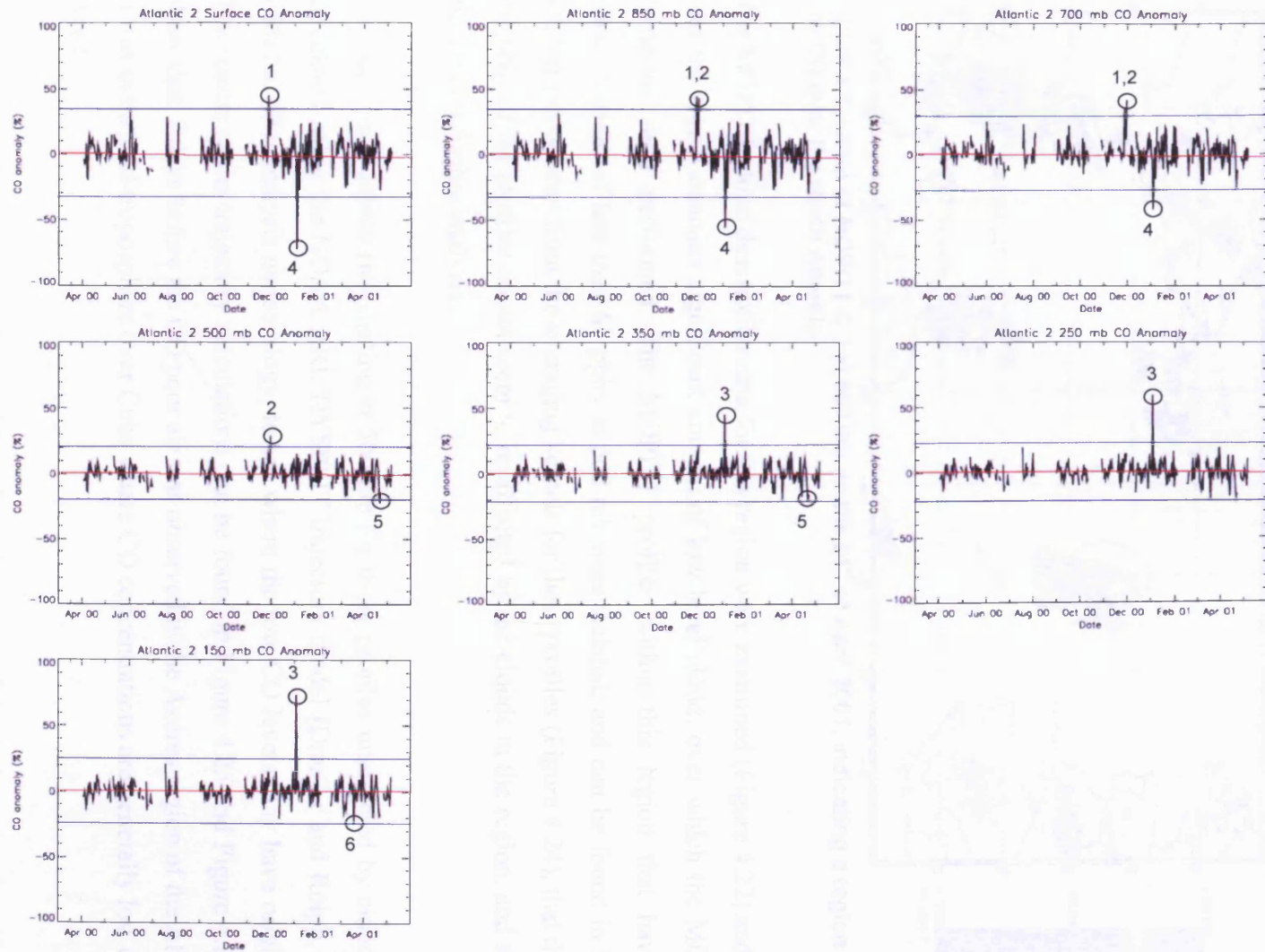


Figure 4.20: Atlantic region 2 (A2) average daily CO anomaly (black), the red line indicates the mean anomaly for the whole time period and the blue lines represent ± 3 standard deviations from this mean.

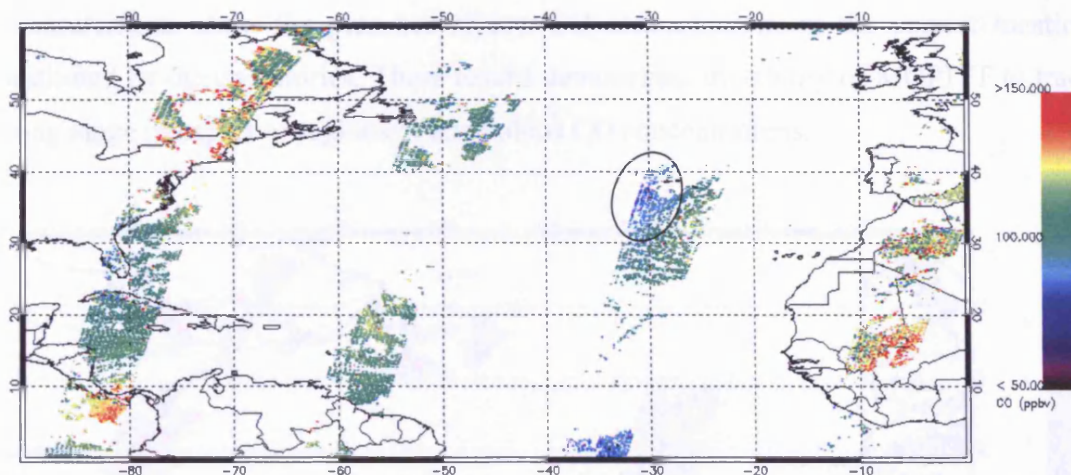


Figure 4.21: Map of MOPITT CO at 500 mb on the 21st of April 2001, indicating a region of low CO over the North Atlantic.

The MOPITT cloud description data for this region were examined (Figure 4.22) and show that the region contains significant amount of low level cloud, over which the MOPITT retrievals were performed. The MOPITT profiles within this region that have CO concentrations of less than 85 ppbv at 500 mb were isolated, and can be found in Figure 4.23. It can be seen from the averaging kernels for these profiles (Figure 4.24), that the vast majority of the profiles do not seem to be affected by the clouds in the region, and so may be used for further analysis.

Five day back trajectories starting at 500 mb for those profiles unaffected by cloud were calculated using the NOAA ARL HYSPLIT trajectory model [Draxler and Rolph, 2003] with NCEP reanalysis meteorology, to see where the low CO levels may have originated. The results of the trajectory calculations can be found in Figure 4.25 and Figure 4.26 and show that, 5 days before the CO poor air was observed in the Azores region of the Atlantic, it was in the mid-troposphere over Cuba where CO concentrations are generally low during April.

An average trajectory was calculated by taking the mean of the trajectories for all of the profiles in the low region, MOPITT data were examined to see if the instrument was able to track the low along this mean trajectory during the five days before it was observed. Figure 4.27 - Figure 4.32 show maps of MOPITT CO concentrations at 500 mb for the 5 days of the trajectory, with the mean trajectory shown in black, and the location of the low in red. With the exception of some cloudy pixels on the 20th, there were coincident MOPITT data with the trajectory locations on each of the 5 days. The MOPITT

measurements show the presence of low CO concentrations in the correct locations as indicated by the trajectories. These results demonstrate the ability of MOPITT to track the long range transport of regions of anomalous CO concentrations.

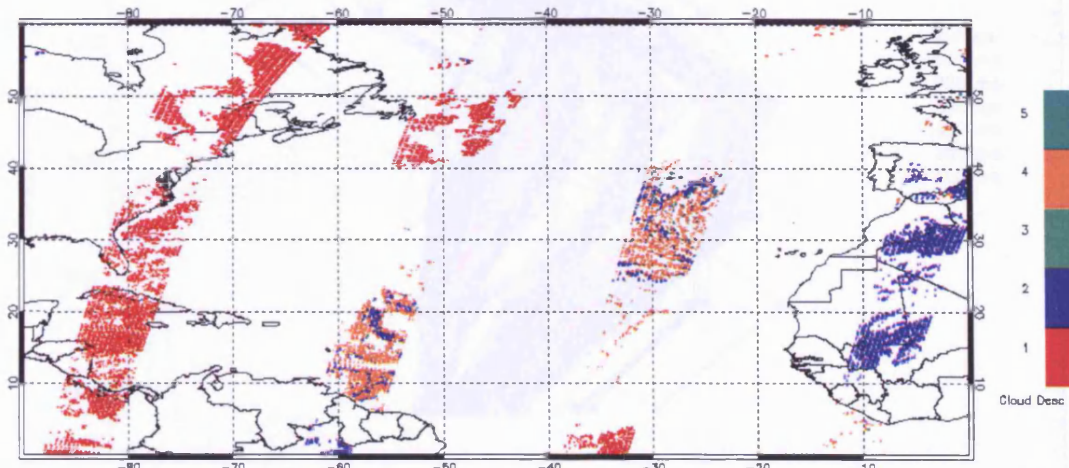


Figure 4.22: Map of MOPITT cloud description flags for the North Atlantic on the 21st April 2001.

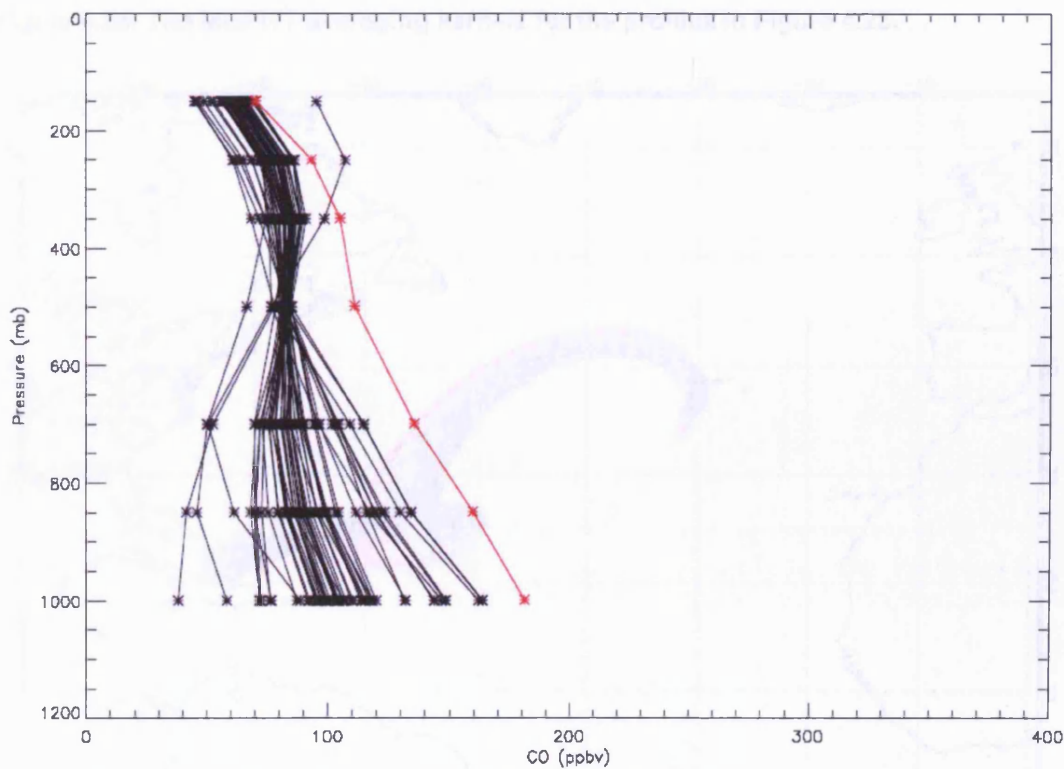


Figure 4.23: MOPITT CO profiles for those pixels in the low CO region in Figure 4.21 with CO concentrations less than 85 ppbv at 500 mb, the red profile indicates the monthly mean profile for the A2 region for April 2001.

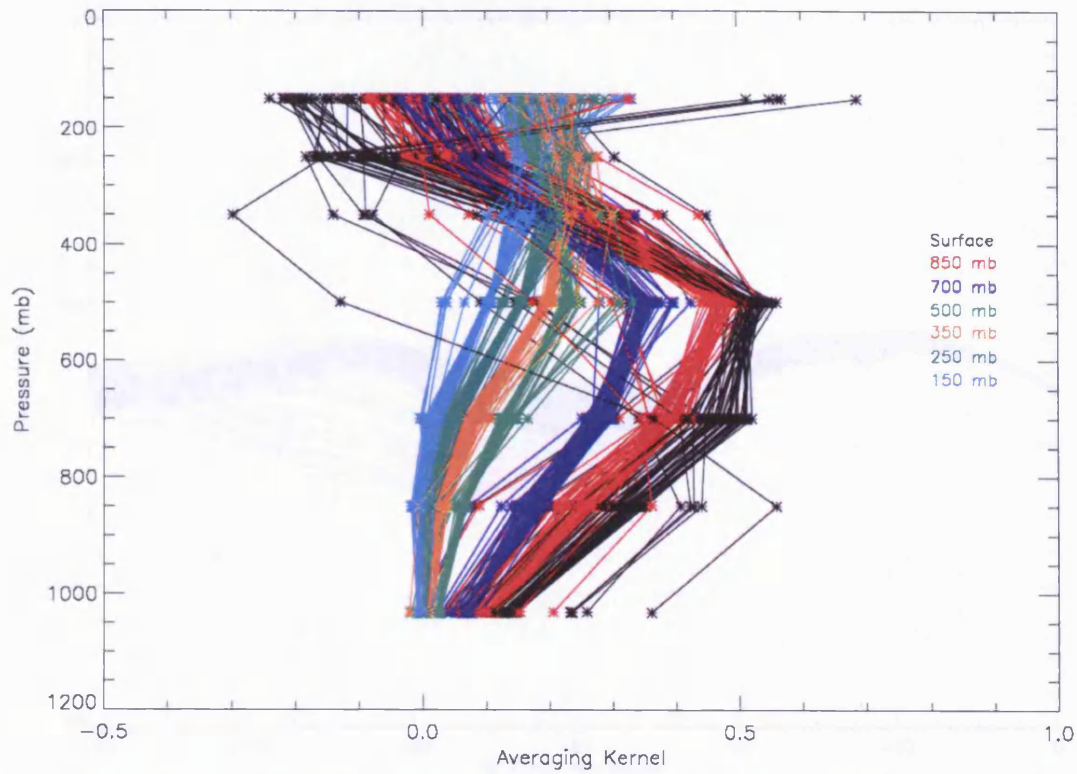


Figure 4.24: The MOPITT averaging kernels for the profiles in Figure 4.23.

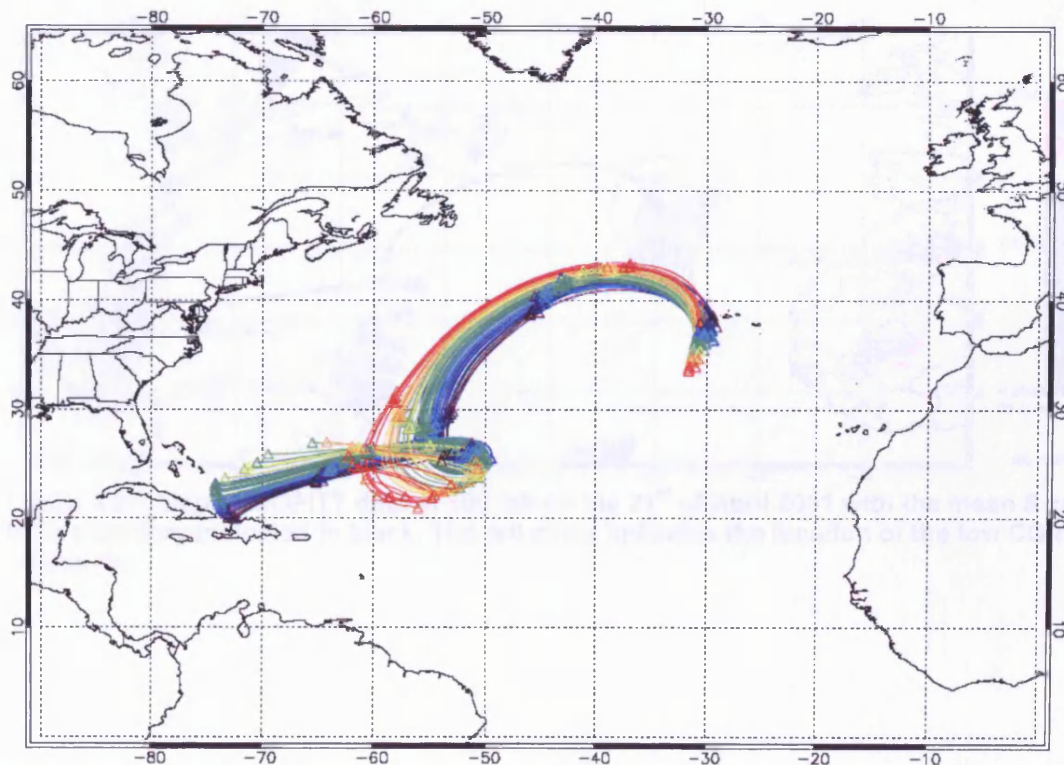


Figure 4.25: 5 day back trajectories for the profiles shown in Figure 4.23 starting at 500 mb on the 21st of April 2001, coloured by starting location.

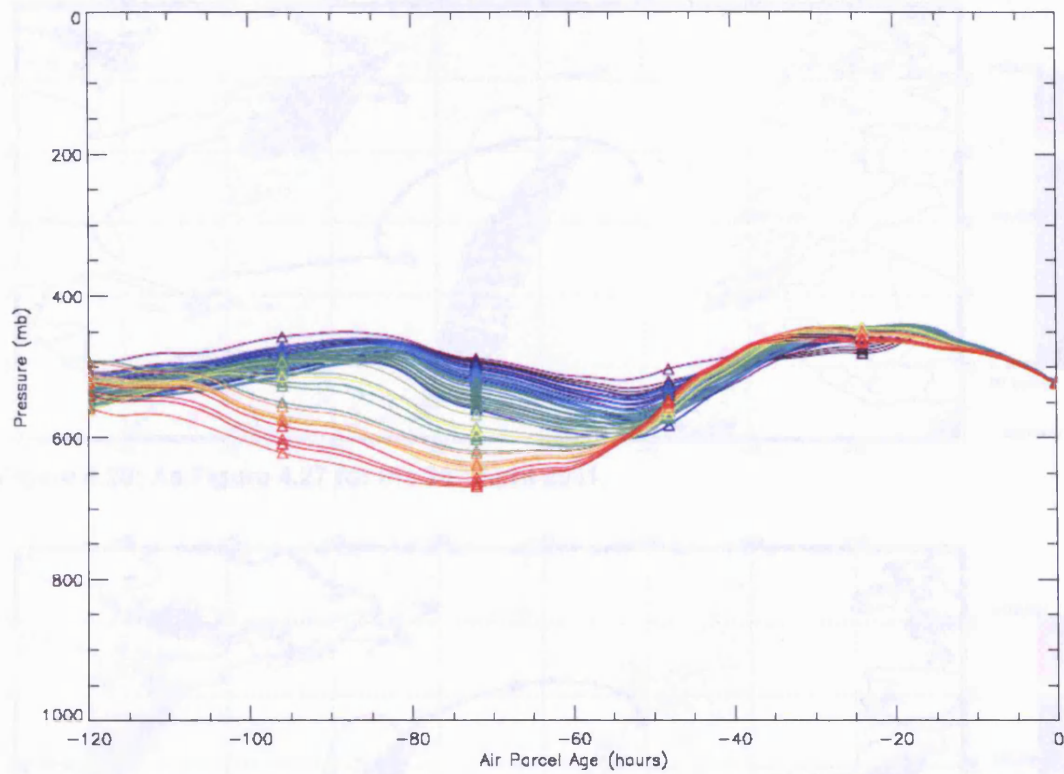


Figure 4.26: Altitude evolution of the 5 day back trajectories shown in Figure 4.25.

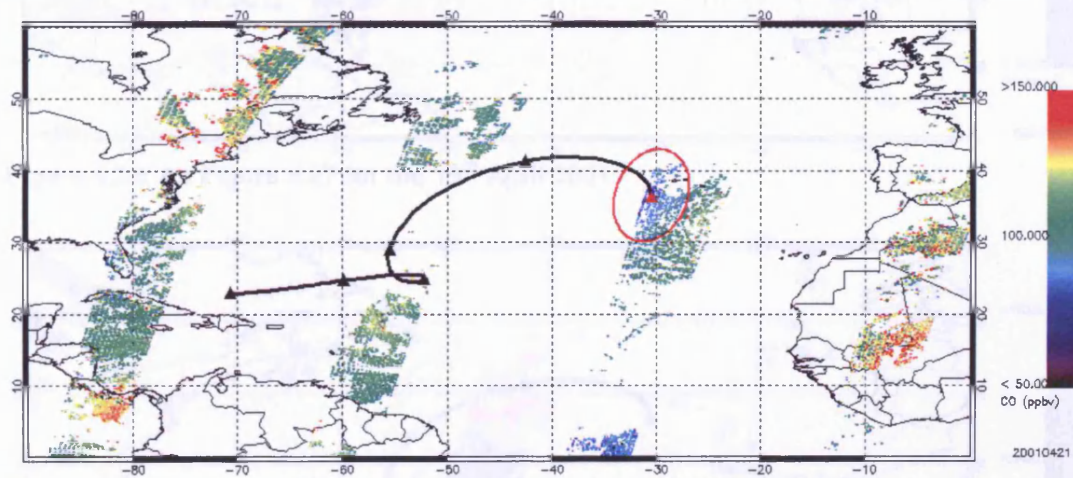
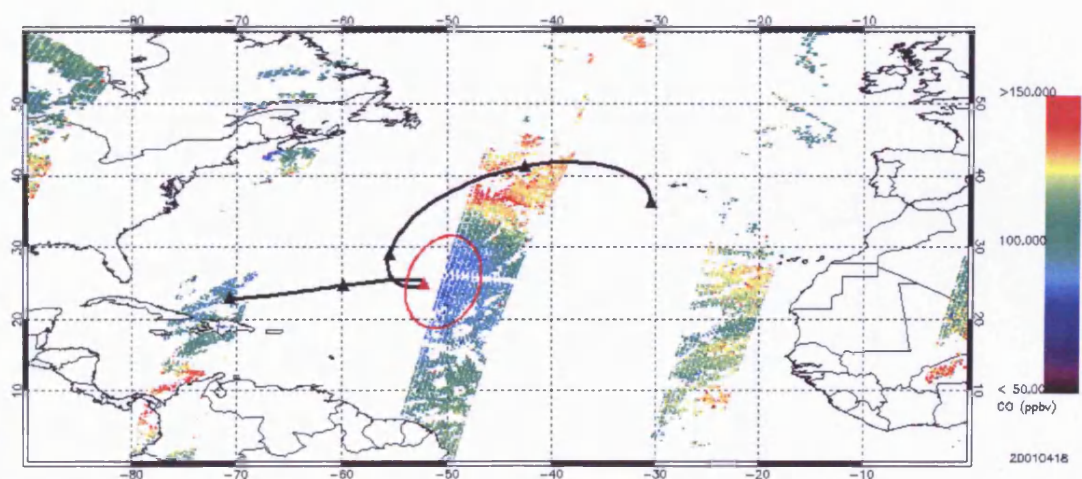
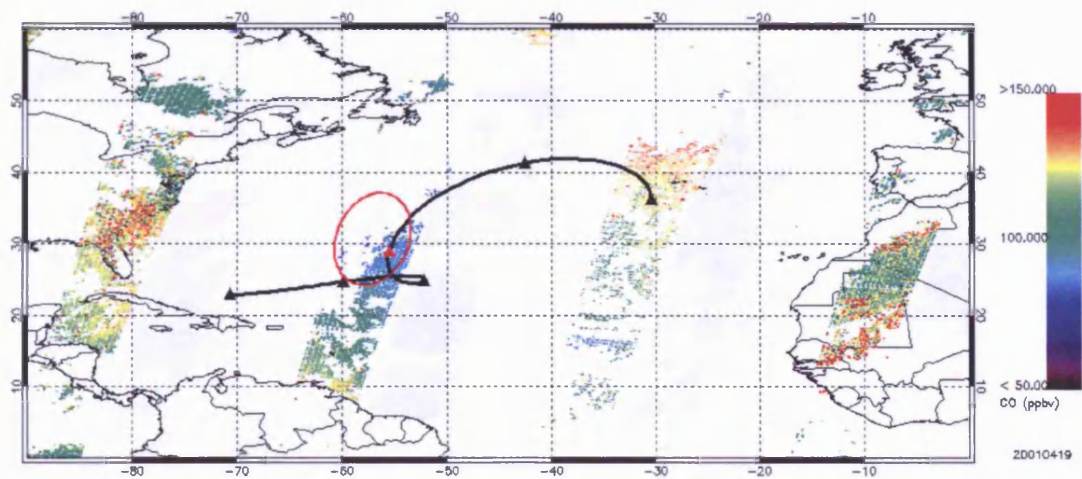
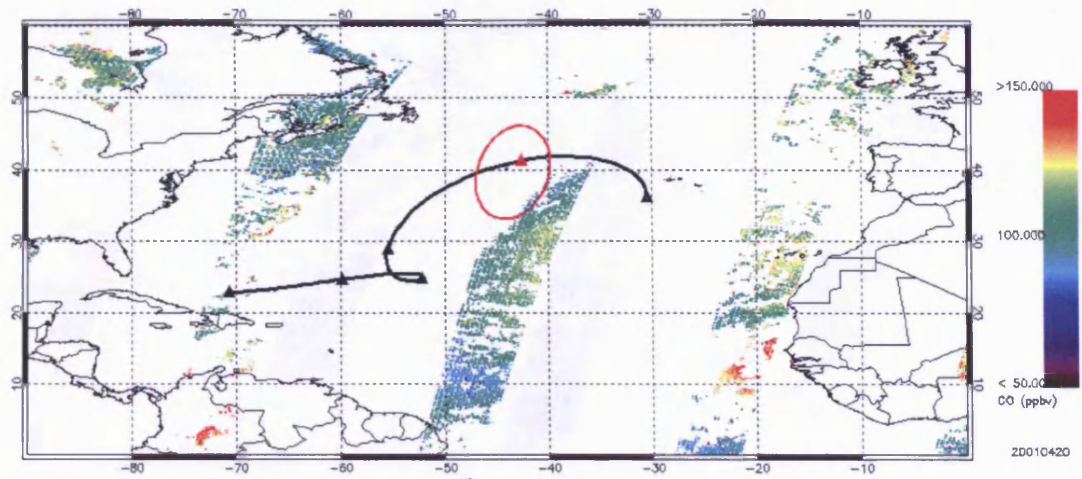


Figure 4.27: Map of MOPITT data at 500 mb on the 21st of April 2001 with the mean 5 day back trajectory indicated in black. The red circle indicates the location of the low CO region on this day.



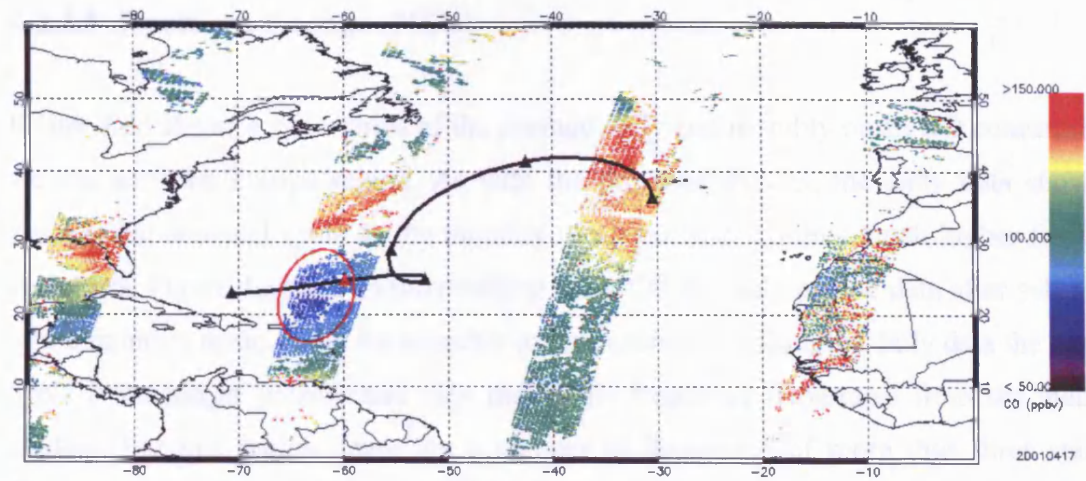


Figure 4.31: As Figure 4.27 for the 17th April 2001

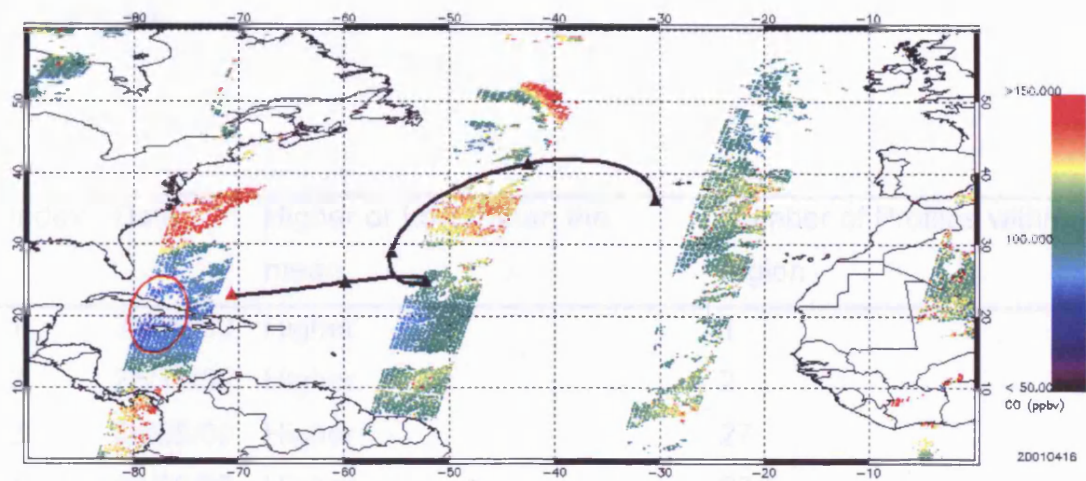


Figure 4.32: As Figure 4.27 for the 16th April 2001

- 1. 200000 Higher
- 2. 150000 Higher
- 3. 100000 Higher
- 4. 50000 Higher
- 5. 20000 Lower

Table 4.3: Rank on which the average MOP-7 CO profile for the NEU region is greater than 2 standard deviations above the mean.

4.2.3.5 Northern Europe (NEU)

Figure 4.33 shows a time series of the average daily and monthly mean CO concentrations for the northern Europe region. As with the previous regions, the daily data shows the same broad seasonal cycle as the monthly mean but also exhibits much higher frequency variations. Figure 4.34 shows the resulting daily CO anomaly profile data after subtraction of the monthly mean. After the monthly mean is subtracted from the daily data the seasonal cycle is no longer present and only the higher frequency departures from the mean are evident. For this region, there are a number of departures of more than three standard deviations from the mean as indicated in Figure 4.34 the details of which are summarised in Table 4.6.

Index	Date	Higher or Lower than the mean	Number of Profiles within region
1	30/09/00	Higher	1
2	26/11/00	Higher	2
3	04/05/00	Higher	27
4	02/09/00	Higher	62
5	23/09/00	Higher	5
6	12/04/00	Higher	1
7	03/09/00	Higher	9
8	25/01/01	Lower	2

Table 4.6: Days on which the average MOPITT CO profile for the NEU region is greater than 3 standard deviations from the mean.

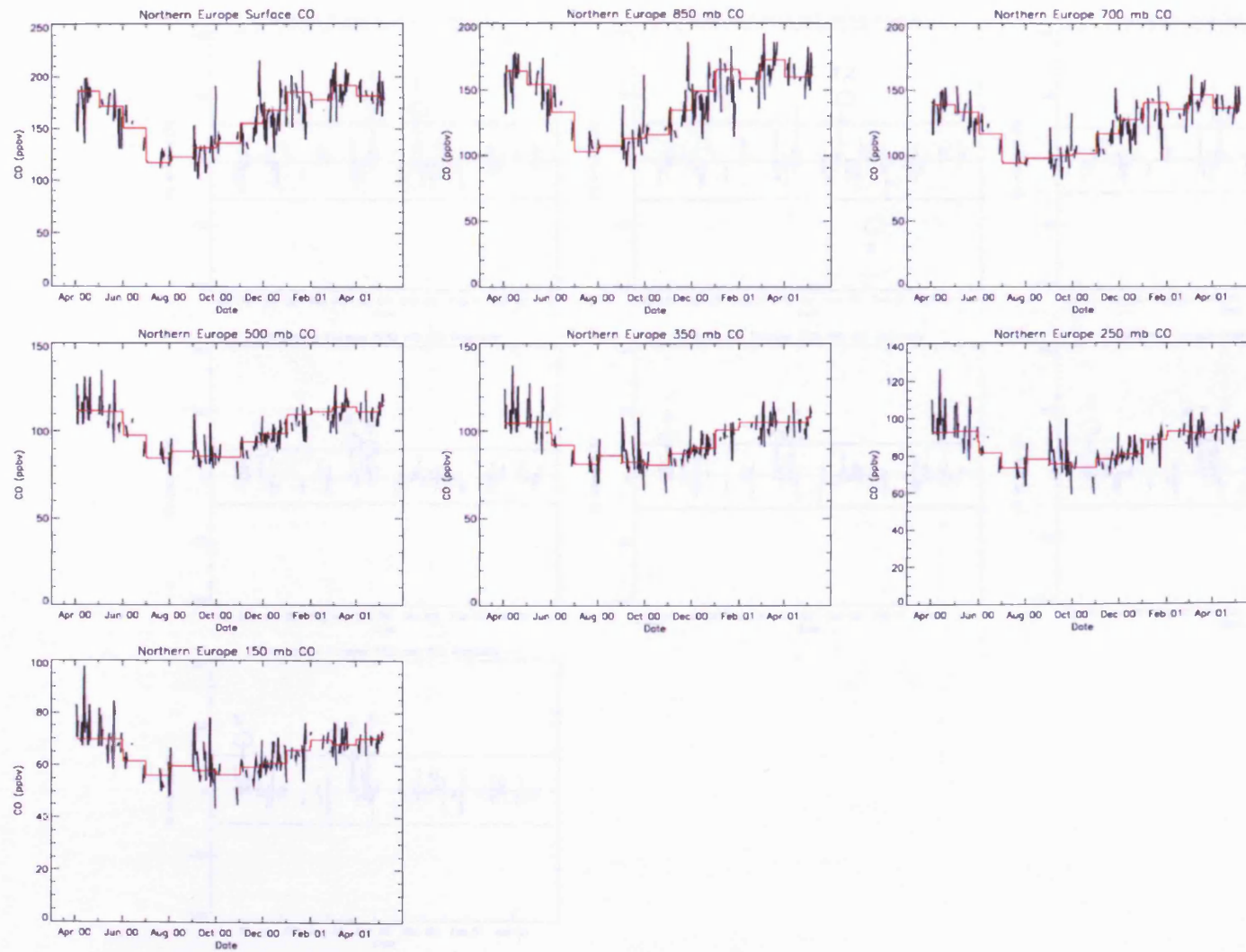


Figure 4.33: Northern Europe (NEU) region average daily (black) and monthly mean (red) CO profile time series.

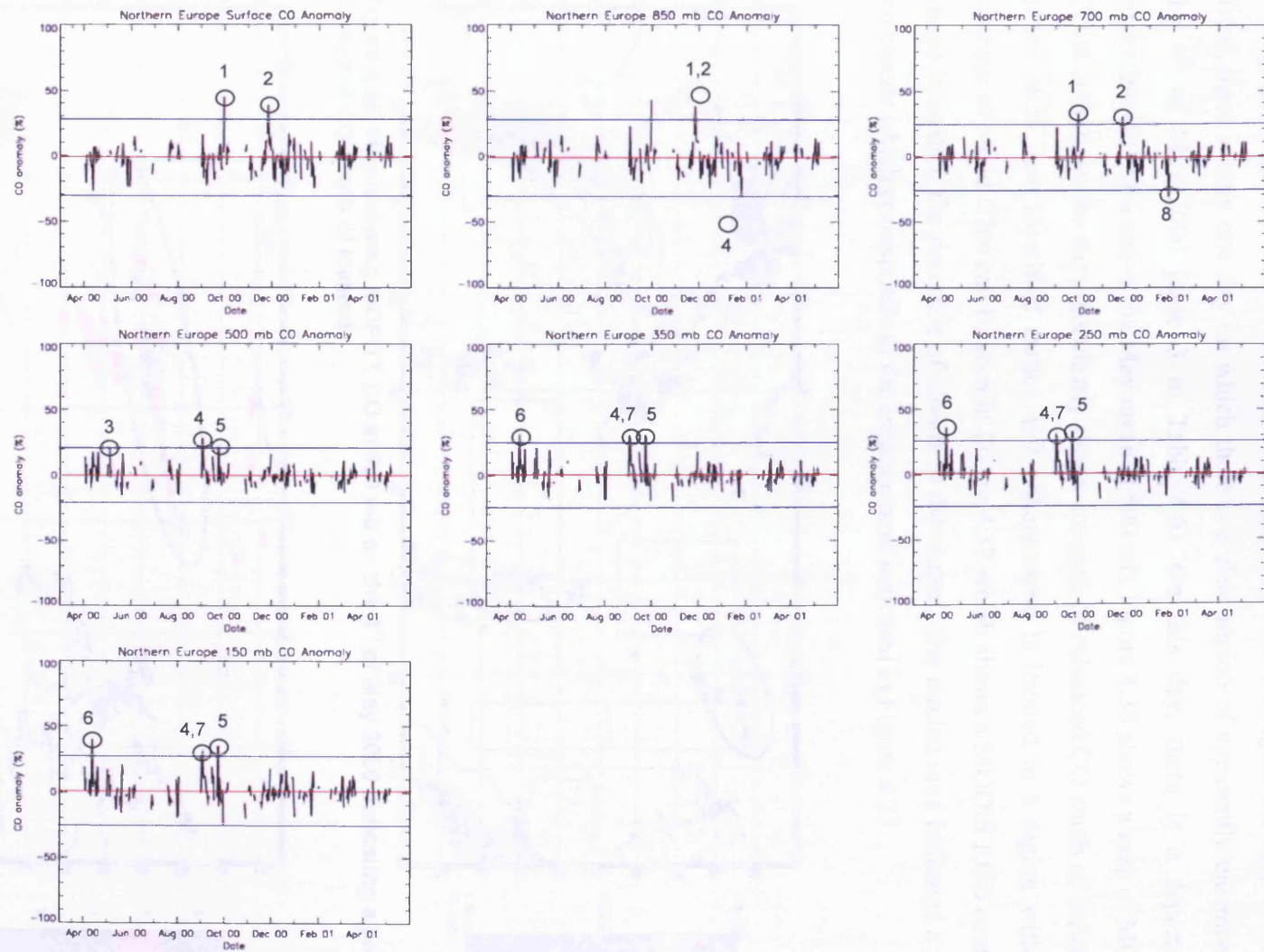


Figure 4.34: Northern Europe region (NEU) average daily CO anomaly (black), the red line indicates the mean anomaly for the whole time period and the blue lines represent ± 3 standard deviations from this mean.

After examining the data and the number of profiles within the region for each of the days listed, there is only one day on which there is a clear region of apparently enhanced CO, the 4th of May 2000 (case 3 in Table 4.6). On this day, there is a departure of approximately 20% above the May mean at 500 mb. Figure 4.35 shows a map of MOPITT CO at 500mb for the day, this clearly shows a region of enhanced CO south of Iceland. As in the NUS case identified earlier, this enhancement is located in a region with large amounts of cloud. This can be seen in Figure 4.37 which shows a MODIS RGB composite image indicating the presence of clouds in the region. The circled area indicates a gap in the clouds which corresponds to the enhancement indicated in Figure 4.35.

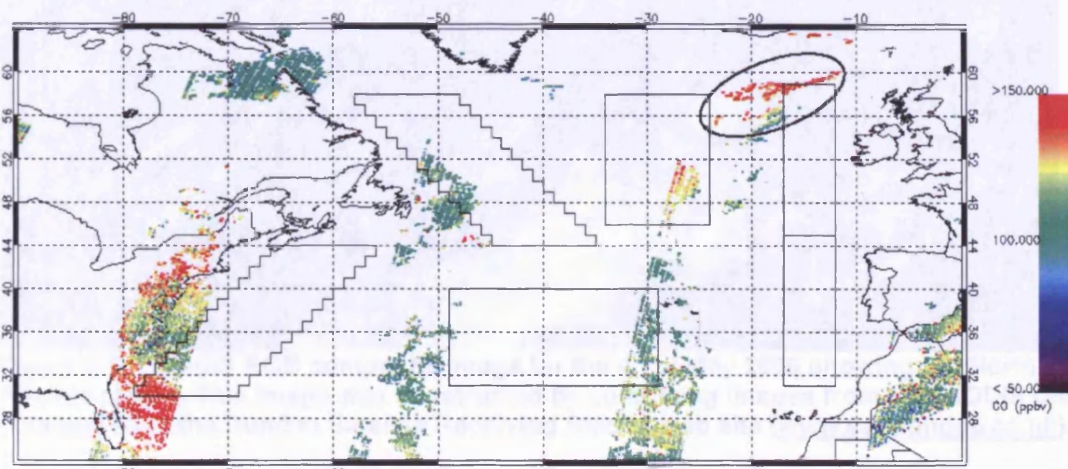


Figure 4.35: Map showing MOPITT CO at 500 mb on the 4th of May 2000 indicating a plume of enhanced CO south of Iceland.

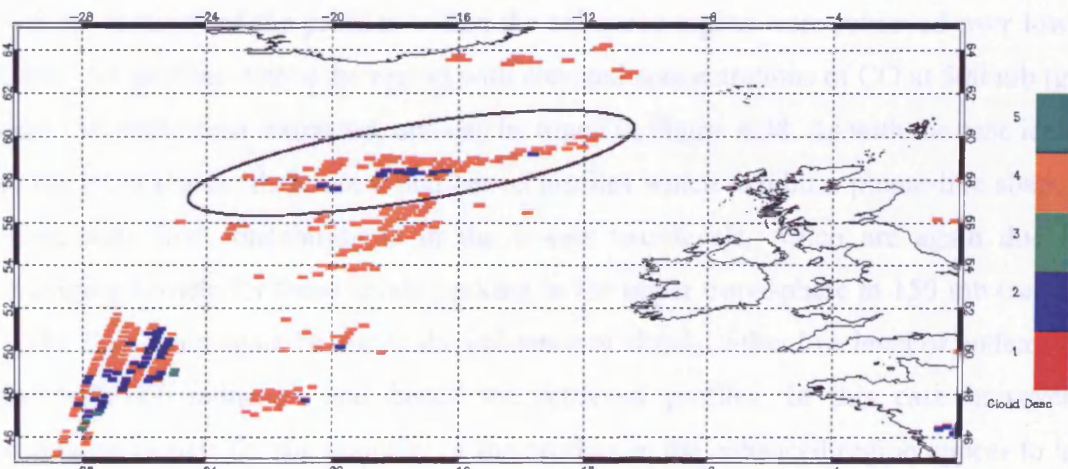


Figure 4.36: Map showing MOPITT cloud description flag values over the North Atlantic on the 4th of May 2000.

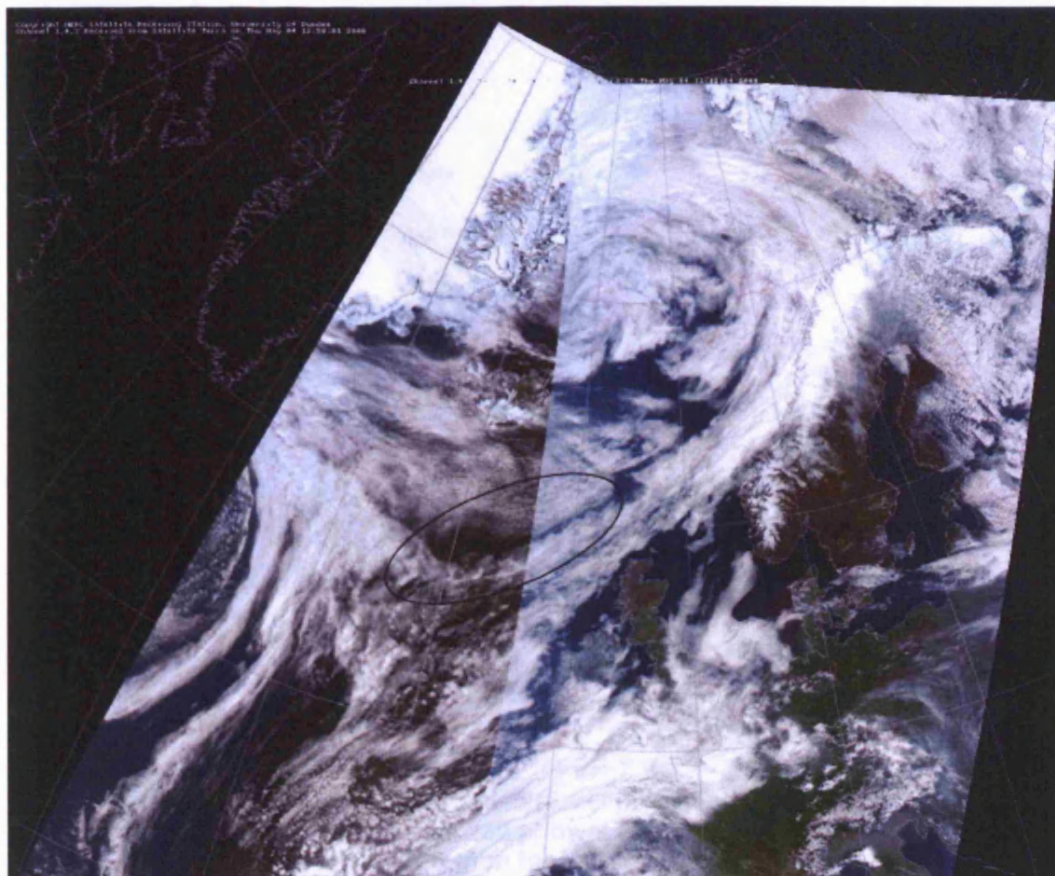


Figure 4.37: MODIS RGB composite image for the 4th of May 2000 showing the North East Atlantic region. This image was constructed by combining images from two MODIS orbits, obtained from the Dundee Satellite Receiving Station web site (www.sat.dundee.ac.uk).

After analysing the MOPITT cloud description flags for this region (Figure 4.36), it is clear that the majority of the profiles within the enhanced region were retrieved over low level cloud. All profiles within the region with elevated concentrations of CO at 500 mb (greater than 130 ppbv) were extracted, and can be found in Figure 4.38. As with the case identified in the NUS region, there are a number of profiles which exhibit a plume-like shape, with abnormally low concentrations in the lowest two levels, which are again due to the averaging kernels for these levels peaking in the upper troposphere at 150 mb (see Figure 4.39). This could again be due to the influence of clouds, either low level or undetected, on the MOPITT radiances and hence the retrieved profiles. In this case however, the averaging kernels for the majority of the profiles in the enhanced region appear to have a more conventional shape, indicating that the retrievals for these profiles were not affected by the low level cloud over which they were retrieved and so may be used in further analysis.

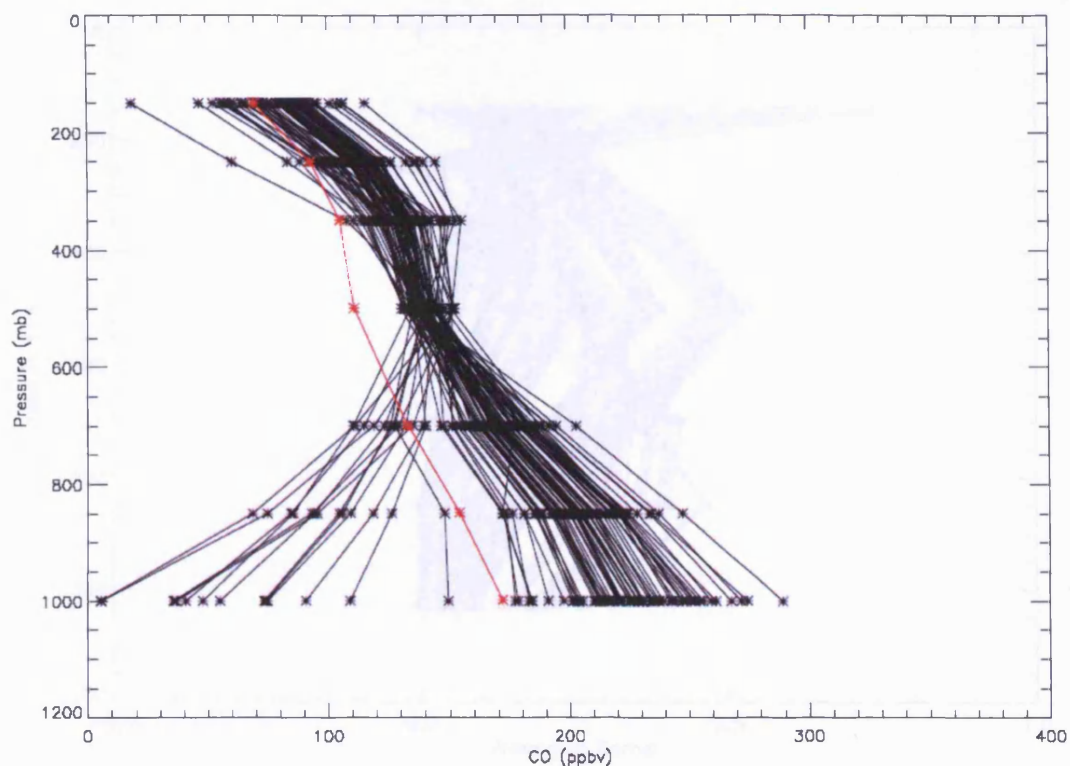


Figure 4.38: MOPITT CO profiles for those pixels in the enhanced CO region in Figure 4.35 with CO concentrations greater than 130 ppbv at 500 mb, the red profile indicates the monthly mean profile for the NEU region for May 2000.

Those profiles which appear to be unaffected by cloud were isolated (see Figure 4.40), and 5 day back trajectories starting at 500 mb were calculated for each. The results of the trajectory run can be found in Figure 4.42 and Figure 4.43. The trajectories appear to take two distinct routes before arriving at their final destination south of Iceland. The first set of trajectories (1 in Figure 4.42) show that some of the 500 mb air in the enhancement originated 5 days earlier over the Pacific coast of Canada in the mid to upper troposphere, between 300 and 500 mb, before moving southeast and descending over the more polluted United States. The air parcels then moved towards the east coast where they mixed with the air parcels from the second set of trajectories (2 in Figure 4.42), which have their origins in the polluted southern United States boundary layer. This mixed air is then uplifted off the coast and travels northeast across the Atlantic, to form the region of enhanced CO observed on the 4th of May. The MOPITT data for the five days of the back trajectories were examined to try and determine if the MOPITT instrument was able to track the enhancement from its source. Unfortunately, due to missing data, owing to coverage problems and clouds, it is not possible to see the CO enhancement along the path indicated by the trajectories.

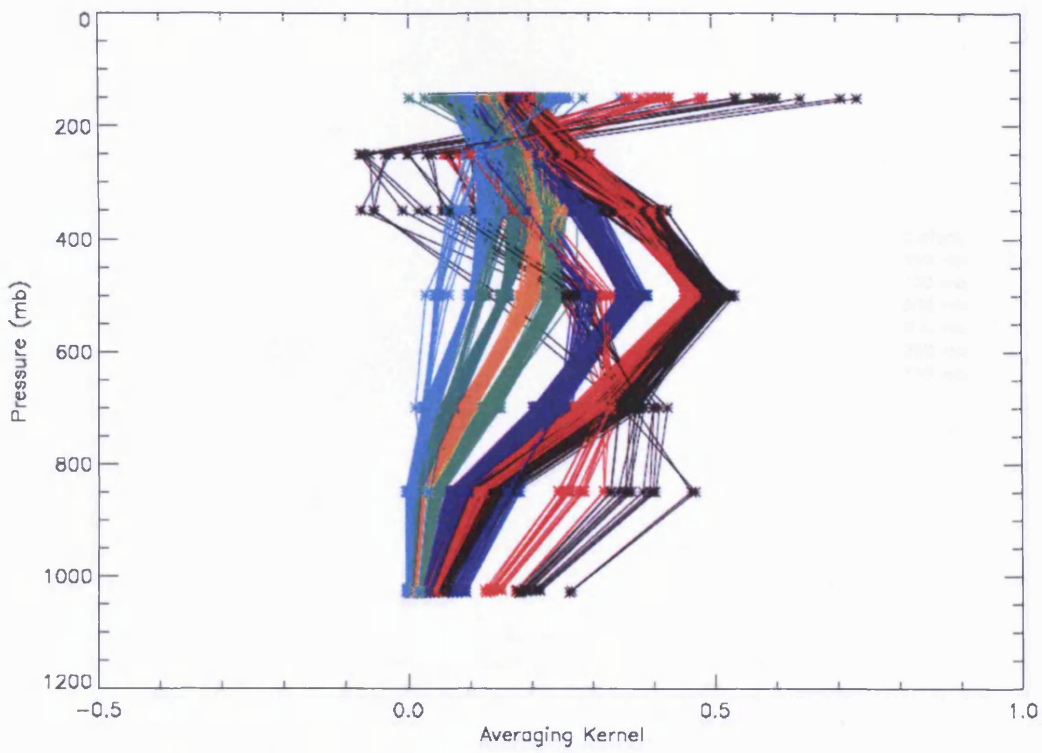


Figure 4.39: The MOPITT averaging kernels for those profiles shown in Figure 4.38.

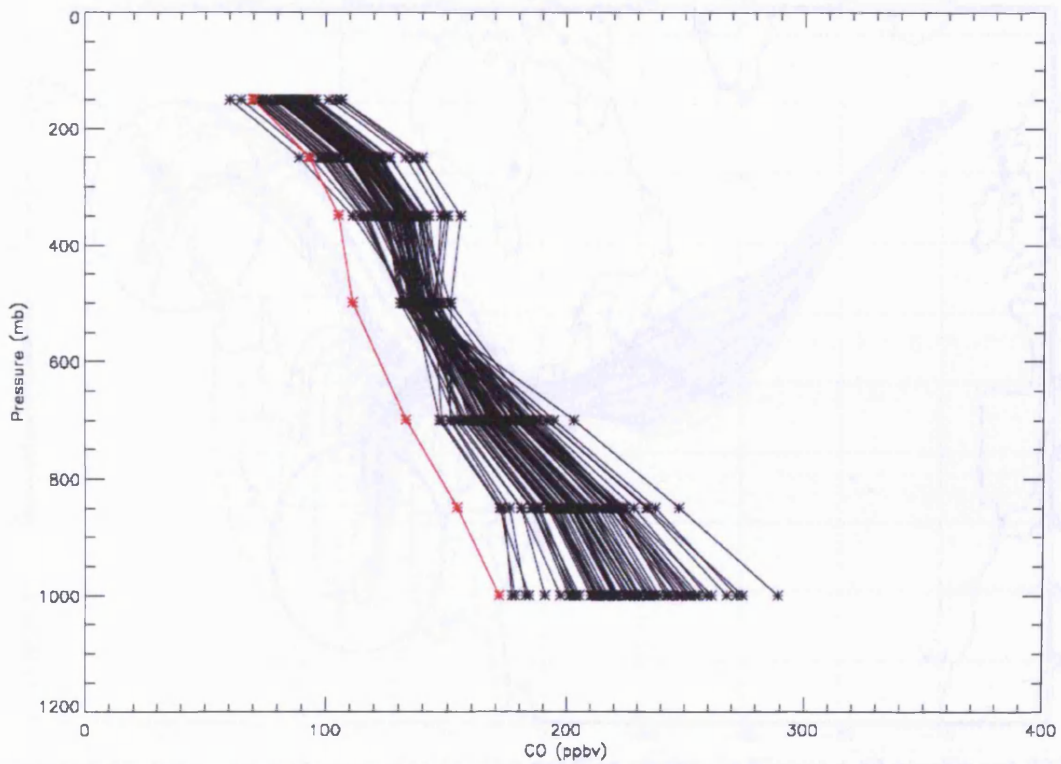


Figure 4.40: Those MOPITT profiles from Figure 4.38 which have conventionally shaped averaging kernels.

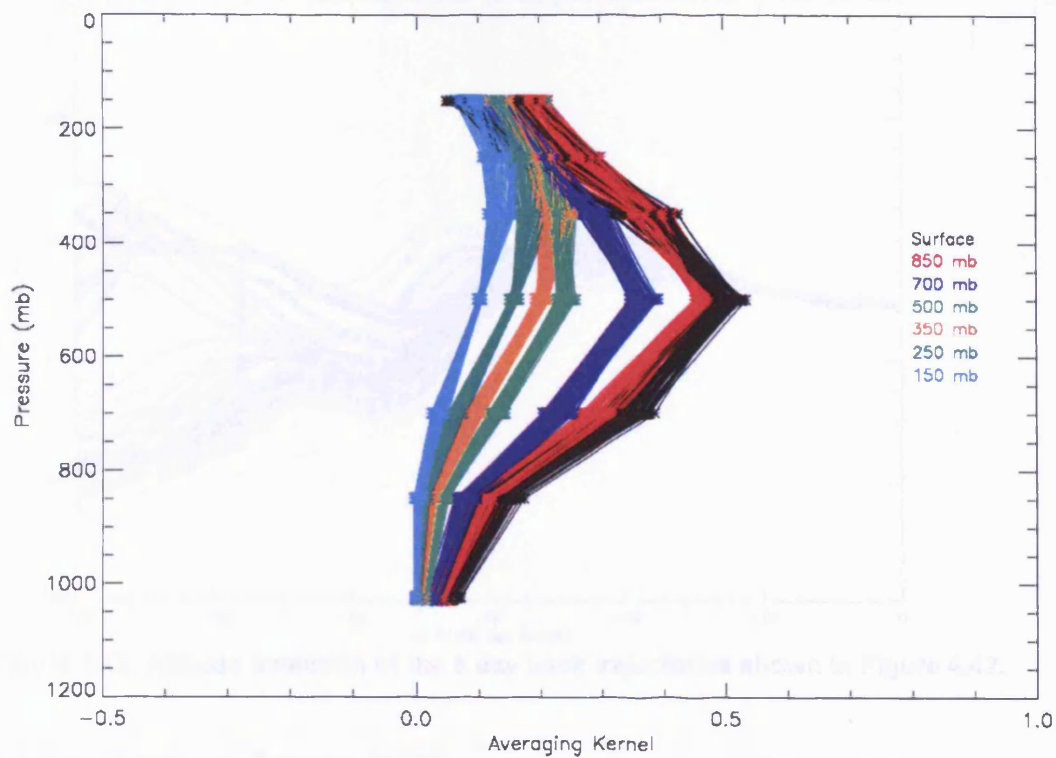


Figure 4.41: The MOPITT averaging kernels for the profiles in Figure 4.40.

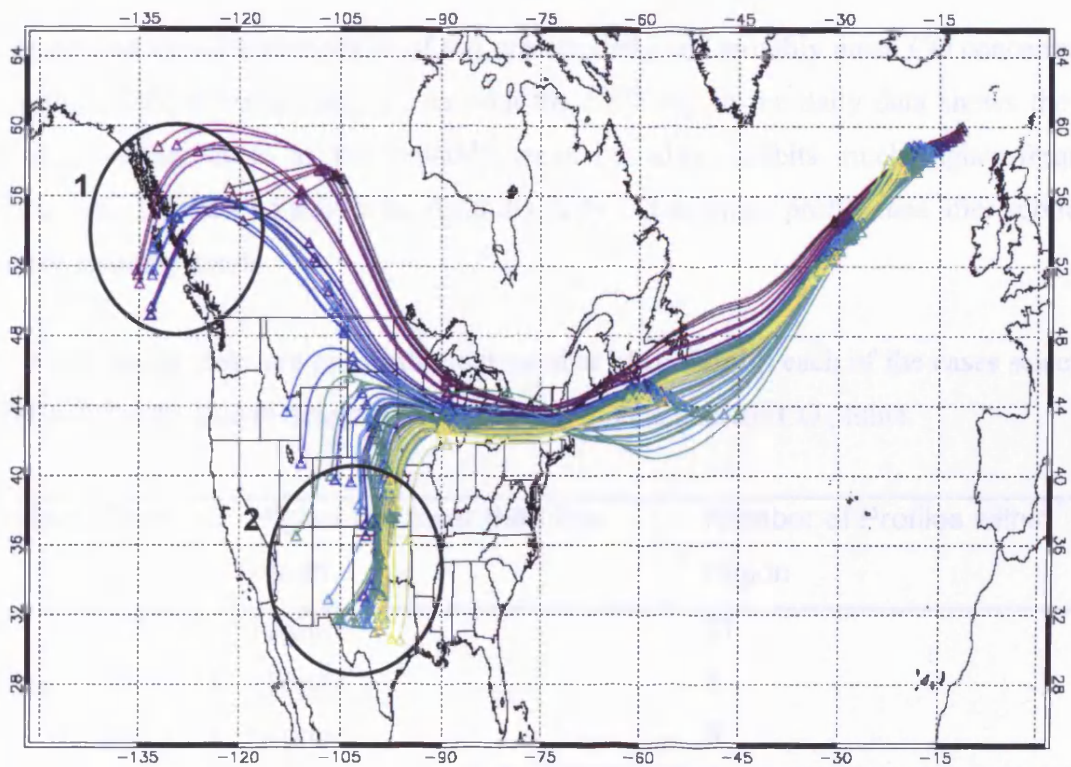


Figure 4.42: 5 day back trajectories for the profiles shown in Figure 4.40 starting at 500 mb on the 4th of May 2000, coloured by starting location.

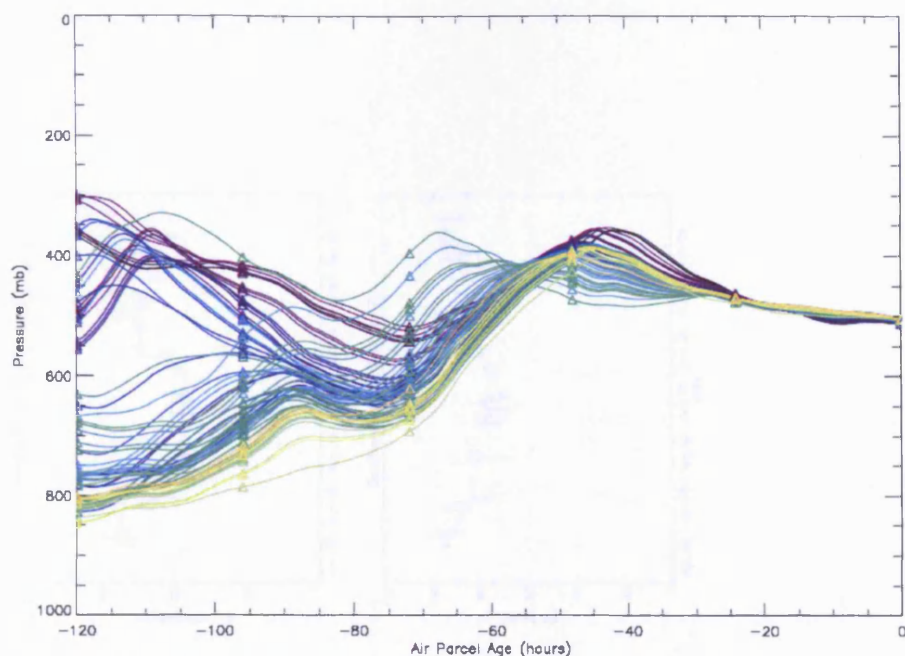


Figure 4.43: Altitude evolution of the 5 day back trajectories shown in Figure 4.42.

4.2.3.6 Southern Europe (SEU)

Figure 4.44 shows a time series of the average daily and monthly mean CO concentrations for the southern Europe region. As with the NEU region the daily data shows the same broad seasonal cycle as the monthly mean but also exhibits much higher frequency variations. Figure 4.45 shows the resulting daily CO anomaly profile data after subtraction of the monthly mean.

For this region there are an insufficient number of profiles in each of the cases selected in Table 4.7 to be able to determine the presence of an enhanced CO plume.

Index	Date	Higher or Lower than the mean	Number of Profiles within region
1	23/11/00	Higher	27
2	04/02/01	Higher	1
3	20/02/01	Higher	5

Table 4.7: Days on which the average MOPITT CO profile for the SEU region is greater than 3 standard deviations from the mean.

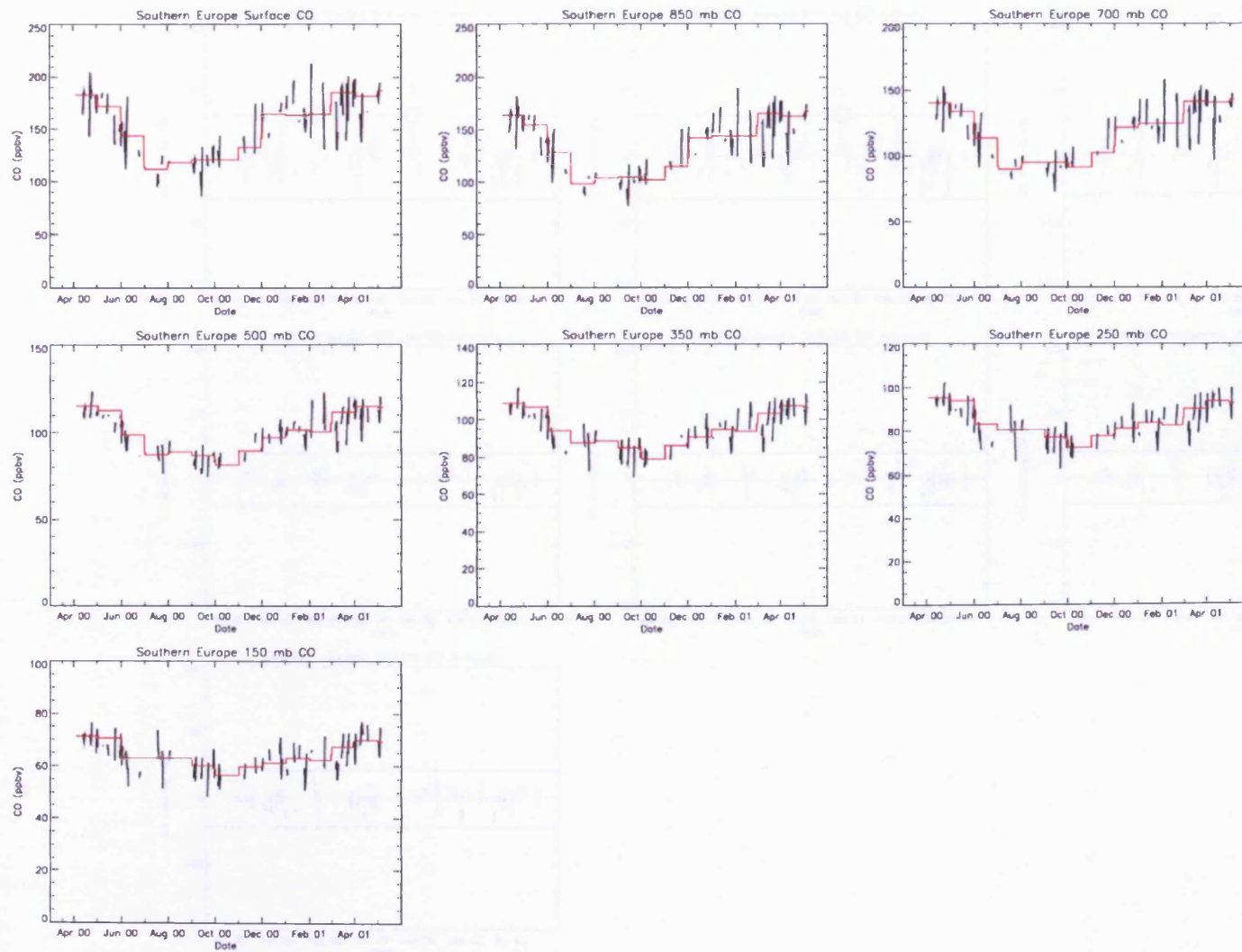


Figure 4.44: Southern Europe (SEU) region average daily (black) and monthly mean (red) CO profile time series.

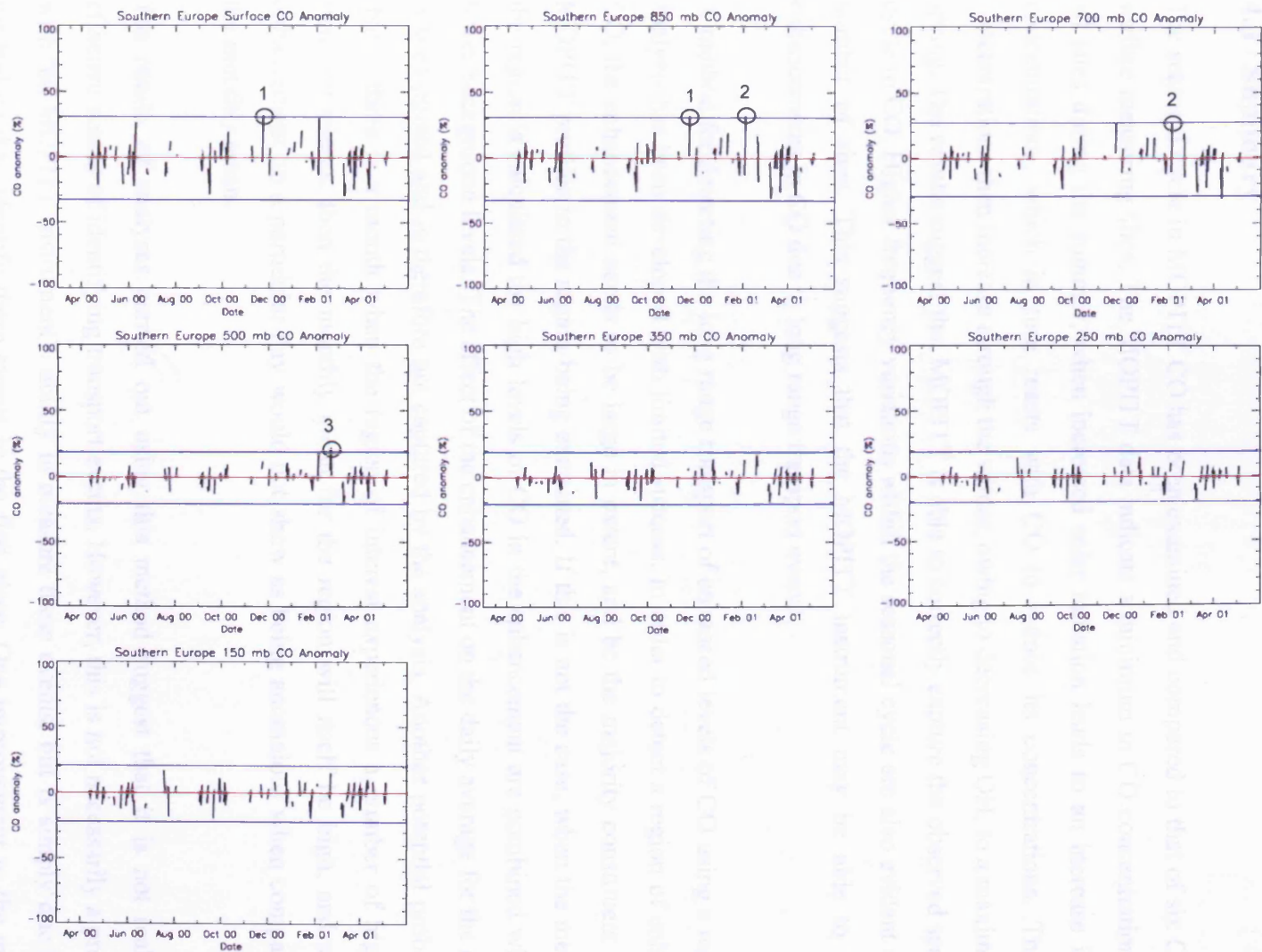


Figure 4.45: Southern Europe region (SEU) average daily CO anomaly (black), the red line indicates the mean anomaly for the whole time period and the blue lines represent ± 3 standard deviations from this mean.

4.3 Summary

The seasonal cycle in MOPITT CO has been examined and compared to that of six CMDL surface measuring sites. The MOPITT data indicate a minimum in CO concentration over all sites during the summer, when increased solar radiation leads to an increase in OH concentrations, which in turn reacts with CO to reduce its concentrations. The CO concentrations then increase through the winter, owing to decreasing OH, to a maximum in spring. The results suggest that MOPITT is able to correctly capture the observed seasonal cycle in CO. Higher frequency variations within the seasonal cycle are also evident over a number of sites. This suggests that the MOPITT instrument may be able to detect enhancements in CO due to long range transport events.

A method for detecting the long range transport of enhanced levels of CO using a regional analysis has been developed with limited success. In order to detect a region of enhanced CO, the enhancement needs to be large in extent, and be the majority constituent of the MOPITT profiles in the region being examined. If this is not the case, when the mean for the region is calculated the high levels of CO in the enhancement are combined with the lower/background levels. The effect of the enhancement on the daily average for the region is then diluted and is therefore not captured by the analysis. Another potential problem is that if there is a month when the region of interest experiences a number of high CO transport events, then the monthly mean for the region will itself be high, and so any enhancement on a particular day would not show as being anomalous when compared to the monthly mean.

The results of analyses carried out using this method suggest that it is not really an effective means of identifying transport events. However, this is not necessarily a problem with the MOPITT instrument's ability to measure these events, but is simply due to the method used to identify these events in the first place. One improvement to the method used, might be to reduce the size of the chosen regions although this would almost certainly reduce the number of coincident measurements. Where coincidences do occur, it might be easier to detect enhanced levels of CO as less dilution will occur during the averaging. Another improvement might be to reduce the three standard deviation limit used in this study. This limit was chosen so that only the most extreme events would be isolated by the analysis, the relaxing of this criterion would result in many more events being

identified. However, it is clear that when an event is detected, for example the anomalously low levels of CO detected in the analysis of the A2 region, the results show that the MOPITT instrument is able to measure and track the event along its trajectory for several days unless there is missing data due to cloud and coverage issues.

The results here suggest that observing and tracking pollution transport events using nadir viewing satellite instruments such as MOPITT is fraught with problems. The major problem is that such transport events tend to be associated with frontal systems which by their very nature are regions of high cloud content. Which, with the exception of some cases where retrieval is possible over very low cloud, means that a nadir viewing instrument would not be able to make measurements of such events. Another problem is coverage, MOPITT is in a sun-synchronous orbit with an altitude of 705 km. This combined with a swath width of 600 km enables the instruments to achieve global coverage only every 3 days. This means that on any particular day around two thirds of the Earth's surface is not observed by MOPITT. This, coupled with missing data due to clouds, makes it very difficult to obtain measurements which are coincident with the trajectory of a transport event. Perhaps a geostationary satellite instrument would be more suited to this task, being able to make measurements over a third of the Earth's surface every few minutes. This would enable much more frequent measurements of a particular region increasing the likelihood of a measurement being coincident with a transport event and cloud-free.

5. Gaining Extra Information from MOPITT profile measurements.

Throughout this thesis, day and night MOPITT data have been treated separately since it is clear from the examination of MOPITT CO profile data and simulations performed using operational MOPITT averaging kernels that MOPITT exhibits different vertical resolution and sensitivity between day and night time measurements. The fact that differences between MOPITT day and night time CO profile retrievals exist has been noted previously [Deeter *et al.*, 2003; Deeter *et al.*, 2004; Crawford *et al.*, 2004; Heald *et al.*], but so far this property of the data has not been exploited to gain extra vertical information from the MOPITT retrievals. In particular, the averaging kernels for the lower three retrieval levels exhibit a considerable diurnal variation in sensitivity especially over locations which have large diurnal surface temperature changes. This shifting of the lower averaging kernels away from the surface during the night may hold the key to gaining extra information about the tropospheric CO profile, in particular the boundary layer and the upper troposphere.

5.1 Day-Night Difference Simulation Studies

5.1.1 Methodology

The simulations performed in Section 3.4 for a layer enhancement of CO, were repeated for both day and night conditions to examine the day/night shifting of sensitivity of the lowermost retrieval levels. Night time ‘retrieved’ profiles are subtracted from daytime profiles to yield a difference profile which is used to investigate the effects of this shifting of sensitivity.

5.1.2 Results

Figure 5.1 shows day and night MOPITT averaging kernels for the Libyan Desert in August 2000. This is a region which experiences large diurnal temperature variations and so one would expect a large day/night sensitivity shift. The averaging kernels show that as expected there is a clear change in the sensitivity of the lower retrieval levels from the day to the night. During the day, the averaging kernels for the lower three retrieval levels peak

in the lower troposphere and show some sensitivity to the surface and boundary layer. At night however, the sensitivity of these averaging kernels shifts to the upper troposphere and show very little sensitivity below 850 mb with no sensitivity to the surface. Figure 5.2 shows the results of simulations conducted using the averaging kernels from the Libyan Desert in August 2000. The results show that day/night sensitivity changes lead to very different retrieved profiles given the same input profile. Lower tropospheric enhancements (below 850 mb) are clearly reflected in the daytime retrieved profiles (below 500 mb) but are not evident in the night profiles. An enhancement at 700 mb clearly has an effect on both day and night profiles with greater sensitivity shown during the day. Enhancements at altitudes above 500 mb act to enhance only the upper tropospheric levels during the day but affect the whole profile during the night. In fact due to the shape of the lower level averaging kernels enhancements at high altitudes during the day act to reduce the CO concentrations in the lower tropospheric levels of the retrieved profiles. It is these differences which may be used to gain information about the vertical structure of CO. Provided that the CO has not changed significantly between day and night time measurements, the result is three averaging kernel groups, compared with the one or two groups observed in day/night retrievals alone.

Although the day profile itself shows sensitivity to the boundary layer, the averaging kernels for the 'surface' and 850 mb levels are very broad and are sensitive to a tropospheric layer from the surface up to 350 mb. This means that it is not possible to separate out the contribution which arises solely from the lower troposphere using the daytime measurements alone. By subtracting the night retrieved profile, whose lower levels have little or no sensitivity to the lower troposphere, from the day retrieved profile, which does have boundary layer information, it is possible to gain information on the lower tropospheric contribution to the daytime retrieved 'surface' level, or the upper tropospheric contribution to the night time 'surface' level. Figure 5.3 shows the result of subtracting the night from the day simulations of layer enhanced profiles for the Libyan Desert in August 2000. The results show that day/night differences have the greatest effect on the retrieved 'surface' level CO with very little or no effect above 500 mb. This is due to the upper level averaging kernels exhibiting little diurnal variation. Figure 5.4 shows how the difference in 'retrieved' 'surface' level CO between day and night varies with the altitude of the CO enhancement in the test profile. An enhancement in CO in the lower troposphere (below 700 mb), manifests itself as a positive difference in the day – night

'surface' CO concentrations with enhancements at 850 mb having the greatest effect. Upper tropospheric enhancements (above 500 mb) show as a negative 'surface' level difference with greatest sensitivity to enhancements at 250 mb.

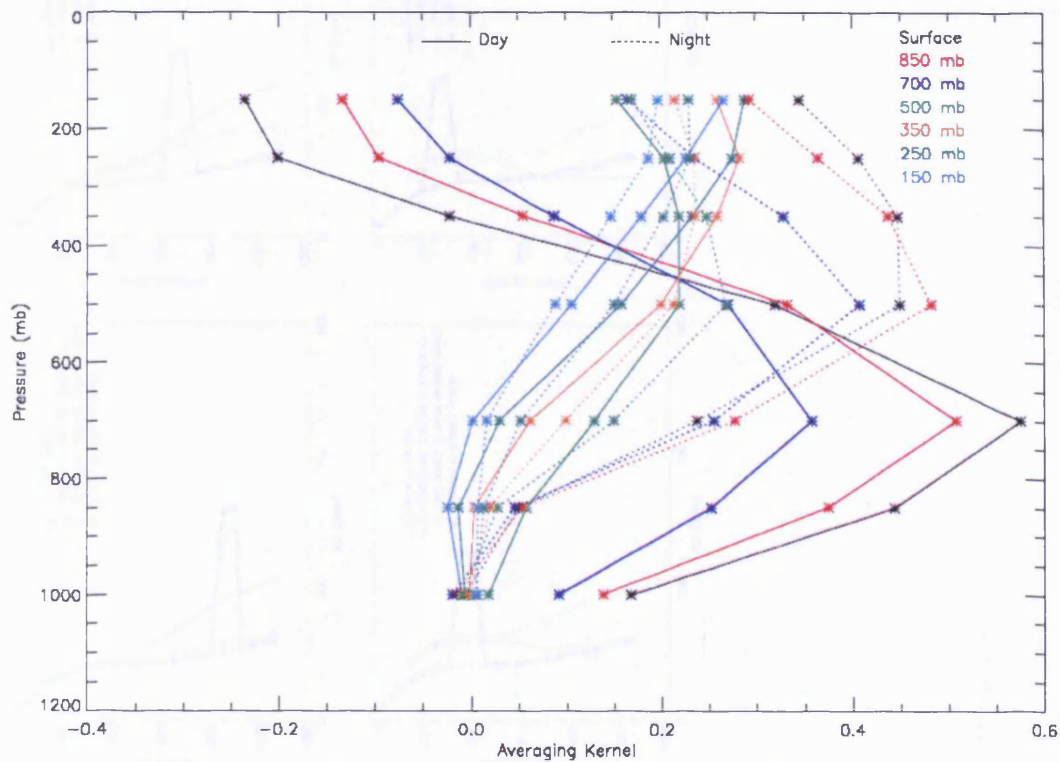


Figure 5.1: Day and night MOPITT averaging kernels for the Libyan Desert in August 2000

Simulations for the Libyan Desert in December 2000 and the UK in August yield similar results to those above as these regions are subject to strong diurnal variations in surface temperature. This is not the case however for the UK in December, where diurnal surface temperature changes are small. The day and night averaging kernels for the UK in December 2000 can be found in Figure 5.5. Due to the lower surface temperatures experienced in the UK in December, the daytime averaging kernels for the lower tropospheric levels peak higher in the atmosphere than the equivalent August kernels. Consequently, the difference between the day and night averaging kernels is much reduced leading to a reduction in day/night differences in the retrieved profiles (see Figure 5.6). Some small day/night differences still persist and the positive peak in sensitivity of the 'surface' difference is shifted upwards to 700 mb further reducing the boundary layer sensitivity of this approach.

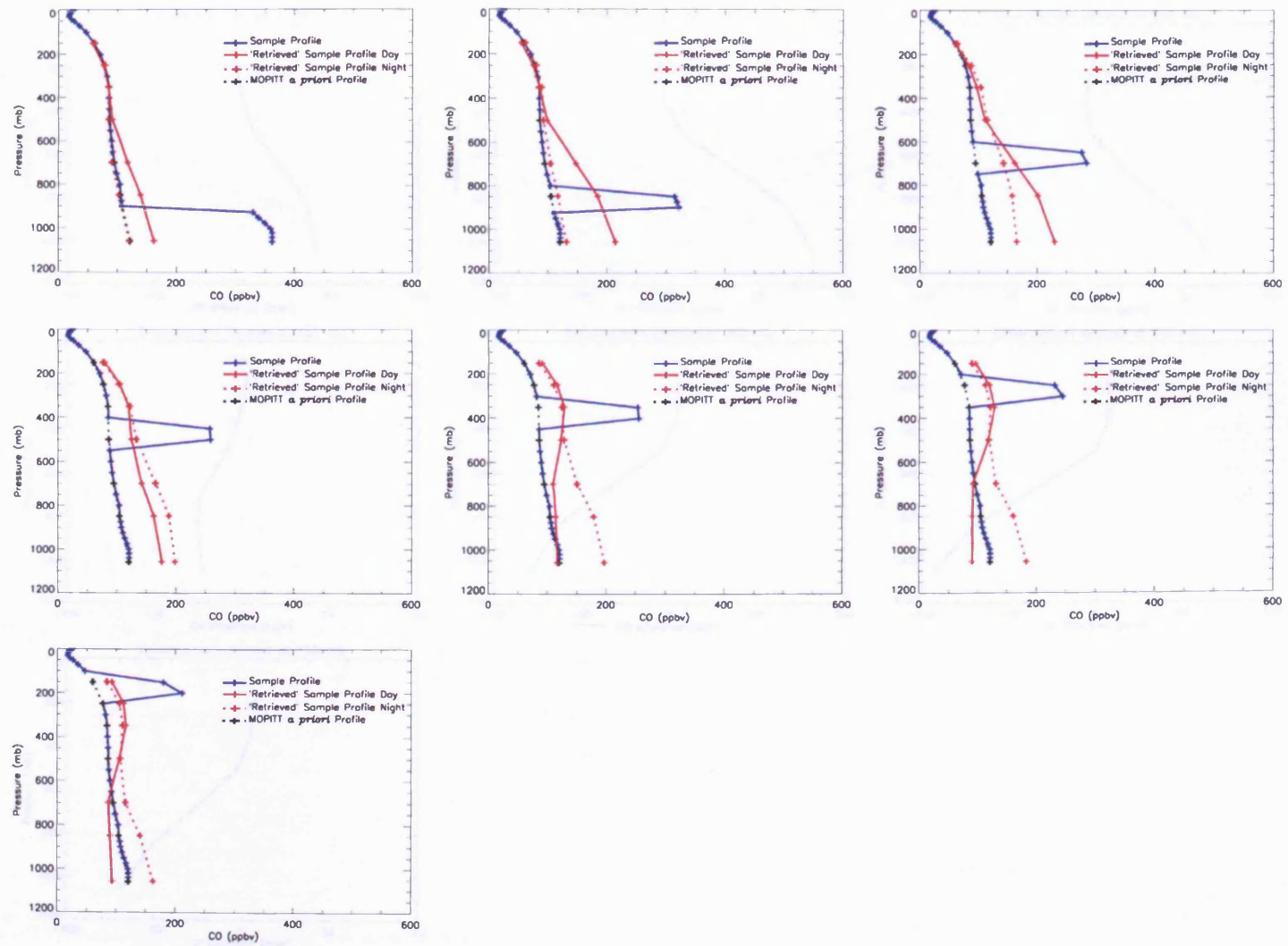


Figure 5.2: The results of simulations conducted using day and night time averaging kernels for the Libyan Desert in August 2000

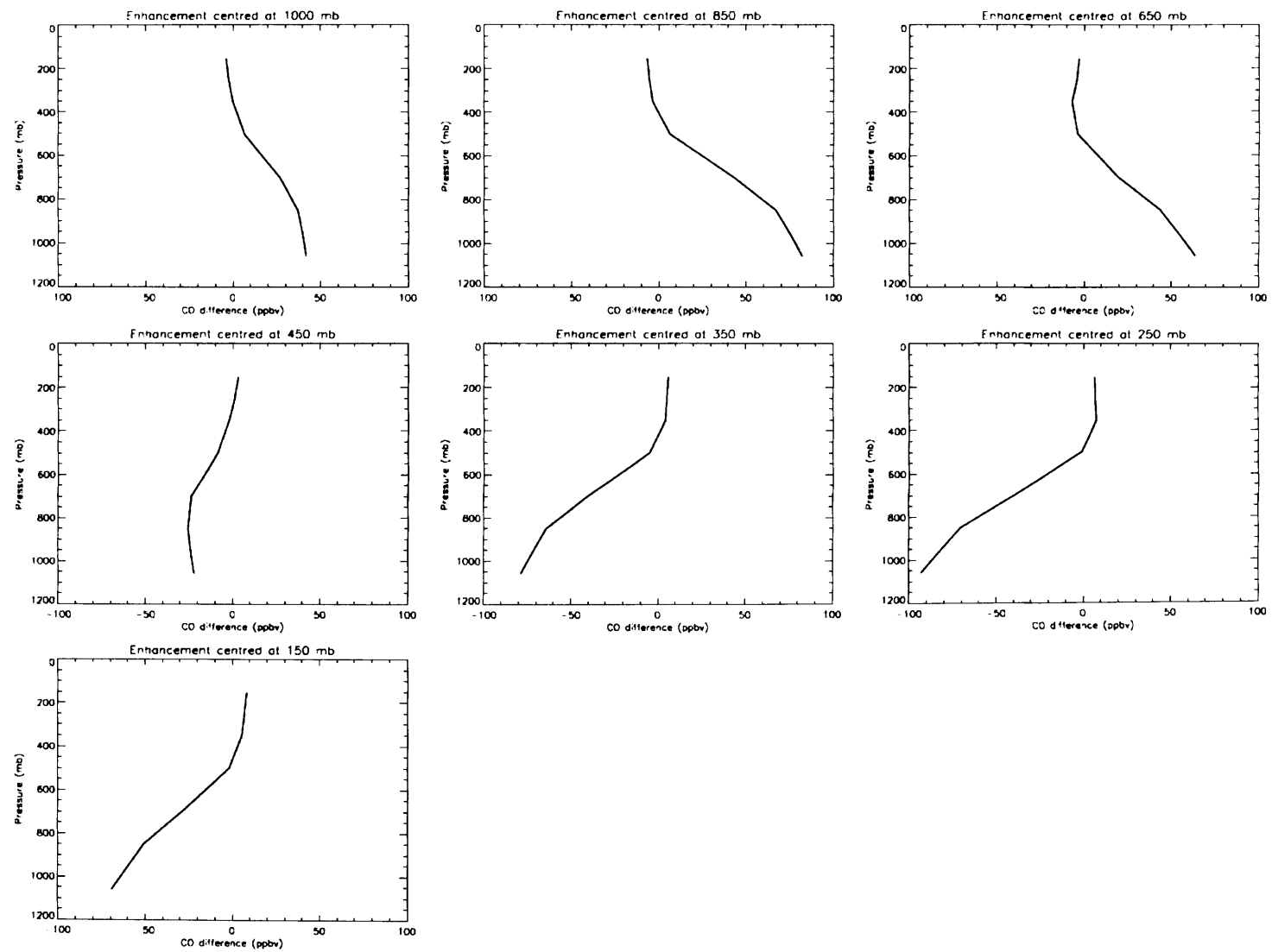


Figure 5.3: Day - night difference profiles for those profiles shown in Figure 5.2.

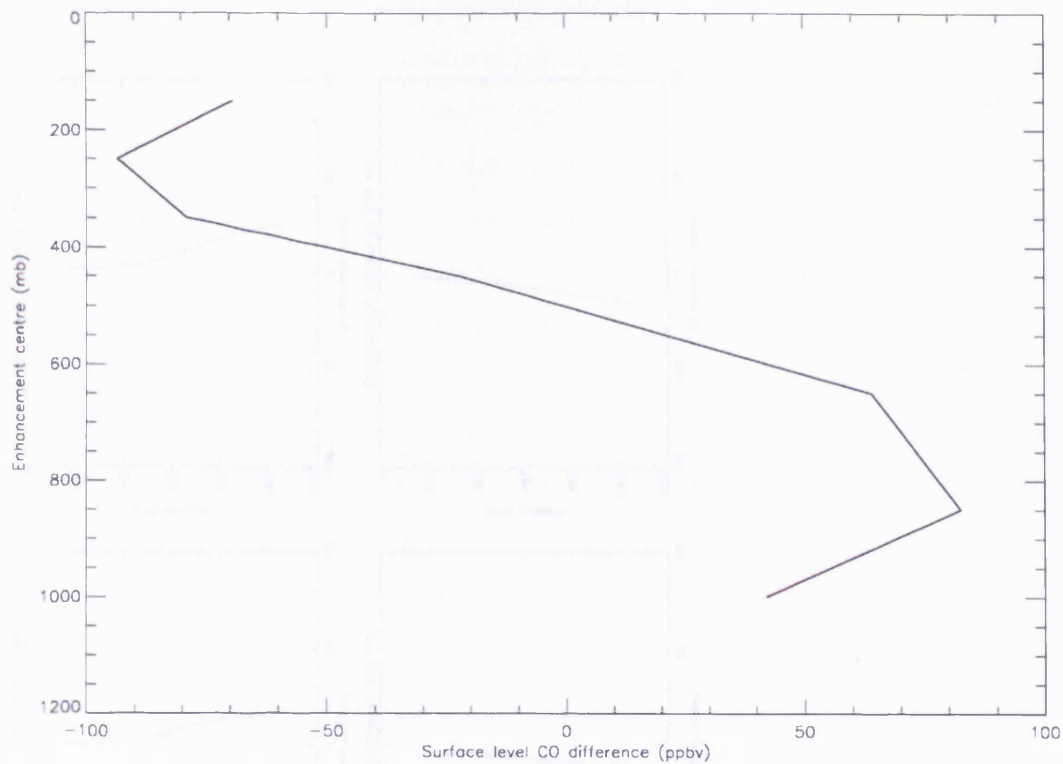


Figure 5.4: Day – Night difference in simulated MOPITT 'retrieved' surface level CO as a function of CO enhancement altitude for the Libyan Desert in August 2000

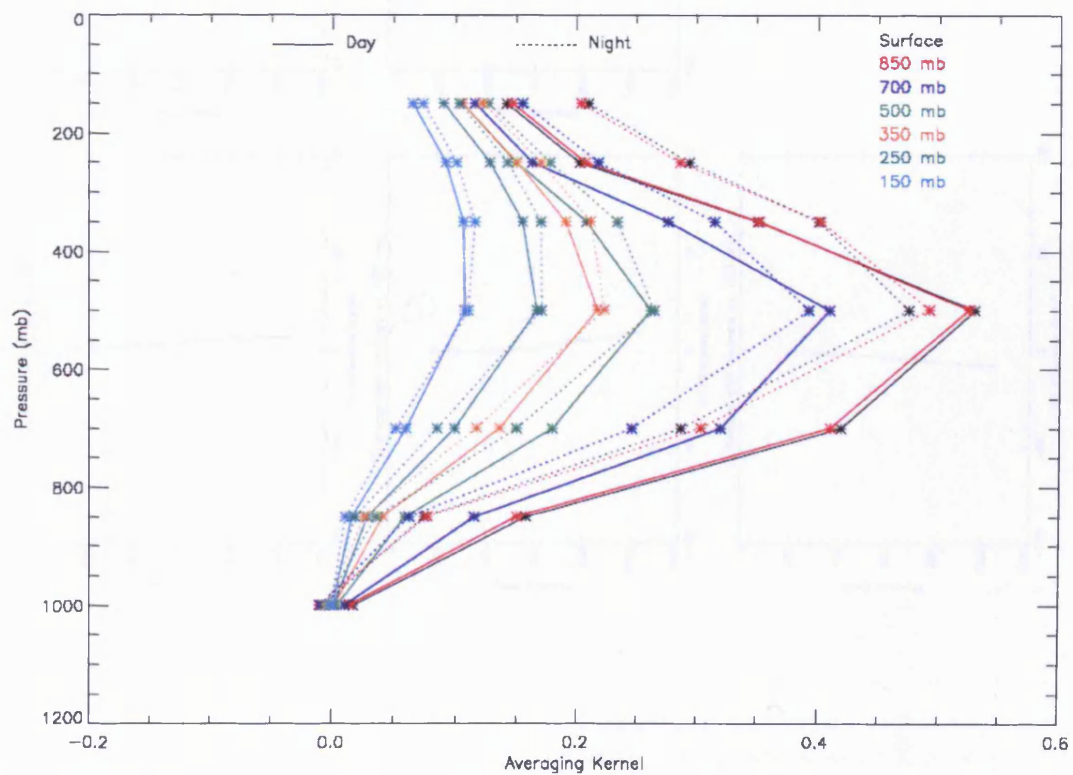


Figure 5.5: Day and night MOPITT averaging kernels for the UK in December 2000.

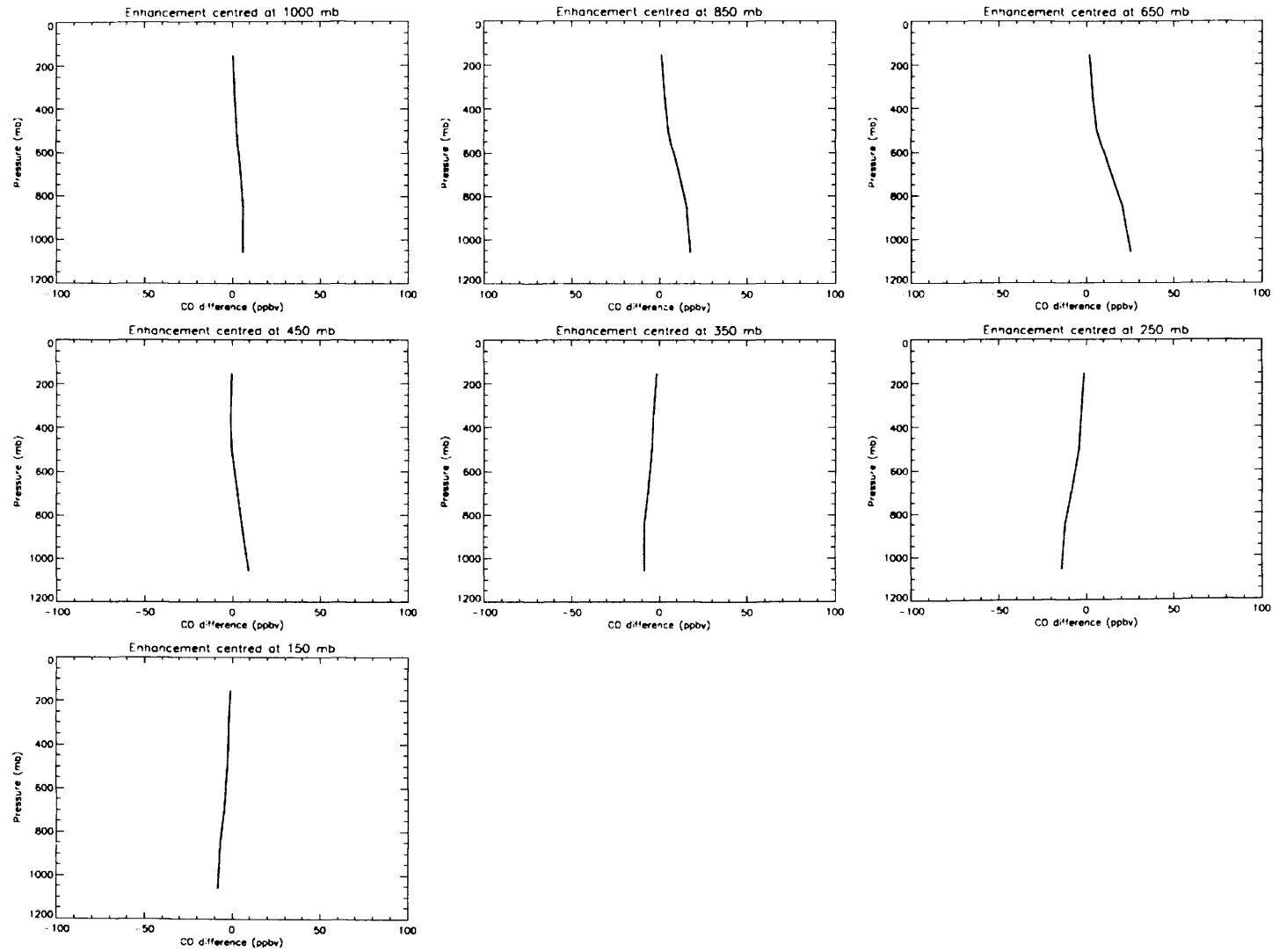


Figure 5.6: Simulated Day - night difference profiles for the UK in December 2000.

Simulations for the North Atlantic in May 2000 were also conducted. The day and night averaging kernels for this simulation can be seen in Figure 5.7. Due to the very small diurnal temperature changes experienced over the oceans, the averaging kernels for the lower levels exhibit very little change between day and night. The greatest change in averaging kernel sensitivity for the lower levels occurs in the upper troposphere, above 500 mb, with very little or no change seen in the lower troposphere. This means that the day/night ‘surface’ level difference is most sensitive to CO in the upper troposphere (see Figure 5.8). This method therefore, is still useful over the ocean since there are no sources, so CO in these regions will have been transported from continental sources, and as such is likely to be at high altitude. Thus, a negative difference in ‘surface’ level CO between day and night would indicate the presence of high altitude CO which may give an indication of transport.

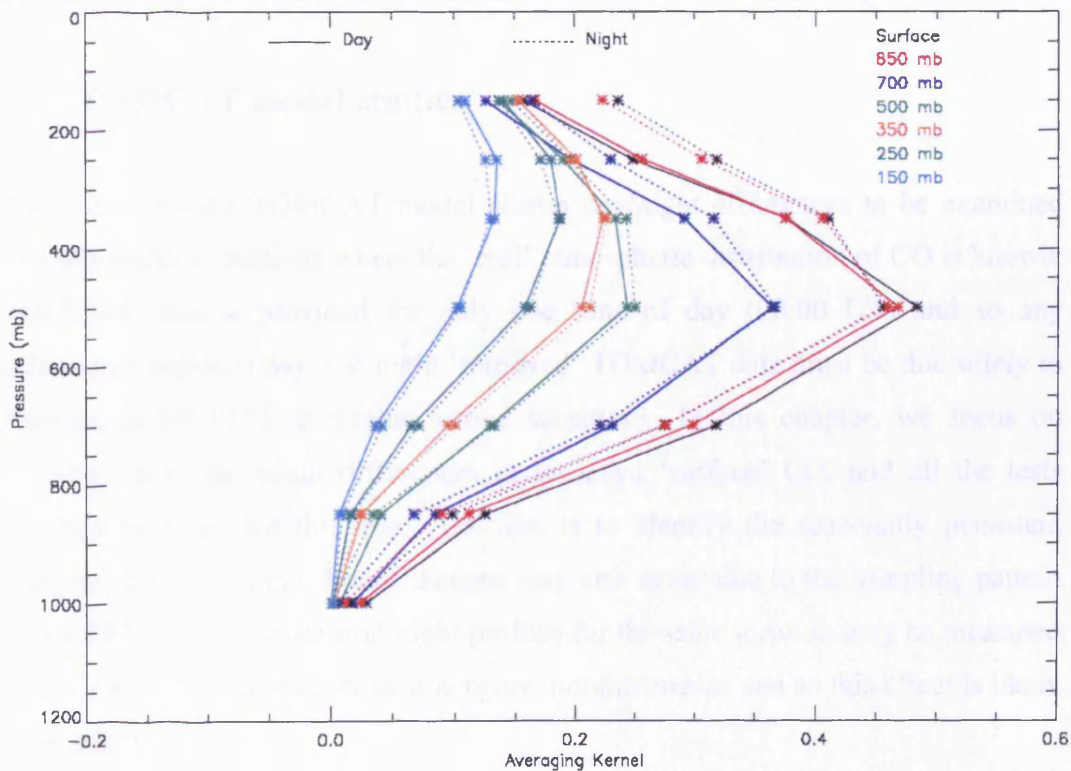


Figure 5.7: Day and night MOPITT averaging kernels for the North Atlantic in May 2000

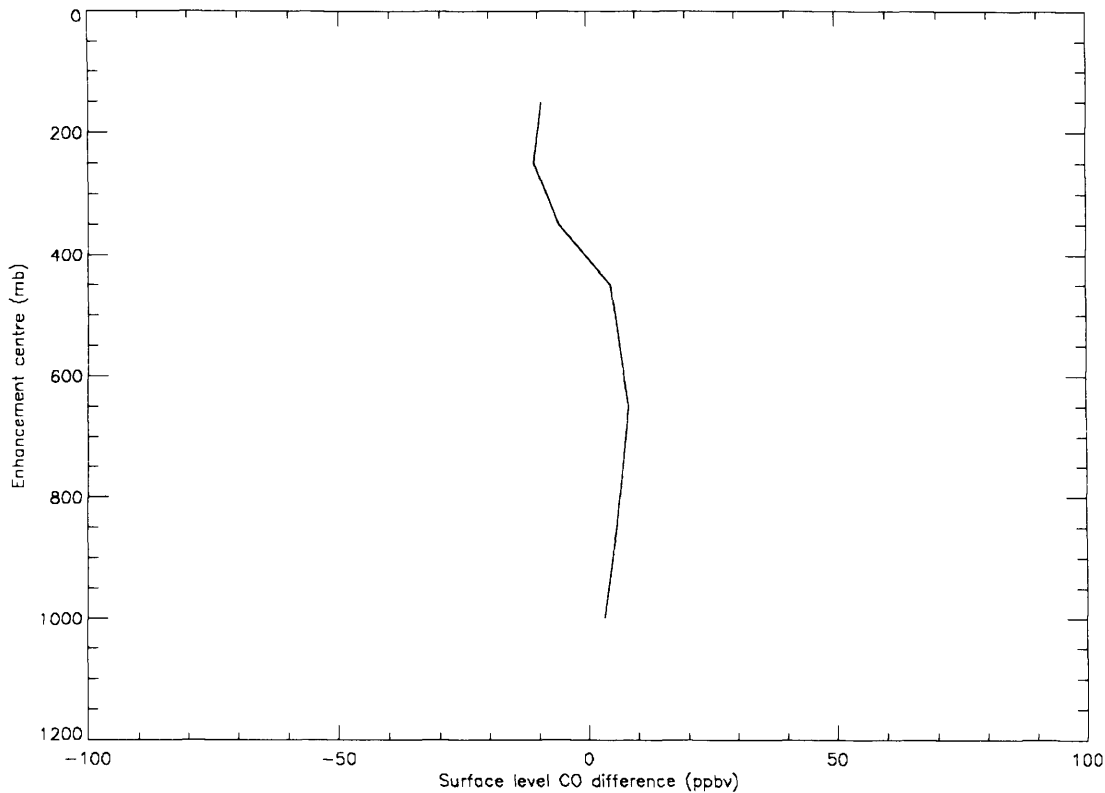


Figure 5.8: Day – Night differences in simulated MOPITT ‘retrieved’ surface level CO as a function of CO enhancement altitude for the North Atlantic in May 2000.

5.2 TOMCAT model studies

The data from the TOMCAT model allows day/night differences to be examined globally under conditions where the ‘real’ atmospheric distribution of CO is known. TOMCAT data is provided for only one time of day (00:00 UT) and so any differences between day and night ‘retrieved’ TOMCAT data must be due solely to changes in MOPITT averaging kernel sensitivity. In this chapter, we focus on monthly mean day-night differences in retrieved ‘surface’ CO, and all the tests reported here are for this case. The aim is to identify the seasonally persistent features of the CO field. Some changes may also occur due to the sampling pattern of MOPITT, whereby day and night profiles for the same location may be measured days apart, but the data examined here are monthly means and so this effect is likely to be small.

5.2.1 Methodology

MOPITT data for each day of May 2000 were split into day and night. Each dataset was then processed as described in Section 3.3.2 to produce monthly mean day and night averaged MOPITT and ‘retrieved’ TOMCAT data. The ‘retrieved’ TOMCAT ‘surface’ level night time data was subtracted from the corresponding daytime data and the differences examined. The ‘surface’ data were chosen as the simulations described above indicate that day/night differences are largest at this retrieval level.

5.2.2 Results

Figure 5.9 shows the day/night differences in ‘surface’ level ‘retrieved’ TOMCAT monthly mean CO for May 2000. The first thing to note is that there are regions of both positive and negative differences. Large positive differences tend to occur over TOMCAT source regions (see Figure 3.19), such as Mexico City, Central Europe, the Eastern Seaboard of the US and East Asia where surface CO concentrations are greatest. This is consistent with simulations, which show that during the day MOPITT exhibits greater sensitivity to the surface and boundary layer where, in these cases, CO concentrations are high, whereas at night the retrieved ‘surface’ concentrations are sensitive to the upper troposphere, thereby leading to lower retrieved concentrations for this level. This leads to MOPITT reporting higher concentrations during the day than at night over such areas hence the day/night difference is positive.

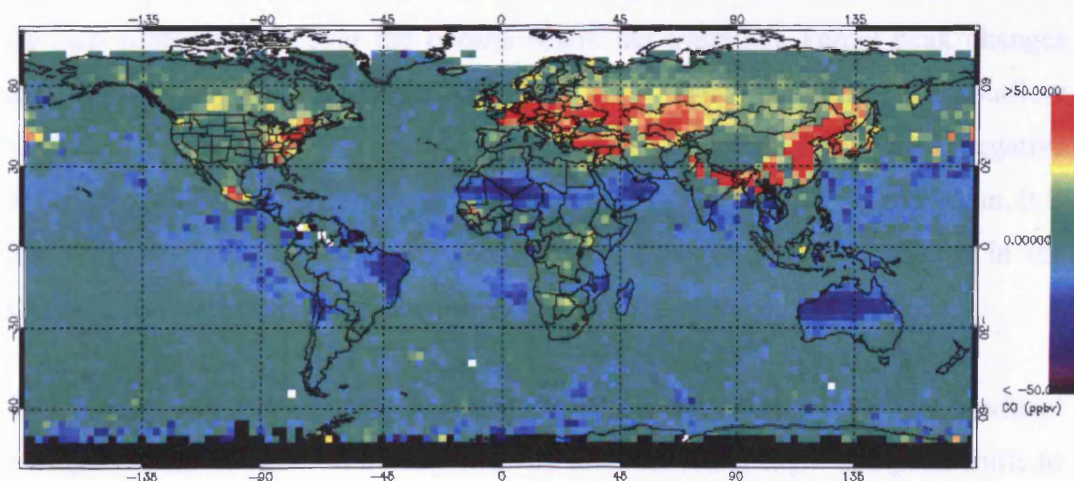


Figure 5.9: Map of ‘Retrieved’ TOMCAT day-night mean surface CO differences for May 2000.

Negative differences occur away from source regions where the CO has been subject to transport. A good example is the Sahara region, which has no CO sources in the TOMCAT model and so surface concentrations are expected to be low. In this region, the large negative day/night difference means that MOPITT would have reported higher CO concentrations at the surface during the night than in the day. Due to the large day/night sensitivity shift in MOPITT averaging kernels over such a region, simulations suggest that this would be consistent with a CO profile which exhibits higher CO concentrations at higher altitudes than at the surface, suggesting that CO in this region has been transported in at high altitude from distant sources. Negative differences also occur over the oceans which could be an indication of high altitude CO transport, since in these regions simulations suggest that the day/night difference is most sensitive to CO enhancements above 500 mb. Large negative differences are also present over the desert regions in Australia where the combination of large day/night sensitivity differences and no CO sources leads to MOPITT being sensitive at night to CO transport at high altitude.

Figure 5.10 shows a monthly mean map of the altitude at which the MOPITT 'surface' averaging kernels peak for daytime retrievals and Figure 5.11 shows the equivalent map for night time retrievals for the month of May 2000. It is clear from examining both sets of data that the areas which exhibit the largest day/night differences in CO concentration also have the largest diurnal shift in altitude of the 'surface' averaging kernel peak. For example, over the Sahara the 'surface' averaging kernel peaks close to the surface at 850 mb during the day whereas at night this peak moves to 350 mb and even as high as 250 mb in some areas. There are also some regions over the oceans where the averaging kernel peak changes altitude particularly close to continental coast lines which could be due to outflow of high CO causing the averaging kernels to shift. Although observed negative day/night differences are not always coincident with these shifts over the ocean, it is likely that the cause of sensitivity changes in these regions is a change in the strength of the averaging kernels rather than the peak altitude.

The averaging kernel maps suggest that during the day in May 2000, the 'surface' averaging kernel peaks, on average, at 700 mb whereas at night this peak shifts to 500 mb and 350 mb. With this information it is possible to use the original

TOMCAT data to construct a map of the differences in CO concentrations between the different MOPITT retrieval levels, using 700 mb to represent the daytime measurements and 500 and 350 mb for the night, to see if positive and negative regions in the day/night difference map correspond to real differences in the shape of the CO profiles. Figure 5.12 shows the result of subtracting the original TOMCAT 500 mb level CO from the 700 mb level and Figure 5.13 shows the same for the 700–350 mb difference. The positive differences in the 700-500 mb map coincide with the positive differences found in the day-night map indicating regions where the surface CO concentrations (in this case 700 mb) are greater than the upper tropospheric (500 mb) levels which again occur predominately, but not exclusively, over source regions. This suggests that strong positive day-night differences in MOPITT data may indicate the presence of quasi-stationary CO sources at the surface. Weaker positive day-night differences do not necessarily indicate source regions but more complicated situations which may be influenced by low level transport from other sources.

Negative differences seen in the day-night analysis over oceans are captured well in both the 500 and the 350 mb differences. This indicates that the CO concentrations at 500 and 350 mb in these regions are higher than at 700 mb suggesting the presence of some high level transport as indicated in the day-night differences. This further reinforces the argument that over the oceans negative differences between day and night MOPITT data can be interpreted as an indication of high altitude CO transport. Negative day-night differences over land however are a little more difficult to interpret. Whereas, there are some regions such as the east coast of Brazil which show good correspondence between negative day-night differences and TOMCAT 700-350 mb differences indicating high level transported CO, this is not the case for all land scenes. One area where there are striking differences is the Sahara region, which shows a very strong negative day-night difference, suggesting high concentrations of CO in the upper troposphere, but the 700-500 and the 700-350 mb differences are closer to zero, indicating that the CO profile in this region is actually quite flat and uniform in the vertical. The reason for this discrepancy can be found by examining the averaging kernels for such a region (see Figure 5.14). Although the daytime ‘surface’ averaging kernel peaks at 700 mb and has some sensitivity to the surface, it also shows a negative contribution from CO at levels

above 350 mb, and in fact the negative contribution from CO at 250 and 150 mb is of the same magnitude as the contribution from the 'surface'. This means that CO at high altitudes during the day will act to reduce the daytime retrieved 'surface' level CO concentration. This situation however, is not present during night time retrievals where the 'surface' level concentration is positively influenced by CO at high altitudes. These two factors combine, leading to the day-night difference parameter being extremely sensitive over this region particularly to high altitude CO enhancements. This also seems to be the case for the Australian desert region, as the TOMCAT 700-350 mb difference map indicates a slight enhancement in CO at 350 mb compared to the concentrations seen at 700 mb due to transport, which combines with the above effect to give an exaggerated day-night negative difference.

It is now possible to apply the knowledge obtained from examining MOPITT day-night differences in conjunction with TOMCAT model data to the examination of MOPITT data alone.

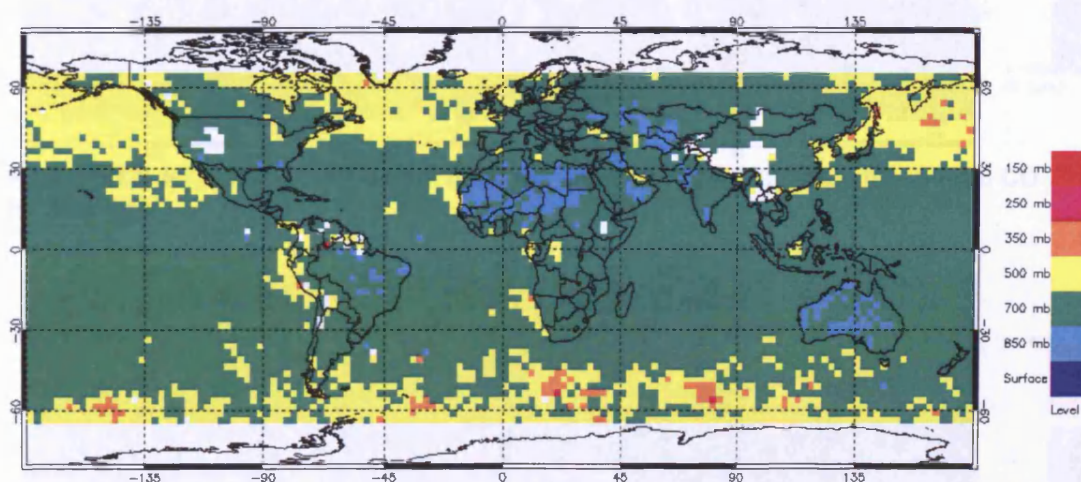


Figure 5.10: Map of MOPITT mean daytime surface averaging kernel peak altitude for May 2000.

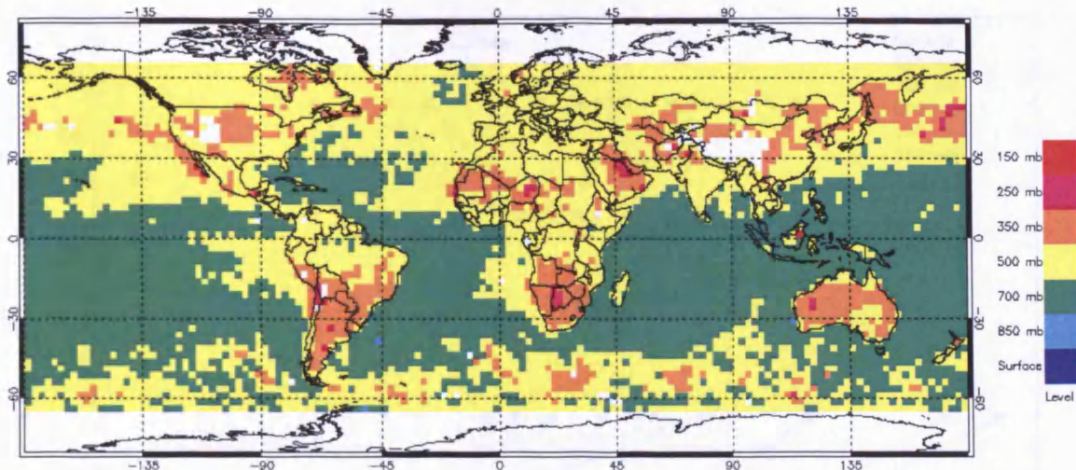


Figure 5.11: Map of MOPITT mean night time surface averaging kernel peak altitude for May 2000.

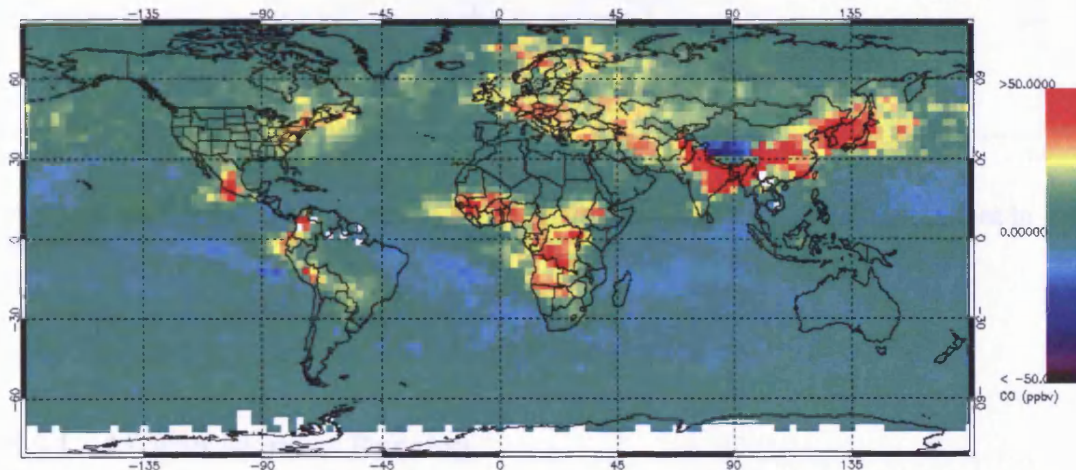


Figure 5.12: Map of the differences between mean TOMCAT 700 mb and 500 mb CO for May 2000.

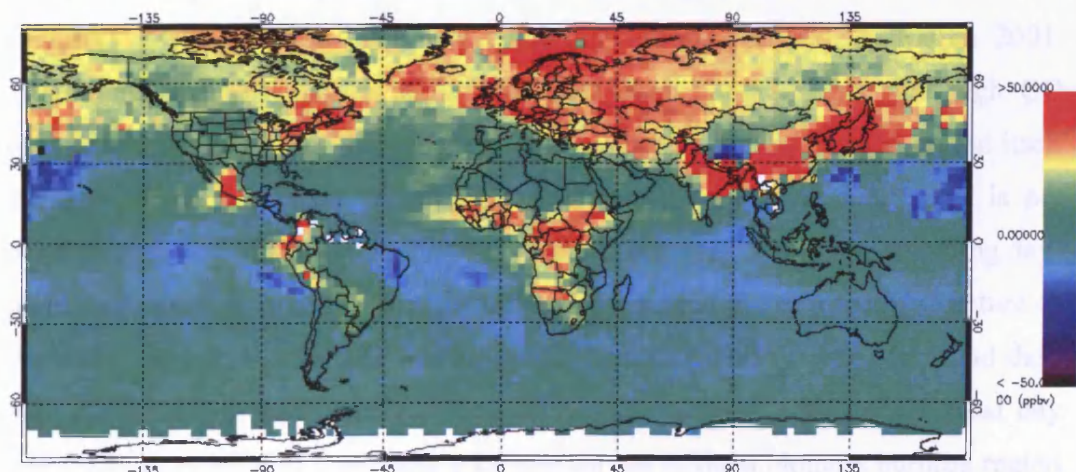


Figure 5.13: Map of the differences between mean TOMCAT 700 mb and 350 mb CO for May 2000.

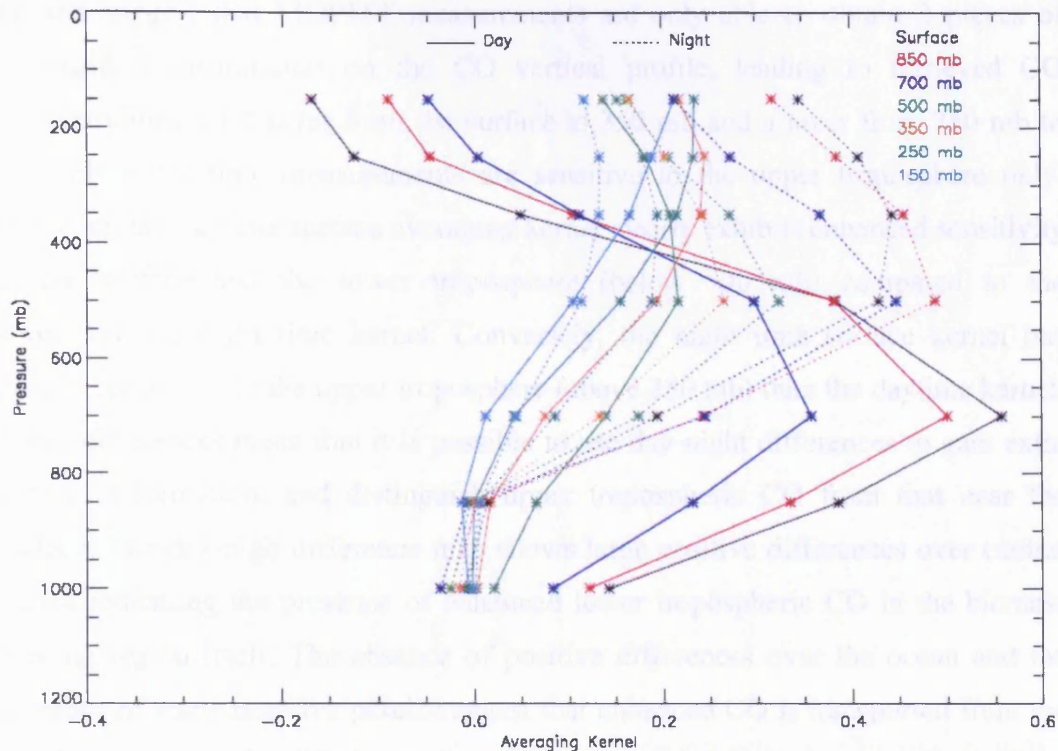


Figure 5.14: Typical MOPITT day and night time averaging kernels for the Sahara in May 2000.

5.3 Day-Night Differences in MOPITT data

5.3.1 African Biomass Burning

MOPITT CO profile data for 2000-2001 indicate high concentrations of ‘surface’ CO over Africa in June 2000 and continuing through to at least March 2001. Examining MOPITT day or night time data alone would imply that high CO concentrations during such burning periods are found over the burning region itself and extend out across the South Atlantic towards South America, but it is not possible to tell at what altitude the CO enhancement is. However by examining day-night differences it is possible to gain extra information on the vertical structure of the enhancement. Figure 5.15 shows monthly mean MOPITT day, night and day-night difference, gridded ‘surface’ CO concentrations over Africa and typical day and night mean MOPITT averaging kernels for the African biomass burning region of 0-10 degrees North, 20-30 degrees East for January 2001. The day and night time data indicate very high ‘surface’ CO concentrations over equatorial Africa which stretches out over the west coast and across the Atlantic. The daytime averaging

kernels suggest that MOPITT measurements are only able to obtain 2 pieces of independent information on the CO vertical profile, leading to retrieved CO concentrations for a layer from the surface to 350 mb and a layer from 350 mb to 150 mb; night time measurements are sensitive to the upper troposphere only. However, the daytime surface averaging kernel clearly exhibits enhanced sensitivity to the surface and the lower troposphere (below 500 mb) compared to the corresponding night time kernel. Conversely, the night time surface kernel has greater sensitivity to the upper troposphere (above 350 mb) than the daytime kernel. These differences mean that it is possible to use day-night differences to gain extra vertical information, and distinguish upper tropospheric CO from that near the surface. The day-night difference map shows large positive differences over central Africa indicating the presence of enhanced lower tropospheric CO in the biomass burning region itself. The absence of positive differences over the ocean and the presence of some negative pixels suggest that enhanced CO is transported from the burning regions and uplifted over the coast to the mid and upper troposphere, where it then undergoes further transport across the South Atlantic to South America.

Rainfall conditions for southern Africa during 2000 were classified as above average [Swap *et al.*, 2003]. This resulted in a more intense growing season for the region that contributed to excess grass biomass and hence fire fuel in the dry season [Hély *et al.*, 2003]. For the year 2000, burning in southern Africa burning took place during June through September and from November through March in the northern sub-Saharan region [Tansey *et al.*, 2004]. MOPITT day-night differences for the period April 2000-March 2001 are consistent with these observations. Positive day-night differences are observed over southern Africa in June and persist through September, whereas positive differences in Northern Africa occur from December 2000 through February 2001, with the greatest number of positive pixels observed in January (see Figure 5.15).

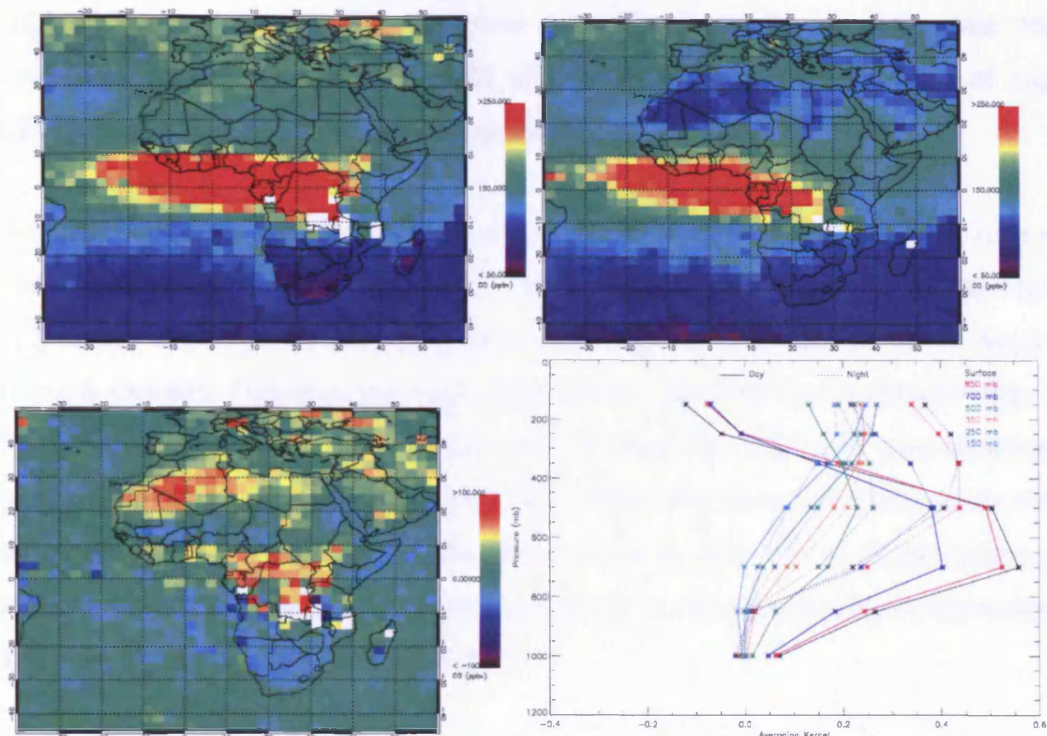


Figure 5.15: MOPITT day (top left), night (top right) and day-night difference (bottom left) 2.5 degree gridded monthly mean surface CO concentrations in the region of Africa for January 2001. Also shown (bottom right) are typical day and night mean MOPITT averaging kernels for the African biomass burning region of 0-10 degrees North, 20-30 degrees East in January 2001.

5.3.2 South American Biomass Burning

MOPITT CO data for 2000-2001 indicates that MOPITT observed high ‘surface’ CO concentrations over South America in August 2000 through to March 2001. Figure 5.16 shows MOPITT gridded day, night and day-night ‘surface’ CO concentrations for South America in September 2000. Mean MOPITT day and night averaging kernels for the region in September 2000 (Figure 5.16) indicate that during the day the surface averaging kernel exhibits sensitivity to the surface and the lower troposphere with little or no sensitivity to the upper troposphere, and even shows a negative sensitivity to CO at 150 mb. At night the averaging kernels look very different, the surface kernel no longer has any sensitivity to the surface and shows reduced sensitivity to the lower troposphere, and its sensitivity to the upper troposphere is greatly enhanced over the daytime. These differences in the day and night averaging kernels indicate that it is possible to use day-night differences in MOPITT surface CO to determine extra vertical information on the CO profile.

High CO concentrations are observed over Brazil in the daytime data and correspond to large positive day-night differences indicating the presence of high CO in the lower troposphere due to biomass burning in the region.

Biomass burning in Brazil during the year 2000 occurred in the period from June to October [Tansey *et al.*, 2004] this corresponds with large positive day-night differences observed in MOPITT data over large areas of Brazil from August through October. Negative day-night differences observed over northwest Brazil, Peru and the eastern South Pacific indicate that the high CO concentrations produced in the biomass burning region are uplifted and transported westwards over the South Pacific. The MOPITT data also indicate the presence of small regions of enhanced boundary layer CO over Argentina due to biomass burning in September and from December 2000 to March 2001.

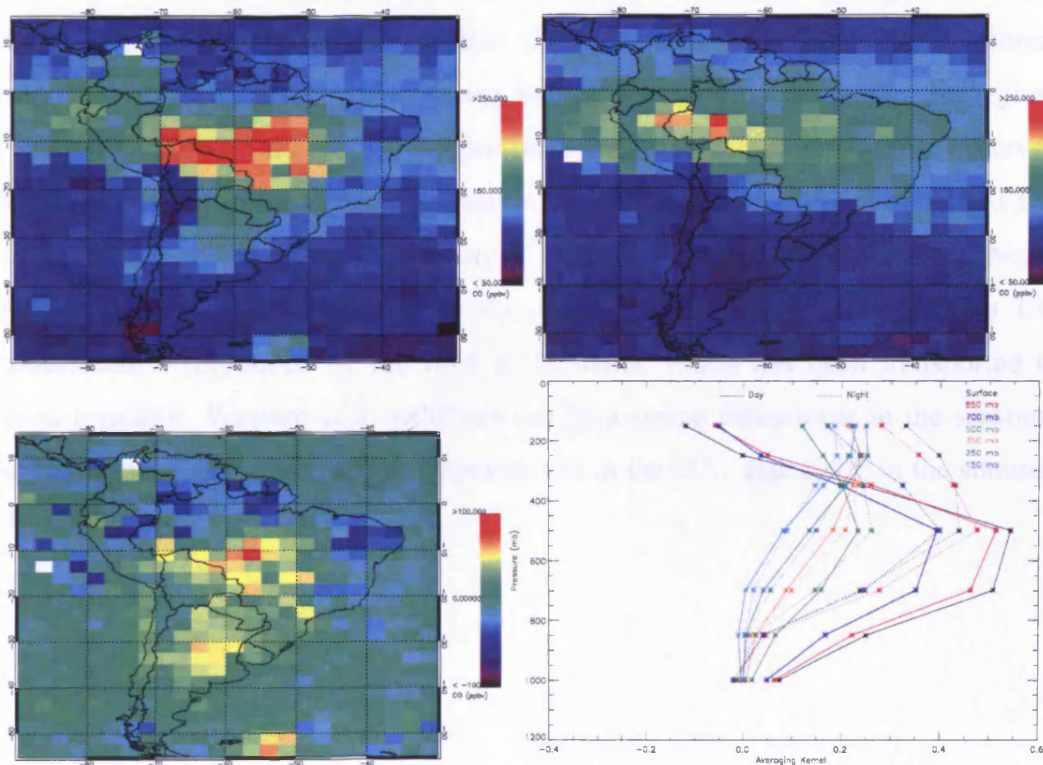


Figure 5.16: MOPITT day (top left), night (top right) and day-night difference (bottom left) 2.5 degree gridded monthly mean surface CO concentrations in the region of South America for September 2000. Also shown (bottom right) are typical day and night mean MOPITT averaging kernels for the South American biomass burning region of 10-15 degrees South, 55-60 degrees West in September 2000.

5.3.3 United States Wildfires

During 2000, the western United States experienced some of the worst forest fires to date with over 8 million acres burned which is more than double the previous 10 year average, at a cost of \$1.3 billion (National Interagency Fire Centre). The largest fire of the year occurred in Montana during August in which 292,070 acres were burned. Figure 5.17 shows monthly mean MOPITT gridded day, night and day-night 'surface' CO concentrations for the United States for August 2000. Examination of the day and night averaging kernels for the wildfire region in August 2000 (Figure 5.17) indicates that the daytime surface kernel exhibits much greater sensitivity to the lower troposphere (below 500 mb) than at night whereas the night time kernel shows enhanced sensitivity to the upper troposphere. These differences indicate that day-night differences in MOPITT surface CO may be used to distinguish lower and upper tropospheric CO enhancements. Daytime data clearly indicate the presence of high CO concentrations over Montana in the vicinity of the fires (also noted by Lamarque *et al.*, 2003). By examining the day-night difference data, it is possible to determine that this enhanced CO resides in the lower troposphere and is associated with the intense forest fires burning in the region. Figure 5.18 shows 5 day forward trajectories for air parcels originating at observed Montana forest fire locations. The results indicate that high altitude enhanced CO concentrations observed in the region of Hudson Bay, over Texas and the North Atlantic, characterised by negative day-night differences, are due to high CO concentrations produced by the fires in Montana, which has been transported to these locations. Western U.S. wildfires can be a strong component in the seasonal and interannual variability of tropospheric CO in the U.S., especially in the summer [Lamarque *et al.*, 2003].

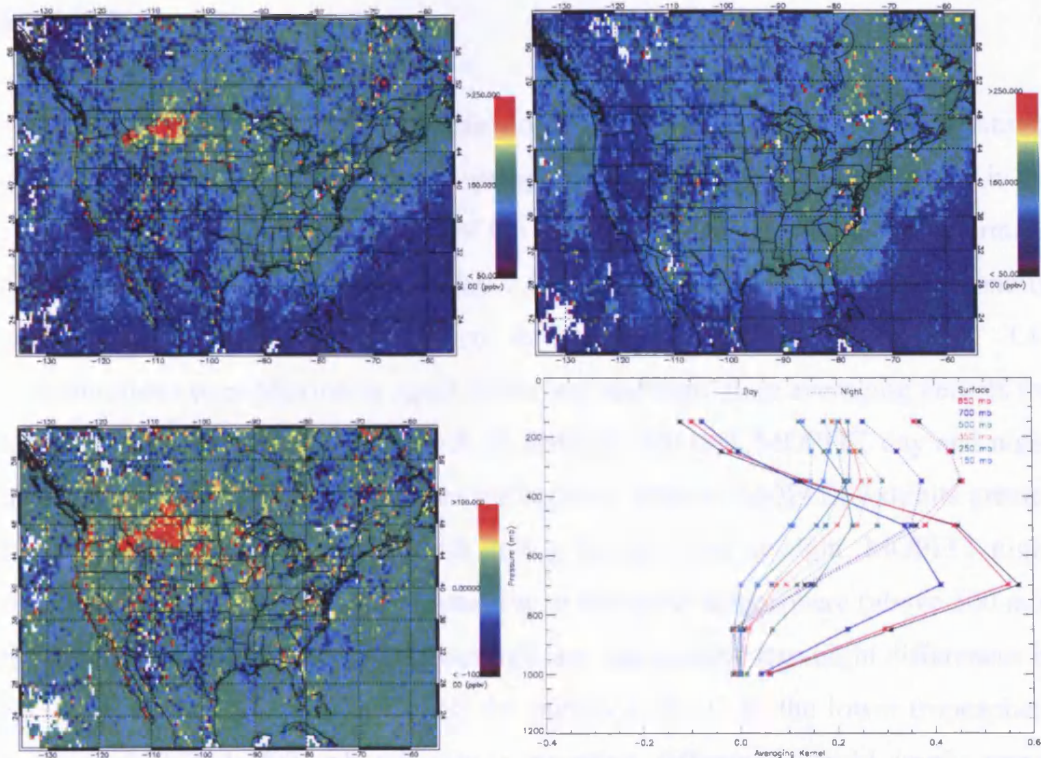


Figure 5.17: MOPITT day (top left), night (top right) and day-night difference (bottom left) 0.5 degree gridded monthly mean surface CO concentrations over the United States for August 2000. Also shown (bottom right) are typical day and night MOPITT averaging kernels for the U.S. wildfire region of 45-48 degrees North, 105-110 degrees West in August 2000.

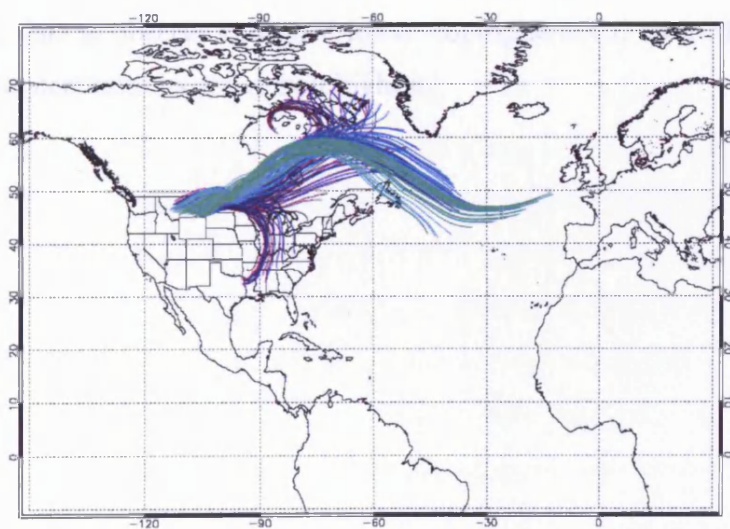


Figure 5.18: 5 day forward trajectories originating at Montana forest fire locations in August 2000.

5.3.4 Mexico City

Mexico City is one of the most polluted locations on Earth, with CO concentrations of up to 9 ppmv observed during spring [Raga *et al.*, 2001]. As such, it is an interesting case study for the ability of the day-night difference method to determine the presence of enhanced boundary layer CO pollution. Figure 5.19 shows monthly mean MOPITT 2.5 degree gridded day, night and day-night 'surface' CO concentrations over Mexico in April 2000. Day and night time averaging kernels for Mexico City in April 2000 (Figure 5.19) indicate that both MOPITT day and night time measurements are insensitive to the surface, whereas MOPITT exhibits greater sensitivity between 850 and 700 mb during the day than at night. MOPITT night time measurements are also more sensitive to the upper troposphere (above 500 mb) than during the day. These differences indicate that positive day-night differences in MOPITT surface CO would suggest the presence of CO in the lower troposphere between 850 and 700 mb whereas a negative difference would imply upper tropospheric CO above 500 mb. The daytime data indicate high levels of CO in the Mexico City region which are not present in the night time data, this leads to a positive day-night difference. The largest observed day-night difference in this region is over Mexico City itself, indicating the presence of enhanced lower tropospheric CO as expected. For the period examined here, it is only possible to use MOPITT data to observe enhanced lower tropospheric CO over Mexico City in spring when concentrations are at their highest.

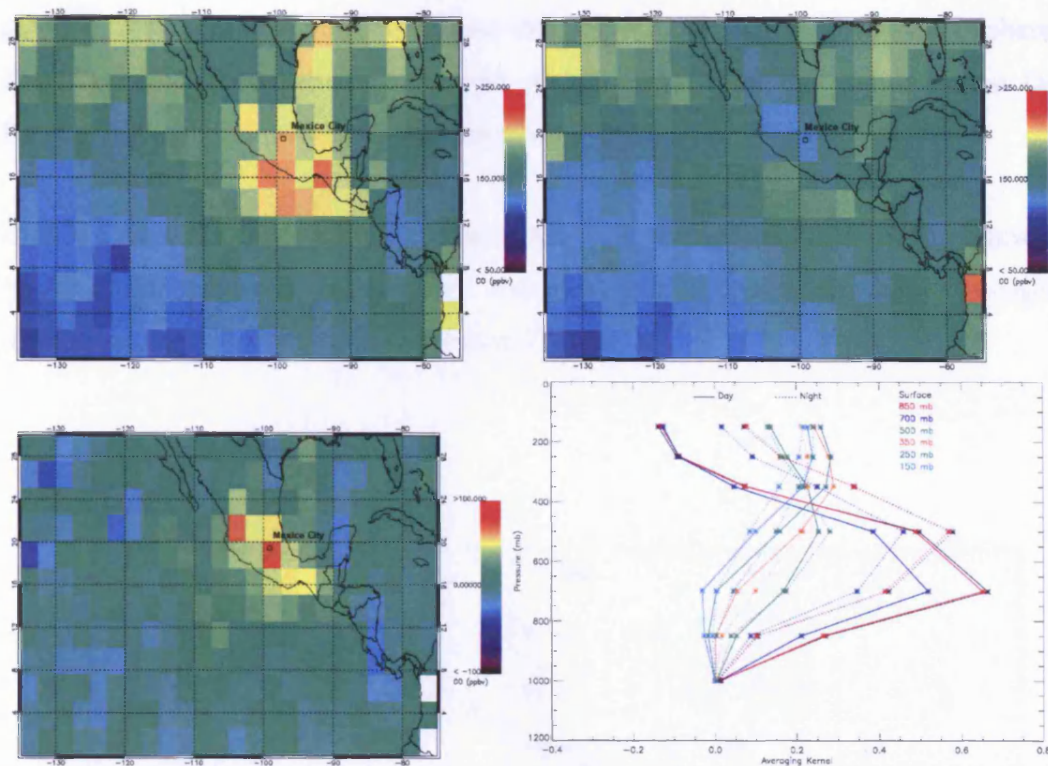


Figure 5.19: MOPITT day (top left), night (top right) and day-night difference (bottom left) 2.5 degree gridded monthly mean surface CO concentrations in the region of Mexico City for April 2000. Also shown (bottom right) are typical day and night mean MOPITT averaging kernels for the Mexico City region of 18-20 degrees North, 98-100 degrees West in April 2000.

5.3.5 East Asia

MOPITT observations indicate large levels of enhanced CO over East Asia all year round. Day-night differences suggest that most of this CO resides in the boundary layer and is likely the result of both biomass burning, which can account for more than 50 % of boundary layer CO over major source regions during spring [Zhang *et al.*, 2003], and fossil fuel burning. Figure 5.21 shows a map of monthly mean gridded day, night and day-night ‘surface’ CO concentrations for April 2000, also shown are mean day and night averaging kernels for the region. The averaging kernels for the lower retrieval levels suggest greater sensitivity to the boundary layer and lower troposphere during the day than at night, and conversely, night time measurements are more sensitive to the upper troposphere than those made during the day. These differences suggest that it is possible to use day-night differences in MOPITT surface CO to determine if CO enhancements exist in the lower, middle or upper troposphere. High concentrations of CO are present over East Asia, where

positive day-night differences suggest that this CO is in the lower troposphere. Enhanced CO levels are also observed stretching out from this region across the Pacific, indicating outflow of pollution to the Pacific.

Data for April 2000-March 2001 suggest that high concentrations of CO are present in the lower troposphere over East Asia, and are evident as positive day-night differences in retrieved MOPITT surface CO all year round.

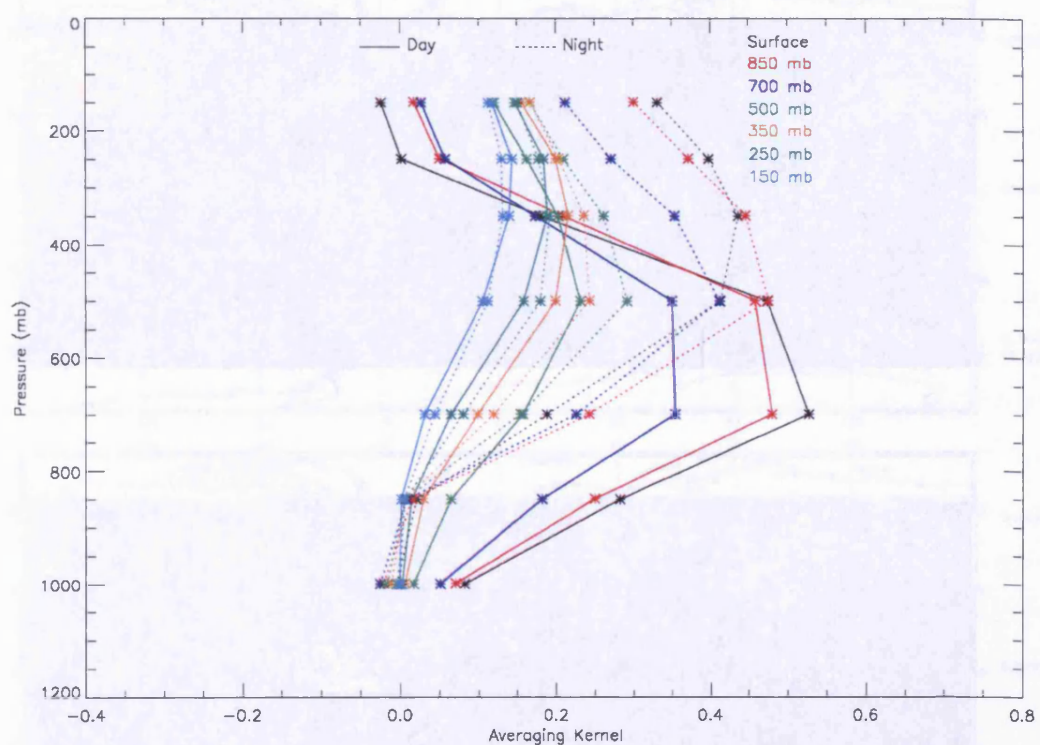


Figure 5.20: Typical day and night mean MOPITT averaging kernels for the East Asian region 30-35 degrees North, 110-115 degrees East in April 2000.

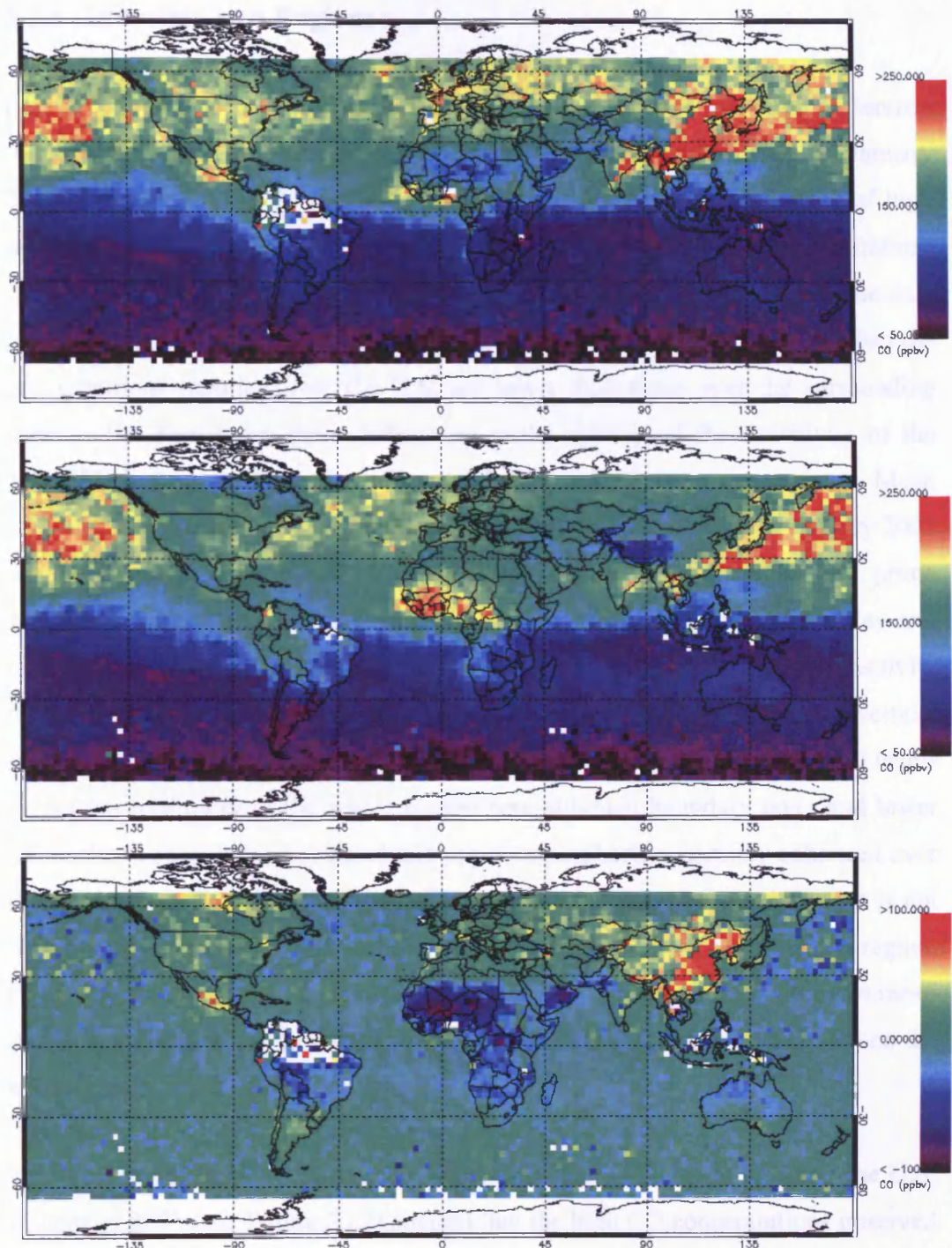


Figure 5.21: MOPITT day (top), night (middle) and day-night difference (bottom) 2.5 degree gridded monthly mean surface CO concentrations for April 2000.

5.3.6 Industrialised Regions

Figure 5.22 shows monthly mean MOPITT day, night and day-night difference 'surface' CO concentrations on a 1 degree grid over the United States in January 2001. Daytime MOPITT surface CO concentrations indicate the presence of high levels of CO over much of the United States, with particularly high concentrations observed over the more heavily populated southeastern states. The night time data however, indicate very low concentrations over the whole of the country, in fact the concentrations reported over the U.S. are lower than those over the surrounding oceans. The reason for these differences is the shifting of the sensitivity of the MOPITT instrument both diurnally and between land and ocean scenes. Mean MOPITT day and night averaging kernels for the southeastern U.S. in January 2001 can be found in Figure 5.22. The averaging kernels for this region are prime examples of when there is only one piece of information in each of the day and night time retrievals. The daytime kernels for all retrieval levels exhibit sensitivity to the whole of the troposphere and it is not possible to gain any vertical information. A similar situation occurs at night, with averaging kernels for all levels exhibiting sensitivity to the whole troposphere although boundary layer and lower tropospheric sensitivity is reduced and upper tropospheric sensitivity enhanced over that of the day. Therefore, by using either the day or night time data alone it is not possible to determine any information on the vertical structure of CO in this region. However, the differences in sensitivity between day and night time retrievals mean that it is possible to use day-night surface CO differences to gain information on the vertical structure of CO in this region.

The presence of largely positive day-night differences in surface CO over the U.S. in January 2001 (see Figure 5.22) suggest that the high CO concentrations observed over much of the U.S. reside in the boundary layer. In particular, large day-night differences are seen in the southeast near to major cities such as Orlando, Atlanta, Dallas and Washington. Some of the large west coast cities such as Los Angeles and San Francisco are also visible as large positive differences. Large positive differences also occur away from major cities such as those observed over Nebraska, Kansas and northern Texas. These differences indicate boundary layer CO which may have been subject to low level transport from more polluted areas,

or in the case of northern Texas could be due to the burning of oil in the oilfields found in this region.

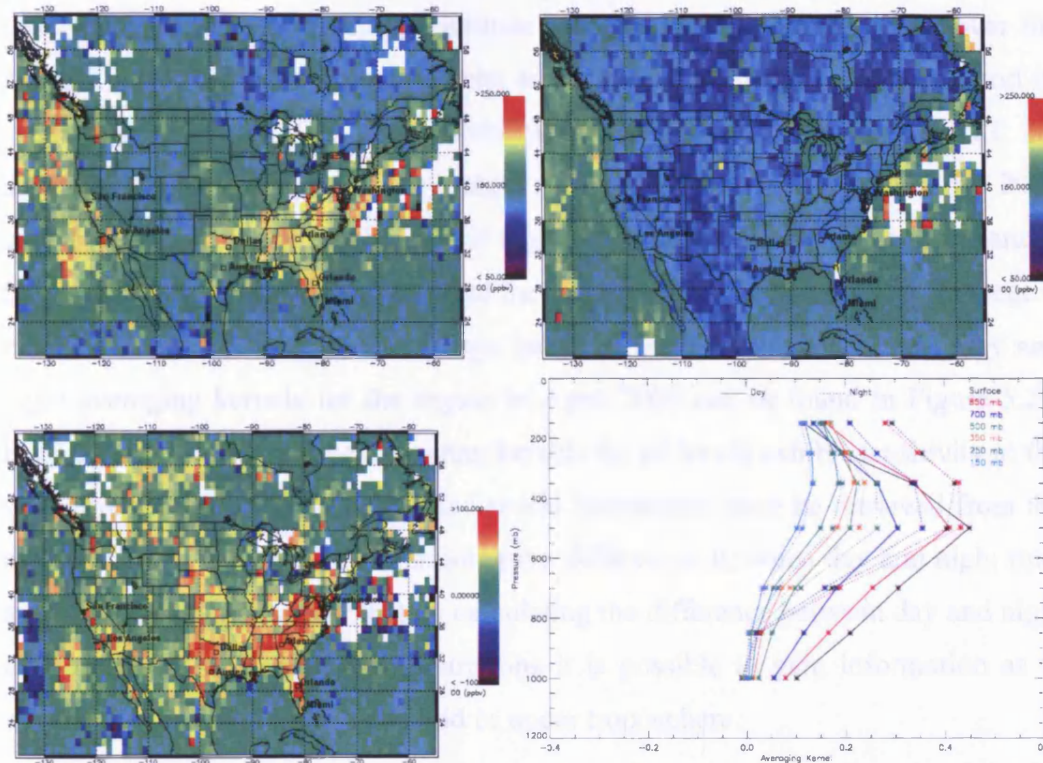


Figure 5.22: MOPITT day (top left), night (top right) and day-night difference (bottom left) 1 degree gridded monthly mean surface CO concentrations over the United States in January 2001. Also shown (bottom right) are typical day and night mean MOPITT averaging kernels for South Eastern United States in the region of 32-37 degrees North, 85-90 degrees West in January 2001.

These results suggest that using this technique it is possible to use MOPITT data to detect high levels of CO in the polluted boundary both over large urban areas and remote regions where high CO concentrations may have been transported from distance source regions.

5.3.7 Long Range Transport

Examination of day-night differences in MOPITT retrieved surface CO, particularly negative differences over oceans may be able to provide information on the long range transport of CO.

5.3.7.1 The North Atlantic

As described in Section 4.2.1 two of the main mechanisms for the transport of pollution from the U.S. are high altitude transport due to frontal lifting over the North Atlantic by warm conveyor belts and middle/upper tropospheric transport of convectively uplifted CO by westerly winds. Figure 5.23 shows MOPITT 2.5 degree gridded monthly mean day, night and day-night surface CO for April 2000 over the North Atlantic. Both day and night data indicate the presence of enhanced CO over the Atlantic which, owing to the lack of strong CO sources in this region must have been subject to long range transport from the United States. Day and night averaging kernels for the region in April 2000 can be found in Figure 5.23. Both the day and night time averaging kernels for all levels exhibit sensitivity to the whole troposphere and therefore no vertical information may be retrieved from the measurements. However, by examining the differences between day and night time averaging kernels it is clear that by calculating the difference between day and night time retrieved surface CO concentrations it is possible to gain information as to whether the CO is present in the mid or upper troposphere.

Examination of the day-night difference data for April 2000 indicates that both of the above transport mechanisms may be present at this time of year. Negative differences indicate the presence of enhanced CO in the upper troposphere which could represent North American pollution which has been uplifted over the western North Atlantic by warm conveyor belts and then transported at high altitude towards Europe. At the same time there are also some areas of enhanced CO which are present both during the day and the night leading to a day-night difference close to zero. These areas represent enhanced CO in the mid troposphere which might have been transported across the Atlantic by westerly winds. Examination of MOPITT data for the period of April 2000 – March 2001 (phase 1) suggests that the transport of North American pollution across the North Atlantic towards Europe occurs all year round, with less CO transport observed during the summer months due to the lower concentrations experienced at this time of year. Conversely the largest amounts of CO cross the Atlantic during the spring when concentrations in the northern hemisphere are at their greatest. Due to the reduced sensitivity of the

daytime averaging kernels to the boundary layer over ocean scenes this technique is most sensitive to CO in the mid and upper troposphere.

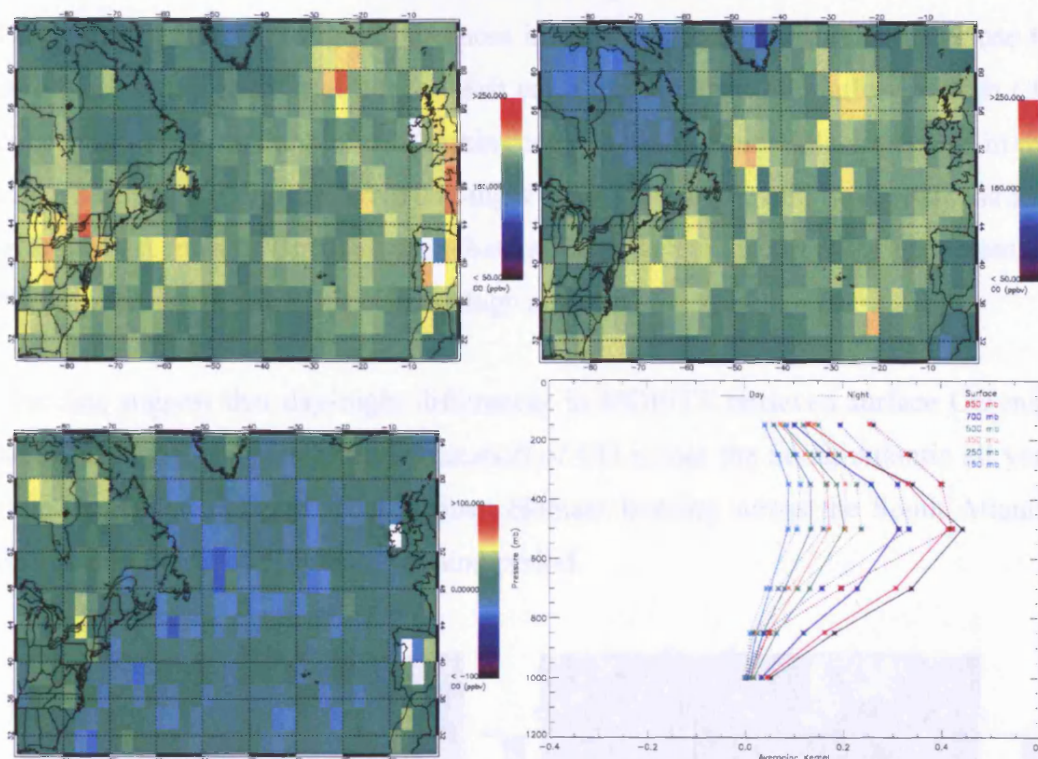


Figure 5.23: MOPITT day (top left), night (top right) and day-night difference (bottom left) 2.5 degree gridded monthly mean surface CO concentrations in the region of the North Atlantic for April 2000. Also shown (bottom right) are typical day and night mean MOPITT averaging kernels for the North Atlantic region of 50-55 degrees North, 45-55 degrees West in April 2000.

5.3.7.2 The South Atlantic

As noted in Section 5.3.1 during biomass burning events it is possible to observe high concentrations of CO stretching from the source regions across the South Atlantic as far as South America. This can be seen in Figure 5.24 which shows MOPITT 2.5 degree gridded monthly mean day, night and day-night surface CO for August 2000 over the South Atlantic. Both the day and night time data indicate the presence of high concentrations of CO over the South Atlantic. Examination of the day and night time averaging kernels for this region (Figure 5.24) indicates that during the day MOPITT retrieved surface CO is sensitive to a broad layer extending from the surface to 350 mb with negative sensitivity to CO in the upper troposphere (above 250 mb). Night time retrievals however show little or no sensitivity below

850 mb and much greater sensitivity to upper tropospheric CO (above 350 mb). These differences suggest that it is possible to use day-night differences in MOPITT surface CO to determine extra information on the vertical location of the enhanced CO in this region. Day-night differences in MOPITT retrieved surface CO close to zero close to the equatorial African east coast indicate that the outflow of high CO concentrations from the biomass burning regions to the South Atlantic occurs in the mid troposphere. Large negative day-night differences in the mid South Atlantic and over the east coast of Brazil suggest that the long range transport of African biomass burning across the Atlantic occurs at high altitudes.

The data suggest that day-night differences in MOPITT retrieved surface CO may be used to observe high altitude transport of CO across the South Atlantic all year round and that transport from African biomass burning across the South Atlantic occurs throughout the biomass burning period.

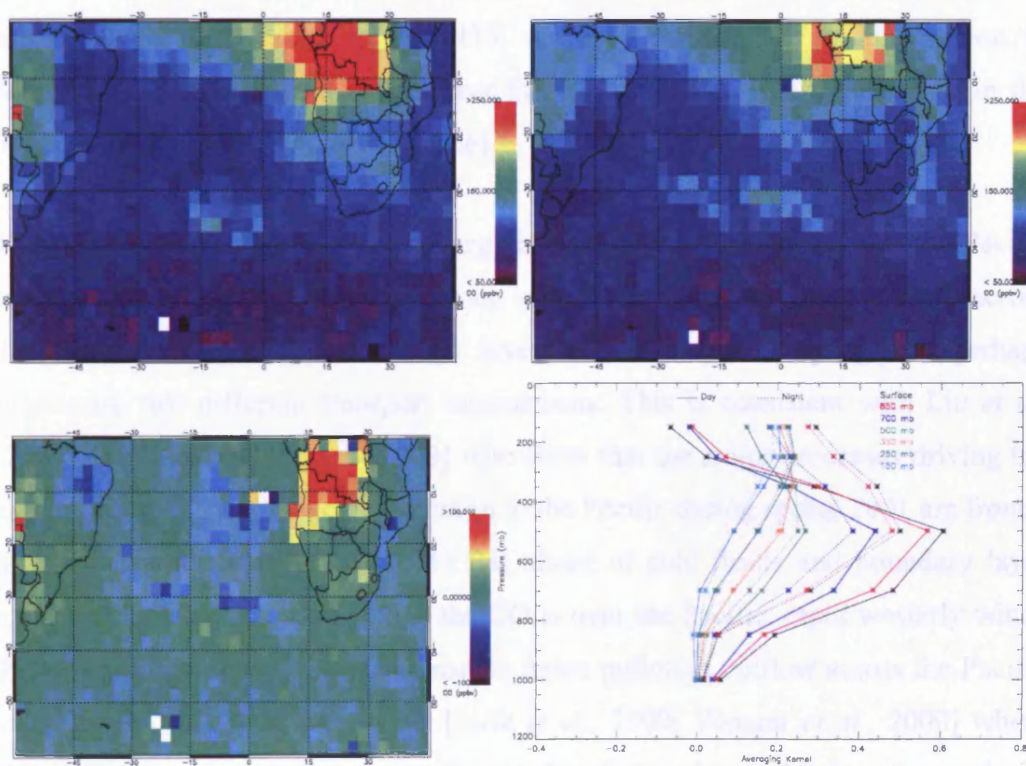


Figure 5.24: MOPITT day (top left), night (top right) and day-night difference (bottom left) 2.5 degree gridded monthly mean surface CO concentrations in the region of the South Atlantic for August 2000. Also shown (bottom right) are typical day and night mean MOPITT averaging kernels for the South Atlantic region of 15-20 degrees South, 0-5 degrees East in August 2000.

5.3.7.3 The North Pacific

Figure 5.25 shows MOPITT 2.5 degree gridded monthly mean day, night and day-night surface CO for April 2000 over the North Pacific. High concentrations of CO are observed over much of the North Pacific, stretching from East Asia to the west coast of the United States and are evident in both the night and day time data. Mean MOPITT averaging kernels for this region in April 2000 are also shown in Figure 5.25 and demonstrate that neither the day or the night time retrievals give any information on the vertical structure of CO, with both exhibiting averaging kernels which are broad and overlap covering the whole troposphere. However, by examining the differences between the day and night averaging kernels it is clear that the daytime surface averaging kernel exhibits greater sensitivity to the boundary layer and lower troposphere than the night time kernel. Also the night time surface averaging kernel shows greater sensitivity to the upper troposphere than the corresponding daytime kernel. These differences mean that it is possible to use day-night differences in MOPITT retrieved surface CO in this region to determine if the enhanced CO is near the surface (positive difference) or in the upper troposphere (negative difference).

The presence of both positive and negative day-night differences over the Pacific suggests that enhanced CO from strong sources in East Asia is transported across the Pacific in both the boundary layer and the upper troposphere, perhaps suggesting two different transport mechanisms. This is consistent with Liu *et al.* [2003] and Carmichael *et al.* [2003] who show that the major processes driving the export of Asian anthropogenic pollution to the Pacific during spring 2001 are frontal lifting in warm conveyor belts (WCBs) ahead of cold fronts and boundary layer transport behind cold fronts. Once the CO is over the Pacific, rapid westerly winds throughout the troposphere can transport Asian pollution outflow across the Pacific to the North American west coast [Jaffe *et al.*, 1999; Yienger *et al.*, 2000] where CO of Asian origin can account for 33 % of the observed lower tropospheric concentrations [Jaeglé *et al.*, 2003].

The results presented here are in contradiction with the findings of Jacob *et al.* [2003] who analysed MOPITT and aircraft data for the TRACE-P campaign which

was conducted over the western Pacific in the spring of 2001 and concluded that MOPITT captures the variability in observed aircraft CO columns but provides no apparent information on the vertical structure for Asian plumes over the Pacific. However, the analysis of Jacob *et al.* used MOPITT day and night data in isolation and as such their conclusions were correct, but if day-night differences are used in conjunction with this data then some limited vertical information may be gained.

The MOPITT data for the period April 2000 – March 2001 indicate that MOPITT is able to observe the transport of CO in the upper and lower troposphere throughout the year, although the amount of CO transported varies according to seasonal variations in the East Asian source strengths and the CO lifetime.

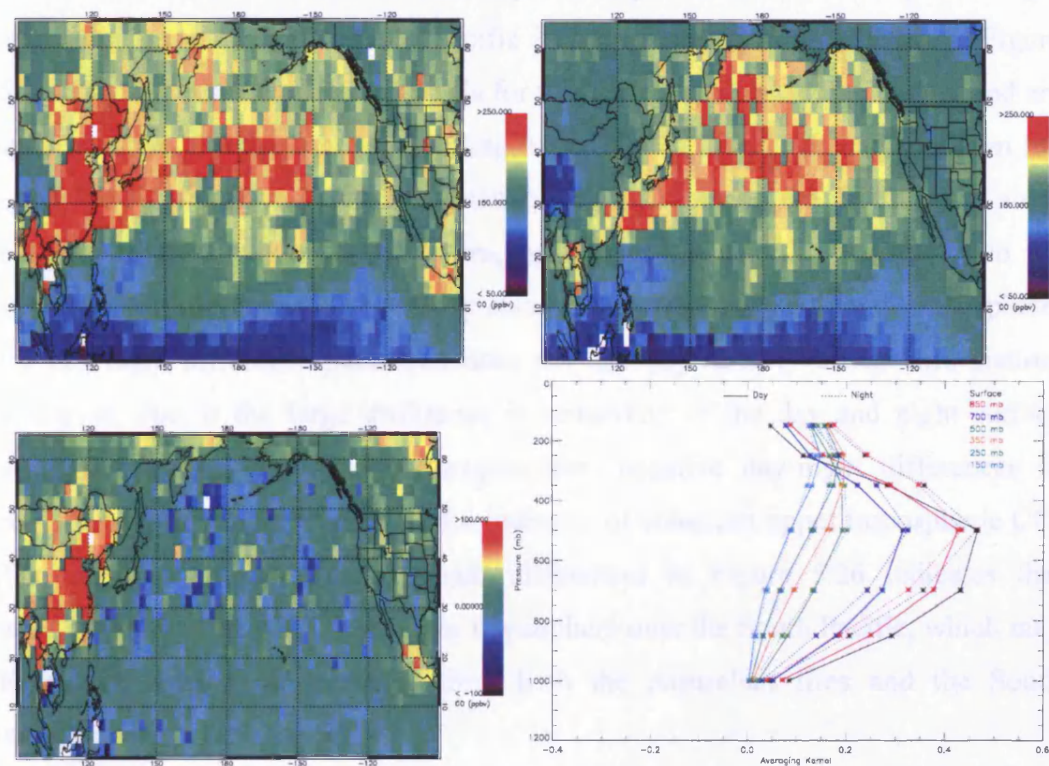


Figure 5.25: MOPITT day (top left), night (top right) and day-night difference (bottom left) 2.5 degree gridded monthly mean surface CO concentrations in the region of the North Pacific for April 2000. Also shown (bottom right) are typical day and night mean MOPITT averaging kernels for the North Pacific region of 30-35 degrees North, 160-165 degrees East in April 2000.

5.3.7.4 The South Pacific

Figure 5.26 shows MOPITT 2.5 degree gridded monthly mean day, night and day-night 'surface' CO for September 2000 over the South Pacific. During September 2000 there were a number of fires burning in northern Australia [Australian Department of Land Information]. The high concentrations of CO produced by these fires can be seen in both the day and night MOPITT retrieved surface CO concentrations as enhanced levels of CO stretching out from the east coast of Australia towards South America. Also at this time of year, biomass burning was occurring in South America (see Section 5.3.2), high concentrations of CO can be seen in MOPITT retrieved surface CO stretching from the biomass burning regions out into the South Pacific in both day and night data. Typical day and night averaging kernels for the South Pacific in September 2000 are shown in Figure 5.26. Day and night averaging kernels for this region exhibit similar shapes, and are split into two distinct groups, enabling MOPITT to distinguish only between the upper (350-150 mb) and the lower (surface-350 mb) troposphere. In this case, since both the day and night surface averaging kernels have similar sensitivity to the surface, and differences in sensitivity occur only in the mid and upper troposphere, the day-night difference parameter does not add any further vertical information. However, due to the large difference in sensitivity of the day and night surface averaging kernels to the upper troposphere, negative day-night differences in retrieved surface CO are still a useful indicator of enhanced upper tropospheric CO. The presence of negative day-night differences in Figure 5.26 indicates that enhanced CO is present in the upper troposphere over the South Pacific, which may have been subject to transport from both the Australian fires and the South American biomass burning.

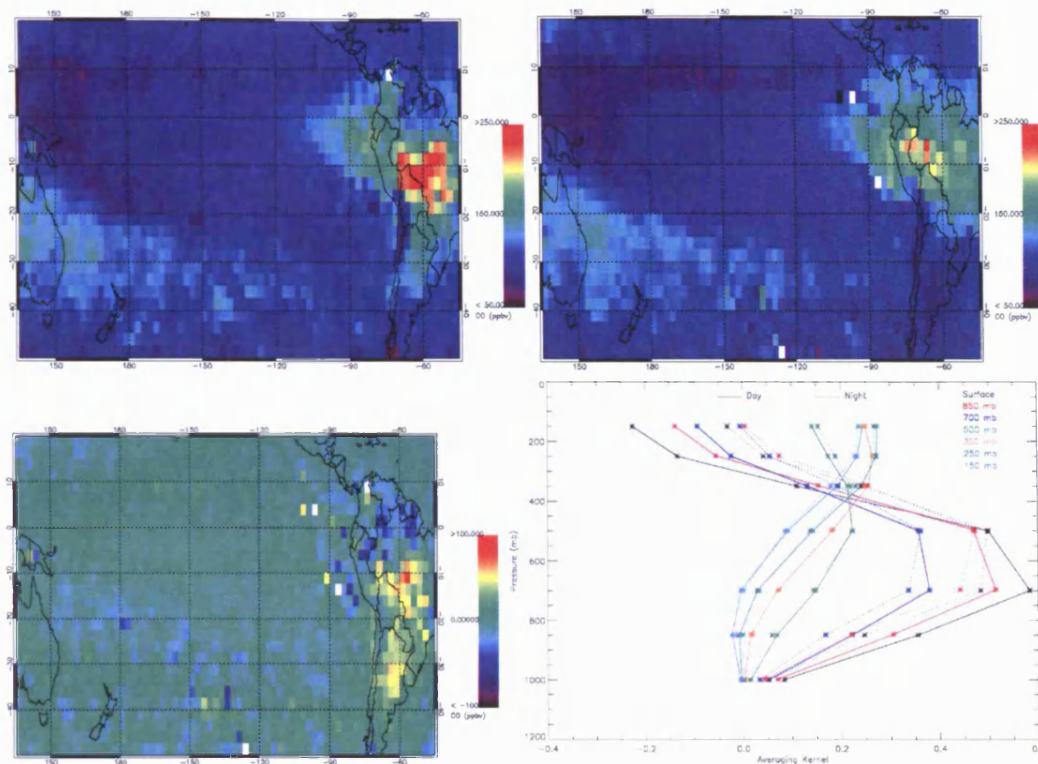


Figure 5.26: MOPITT day (top left), night (top right) and day-night difference (bottom) 2.5 degree gridded monthly mean surface CO concentrations in the region of the South Pacific for September 2000. Also shown (bottom right) are typical day and night mean MOPITT averaging kernels for the South Pacific region of 0-5 degrees South, 145-150 degrees West in September 2000.

5.3.7.5 The Indian Ocean

Figure 5.27 shows 2.5 degree gridded MOPITT day, night and day-night ‘surface’ CO concentrations for September 2000. The day and night data both indicate high concentrations of CO over the Indian Ocean which are likely the result of transport of high CO air from biomass burning regions in Africa. Figure 5.27 also shows typical day and night MOPITT averaging kernels for the Indian Ocean in September 2000. The daytime averaging kernels are split into two distinct groups (surface-350 mb and 350-150 mb) providing upper and lower tropospheric sensitivity, whereas the night time kernels show no apparent vertical resolution. It is clear by examining the day-night differences in surface averaging kernel sensitivity, that the day-night difference parameter does not provide any extra information on CO in the lower troposphere over the daytime measurements themselves. However, large changes in surface average kernel sensitivity between day and night occur in the upper

troposphere (above 500 mb). This means that the day-night difference parameter is useful for examining upper tropospheric CO which, over the oceans, is characteristic of long range transport.

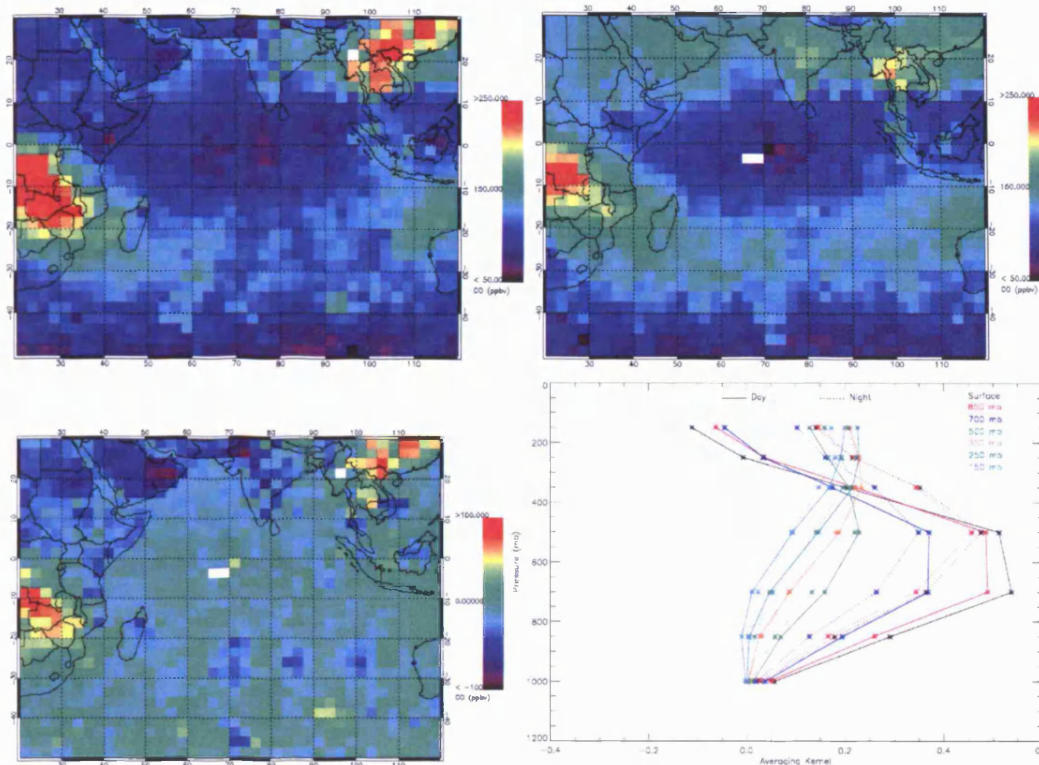


Figure 5.27: MOPITT day (top left), night (top right) and day-night difference (bottom left) 2.5 degree gridded monthly mean surface CO concentrations in the region of the Indian Ocean for September 2000. Also shown (bottom right) are typical day and night mean MOPITT averaging kernels for the South Pacific region of 25-30 degrees South, 60-65 degrees East in September 2000.

Large negative differences are present over the Indian Ocean between southern Africa and Australia (see Figure 5.27). These differences represent high CO concentrations in the upper troposphere which are caused by the transport of high CO from biomass burning regions in Africa [de Laat, 2002; Swap *et al.*, 2003].

The analysis of day-night difference data for the period April 2000-March 2001 suggests that it is possible to use day-night differences to observe upper tropospheric CO enhancements whenever they occur. The data suggest that the transport of high CO concentrations in the upper troposphere across the Indian Ocean occurs whenever biomass burning is occurring in southern Africa (May-November 2000), or during large wildfire events in northwestern Australia (September 2000-February 2001).

5.4 Summary

The results presented here demonstrate that differences between day and night MOPITT retrievals may be exploited in order to gain further information on the vertical distribution of CO on a global scale. Simulations show that in regions with large diurnal variations in surface temperature the day-night differences in MOPITT surface level CO give an indication as to the altitude at which a CO enhancement is present. Simulations for the Libyan Desert and the UK in August 2000 suggest that when surface temperature differences occur over land the day-night difference is positive for CO enhancements below 500 mb with greatest sensitivity to enhancements at 850 mb. Negative day-night differences indicate the presence of enhanced CO above 500 mb with greatest sensitivity to enhancements at 250 mb. Simulations for the Atlantic in May 2000 where surface temperature changes are small suggest that the day-night difference parameter is sensitive only to high altitude enhancements (above 500 mb) where the 'surface' averaging kernel is stronger at night than during the day, and so is useful for investigating high levels CO transport.

The application of TOMCAT data to this investigation has allowed the effects of day-night differencing to be quantified globally on a monthly mean basis. The day-night differences calculated for the month of May show a very good correspondence between large positive day-night differences seen in 'retrieved' TOMCAT data with the locations of source regions in the model, for example Mexico City and East Asia. The results also show that while positive differences are likely to be an indication of surface CO sources this is not always the case. Areas where positive differences are observed which do not coincide with model source regions are likely the result of the presence of more complicated mixed air which has been subject to low level CO transport. Negative day-night differences over the oceans correspond with high altitude CO enhancements observed in TOMCAT data, these differences therefore may be considered to be a signature of long range CO transport. Negative differences over land however are not so straight forward. In order to interpret such differences, the appropriate MOPITT averaging kernels must be examined since in some regions such as the Sahara the daytime retrieved 'surface' CO concentrations

may be artificially reduced due to a negative averaging kernel sensitivity to high altitudes.

An examination of monthly mean day-night differences in MOPITT 'surface' CO concentrations for phase 1 data (April 2000 – March 2001) has been performed. The results show that the use of day-night data to detect boundary layer pollution is most effective when the boundary layer CO concentrations are large as this has the effect of enhancing the sensitivity of the daytime averaging kernels to the boundary layer. This means that it is possible to observe large pollution events such as biomass burning in Africa and South America and wildfires, for example those observed in the U.S. in August 2000. These events manifest themselves as large positive day-night differences in MOPITT retrieved surface CO indicating high concentrations of CO in the lower troposphere. High levels of lower tropospheric pollution over cities and industrialised regions, such as the U.S. and Europe, are also present as positive day-night differences in day-night data, particularly during winter and the spring when CO concentrations are at their highest.

The results suggest that it is also possible to use day-night differences in retrieved surface CO to detect high altitude CO transport over the oceans. For example, negative day-night differences are observed over the North and South Atlantic all year round indicating the presence of persistent high altitude transport of enhanced CO from the United States to Europe, and biomass burning pollution from Africa to South America. Day-night differences over the North Pacific suggest that it is possible to observe both boundary layer and high altitude transport of enhanced CO from East Asia to the United States. Negative differences over the South Pacific and the Indian Ocean also suggest that it is possible to observe high altitude CO transport in these regions.

Due to the orbit of the MOPITT instrument, day and night time measurements over a particular location may be separated by a period of days. It is therefore only possible to apply this analysis globally on a monthly mean basis.

6. Summary, Conclusions and Future Work

6.1 Carbon Monoxide in the troposphere

Carbon Monoxide is a very important atmospheric gas and through its interaction with the OH radical is partly responsible for controlling the oxidising capacity of the troposphere. Due to its relatively short lifetime of just a few months its distribution is complex, varying both spatially and temporally due to seasonal variations in its sources and sinks. Large uncertainties still exist in estimates of the magnitudes of CO sources and sinks, and consistent global observations are needed to reduce these. Satellite instruments offer the opportunity to make continuous global measurements of CO and may be used in conjunction with data from other sources to further improve our understanding of CO in the global atmosphere. It has been shown in this thesis that MOPITT can contribute substantially in this way. However, spatial and temporal variations in altitude sensitivity occur, and these need to be accounted for carefully by examining the appropriate retrieval averaging kernels.

6.2 Characteristics of MOPITT CO profiles

The MOPITT vertical resolution is intrinsically linked to the retrieval averaging kernels for each measured profile which themselves are highly variable in both space and time. Typically MOPITT profiles contain, at most, two pieces of independent information, providing only lower and upper tropospheric CO concentrations. In some regions, such as above the UK in winter, only one piece of information is present.

Profiles measured by the MOPITT instrument were compared to those constructed using data from research aircraft flights conducted as part of the ACTO campaign. Despite large differences in the temporal and spatial collocation of the two sets of measurements they compare very well. The comparisons suggest that MOPITT CO profiles may have a positive bias of up to 25 % in the lower troposphere which decreases with increasing altitude for the two flights examined. This is consistent with the results of the MOPITT validation campaign, which at the time of this thesis was ongoing. Although the biases suggested by the validation results are smaller than those found in the ACTO comparison

(< 10%), there is however a large variability about these mean biases, particularly in the lower troposphere (20 ppbv, 20%), as indicated by the standard deviations of the biases.

The results of the comparisons of MOPITT profile with *in situ* aircraft data from the ACTO campaign indicate that one should be careful when using MOPITT data to examine the vertical distribution of CO. There is a clear need to take into account the effects of vertical resolution and the influence of the *a priori* used in the retrieval of MOPITT profiles through the use of MOPITT averaging kernels. The results clearly show that the corresponding averaging kernel for each MOPITT profile should be examined and must be applied to *in situ* data before any meaningful comparison can be made.

Simulations have been conducted using MOPITT averaging kernels to investigate the ability of the instrument to conduct measurements of layers or plumes of enhanced CO under differing conditions. The results show that the ability of MOPITT to measure the vertical structure of CO depends greatly on both the surface and atmospheric conditions of the measurement scene. A major factor is surface temperature. Regions with a high surface temperature enable the MOPITT instrument to gain greater sensitivity to the lower troposphere and the boundary layer. The atmospheric temperature profile also has important implications for MOPITT profile measurements. In areas where the temperature profile through the atmosphere is quite uniform, MOPITT is unable to gain any information on the vertical structure of CO since it relies on thermal contrast between layers to make such measurements. The amount of CO itself in the profile being measured also affects the MOPITT sensitivity, with higher concentrations leading to increased sensitivity. These effects combine leading to complex variations in the vertical resolution of MOPITT depending on location and surface type as well as time of year and even time of day for some locations such as desert regions. The simulations suggest that it is possible for the MOPITT instrument to measure plumes of enhanced CO under the right conditions. Although it is possible to detect enhanced concentrations over most surface types, it is difficult to determine that altitude at which it occurs. If vertical information is required then these measurements are best made over land during the summer where there is a large thermal contrast between the surface and lower troposphere.

An investigation of the combined use of the differing sensitivity of MOPITT between day and night in order to gain extra vertical information from MOPITT data has been

conducted. This is the first such study of its kind and the results are encouraging. The results show that by examining the difference between day and night MOPITT 'surface' measurements it is possible, in a number of regions and seasons, to determine whether an enhancement in CO is near the surface, in the mid-troposphere or in the upper troposphere. The results have been validated using the TOMCAT model to represent the 'real' atmosphere. Surface level enhancements appear as positive day-night differences whereas negative differences indicate the presence of enhanced CO in the upper troposphere. A difference of zero means that a CO enhanced layer is likely to be present in the mid troposphere.

An examination of phase 1 MOPITT data suggests that by using this technique it is possible to identify strong CO sources such as biomass burning in Africa and South America and wildfires, for example those observed in the U.S. during August 2000. It is also possible to observe lower tropospheric pollution over cities and industrialised regions, such as the United States, Europe and Mexico City, although this appears to only be possible during the winter and spring when CO concentrations are at their greatest.

These results indicate that in order to determine the vertical structure of CO using MOPITT profile data, a reference profile is required. This profile may be obtained either spatially or temporally. The method developed in this thesis is one based in the temporal domain, using MOPITT night time profile measurements as a reference to subtract from daytime profiles obtained over the same location. Spatial referencing could be accomplished by comparing the profile of interest to surrounding profiles.

The seasonal cycle in MOPITT CO has been derived and compared to that of six CMDL surface measuring sites. The MOPITT data indicate a minimum in CO concentration over all sites during the summer when increased solar radiation leads to an increase in OH concentrations, which in turn reacts with CO to reduce its concentrations. The CO concentrations then increase through the winter, owing to decreasing OH, to a maximum in spring. The seasonal cycle found in the MOPITT profile measurements compares well with that of the surface sites examined. The results suggest that MOPITT data are able to correctly capture the observed seasonal cycle in CO.

6.3 Comparisons of MOPITT CO Profiles with TOMCAT

Global mean comparisons of MOPITT CO profiles with those reported by TOMCAT also suggest that MOPITT has a positive bias throughout the troposphere. This bias is largest in the lower troposphere and decreases with increasing altitude, falling from 24% at 850 mb to 11% at 150 mb. Regional variations in MOPITT-TOMCAT differences are also evident, with the largest differences observed near TOMCAT source regions. For example, excluding Antarctica, where snow and ice cover may affect the MOPITT retrievals, the only locations where the 'retrieved' TOMCAT CO levels are higher than those of MOPITT are over a very intense TOMCAT emission in the region of Calcutta and a smaller source region over northeast Columbia. Conversely over Mexico City, MOPITT reports higher CO levels than TOMCAT of up to 50%. These differences could indicate that the sources in the model may give approximately the correct amount of CO release globally but the relative strengths of the different source locations may be underestimated. Large differences are also observed over the North Pacific off the east coast of Russia and over Japan, stretching as far as the west coast of the U.S. These differences indicate that the model may underestimate the amount of CO transport across the North Pacific.

Zonal mean comparisons of MOPITT and TOMCAT CO profiles are excellent, with correlation coefficients of in excess of 0.97 for all altitudes. These comparisons also suggest a positive bias in MOPITT data of approximately 25% at the surface, falling to approximately 5% at 150 mb. However, these biases vary considerably with latitude. The largest differences are observed in the lower troposphere, over those latitudes which contain strong source regions such as 30-50 degrees north, which encompasses strong North American, European and East Asian sources. These differences may again be due to problems with source strengths, or with the transport of CO from sources in the boundary layer up to the free troposphere in the TOMCAT model.

MOPITT CO profile data has also been compared to TOMCAT profiles on an individual case study basis. The results suggest that MOPITT profiles are representative of the real atmosphere when used to examine regions of low CO concentrations away from source regions where the air is considered to be well mixed, this could be due to the influence of the *a priori* profile. In regions such as the northern hemisphere where CO concentrations

are higher and more variable MOPITT measurements are able to well represent the mid troposphere between 850 and 250 mb showing greater sensitivity to the surface over land.

6.4 Observing the Intercontinental Transport of CO with MOPITT

A method for detecting long range transport of events with anomalous CO using a regional analysis has been developed with limited success. Analysis using this method was only able to detect the presence of two anomalous events in one year of MOPITT data, one with high CO and one with low CO. The inability of the analysis to identify events is most likely due to the method itself and not the ability of the MOPITT instrument. In order to detect a region of enhanced CO using this method the enhancement would need to be large in extent and fill most of the region being examined. Otherwise the effect of a small plume of enhanced CO due to transport may become diluted when an average is taken over a large area such as the regions examined here. In order to improve the detection method, smaller regions might be selected although this might reduce the number of days on which there is coincident MOPITT data. When coincidences do occur it might be easier to detect the enhanced CO levels. Another improvement might be to reduce the three sigma limit used in this study. This limit was chosen so that only the most extreme events would be isolated by the analysis. Reduction of this criterion would result in many more events being identified.

It is also possible to use day-night differences in retrieved surface CO to detect high altitude CO transport over the oceans. For example negative day-night differences are observed over the North and South Atlantic all year round indicating the presence of persistent high altitude transport of enhanced CO from the United States to Europe, and biomass burning pollution from Africa to South America. Day-night differences over the North Pacific suggest that it is possible to observe both boundary layer and high altitude transport of enhanced CO from East Asia to the United States. Negative differences over the South Pacific and the Indian Ocean also suggest that it is possible to observe high altitude CO transport in these regions.

The results here suggest that observing and tracking the long range transport of pollution events with a nadir viewing instrument such as MOPITT is difficult. The main problem is missing data due to both problems with coverage and clouds. Unfortunately the long range

transport of such events is usually associated with the movement of frontal systems which tend to be regions of high cloud content and as such are not conducive to measurements using nadir viewing instruments. However when a transport event is identified results show that it is possible for the MOPITT instrument to measure and track the event along its trajectory for several days providing cloud free measurements are available.

6.5 Conclusions

- MOPITT CO profiles show a positive bias throughout the troposphere which decreases with increasing altitude.
- It is necessary to take into account the retrieval averaging kernels when using MOPITT data to look at the vertical structure of CO.
- The vertical resolution of the MOPITT instrument has both diurnal and seasonal variations and also varies from location to location, mainly due to changes in surface temperature and type.
- The MOPITT instrument is able to capture the seasonal cycle in tropospheric CO.
- Under the right conditions the MOPITT instrument is able to detect and track enhanced plumes of CO as they undergo long range transport.
- Problems with missing data due to cloud and surface coverage greatly inhibit the ability of nadir viewing instruments such as MOPITT to monitor pollution episodes.
- Monthly mean day/night differencing of MOPITT 'surface' CO provides additional information on the vertical structure of CO, and may be used to identify strong CO sources and high altitude transport.

6.6 Future Work

6.6.1 Characteristics of MOPITT CO profile Measurements

So far, the characterisation of MOPITT CO profile measurements in this thesis with *in situ* data has been conducted using data from only one aircraft campaign, ACTO, which occurred in May 2000. The extension of these comparisons to other aircraft campaigns, conducted at different times of year, and covering a range of geographical locations would be desirable. Interesting regions not included in this thesis or in the MOPITT validation campaign would include the North and South Atlantic and Europe. Profile comparisons over desert regions, such as the Libyan Desert, and major urban areas, would also be very useful for validation of the MOPITT day-night differencing technique.

Comparisons of MOPITT profile measurements to TOMCAT model profiles have been confined to data obtained for May 2000 only. It would be very useful to compare MOPITT and TOMCAT data from other months to examine any seasonal variability in the characteristics of MOPITT retrievals and to compare with the source/transport identifications made using the day-night differencing of MOPITT data. Also, the model data used in this study are for 00:00 UT only. The use of time coincident model data may improve the comparisons, and this should be investigated.

The characterisation of MOPITT profile measurements should also be extended to include MOPITT phase 2 data. These data exhibit reduced vertical resolution and this must be characterised before the data can be used in further studies. These data may then be combined with phase 1 data and employed to examine the long term trend of CO.

6.6.2 Observing Intercontinental Transport with MOPITT

Refinements to the regional analysis technique to detect long range transport events might include a reduction in the size of the regions in order to reduce the effects of dilution. A reduction in the three sigma detection limit used could also be of benefit as it would result in a higher number of candidate events being identified.

Another method to detect long range transport event in MOPITT data would be to use the results of aircraft campaigns to identify anomalously high CO concentrations which may be the result of pollution transport. Backward/forward trajectories could be employed to

determine the origin/fate of the enhancement. MOPITT data along these trajectories could then be examined to determine if the instrument is able to track such events. Such a study has already been conducted successfully using MOPITT CO total column data for the TRACE-P campaign over the Pacific [Crawford *et al.*, 2004]. This technique could usefully be adapted to other regions of interest such as the North Atlantic, and to include use of MOPITT CO profile data and day-night differencing techniques to obtain information on the vertical structure of CO transport.

MOPITT measurements may be combined with information from global chemical transport models in a more sophisticated manner than presented here in order to determine global mass flux budgets for the intercontinental transport of CO. This might include techniques such as data assimilation, although in any such study, factors such as the apparent bias and large errors on MOPITT profile data, as well as the vertical resolution issues discussed in this thesis must be considered.

6.6.3 Gaining Extra Information from MOPITT profile Measurements

Day-night differences in ‘retrieved’ model data should be examined further. The investigation could be extended to include model data from different months to determine any seasonal variability in the ability of day-night differencing to provide extra vertical information. Layer enhancement simulations similar to those described in Section 3.4 could be conducted to examine the ability of day-night differencing to determine the altitude of a CO enhancement over a wide range of situations.

Day-night differences could be used to identify the presence of high altitude CO over the oceans due to transport. Back trajectory calculations could then be performed and MOPITT day, night and day-night data examined along the trajectories to investigate the ability of the MOPITT instrument to identify and track the intercontinental transport of CO.

A study could be performed to determine the temporal coincidence of MOPITT day/night measurements. Locations where day and night overpasses occur during the same day could be identified, and day-night differences over such locations could be compared to other

locations to determine the effect of differencing measurements which are several days apart.

6.6.4 Improvements to the MOPITT Instrument

Problems with the limited vertical resolution of MOPITT could be improved with the inclusion of near infrared channels, not currently employed in MOPITT operational retrievals due to signal-to-noise and characterisation issues. These channels are more sensitive to the surface and the lower troposphere, and so could provide information on a region of the atmosphere where current MOPITT measurements are least sensitive. This technique has been employed successfully by the SCHIAMACHY instrument onboard Envisat.

Improved vertical resolution could be achieved using a MOPITT-like instrument which has channels with weighting functions that peak in different parts of the atmosphere, resulting in averaging kernels for each retrieved level which are more unique and providing a greater number of independent measurements for the retrieval process. This could be achieved through the use of different cell pressures, or by exploiting different wavelength regions, such as the near infrared as discussed above.

A problem of the current MOPITT instrument is coverage particularly cloud free measurements. MOPITT is in a sun-synchronous orbit with an altitude of 705 km. This combined with a swath width of 600 km enables the instruments to achieve global coverage only every 3 days. This means that on any particular day around two thirds of the Earth's surface is not observed by MOPITT. A geostationary orbit would enable MOPITT to make measurements over a third of the Earth's surface every few minutes. This improvement to the temporal and spatial coverage of MOPITT would be very useful for observing pollution transport. The extension of this idea to include three MOPITT instruments in geostationary orbit would provide total global coverage.

Appendix 1. Day-Night Differences in MOPITT 'surface' CO

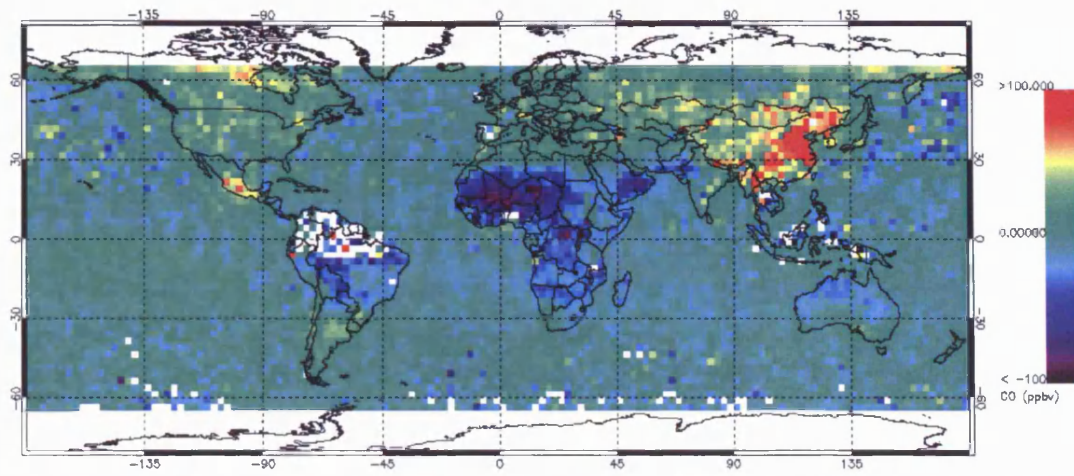


Figure A1.1: MOPITT monthly mean day-night retrieved surface CO difference map for April 2000

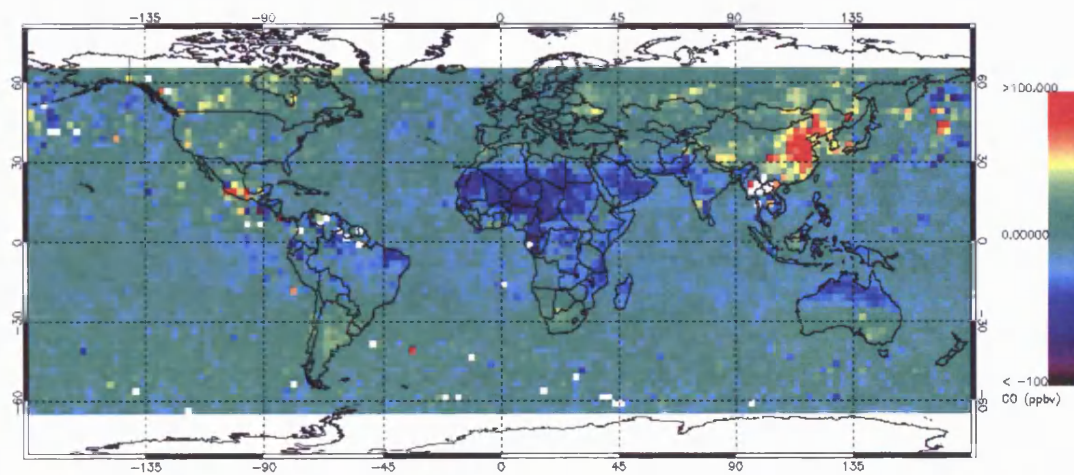


Figure A1.2: MOPITT monthly mean day-night retrieved surface CO difference map for May 2000

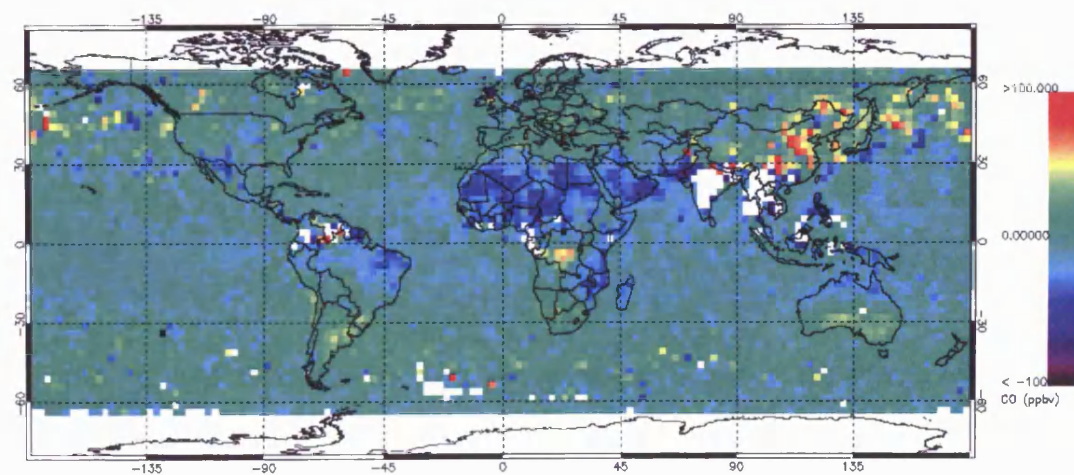


Figure A1.3: MOPITT monthly mean day-night retrieved surface CO difference map for June 2000.

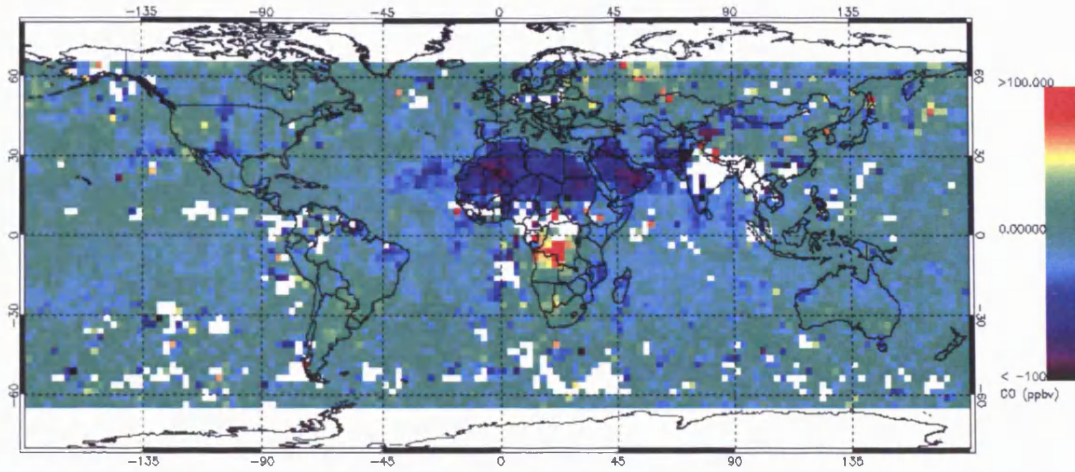


Figure A1.4: MOPITT monthly mean day-night retrieved surface CO difference map for July 2000

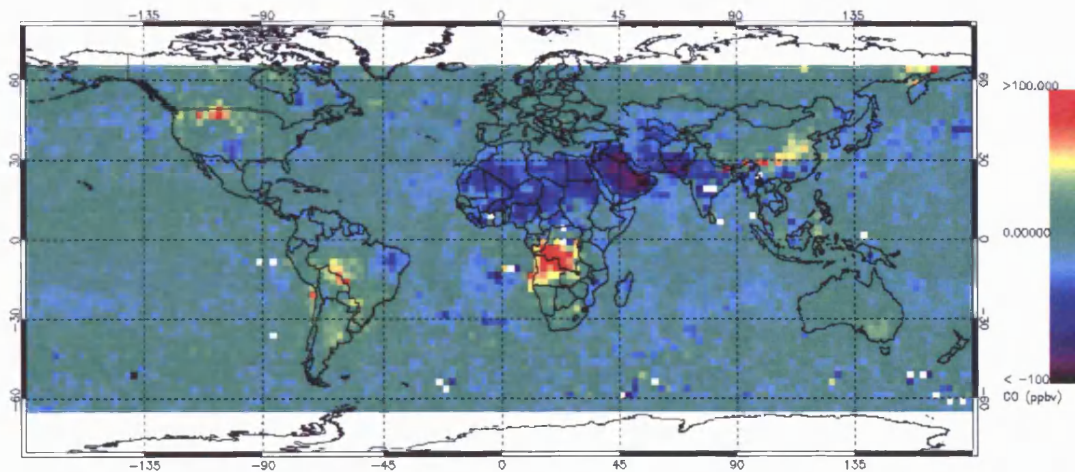


Figure A1.5: MOPITT monthly mean day-night retrieved surface CO difference map for August 2000

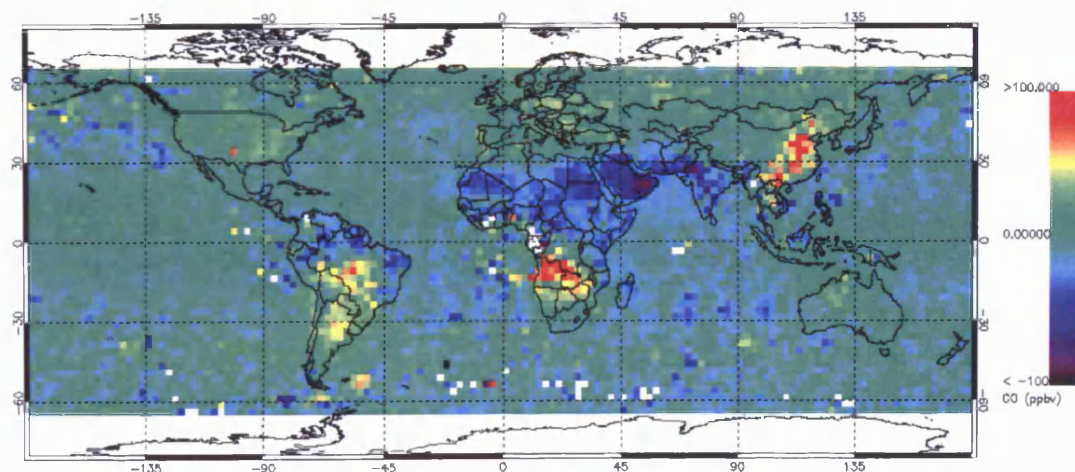


Figure A1.6: MOPITT monthly mean day-night retrieved surface CO difference map for September 2000

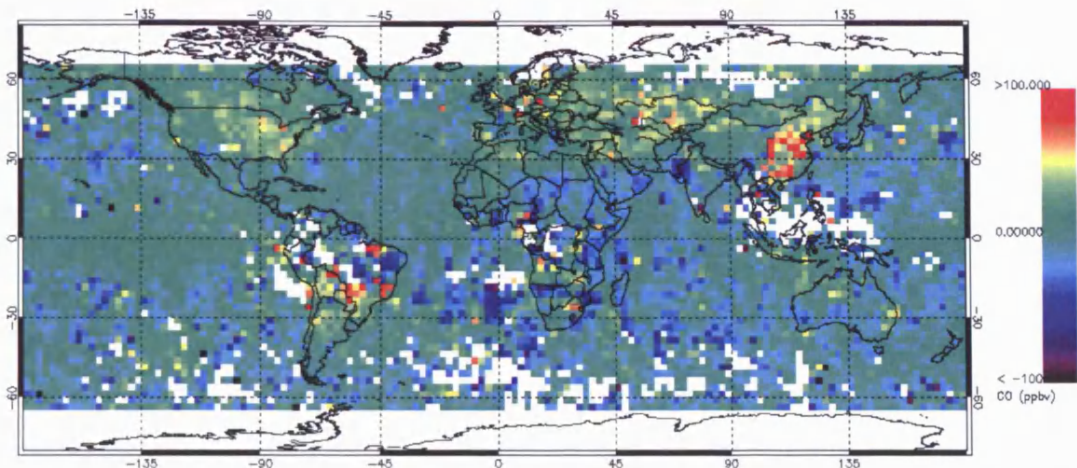


Figure A1.7: MOPITT monthly mean day-night retrieved surface CO difference map for October 2000

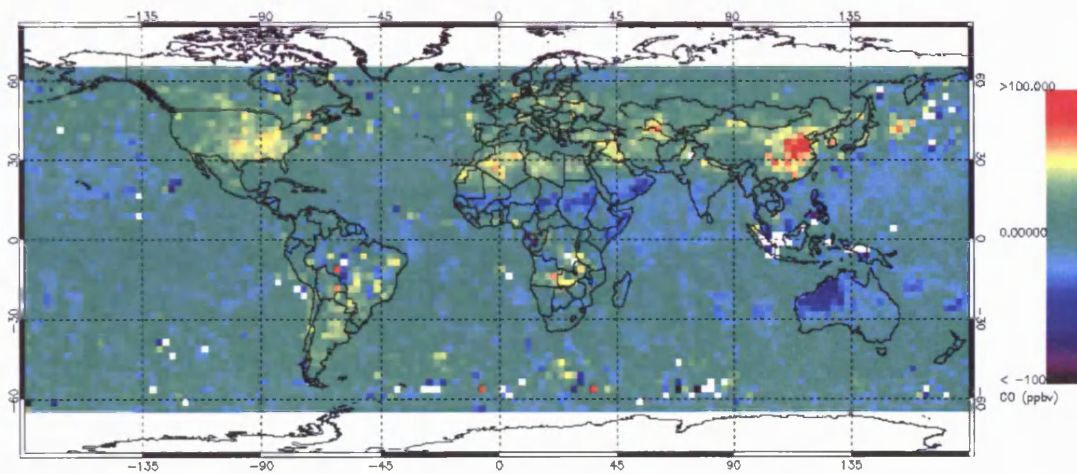


Figure A1.8: MOPITT monthly mean day-night retrieved surface CO difference map for November 2000

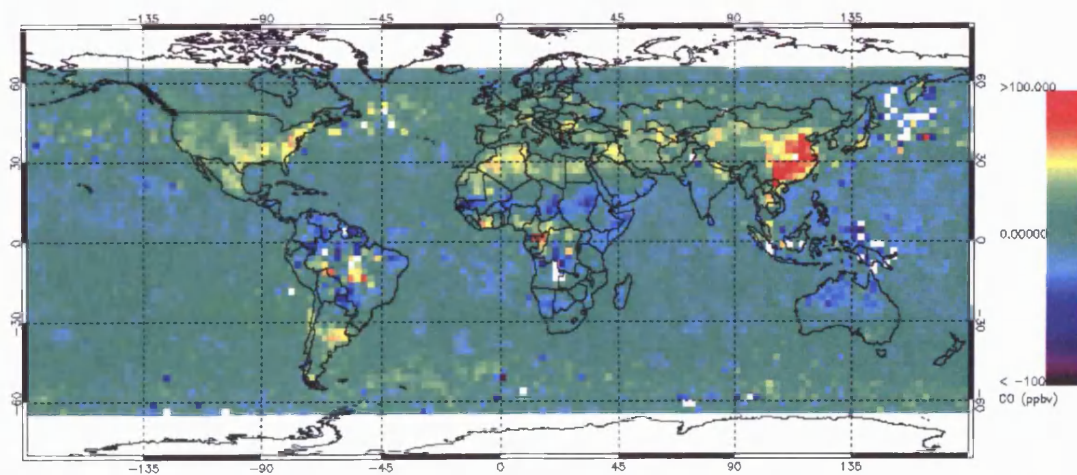


Figure A1.9: MOPITT monthly mean day-night retrieved surface CO difference map for December 2000

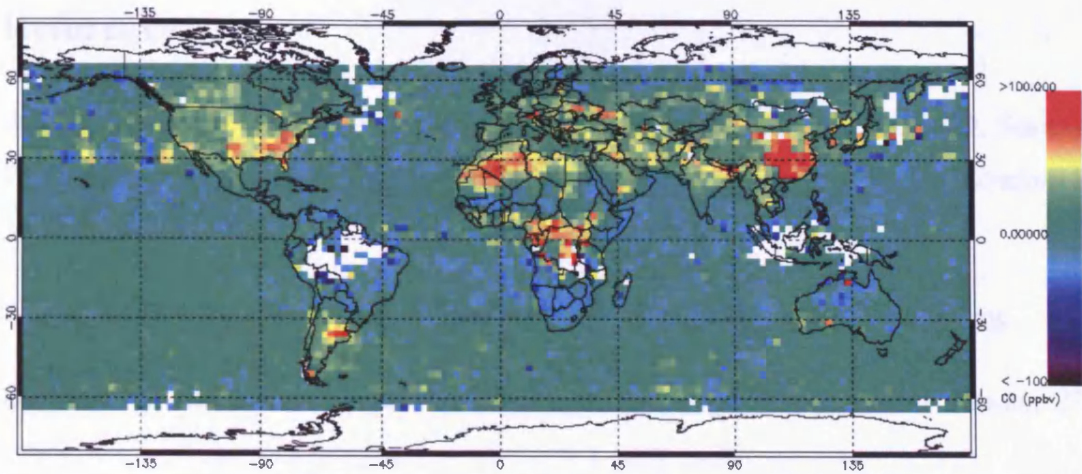


Figure A1.10: MOPITT monthly mean day-night retrieved surface CO difference map for January 2001

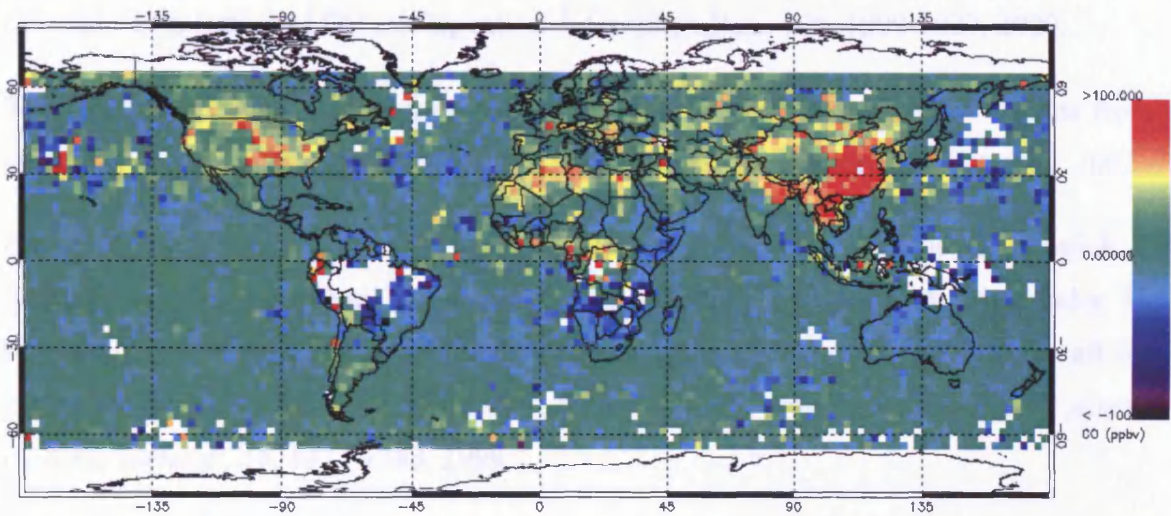


Figure A1.11: MOPITT monthly mean day-night retrieved surface CO difference map for February 2001

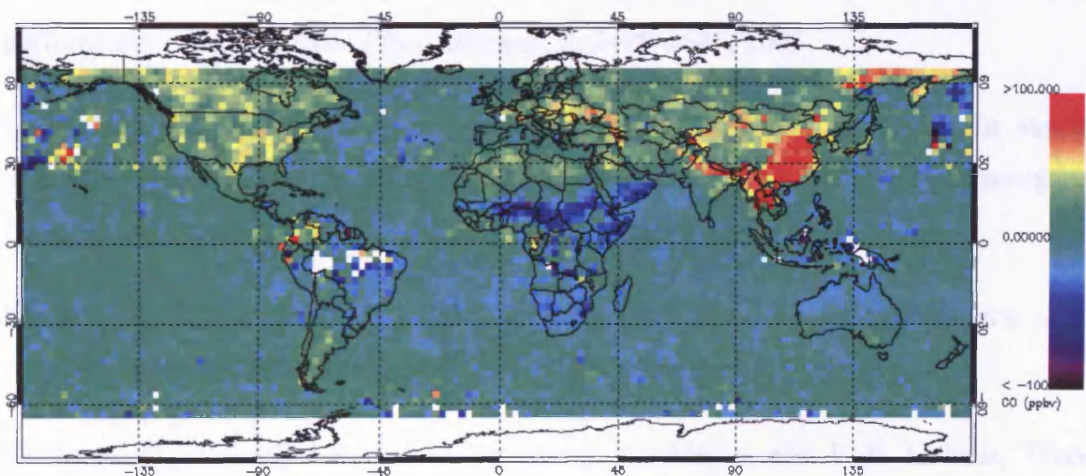


Figure A1.12: MOPITT monthly mean day-night retrieved surface CO difference map for March 2001

References

Abel, P. G., P. J. Ellis, J. T. Houghton, G. Peckham, C. D. Rodgers, S. D. Smith, E. J. Williamson, The selective chopper radiometer for Nimbus-D, *Proc. R. Soc. London, Ser A*, 320, 35, 1970.

Australian Department of Land Information web site: <http://www.dli.wa.gov.au>.

Belward, T., and T. Loveland, The DIS 1-km land cover data set, *IGBP Newsl.*, 27, 7-9, 1996.

Bergamaschi, P., R. Hein, M. Heimann and P.J. Crutzen, Inverse modeling of the global CO cycle 1. Inversion of CO mixing ratios. *J. Geophys. Res.*, 105, 1909-1927, 2000.

Bey I, Intercontinental transport of pollution in the Northern Hemisphere: insights from modelling studies, *Eurotrac-2 Symposium 2002*, Garmisch-Partenkirchen, Germany, 2002.

Brenninkmeijer, C. A. M., P. J. Crutzen, H. Fischer, H. Gusten, W. Hans, G. Heinrich, J. Heintzenberg, M. Hermann, T. Immelmann, D. Kersting, M. Maiss, A. Pitscheider, H. Pohlkamp, D. Scharffe, K. Specht and A. Wiedensohler, CARABIC – Civil aircraft for global measurement of trace gases and aerosols in the tropopause region, *J. Atmos. Oceanic Technol.*, 16, 1373-1383, 1999.

Brunner, D., *et al.*, An evaluation of the performance of chemistry transport models by comparison with research aircraft observations. Part1: Concepts and overall model performance, *Atmos. Chem. Phys. Discuss.*, 3, 2499-2545, 2003.

Carmichael, G. R., *et al.*, Regional-scale chemical transport modelling in support of intensive field experiments: Overview and analysis of the TRACE-P observations, *J. Geophys. Res.*, 108(D21), 8823, doi:10.1029/2002JD003117, 2003.

Chameides, W.L. & Walker, J.C.G., A photochemical theory for tropospheric ozone, *J. Geophys. Res.*, 78, 8751-8760, 1973.

Clerbaux, C., J. Hadji-Lazaro, S. Turquety, G. Mégie, and P.-F. Coheur, Trace gas measurements from infrared satellite for chemistry and climate applications. *Atmos. Chem. Phys.*, 3, 1495-1508, 2003.

Crawford, J. H., *et al.*, Relationship between Measurements of Pollution in the Troposphere (MOPITT) and in situ observations of CO based on a large-scale feature sampled during TRACE-P, *J. Geophys. Res.*, 109, D15S04, doi:10.1029/2003JD004308, 2004.

Cros, B., R. Delas, D. Nganga, B. Clairac, and J. Fontan, Seasonal trends of ozone in equatorial Africa: Experimental evidence of photochemical production, *J. Geophys. Res.*, 93, 8355-8366, 1988.

Crutzen, P.J., A discussion of the chemistry of some minor constituents in the stratosphere and troposphere, *Pure Appl. Geophys.*, 106-108, 1385-1399, 1973.

Crutzen, P.J., "An Overview of Atmospheric Chemistry", chapter in "Topics in Atmospheric and Interstellar Physics and Chemistry", Editor. C. F. Boutron., Les Editions de Physique, Les Ulis, 1994.

Daniel, J.S. and S. Solomon, On the climate forcing of carbon monoxide. *J. Geophys. Res.*, 103, 13249-13260, 1998.

Deeter, M. N., *et al.*, Operational carbon monoxide retrieval algorithm and selected results for the MOPITT instrument, *J. Geophys. Res.*, 108(D14), 4399, doi:10.1029/2002JD003186, 2003.

Deeter, M. N., *et al.*, Evaluation of operational radiances for the Measurements of Pollution in the Troposphere (MOPITT) instrument CO thermal band channels, *J. Geophys. Res.*, 109, D03308, doi:10.1029/2003JD003970, 2004.

de Laat, A. T. J., On the origin of tropospheric O₃ over the Indian Ocean during the winter monsoon: African biomass burning vs. stratosphere-troposphere exchange, *Atmos. Chem. Phys.*, 2, 325-341, 2002.

Draxler, R. R. and G. D. Rolph, 2003. HYSPLIT (Hybrid Single-Particle Lagrangian Integrated Trajectory) Model access via NOAA ARL READY Website (<http://www.arl.noaa.gov/ready/hysplit4.html>). NOAA Air Resources Laboratory, Silver Spring, MD.

Drummond, J. R., Novel correlation radiometer: the length-modulated radiometer, *Appl. Optics*, 28 (13), 2451-2452, 1989.

Drummond, J. R., Measurements of Pollution in the Troposphere (MOPITT), in *The Use of EOS for Studies of Atmospheric Physics*, edited by J. C. Gille and G. Visconti, pp. 77-101, North-Holland, New York, 1992.

Drummond, J. R., MOPITT Mission Description Document, University of Toronto Internal Report, 1996.

Edwards, D. P., GENLIN2: A general line-by-line atmospheric transmittance and radiance model: Version 3.0 description and users guide, *Rep. NCAR/TN-367+STR*, Natl. Cent. For Atmos. Res., Boulder, Colo., 1992.

Edwards D. P., C. M. Halvorson, and J. C. Gille, Radiative transfer modelling for the EOS Terra satellite Measurements of Pollution in the Troposphere (MOPITT) instrument, *J. Geophys. Res.*, 104, 16, 755-16,775, 1999.

Ehhalt, D., Photooxidation of trace gases in the troposphere, *Phys. Chem. Chem. Phys.*, 24, 5401-5408.

European Council of Ministers (ECM), Council Directive 92/72/EEC of 21 September 1992 on air pollution by ozone, Off. J. Eur. Communities, Legis., L297, 1-7, 1992.

Emmons L. K., D. A. Hauglustaine, JF. Muller, M. A. Carroll, G. P. Brasseur, D. Brunner, J. Staehelin, V. Thouret, and A. Marengo, Data composites of airborne observations of tropospheric ozone and its precursors, *J. Geophys. Res.*, 105, 20497-20538, 2000.

Emmons, L. K., et al., Validation of Measurements of Pollution in the Troposphere (MOPITT) CO retrievals with aircraft in situ profiles, *J. Geophys. Res.*, 109, D03309, doi:10.1029/2003JD004101, 2004.

Faluvegi, G. S., K. Alapaty, H. G. Reichle Jr., R. Mathur, S. Raman and V. S. Connors, Simulation of carbon monoxide transport during April 1994, *J. Geophys. Res.*, 104, 21471-21485, 1999.

Fishman, J., and W. Seiler, Correlative nature of ozone and carbon monoxide in the troposphere: Implications for tropospheric ozone budget, *J. Geophys. Res.*, **88**, 3662-3670, 1983.

Hauglustaine, D.A., G.P. Brasseur, S. Walters, P.J. Rasch, J.-F. Müller, L.K. Emmons and M.A. Carroll, MOZART, a global chemical transport model for ozone and related chemical tracers: 2. Model results and evaluation. *J. Geophys. Res.*, **103**, 28291-28335, 1998.

Hauglustaine, D. A., G. P. Brasseur, S. Walters, P. J. Rasch, J.-F. Muller, L. K. Emmons, and M. A. Carroll, MOZART, a global chemical transport model for ozone and related chemical tracers: 2. Model results and evaluation, *J. Geophys. Res.*, **104**, 5567-5583, 1999.

Heald, C. L., et al., Asian outflow and trans-Pacific transport of carbon monoxide and ozone pollution: An integrated satellite, aircraft, and model perspective, *J. Geophys. Res.*, **108(D24)**, 4804, doi:10.1029/2003JD003507, 2003.

Hély, C., S. Alleaume, R. J. Swap, H. H. Shugart, and C. O. Justice, SAFARI 2000 characterisation of fuels, fire behaviour, combustion completeness and emissions from experimental burns in infertile grass savannas in western Zambia, *J. Arid Environ.*, **54(2)**, 381-394, 2003.

IPCC, 1996 Climate Change 1995: The Science of Climate Change. Contribution of Working Group I to the Second Assessment Report of the Intergovernmental Panel on Climate Change [Houghton, J.T., L.G. Meira Filho, B.A. Callander, N. Harris, A. Kattenberg, and K. Maskell (eds.)]. Cambridge University Press, Cambridge, United Kingdom and New York, NY, USA, pp 572, 1996.

IPCC, 2001: Climate Change 2001: The Scientific Basis Contribution of Working Group I to the Third Assessment Report of the Intergovernmental Panel on Climate Change (IPCC) [J. T. Houghton, Y. Ding, D.J. Griggs, M. Noguer, P. J. van der Linden and D. Xiaosu (Eds.)] Cambridge University Press, UK. pp 944, 2001.

Jacob, D., J. A. Logan, G. M. Gardner, R.M. Yevich, C. M. Spivakovsky,, and S. C. Wofsy, Factors regulating ozone over the United States and its export to the global atmosphere, *J. Geophys. Res.*, **98**, 14,817 – 14,826, 1993.

Jacob, D. J., J. H. Crawford, M. M. Kleb, V. S. Connors, R. J. Bendura, J. L. Raper, G. W. Sachse, J. C. Gille, L. Emmons and C. L. Heals, Transport and Chemical Evolution Over the Pacific (TRACE-P) aircraft mission: Design, execution, and first results, *J. Geophys. Res.*, 108(D20), 8802, doi:10.1029/2002JD003121, 2003.

Jaeglé, L., D. A. Jaffe, H. U. Price, P. Weiss-Penzias, P. I. Palmer, M. J. Evans, D. J. Jacob, and I. Bey, Sources and budgets for CO and O₃ in the northeastern Pacific during the spring of 2001: Results from the PHOBEA-II Experiment, *J. Geophys. Res.*, 108(D20), 8802, doi:10.1029/2002JD003121, 2003.

Jaffe, D. A., *et al.*, Transport of Asian air pollution to North America, *Geophys. Res. Lett.*, 26, 711-714, 1999.

Junge, C.E., Global ozone budget and exchange between the stratosphere and troposphere, *Tellus*, 14, 363-377, 1962.

Khalil, M. A. K., and R. A. Rasmussen, The global cycle of carbon monoxide: trends and mass balance. *Chemosphere*, 20, 227-242, 1990.

Kobayashi, H., A. Shimota, K. Kondo, E. Okumura, Y. Kameda, H. Shimoda, and T. Ogawa. Development and evaluation of the interferometric monitor for greenhouse gases: a high-throughput Fourier-transform infrared radiometer for nadir Earth observation, *Appl. Opt.*, 38, 6801-6807, 1999.

Law, K. S., *et al.*, Evaluation of modelled O₃ using MOZAIC data, *J. Geophys. Res.*, 103, pp. 25721-25737, 1998.

Law, K. S., *et al.*, Comparison between global chemistry transport model results and Measurement of Ozone by Airbus In-Service Aircraft (MOZAIC) data., *J. Geophys. Res.*, 105, 1503-1525, 2000.

Lamarque, J.-F., *et al.*, Identification of CO plumes from MOPITT data: Application to the August 2000 Idaho-Montana forest fires, *Geophys. Res. Lett.*, 30(13), 1688, doi:10.1029/2003GL017503, 2003.

Li, Q., *et al.* Transatlantic transport of pollution and its effects on surface ozone in Europe and North America, *J. Geophys. Res.*, 107, D13, 10.1029/2001JD001442, 2002.

Liu, H., D. J. Jacob, I. Bey, R. M. Yantosca, B. N. Duncan, and G. W. Sasche, Transport pathways for Asian combustion outflow over the Pacific: Interannual and seasonal variations, *J. Geophys. Res.*, 108(D20), 8786, doi:10.1029/2002JD003102, 2003.

Logan, J.A., M.J. Prather, S.C. Wofsy, and M.B. McElroy, Tropospheric chemistry: A global perspective, *J. Geophys. Res.*, 86, 7210-7254, 1981.

McKernan, É., MOPITT Spectral Characterisation and Forward Modelling, PhD Thesis, Graduate Department of Physics, University of Toronto, Canada, 2001.

Monks, P. S., Personal communication, 2002.

MOPITT validation web site: <http://www.eos.ucar.edu/mopitt/validation/index.html>

NASA Langley DAAC, MOPITT data access via the world wide web: http://eosweb.larc.nasa.gov/PRODOCS/mopitt/table_mopitt.html

National Interagency Fire Centre, <http://www.nifc.gov>.

NOAA (National Oceanic and Atmospheric Administration) CMDL (Climate Modelling & Diagnostics Laboratory) CCGG (Carbon Cycle Greenhouse Gases), <http://www.cmdl.noaa.gov/ccgg>

Novelli, P.C., K.A. Masarie, and P.M. Lang, Distributions and recent changes of carbon monoxide in the lower troposphere, *J. Geophys. Res.*, 103, 19015-19033, 1998.

Novelli, P. C., V. S. Connors, H. G. Reichle Jr, B. E. Anderson, C. A. M. Brenninkmeijer, E. G. Brunke, B. G. Doddridge, V. W. J. H. Kitchhoff, K. S. Lam, K. A. Masarie, T. Matsuo, D. D. Parrish, H. E. Sheeel, and L. P. Steele, An internally consistent set of globally distributed atmospheric carbon monoxide mixing ratios developed using results from an intercomparison of measurements, *J. Geophys. Res.*, 103, 19285-19293, 1998.

Pacyna, J. M., and T. E. Graedel, Atmospheric emissions inventories: status and prospects. *Annu. Rev. Energy Environ.* 20, 265-300, 1995.

Pan, L., D. P. Edwards, J. C. Gille, M. W. Smith, and J. R. Drummond, Satellite remote sensing of tropospheric CO and CH₄: Forward model studies for the MOPITT instrument, *Appl. Opt.*, 34, 6976-6988, 1995.

Pan, L., J. Gille, D. P. Edwards, P. L. Bailey, and C. D. Rodgers, Retrieval of carbon monoxide for the MOPITT instrument, *J. Geophys. Res.*, 103, 32,277-32,290, 1998.

Poisson, N., M. Kanakidou, and P.J. Crutzen, Impact of non-methane hydrocarbons on tropospheric chemistry and the oxidising power of the global troposphere: 3-dimensional modelling results, *J. Atmos. Chem.*, 36, 157-230.

Pougatchev, N. S., G. W. Sachse, H. E. Fuelberg, C. P. Rinsland, R. B. Chatfield, V. S. Connors, N. B. Jones, J. Notholt, P. C. Novelli, and H. G. Reichle Jr., *J. Geophys. Res.*, 104, 26195-26207, 1999.

Prather, M. J., Ehhalt, D. Dentener, F., *et al.*, Atmospheric chemistry and greenhouse gases, in *Climate Change 2001: The Scientific Basis. Contribution of Working Group I to the Third Assessment Report of the Intergovernmental Panel on Climate Change (IPCC)*, edited by Houghton, J. T. *et al.*, 881, Cambridge University Press, New York, 2001

Raga, G. B., D. Baumgardner, T. Castro, A. Martinez-Arroyo, R. Navarro-Gonzalez, Mexico City air quality: a qualitative review of gas and aerosol measurements (1960-2000), *Atmos. Environ.*, 35, 4041-4058, 2001.

Reichle, H. G. Jr., V. S. Connors, J. A. Holland, W. D. Hypes, H. A. Wallio, J. C. Casas, B. B. Gormsen, M. S. Saylor, and W. D. Hesketh, Middle and upper tropospheric carbon monoxide mixing ratios as measured by a satellite-borne remote sensor during November 1981, *J. Geophys. Res.*, 91, 10865-10887, 1986.

Reichle, H. G. Jr., V. S. Connors, J. A. Holland, R. T. Sherrill, H. A. Wallio, J. C. Casas, E. P. Condon, B. B. Gormsen, and W. Seiler, The distribution of middle tropospheric carbon monoxide during early October 1984, *J. Geophys. Res.*, 95, 9845-9856, 1990.

Reichle, H. G. Jr., B. E. Anderson, V. S. Connors, T. C. Denkins, D. A. Forbes, B. B. Gormsen, R. L. Langenfelds, D. O. Neil, S. R. Nolf, P. C. Novelli, N. S. Pougatchev, M. M. Roell, and L. P. Steele, Space shuttle based global CO measurements during April and October 1994, MAPS instrument, data reduction and data validation, *J. Geophys. Res.*, 104, 21443-21454, 1999.

- Rinsland, C. P., A. Meier, D. W. T. Griffith, and L. S. Chiou, Ground based measurements of tropospheric CO, C₂H₆, and HCN from Australia at 34°S latitude during 1997-1997, *J. Geophys. Res.*, 106, 20913-20924, 2001.
- Rodgers, C. D., *Inverse Methods for Atmospheric Sounding, Theory and Practice*, World Sci., River Edge, N. J., 2000.
- Seiler, W., The cycle of atmospheric CO. *Tellus*, 26, 116-135, 1974.
- Seiler, W., and R. Conrad, Contribution of tropical ecosystems to the global budgets of trace gases, especially CH₄, H₂, CO, and N₂O. In "Geophysiology of Amazonia" (R. Dickinson, ed.), pp. 133-162. Wiley, New York, 1987.
- Stohl, A., A 1-year Lagrangian "climatology" of airstreams in the Northern Hemisphere troposphere and lowermost stratosphere, *J. Geophys. Res.*, 106(D7), 7263-7279, 2001.
- Stohl, A., S. Eckhardt, C. Forster, P. James, N. Spichtinger, P. Seibert, A replacement for simple back trajectory calculations in the interpretation of atmospheric trace substance measurements, *Atmos. Env.*, 36, 4635-4648, 2002.
- Swap, R. J., H. J. Annegarn, J. T. Suttles, M. D. King, S. Platnick, J. L. Privette, and R. J. Scholes, Africa burning: A thematic analysis of the Southern African Regional Science Initiative (SAFARI 2000), *J. Geophys. Res.*, 108(D13), 8465, doi:10.1029/2003JD003747, 2003.
- Tansey, K., *et al.*, Vegetation burning in the year 2000: Global burned area estimates from SPOT VEGETATION data, *J. Geophys. Res.*, 109, D14S03, doi:10.1029/2003JD003598, 2004.
- Taylor, F. W., C. D. Rodgers, E. J. Williams, G. D. Peskett, J. T. Houghton, Radiometer for remote sounding of the upper atmosphere, *Applied Optics*, 11, 135-141, 1972.
- The Oxford Reference Forward Model (RFM), <http://www.atm.ox.ac.uk/RFM>
- Tolton, B. T., and J. R. Drummond, Characterisation of the length-modulated radiometer, *Appl. Optics*, 36, 5409-5419, 1997.

Tucker, G. B., and R. G. Barry, Climates of the North Atlantic Ocean, in World Survey of Climatology, vol. 15, Climates of the Oceans, edited by H. Van Loon, chap. 2, pp. 193-262, Elsevier Sci., New York, 1984.

U.S. Environmental Protection Agency (EPA), National air pollution emission trends, 1900-1994, *Rep. EPA-454/R-95-011*, Washington D.C., 1995.

Wang, Y., W.K. Tao, K. E. Pickering, A. M. Thompson, R. Adler, J. Simpson, P. Keehn, and G. Lai, Mesoscale model (MM5) simulations of TRACE A and PRESTORM convective events and associated tracer transport, *J. Geophys. Res.*, *101*, 24013-24027, 1996.

Warneck, P., 2000. Chemistry of the Natural Atmosphere. Academic Press, New York.

Warner, J., J. C. Gille, D. P. Edwards, D. Ziskin, M. Smith, P. Bailey, and L. Rokke, Cloud detection and clearing for the Earth observing system Terra satellite Measurements of Pollution in the Troposphere (MOPITT) experiment, *Appl. Opt.*, *40*, 1269-1284, 2001.

Wayne, R.P., "Chemistry of Atmospheres", 2nd Ed., Oxford University Press, Oxford, 1991.

Wilber, A. C., D. P. Kratz, and S. K. Gupta, Surface emissivity maos for use in satellite retrievals of longwave radiation, *NASA Tech. Pap. 1999-209362*, NASA Langley Res. Cent., Hampton, Va., 1999.

WMO, Scientific Assessment of Ozone Depletion: 1998. Global Ozone Research and Monitoring Project - Report No. 44, World Meteorological Organization, Geneva, Switzerland, 732 pp, 1999.

Yienger, J. J., M. Galanter, T. A. Holloway, M. J. Phadnis, S. K. Guttikunda, C. R. Carmichael, W. J. Moxim, and H. Levy II, The episodic nature of air pollution transport from Asia to North America, *J. Geophys. Res.*, *105*, 26,931-26,945, 2000.

Zhang *et al.*, Large-scale structure of trace gas and aerosol distributions over the western Pacific Ocean during the Transport and Chemical Evolution Over the Pacific (TRACE-P) experiment, *J. Geophys. Res.*, *108*(D21), 8820, doi:10.1029/2002JD002946, 2003.